Unclassified

SECURITY CLASSIFICATION OF THIS PAGE (When Data Entered)

AD-A030 806

REPORT DOCUMENTATION PAGE

READ INSTRUCTIONS BEFORE COMPLETING FORM

1. REPORT NUMBER: Contract Report S-76-11	2. GOVT ACCESSION NO. / 3. RECIPIENT'S CATALOG NUMBER: WES/CR-S-76-11
4. TITLE (and Subtitle): DATA COLLECTION AND ANALYSIS, RUNWAY 4R-22L, O'HARE INTERNATIONAL AIRPORT	5. TYPE OF REPORT & PERIOD COVERED: Final report
	6. PERFORMING ORG. REPORT NUMBER
7. AUTHOR(s): Harvey J. Treybig, Harold L. Von Quintus and B. Frank McCullough	8. CONTRACT OR GRANT NUMBER(s): Contract DACW39-75-C-0090
9. PERFORMING ORGANIZATION NAME AND ADDRESS: Austin Research Engineers, Inc. Engineering Consultants 5706 Bee Cave Road, Austin, Texas 78746	10. PROGRAM ELEMENT, PROJECT, TASK AREA & WORK UNIT NUMBERS: 181p.
11. CONTROLLING OFFICE NAME AND ADDRESS: Federal Aviation Administration Systems Research and Development Service Washington, D. C. 20591	12. REPORT DATE: Sept 1976
	13. NUMBER OF PAGES: 178
MONITORING AGENCY NAME & ADDRESS (if different from Controlling Office): U. S. Army Engineer Waterways Experiment Station Soils and Pavements Laboratory P. O. Box 631, Vicksburg, Miss. 39180	15. SECURITY CLASS. (of this report): Unclassified
	15a. DECLASSIFICATION/DOWNGRADING SCHEDULE

16. DISTRIBUTION STATEMENT (of this Report)

Approved for public release; distribution unlimited.

17. DISTRIBUTION STATEMENT (of the abstract entered in Block 20, if different from Report)

18. SUPPLEMENTARY NOTES

19. KEY WORDS (Continue on reverse side if necessary and identify by block number)

Continuously reinforced concrete	Overlays (Pavements)
Data collection	Reinforced concrete
Data processing	Rigid pavements
O'Hare International Airport	Runways

20. ABSTRACT (Continue on reverse side if necessary and identify by block number)

This report documents and discusses data obtained from field studies of continuously reinforced concrete (CRC) airfield pavement. It includes a discussion and analysis of deflection measurements, material properties, traffic distribution, climatological data, and the pavement's physical condition, as they pertain to the design of CRC pavements and overlays. A comparison is presented between predicted characteristics, developed using the design procedures for CRC pavement, and actual observations made on Runway 4R-22L at (continued)

DD FORM 1 JAN 73 1473 EDITION OF 1 NOV 65 IS OBSOLETE

Unclassified

SECURITY CLASSIFICATION OF THIS PAGE (When Data Entered)

20. ABSTRACT (continued).

O'Hare International Airport. A summary of the analysis is presented which includes conclusions concerning components of the design procedure and a list of recommendations for future revisions and additions to the procedure. Every attempt was made to summarize and establish the initial behavior and performance data of Runway 4R-22L, so that it can be used in future performance studies of CRC airfield pavements.

PREFACE

This report documents and presents analyses of data collected on Runway 4R-22L at O'Hare International Airport for the purpose of verifying and/or modifying the CRC airfield pavement design procedures developed for USAF and the FAA. The data obtained are summarized and presented such that it may be used in future evaluations and analysis.

Support for the contract was provided by the Federal Aviation Administration (FAA) through the U. S. Army Engineers Waterways Experiment Station (WES).

The authors are grateful and acknowledge the cooperation of the City of Chicago, particularly Mr. Donald M. Arntzen. Special thanks are extended to Mr. Phil Smith, Staff Engineer for ARE Inc., who supervised and coordinated the gathering of field data. Recognition and thanks also go to Mr. Jim W. Hall, Jr. (USAE/WES) for collection of the WES Vibrator data, and to USAE/WES for providing deflection measurements for this study. The technical coordination for the contract was supplied by Dr. Frazier Parker and Mr. Gary Harvey both from USAE/WES.

HARVEY J. TREYBIG
HAROLD L. VON QUINTUS
B. FRANK MCCULLOUGH

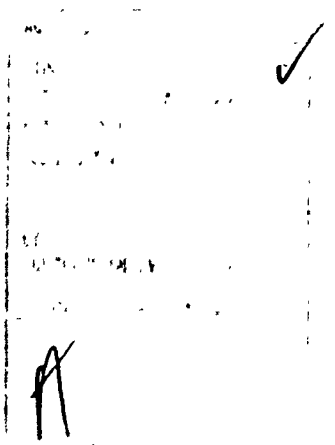

DISCLAIMER

The opinion, findings and conclusions expressed in this publication are those of the Authors and not necessarily those of the U.S. Army Engineer Waterways Experiment Station.

TABLE OF CONTENTS

	Page
PREFACE	i
DISCLAIMER	iii
LIST OF TABLES	iv
LIST OF FIGURES	vi
CONVERSION FACTORS, U.S. CUSTOMARY TO METERIC (SI) UNITS OF MEASUREMENT	xii
PART I INTRODUCTION	1
Objective	1
Scope	2
PART II FIELD STUDIES	3
Deflection Profile Measurements	3
LVDT Deflection Measurements	3
Strain Measurements	33
Pavement Condition Observations	33
Material Properties	37
Environmental Data	53
Traffic Survey	53
PART III PAVEMENT CHARACTERIZATION AND ANALYSIS	61
Elastic Layer Theory	61
Slab Theory	72
PART IV DISCUSSION AND INTERPRETATION OF RESULTS	93
Comparison of Observed and Predicted Deflections	93
Design Implications of Data	97
PART V SUMMARY	100
Conclusions	100
Recommendations	103
REFERENCES	104
APPENDICES	
APPENDIX A DEFLECTION MEASUREMENTS ON RUNWAY 4R-22L	A1
APPENDIX B CRACK SPACING	B1
APPENDIX C CRACK WIDTH AND CONCRETE MOVEMENT	C1

LIST OF TABLES

Tables		Page
1.	Summary of Load Data on Test Equipment	5
2.	Change in WES Vibrator Deflection Values with Time at Each Section Along Runway 4R-22L for 10 kip load	10
3.	Change in WES Dynaflect Deflection Values with Time at Each Section Along Runway 4R-22L	13
4.	Average Crack Spacing for Each Section Along Runway 4R-22L	35
5.	Summary of Portland Cement Concrete Test Data Available For Runway 4R-22L (Ref 5, 9)	41
6.	Summary of Cement Aggregate Mixture (CAM) Test Data.	43
7.	Subsurface Soil Condition Beneath Centerline of Runway 4R-22L	50
8.	Traffic Survey Comparisons for O'Hare International Airport, Chicago, Illinois	60
9.	Deflection Values Used to Characterize Each Site	69
10.	Subgrade Resilient Modulus Based on the Dynaflect and WES Vibrator Loads Considering Concept of Stress Sensitivity	70
11.	Comparison of Deflection Measurements and Predictions With and Without Stress Sensitivity Considerations	96
12.	Maximum Tensile Stress That Occurs At the Bottom Of The CRC Layer	99
A1.	Dynaflect Deflection Collected on Runway 4R-22L, O'Hare International Airport	A8
A2.	Dynaflect Deflection Collected on Runway 4R-22L, O'Hare International Airport	A15
A3.	Dynaflect Deflection Collected on Runway 4R-22L, O'Hare International Airport	A19
A4.	WES Vibrator Deflection Data for Runway 4R-22L, O'Hare International Airport	A24

LIST OF TABLES (continued)

Tables		Page
A5.	WES Vibrator Deflection Data for Runway 4R-22L, O'Hare International Airport (Lane 3).	A26
A6.	WES Vibrator Deflection Data for Runway 4R-22L, O'Hare International Airport (Lane 4).	A28
A7.	WES Vibrator Deflection Data for Runway 4R-22L, O'Hare International Airport, Site 1 - 4	A29
A8.	Plate Load Deflection Data for Site 1 on Runway 4R-22L.	A31
A9.	Plate Load Deflection Data for Site 3 on Runway 4R-22L.	A32
A10.	Plate Load Deflection Data for Site 4 on Runway 4R-22L.	A33
A11.	727 Aircraft Load Deflection Data for Site 1 on Runway 4R-22L.	A34
A12.	727 Aircraft Load Deflection Data for Site 3 on Runway 4R-22L.	A35
A13.	727 Aircraft Load Deflection Data for Site 4 on Runway 4R-22L.	A36
A14.	Tug (747) Load Deflection Data for Site 1 on Runway 4R-22L.	A37
A15.	Tug (747) Load Deflection Data for Site 3 on Runway 4R-22L.	A38
A16.	Tug (747) Load Deflection Data for Site 4 on Runway 4R-22L.	A39
C1.	Crack Width Measurements Taken With A Microscope on Runway 4R-22L	C5
C2.	Crack Width Data Taken with the Whitmore Strain Gage on Runway 4R-22L.	C6

LIST OF FIGURES

Figure		Page
1.	Location of the special test sections along Runway 4R-22L at O'Hare International Airport in Chicago, Illinois. . . .	4
2.	WES Vibrator deflection measurements for different time periods in lane 3 for a 10 kip load at a frequency of 15 cps	7
3.	WES Vibrator deflection data taken in 1975 with a 10 kip load at a frequency of 15 cps.	8
4.	Typical frequencies of sweep data taken on Runway 4R-22L with the WES Vibrator for a load of 7,000 lb.	9
5.	Dynaflect deflection profile along center of Lane 3, Runway 4%-22L for October 1971 and September 1972	11
6.	Dynaflect deflection profile along runway 4R-22L for October 1971.	12
7.	In-place LVDT installed on Runway 4R-22L at O'Hare International Airport	15
8.	Illustration and description of where the test sites are located on Runway 4R-22L.	16
9.	Underside view of the prefabricated plate used to simulate the Boeing 727 aircraft gear.	17
10.	Illustration showing the crane which was used to apply the 76 kip load	18
11.	Side view of the plate and jeep which was used to position the plate at the selected offset	18
12.	Plate load deflection data for Site 1 (sta 329 + 48) on Runway 4R-22L	20
13.	Plate load deflection data for Site 3 (sta 305 + 66) on Runway 4R-22L	21
14.	Plate load deflection data for Site 4 (sta 305 + 77) on Runway 4R-22L	22
15.	Normalized deflections for the plate load for adjacent to crack measurements	23

LIST OF FIGURES (continued)

Figure		Page
16.	Boeing 727 Aircraft load deflection data for Site 1 (sta 329 + 28) on Runway 4R-22L.	25
17.	Boeing 727 aircraft load deflection data for Site 3 (sta 305 + 66) on Runway 4R-22L.	26
18.	Boeing 727 aircraft load deflection data for Site 4 (sta 305 + 77) on Runway 4R-22L.	27
19.	Normalized deflections for the Boeing 727 aircraft for adjacent to crack measurements	28
20.	Aircraft tug (B747) load deflection data for Site 1 (sta 329 + 48) on Runway 4R-22L.	29
21.	Aircraft tug (B747) load deflection data for Site 3 on Runway 4R-22L	30
22.	Aircraft tug (B747) load deflection data for Site 4 (sta 305 + 77) on Runway 4R-22L.	31
23.	Normalized deflections for the tug load for adjacent to crack measurements	32
24.	General view of transverse cracking and aggregate popout along Runway 4R-22L.	34
25.	Close-up of an aggregate popout with some distress developing around popout	34
26.	Crack width measurements taken with the Whitmore Strain gage at Sta 306 + 50 (Interior lane) expressed as a function of crack spacing	38
27.	Crack width measurements taken with the Whitmore Strain gage at Sta 305 + 50 (outer lane) expressed as a function of crack spacing	39
28.	Crack width measurements taken with the Whitmore Strain gage at Sta 304 + 60 (outer lane) expressed as a function of crack spacing	40
29.	Laboratory test data for the granular subbase material sampled in May 1975.	45

LIST OF FIGURES (continued)

Figures		Page
30.	Laboratory test results of the subgrade material at a depth of 3.5 - 6 feet below the surface.	47
31.	Laboratory test results of the subgrade material at a depth of 8-11 feet below the surface	48
32.	Laboratory test results of the subgrade material at a depth of 6-8 feet below the surface	49
33.	General increase in moisture content with time on Runway 4R-22L	51
34.	General decrease in dry density with time on Runway 4R-22L	52
35.	Average monthly high and low temperatures, for the O'Hare International Airport	54
36.	Yearly snow and ice precipitation of O'Hare International Airport	55
37.	Monthly rainfall for O'Hare International Airport. . . .	56
38.	Temperature variation with depth of CRCP, taken with thermistors located at Site 4 on 21 May 1975	57
39.	Distribution of arrivals and departures of the traffic survey on 22 May 1975 for O'Hare International Airport .	59
40.	Theoretical deflection versus subgrade modulus for dynamic load conditions at Site 1.	62
41.	Theoretical deflection versus subgrade modulus for dynamic load conditions at Site 3.	63
42.	Theoretical deflection versus subgrade modulus for dynamic load conditions at Site 4.	64
43.	Theoretical deviator stress (top of subgrade) versus subgrade modulus for dynamic and static load conditions at Site 1.	66
44.	Theoretical deviator stress (top of subgrade) versus subgrade modulus for dynamic and static load conditions at Site 3.	67

LIST OF FIGURES (continued)

Figures		Page
45.	Theoretical deviator stress (top of subgrade) versus subgrade modulus for dynamic and static load conditions at Site 4.	68
46.	Comparison of predicted and observed deflections for the plate load at Site 1	73
47.	Comparison of predicted and observed deflections for the plate load at Site 3	74
48.	Comparison of predicted and observed deflections for the plate load at Site 4	75
49.	Comparison of predicted and observed deflections for the B727 load at Site 1	76
50.	Comparison of predicted and observed deflections for the B727 load at Site 3	77
51.	Comparison of predicted and observed deflections for the B727 load at Site 4	78
52.	Comparison of predicted and observed deflections for the tug (B747) load at Site 1	79
53.	Comparison of predicted and observed deflections for the tug (B747) load at Site 3	80
54.	Comparison of predicted and observed deflections for the tug (B747) load at Site 4	81
55.	Determiniation of the composite k-value from deflection matching using the WES Vibrator	82
56.	Comparison of predicted deflections, using plate theory, and observed deflections for the plate load at Site 1. .	84
57.	Comparison of predicted deflections, using plate theory, and observed deflections for the plate load at Site 3. .	85
58.	Comparison of predicted deflections, using plate theory, and observed deflections for the plate load at Site 4. .	86
59.	Comparison of predicted deflections, using plate theory, and observed deflections for the B727 load at Site 1 . .	87

LIST OF FIGURES (continued)

Figures		Page
60.	Comparison of predicted deflections, using plate theory, and observed deflections for the B727 load at Site 3	88
61.	Comparison of predicted deflections, using plate theory, and observed deflections for the B727 load at Site 4	89
62.	Comparison of predicted deflections, using plate theory, and observed deflections for the tug (B747) load at Site 1 .	90
63.	Comparison of predicted deflections, using plate theory, and observed deflections for the tug (B747) load at Site 3 .	91
64.	Comparison of predicted deflections, using plate theory, and observed deflections for the tug (B747) load at Site 4 .	92
65.	Typical comparison of predicted and observed deflections (B727 load at Site 3) that occurred in the first analysis (who reduced CAM modulus and w/o rigid layer).	95
A1.	Site 1 Station 328 + 48, End of runway in wheel path of B747 either interior paving lane.	A2
A2.	Site 2 Station 320 + 88, Touchdown area, in wheel path of B747, either interior paving lane	A3
A3.	Site 3 Station 305 + 66, Rotation area in wheel path of B747, either interior paving lane	A4
A4.	Site 4 Station 305 + 77, No traffic, outer paving lane, (adjacent to site 3).	A5
A5.	General layout for longitudinal and transverse offsets at Sites 1 and 2 for the three test loads (not to scale). . . .	A6
A6.	General layout for longitudinal and transverse offsets at sites 3 and 4 for the three test loads (not to scale). . . .	A7
B1.	Distribution of crack spacing for two time periods at Section A.	B2
B2.	Distribution of crack spacing for two time periods at Section B.	B3
B3.	Distribution of crack spacing for two time periods at Section C.	B4

LIST OF FIGURES (continued)

Figures		Page
B4.	Distribution of crack spacing for two time periods at Section D.	B5
B5.	Distribution of crack spacing for two time periods at Section E.	B6
B6.	Distribution of crack spacing for two time periods at Section F.	B7
B7.	Crack pattern, in feet, for Section A from the May 1975 condition survey	B8
B8.	Crack pattern, in feet, for Section B from the May 1975 condition survey	B9
B9.	Crack pattern, in feet, for Section C from the May 1975 condition survey	B10
B10.	Crack pattern, in feet, for Section D from the May 1975 condition survey	B11
B11.	Crack pattern, in feet, for Section E from the May 1975 condition survey	B12
B12.	Crack pattern, in feet, for Section F from the May 1975 condition survey	B13
C1.	General layout for Whitmore Gage measurments at about station 306 + 50 (outer lane).	C2
C2.	General layout for Whitmore Gage measurements at about station 306 + 50 (interior lane)	C3
C3.	General layout for Whitmore Gage measurements at about station 304 + 60 (outer lane)	C4

CONVERSION FACTORS, U.S. CUSTOMARY TO METRIC (SI) UNITS OF MEASUREMENT

U. S. customary units of measurement used in this report can be converted to metric (SI) units as follows:

Multiply	By	To Obtain
inches	0.0254	meters
feet	0.3048	meters
pounds (mass)	0.4535924	kilograms
pounds per square inch	6894.757	pascals

PART I INTRODUCTION

1. Continuously reinforced concrete pavement (CRCP) has been used successfully, both as new pavement and as rehabilitation or overlay pavement (Ref 1, 2). Engineers in recent years have begun to use this pavement type for airfields too. The use of CRCP for rehabilitating existing airfield pavements has begun, but there have been some problems in design. Continuously reinforced pavement was used for runways the first time at Chicago's O'Hare International Airport in 1967 as well as an extension of an existing runway. These pavements have experienced problems (Ref 3) that have been investigated and explained, thus providing background indicating continuously reinforced concrete pavement is applicable for new airfield pavements. Continuously reinforced concrete pavements have also been used as overlays at several airports. An extensive use was made of continuously reinforced concrete at U.S. Air Force Plant 42 at Palmdale, California (Ref 4). Other significant uses of CRCP as airfield pavement overlays have been made at Chicago's Midway Airport, U. S. Navy's Patuxent Air Base in Maryland, and at John F. Kennedy International Airport in New York (Ref 1).

2. During the years 1972-73, the first design procedures for airfield CRC pavements and overlays were developed (Ref 5, 6, 7). Along with these design procedures, a working guide specification was prepared for airfield CRCP (Ref 8). During April and May 1973, deflection and strain measuring instrumentation was installed in the CRC pavement on Runway 4R-22L at O'Hare International Airport in Chicago by the USAE/WES. This runway was first studied by ARE Inc in 1972 during an evaluation immediately after construction (Ref 9).

Objective

3. The general objective of this effort was to obtain and analyze additional data on Runway 4R-22L at O'Hare International Airport. The initial behavioral and performance observations were used to accomplish the following objectives:

a. To lend credibility to or identify needed alterations to the CRCP design procedures previously developed (Ref 6,7).
b. Establish the condition on Runway 4R-22L and present all data available for future reference.

Scope

4. This study reviews the design concepts for CRC airfield pavements and presents observations, evaluation and analysis of performance and behavior data for Runway 4R-22L. The work performed consisted of the following:

a. Analysis of initial measurements,
b. Collection and analysis of additional measurements,
c. Collection and analysis of the pavement condition, environmental data, and traffic data, and
d. Development of support for the analytical response models used in the proposed CRCP design procedures (Ref 6, 7).

PART II FIELD STUDIES

5. The purpose of the field study was to obtain information to verify and/or modify the recommended CRCP design procedures for airfields developed for USAF and the FAA (Ref 5, 6, 7). Data collected included deflection measurements (dynamic and static), material properties, traffic distribution, climatological data, and a survey of the pavement's condition. Measurements on Runway 4R-22L were obtained along the entire runway as well as at specified sections. These special sections, shown in Figure 1, were selected and based on deflection measurements (Ref 9) taken shortly after construction. These data may be used to document the behavior and performance of Runway 4R-22L under actual traffic and environmental conditions. An attempt was made to collect as much data as possible even though the runway closure time was limited.

Deflection Profile Measurements

6. The field study consisted largely of deflection profile measurements made on the CRC pavement with various dynamic loads placed between and adjacent to transverse cracks. The Dynaflect and the Waterways Experiment Station (WES) electrohydraulic heavy load deflection device were used to measure the deflection profiles along Runway 4R-22L. These deflection profiles were used in the analysis to characterize the runway. Table 1 lists information pertinent to the above loading devices.

USAE/WES Vibrator

7. Deflection profiles obtained with the WES Vibrator in September 1972 and May 1975 are contained in Tables A4-A7, Appendix A. The 1972 data were collected on a line about 12 feet east of the runway centerline from station 270+00 to station 334+00 measuring between and adjacent to cracks. As tabulated in Appendix B for 1972, the average deflection value for the 10 kip load adjacent to the cracks, .00193 inches, is slightly

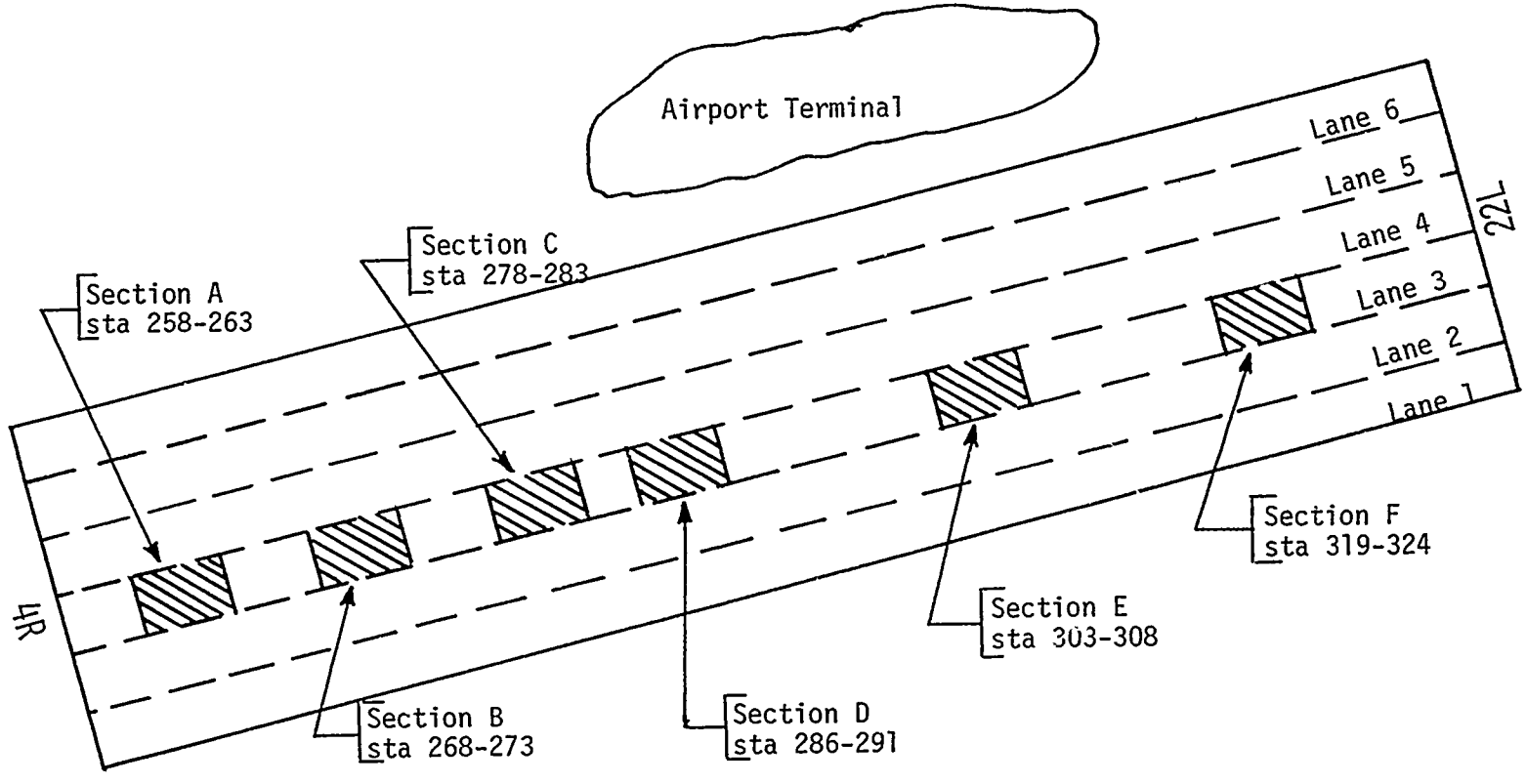

Figure 1. Location of the special test sections along Runway 4R-22L at O'Hare International Airport in Chicago, Illinois.

Table 1

Summary of Load Data on Test Equipment

Type of Loading Device	Load per Footprint (lbs.)	Contact or Tire Pressure (psi)	Equivalent Load Radius (in.)	Dates of Measurements
Dynaflect	500	167.0	0.98	October 1971 September 1972
USAL-WES Vibrator	10,000	39.3	9.00	September 1972 May 1975
Plate (Simulated Boeing 727)	38,000	148.0	9.04	May 1975
Boeing 727 Aircraft	27,100 31,050	175.0	7.02 7.52	June 1973
Aircraft Tug (B747)	31,250	115.0	9.30	June 1973

greater than the deflection value between the cracks, .00172 inches. The deflection profile for the 1972 data is shown in Figure 2 which represents the average deflection. Similarly, a deflection profile was made in May 1975 for different locations along the runway. Measurements were taken at random without any regard to crack location from station 254+00 through station 334+00 in lanes 3 and 4 19 feet from centerline. These data are also shown in Figures 2 and 3.

8. At various locations along the runway (1975 data), frequency sweeps were run with the WES Vibrator, (Figure 4), to determine the deflection variation with frequency. An operating frequency of 15 cps was selected since it gave the maximum stable deflection while increasing the frequency through operational levels. The WES vibrator applied loads of up to 15 kips, however only the deflection data for 10 and 15 kip loads are reported (Appendix A). In the analysis, only the deflection produced by the 10 kip load is used since the 1972 data is for the same 10 kip load. The average deflection of the entire runway and of each specific section has increased slightly with time as shown in Table 2. Figure 2 illustrates the slight increase in deflection between 1972 and 1975 as observed using the WES Vibrator deflection data. Figure 3 compares the deflection profiles of lanes 3 and 4 for the 1975 measurements.

Dynaflect

9. Deflection measurements were made with the Dynaflect in October 1971 and September 1972 for its fixed loading of 1000 lbs. Deflections were obtained in lane 3 twelve feet from the runway centerline, (Figure 5) and in lane 1, near the runway edge, (Figure 6). Measurements were taken with the load placed between and adjacent to cracks along the entire runway. These data are contained in Appendix A. The average deflection value adjacent to the cracks .000217 inches, is slightly greater than the average deflection value between cracks, .000208 inches, as was observed for the WES Vibrator. The average deflection and variation in readings for the Dynaflect has increased with time as shown in Table 3.

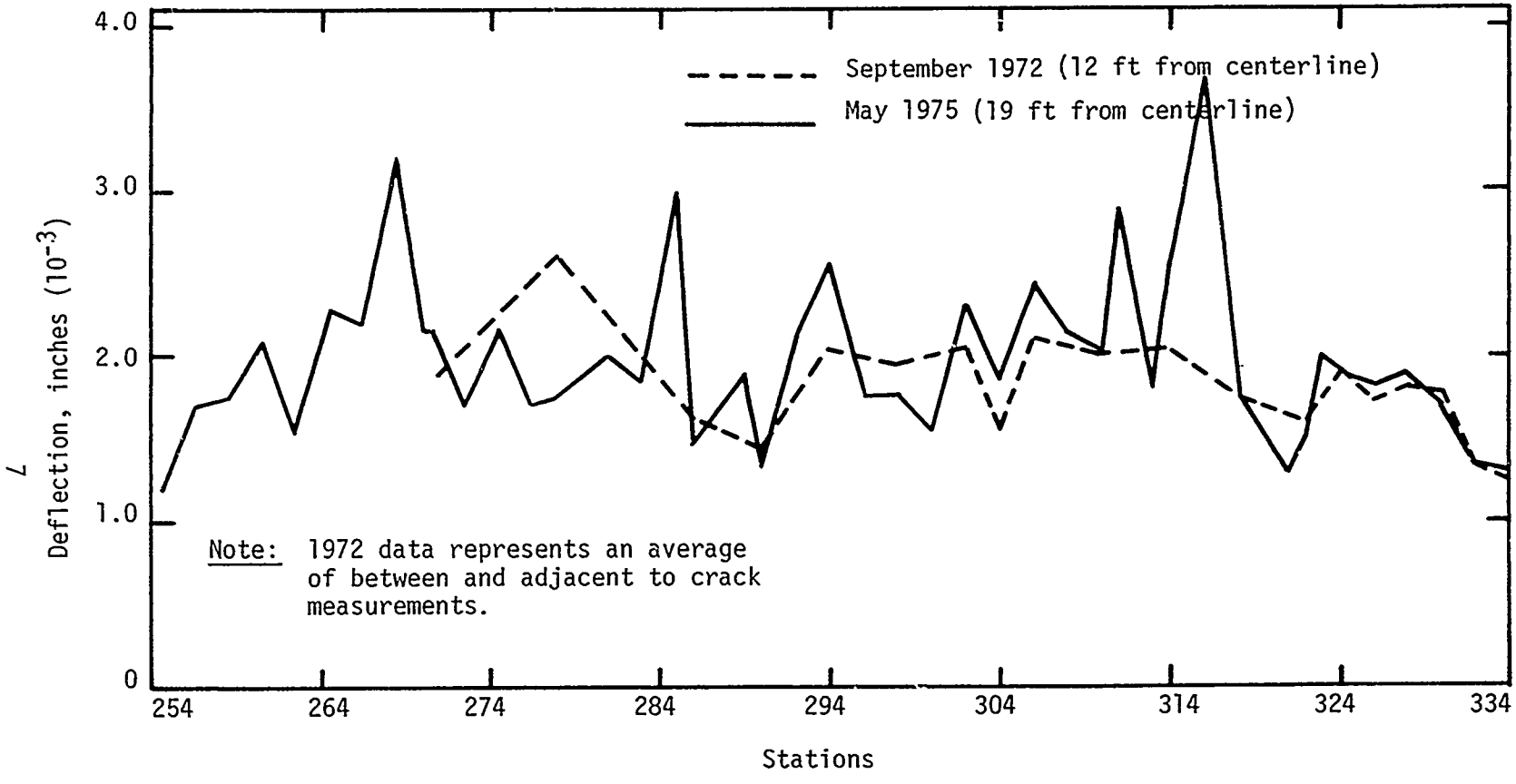

Figure 2. WES Vibrator deflection measurements for different time periods in lane 3 for a 10 kip load at a frequency of 15 cps.

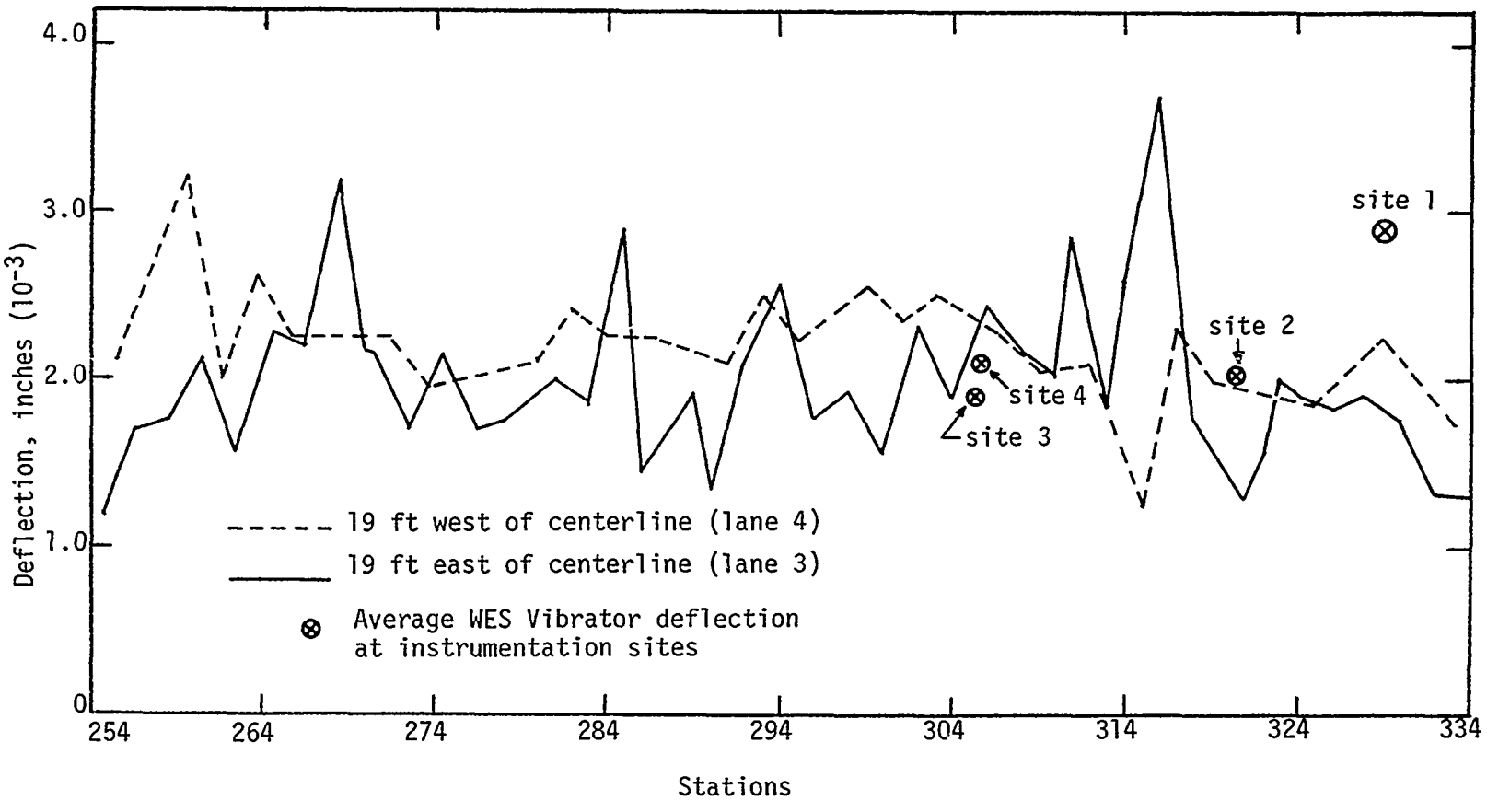

Figure 3. WES Vibrator deflection data taken in 1975 with a 10 kip load at a frequency of 15 cps.

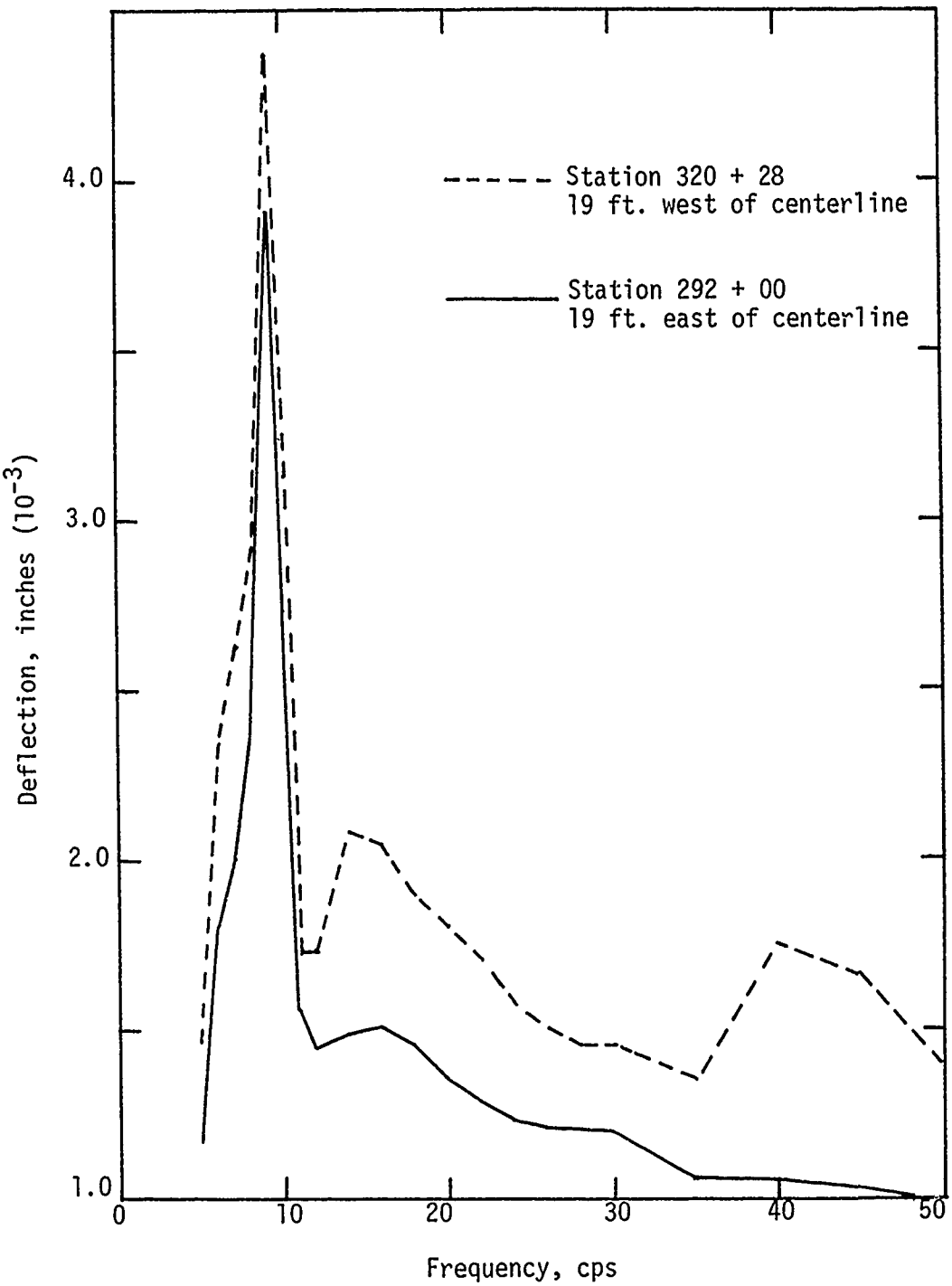

Figure 4. Typical frequency sweep data taken on Runway 4R-22L with the WES Vibrator for a load of 7,000 lb.

Table 2

Change in WES Vibrator Deflection Values with Time at Each Section Along Runway 4R-22L for 10 kip load

Section Number (Fig 1 & 3)	1972 Measurements Average Deflection, inches (10^{-3})	1972 Measurements Coefficient of Variation (%)	1975 Measurements Average Deflection inches (10^{-3})	1975 Measurements Coefficient of Variation (%)
A	-	-	1.80	15.5
B	-	-	2.30	27.7
C	2.62*	-	1.87	6.7
D	1.50	11.9	1.50	18.7
E	1.83	18.9	2.11	16.7
F	1.77	14.1	1.71	19.4
Site 1	1.65	21.6	2.89**	14.1
Site 2	1.68	8.1	2.04	19.9
Site 3	1.83	18.9	1.98	9.6
Site 4	-	-	2.10	15.3
Entire Runway (Lane 3)	1.82	18.0	1.97	25.1
Entire Runway (Lane 4)	-	-	2.26	15.0

*Only one deflection value

**Represents average deflection value at Site 1, but believed to be in error when compared to other deflection values (Fig. 3).

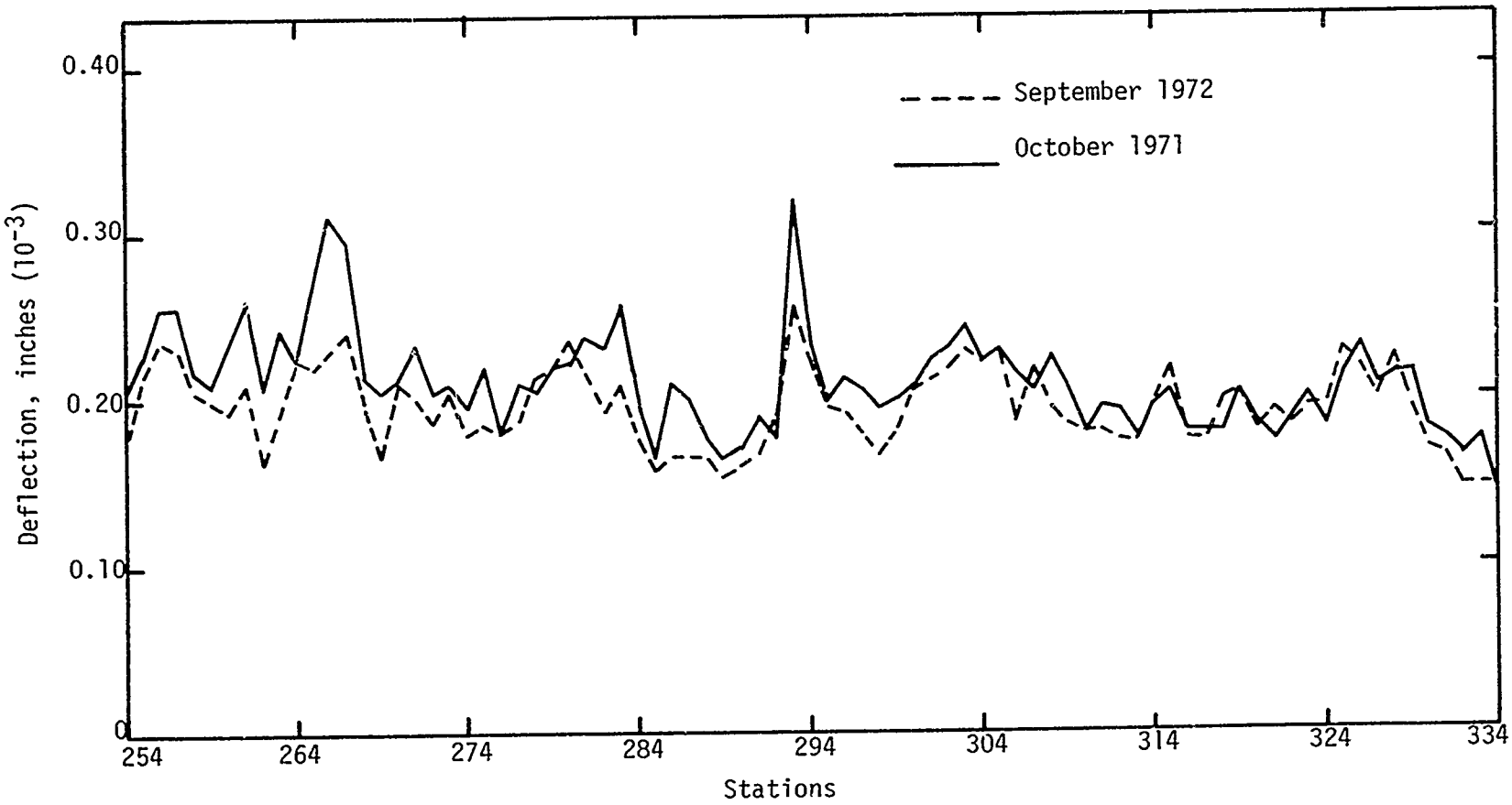

Figure 5. Dynaflect deflection profile along center of Lane 3, Runway 4R-22L for October 1971 and September 1972. (12' from Runway centerline)

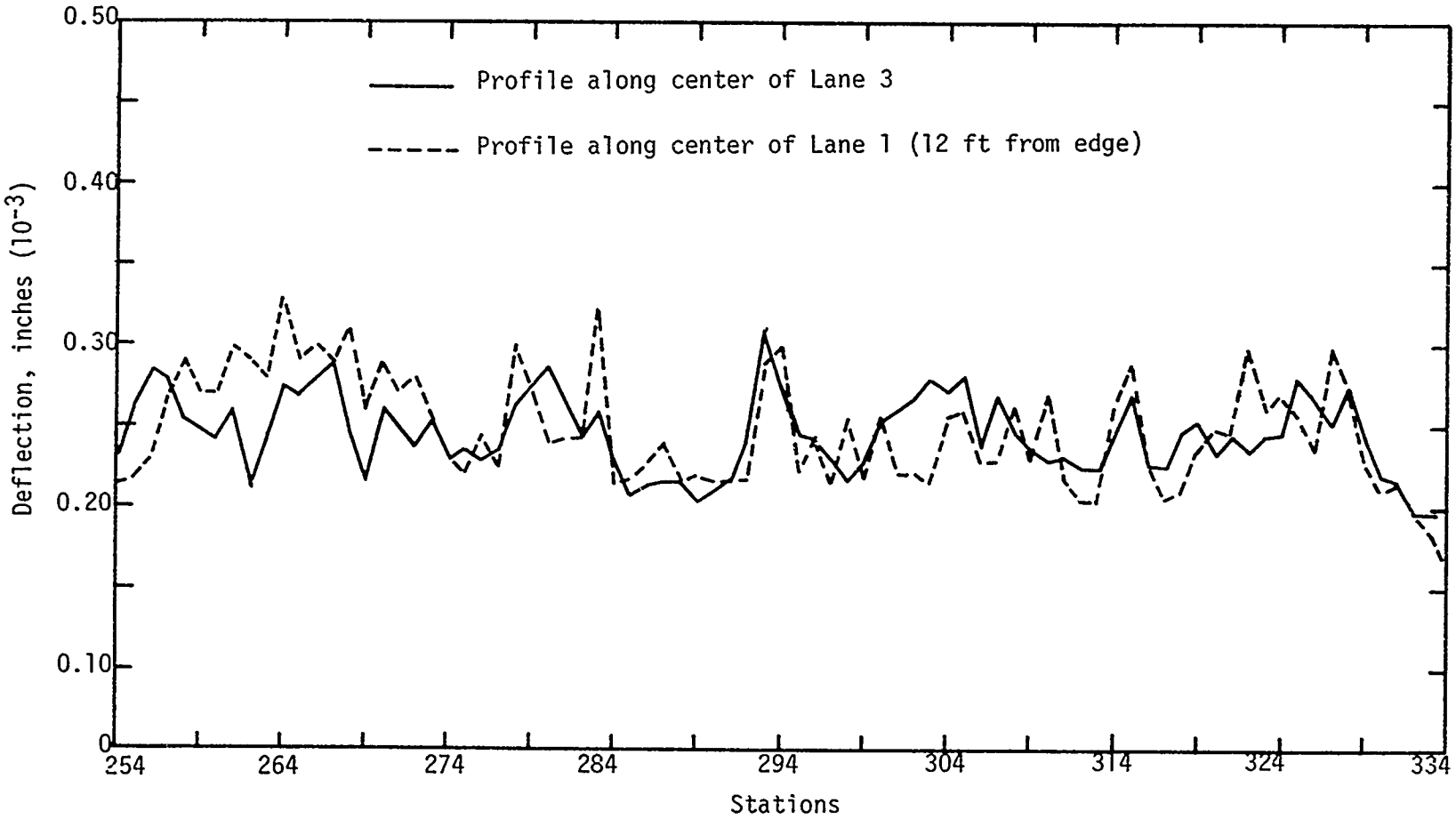

Figure 6. Dynaflect deflection profile along runway 4R-22L for October 1971.

Table 3

Change in Dynaflect Deflection Values with Time at Each Section Along Runway 4R-22L

Section Number	1971 Measurements Average Deflection inches, (10^{-3})	1971 Measurements Coefficient of Variation (%)	1972 Measurements Average Deflection inches, (10^{-3})	1972 Measurements Coefficient of Variation (%)
A	.198	10.9	.229	9.4
B	.195	11.0	.212	5.6
C	.217	9.5	.238	8.5
D	.163	4.7	.186	9.9
E	.216	11.2	.224	6.7
F	.192	5.2	.190	6.7
Site 1	.191	15.6	.199	12.7
Site 3	.216	11.2	.224	6.7
Site 4	.192	10.4	-	-
Entire Runway (Lane 3)	.196	13.9	.213	15.6
Entire Runway (Lane 1)	.198	17.4	-	-

LVDT Deflection Measurements

10. The field study also consisted of deflection measurements made with static loads placed between and adjacent to transverse cracks. These loads included a Boeing 727 aircraft, an aircraft tug (B747) and a specially built plate for B727 load simulation. Table 1 lists information pertinent to the above loads.

11. For the three test loads (plate, 727, tug), deflections were measured using the linear variable differential transformers (LVDT) and a digital volt-meter. A schematic diagram of an in-place LVDT is shown in Figure 7. Measurements were taken at each of the locations where the LVDT's were installed in the pavement as shown in Figure 8. Measurements were not taken at Site 2 because the LVDT was inoperative. Deflections were measured with gages that were located adjacent to cracks and gages that were located between cracks (See Figures A1-A4 for gage locations). The loads were placed at both logitudinal and transverse offsets from the gages as illustrated in Figures A5 and A6.

Simulated B727

12. Collection of the simulated Boeing 727 or plate load deflection was accomplished in May 1975 by the use of a prefabricated plate designed and furnished by the City of Chicago, a crane, and a jeep. The prefabricated plate illustrated in Figure 9 was used to support the load on two 16" x 16" pads, simulating a B727 footprint, spaced 50" center to center. The crane, Figure 10, was used to apply a 76 kip load and the jeep, figure 11, was used to position the plate at various offsets. Shown in Figures A5 and A6 Appendix A, for deflection measurements. The procedure used for collecting the deflection data was:

a. Position plate directly over the LVDT
b. The initial reading, without any load, was taken one minute after the plate was in position (Figure 11)
c. The crane was positioned on the plate for load application. The beams used for support had to be free of pavement contact (Figure 10).
d. The reading due to the 76 kip load was taken one minute after the crane had been positioned on the plate.

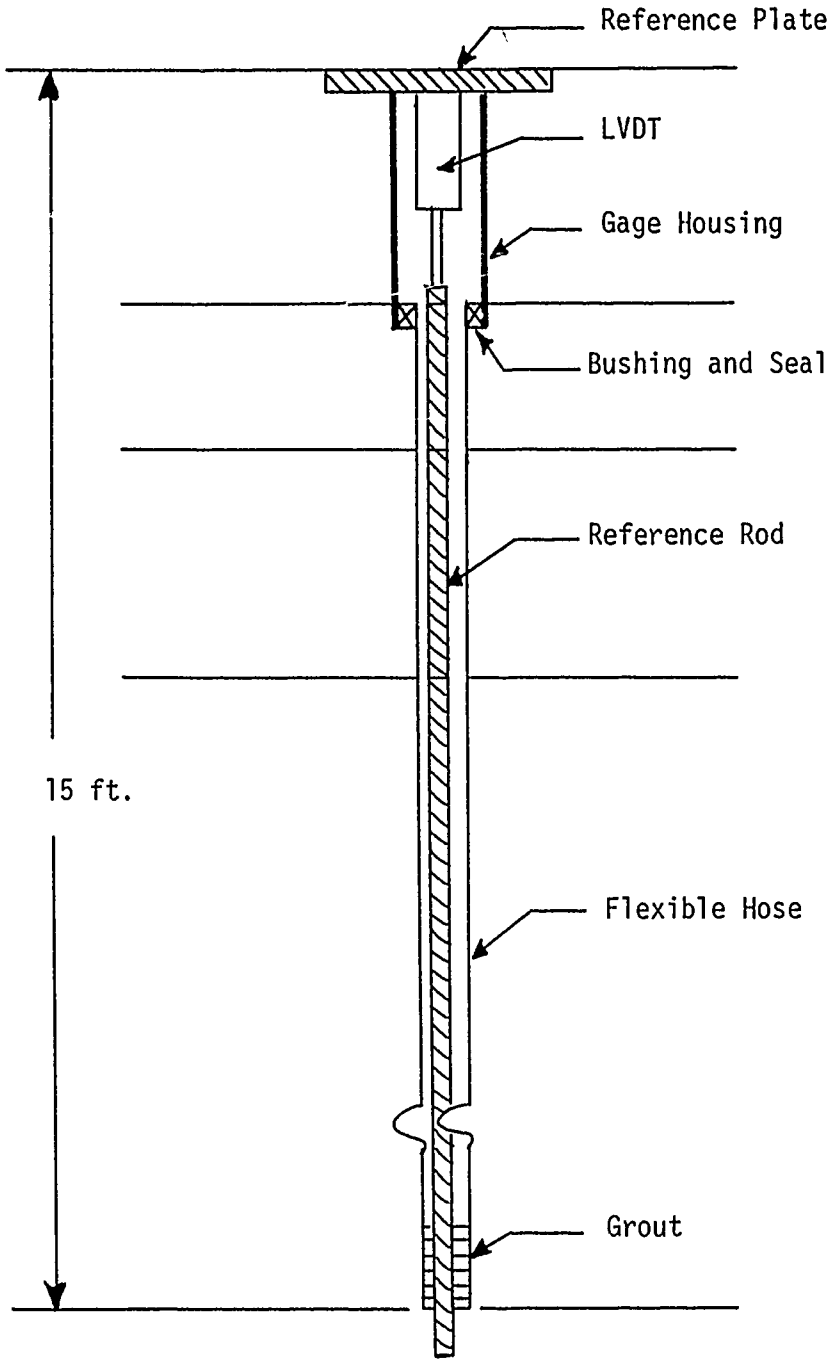

Figure 7. In-place LVDT installed on Runway 4R-22L at O'Hare International Airport.

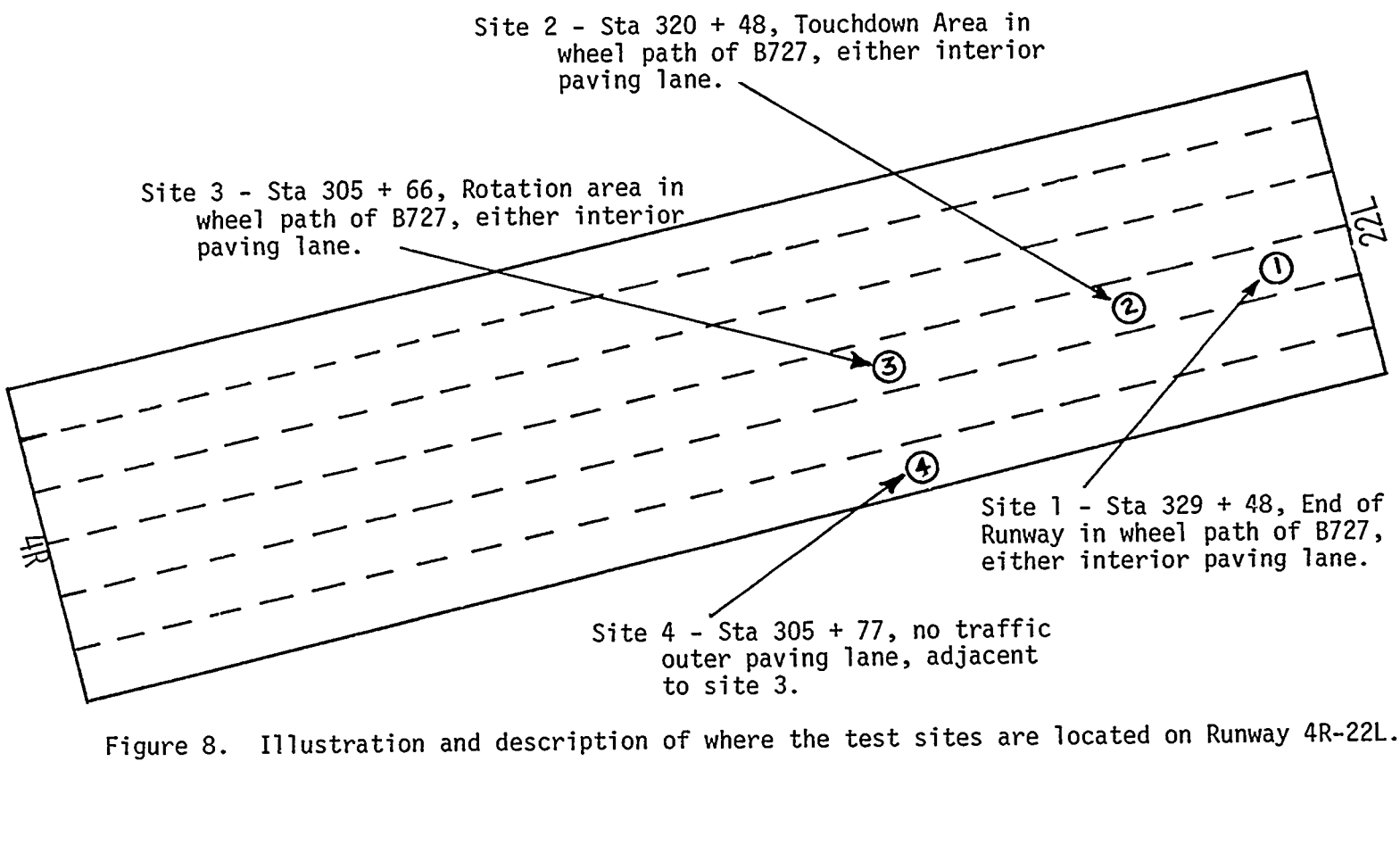

Figure 8. Illustration and description of where the test sites are located on Runway 4R-22L.

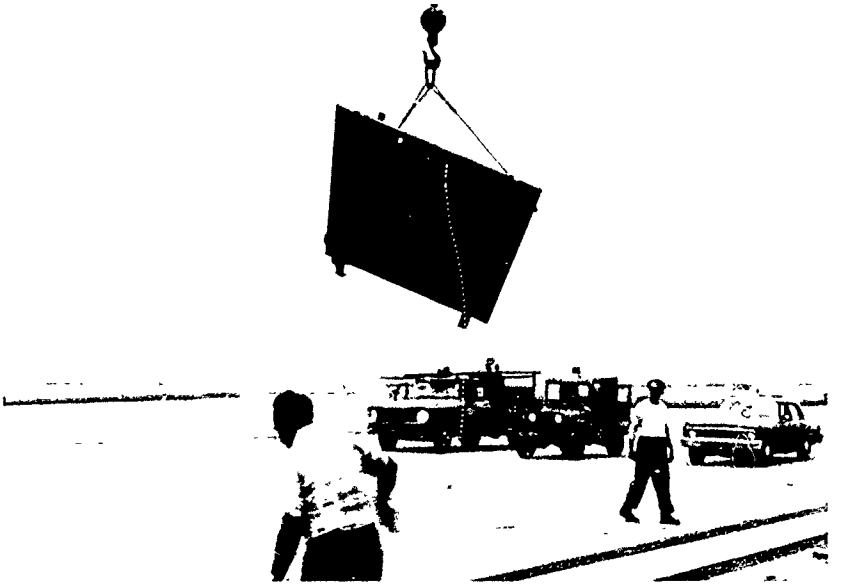

Figure 9. Underside view of the prefabricated plate used to simulate the Boeing 727 aircraft gear.

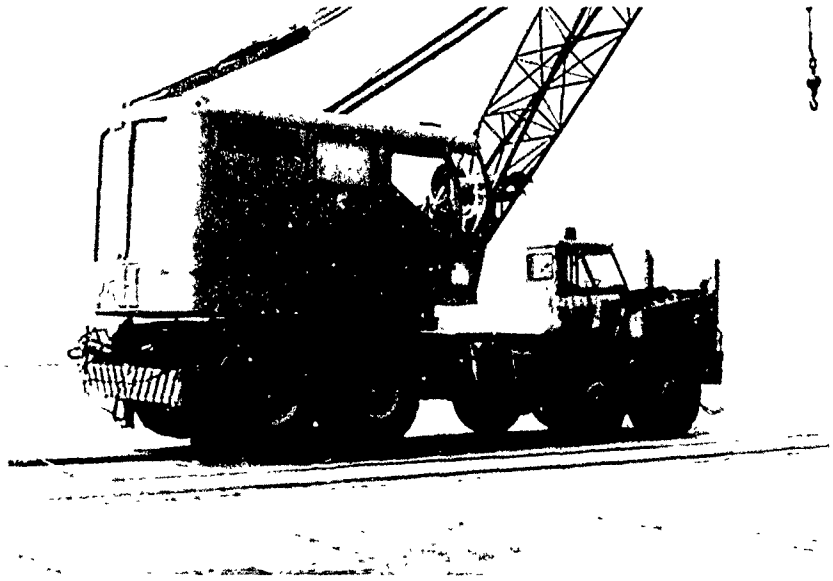

Figure 10. Illustration showing the crane which was used to apply the 76 kip load.

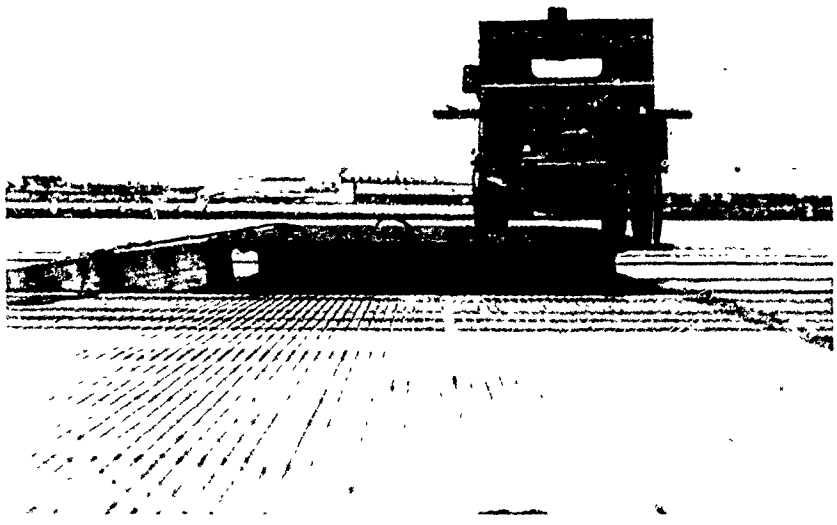

Figure 11. Side view of the plate and jeep which was used to position the plate at the selected offset.

a. The crane was then moved a distance of approximately 35-50 feet from the plate.

b. The plate was then moved to the next selected offset distance from the in-place LVDT.

c. Steps 2-6 were then repeated to obtain deflections at all offsets.

The observed deflections for the plate load are plotted in Figures 12-14. Deflections for transverse and longitudinal movement of load are given for each site for the two gage positions, between and adjacent to cracks, with the exception of Site 3. The deflection measurements for the plate loadings are contained in Tables A8-A10 in Appendix A. Figure 12 shows that the deflection for the gage located adjacent to a crack at Site 1 are much less than the deflection values for the gage located between cracks, a contrast to the Dynaflect and WES Vibrator results. At the time when the measurements were made at Site 1, there was a temperature drop due to rain as noted on the data sheet in Appendix A. It is believed that the moisture and/or sudden change in temperature could have caused the readings to be in error for the LVDT adjacent to the crack.

13. After reviewing the deflection basins at each site, it was concluded that the deflection between cracks is approximately equal in shape and magnitude to the deflection adjacent to cracks, with the exclusion of the LVDT adjacent to crack measurements at Site 1. Sites 1 and 3, interior lanes, have approximately the same deflection magnitude (Figure 12 and 13). It is hypothesized that Site 4 has greater deflections (Figure 14) due to its being an edge lane and the load no longer represents an interior load position. The shapes of each site are compared in Figure 15 where the deflection is normalized for each site. Sites 1 and 3 had comparable basin shapes. Site 4 (edge lane) had a larger deflection basin with respect to Sites 1 and 3 (Figure 15).

Boeing 727 Aircraft

14. When the LVDT's were installed in 1973, deflection measurements were made using a Boeing 727. Basically, the same procedure was used to collect the data as for the plate load. The deflection values for

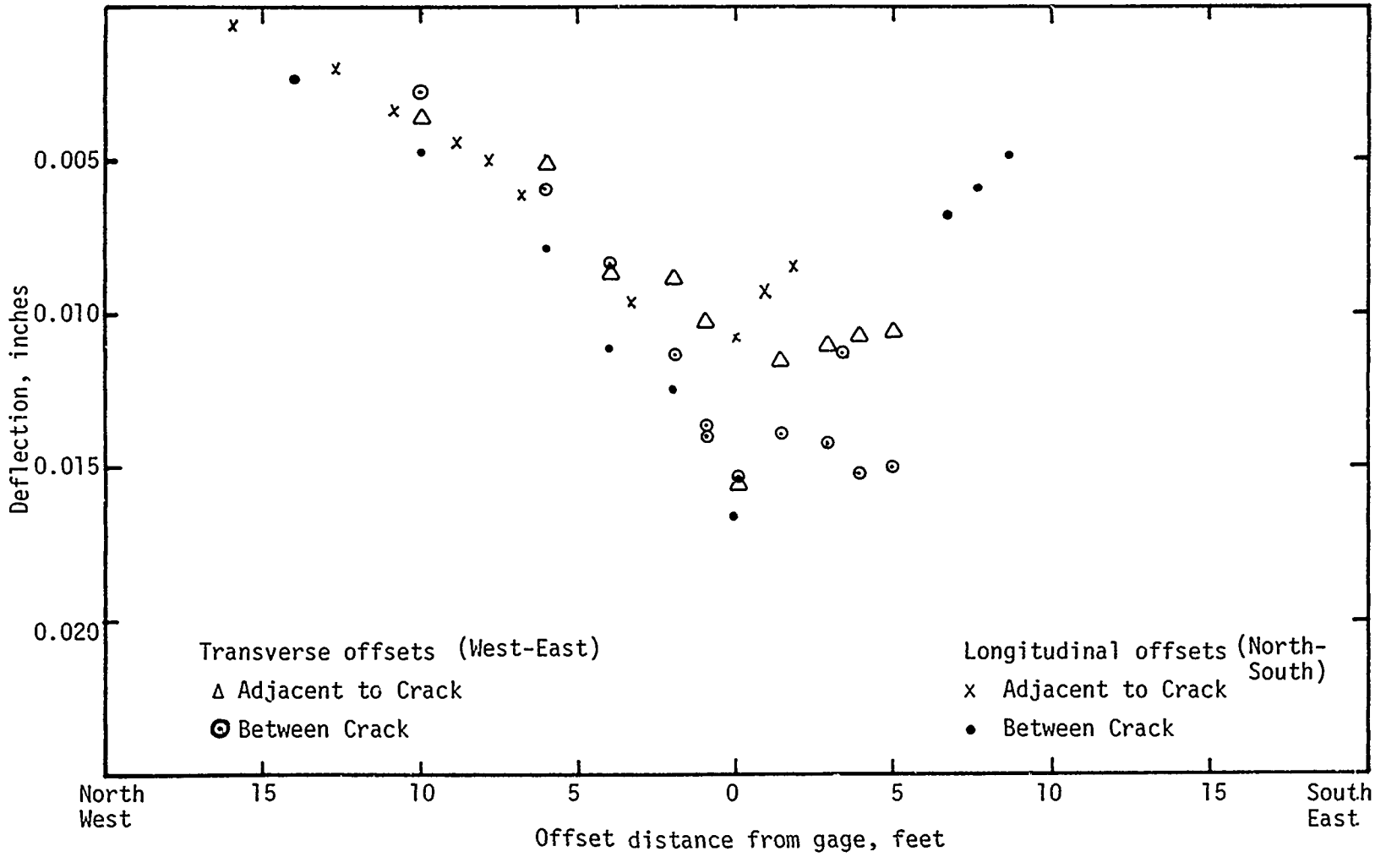

Figure 12. Plate load deflection data for Site 1 (sta 329 + 48) on Runway 4R-22L.

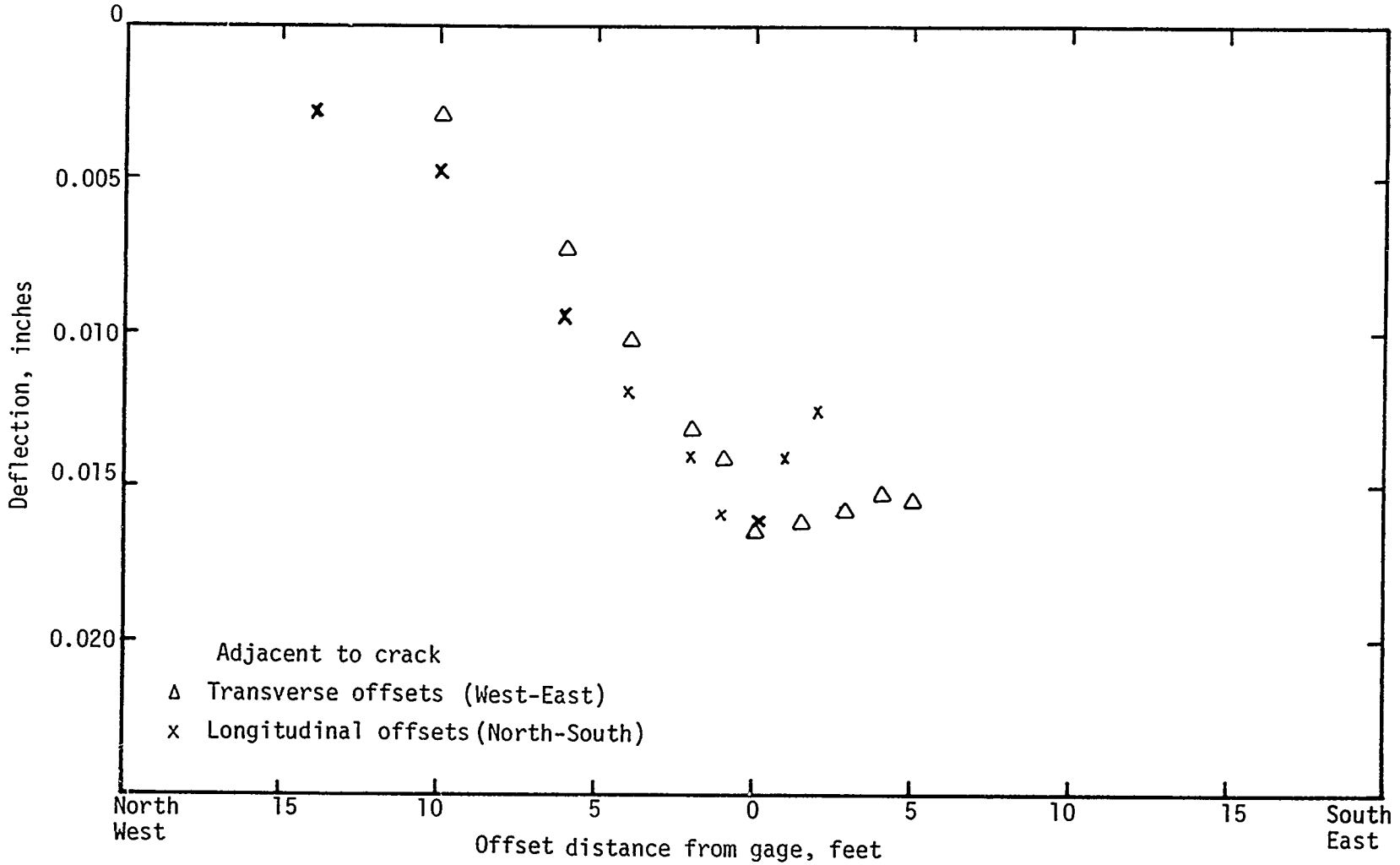

Figure 13. Plate load deflection data for Site 3 (sta 305 + 66) on Runway 4R-22L.

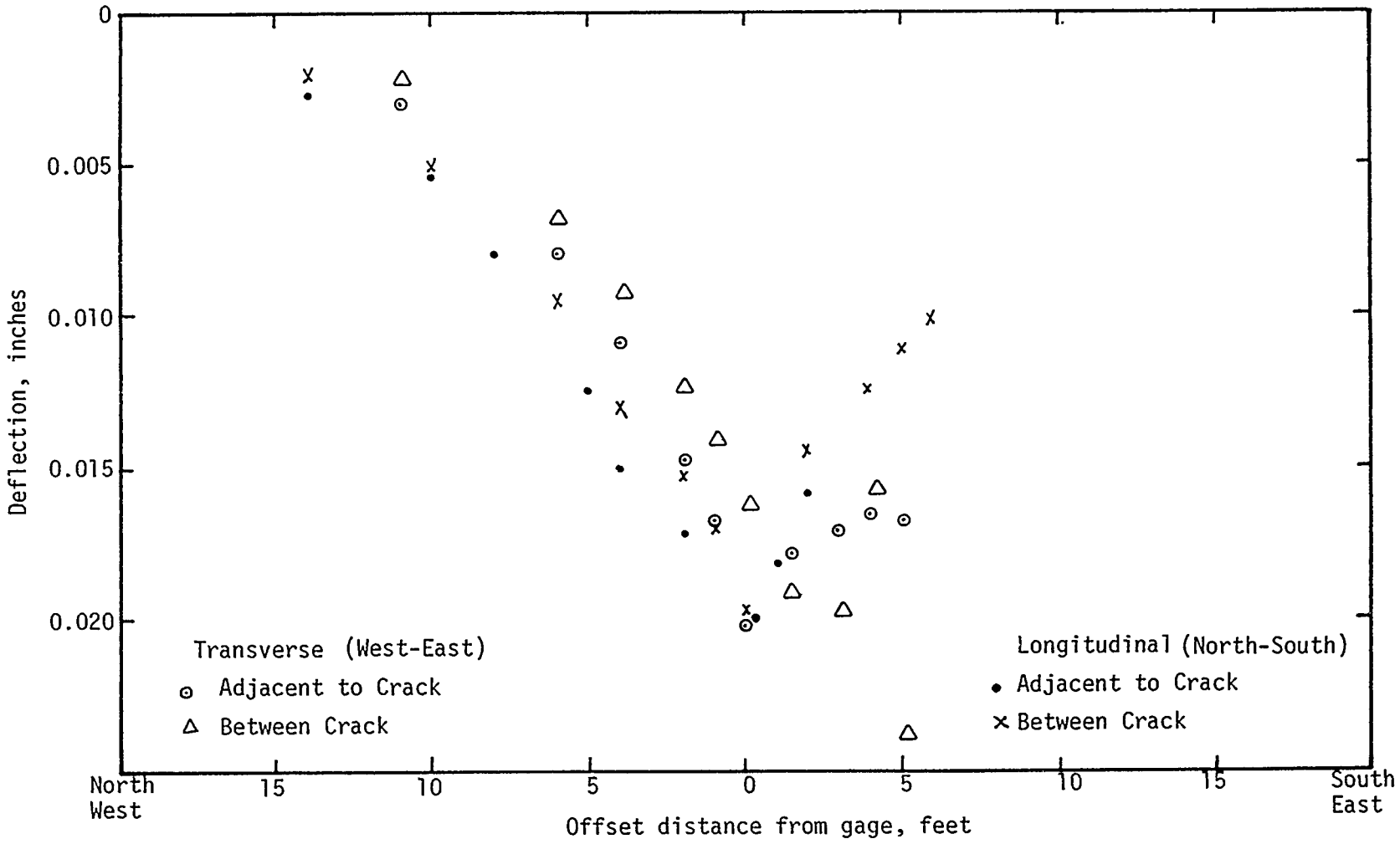

Figure 14. Plate load deflection data for Site 4 (sta 305 + 77) on Runway 4R-22L.

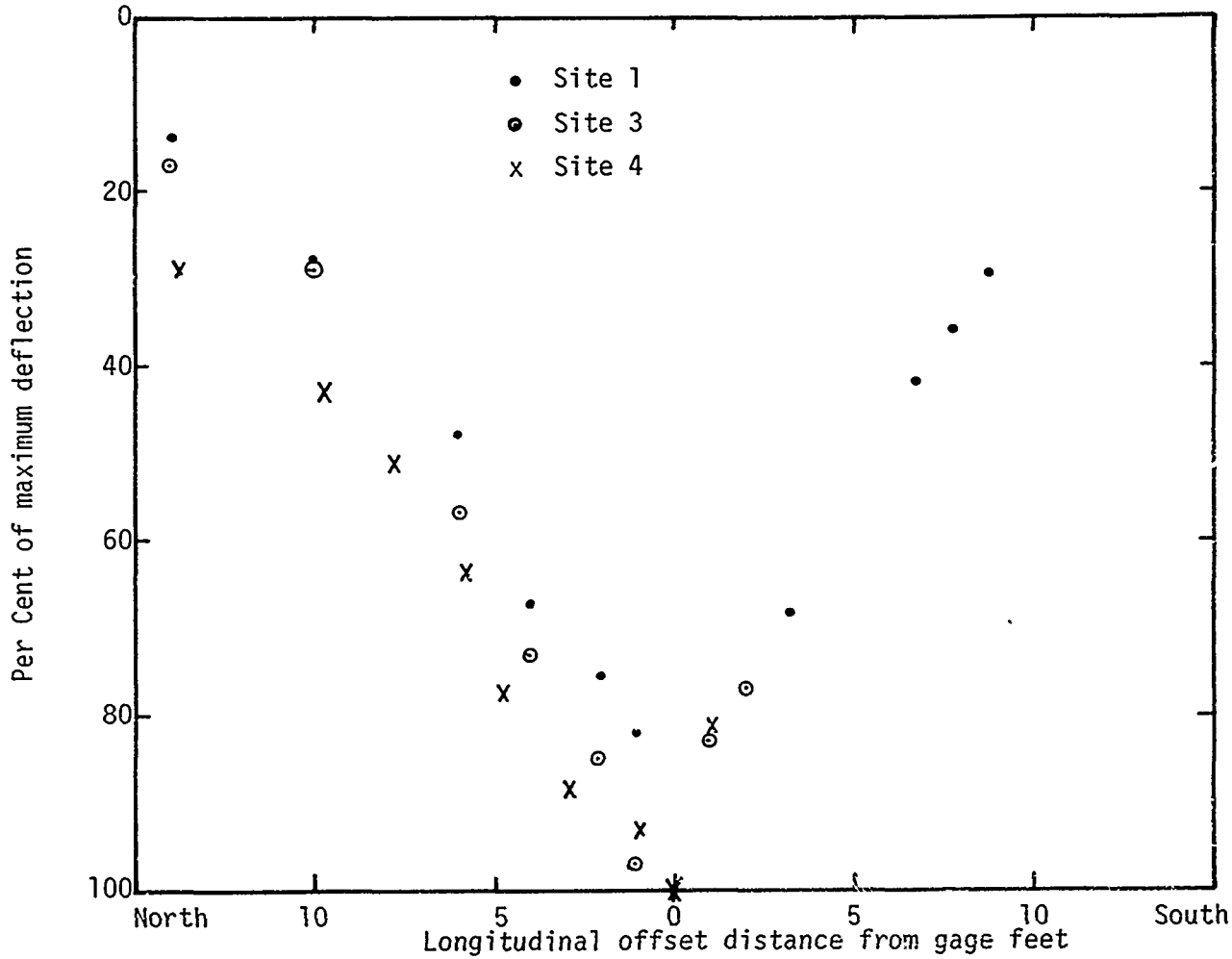

Figure 15. Normalized deflections for the plate load for adjacent to crack measurements.

deflection values for the Boeing 727 are shown in Figures 16-18 for sites 1, 3, and 4. Measurements were made with the load located at longitudinal offsets only and these measurements are tabulated in Tables A11-A13 Appendix A. As illustrated in Figures 16-18 the deflection values for the gages adjacent to and between cracks were similar in magnitude and shape for each site. Sites 1 and 3 had deflection magnitudes (Figure 16 and 17) that were comparable but Site 4 had greater maximum deflections (Figure 18) as was observed for the plate load. The basin shapes are compared in Figure 19 where the deflection is normalized for each site, i.e. the deflection is expressed as a percentage of the maximum values. Sites 1 and 4 had similar basin shapes which was not the case for the plate load basins. Site 3 had a different basin shape near the LVDT (Figure 19), but approached the shape at Sites 1 and 4 at offsets further from the LVDT.

Tug B747

15. Deflections were measured with the pavement loaded with a tug (B747) at the same time of the 727 aircraft using the same procedure. The basins shown in Figures 20-22 represent deflections measured with the gages located between and adjacent to cracks with the load positioned at transverse and longitudinal offsets. The data are also tabulated in Tables A14-A16 Appendix A. The deflection magnitudes are approximately the same for loading between and adjacent to cracks at each site. Sites 1 and 3, interior lanes, have deflection values that are approximately equal in magnitude. Site 4 deflections are greater since it is an edge lane. It may be noted from Figure 23, where the deflection is normalized, that the deflection basins are similar for each site.

Deflection Summary

16. After reviewing all deflection basins at each site for each test load, it was concluded that the deflection basins between cracks are approximately equal in shape and magnitude to deflection adjacent to cracks. By comparing Figure 15, 19 and 23, where the deflection was normalized for each test load at each site, several observations were apparent.

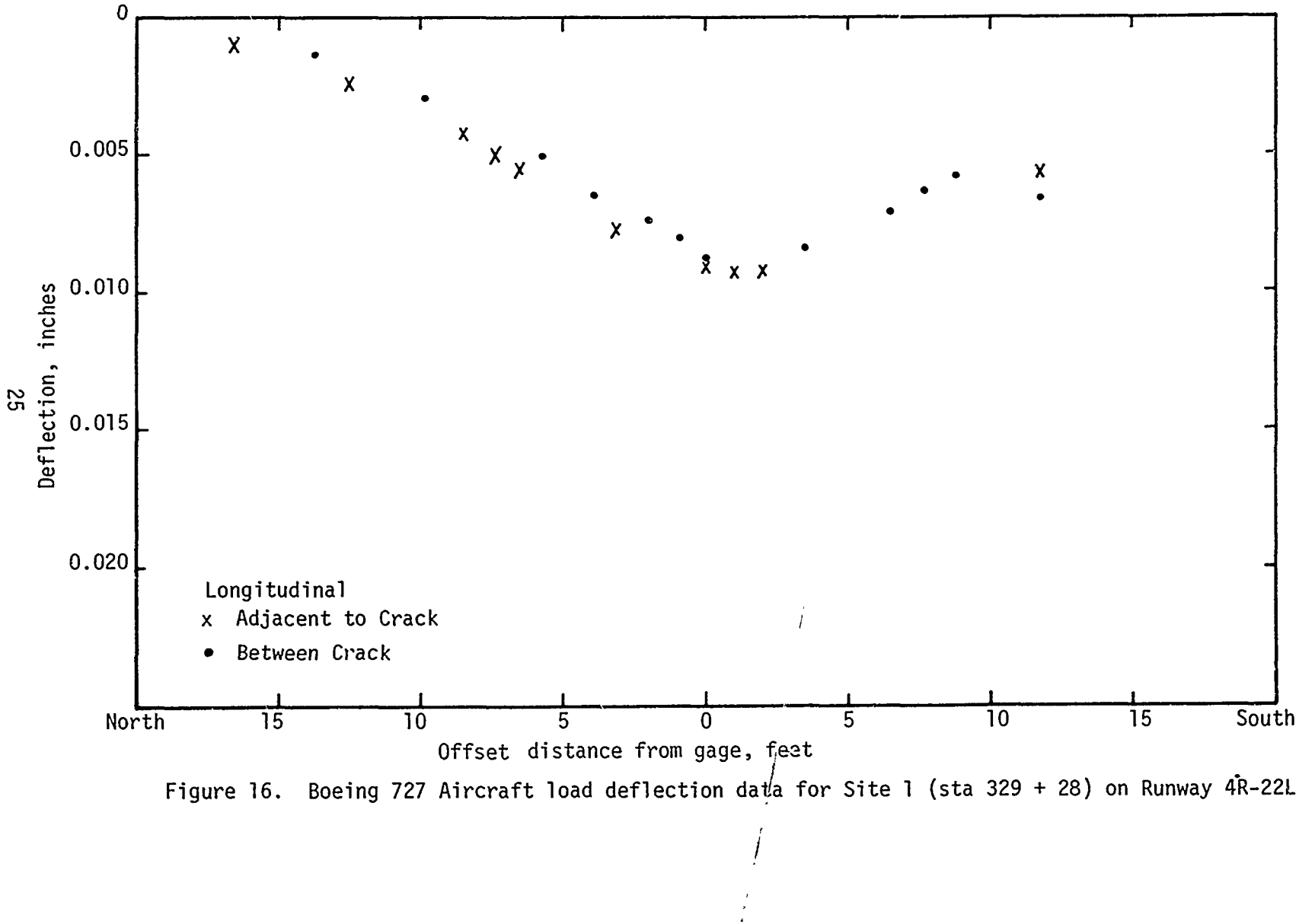

Figure 16. Boeing 727 Aircraft load deflection data for Site 1 (sta 329 + 28) on Runway 4R-22L.

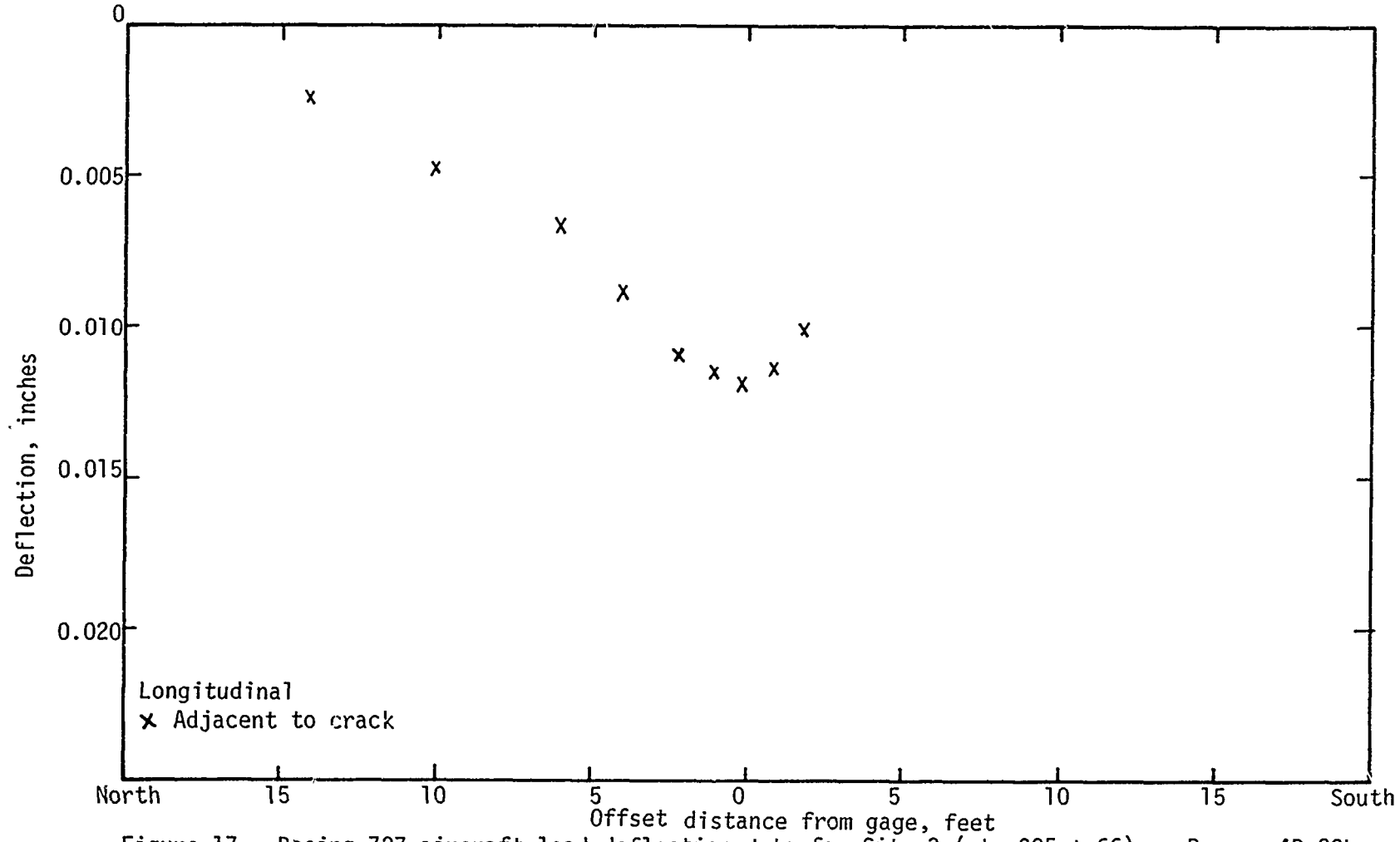

Figure 17. Boeing 727 aircraft load deflection data for Site 3 (sta 305 + 66) on Runway 4R-22L.

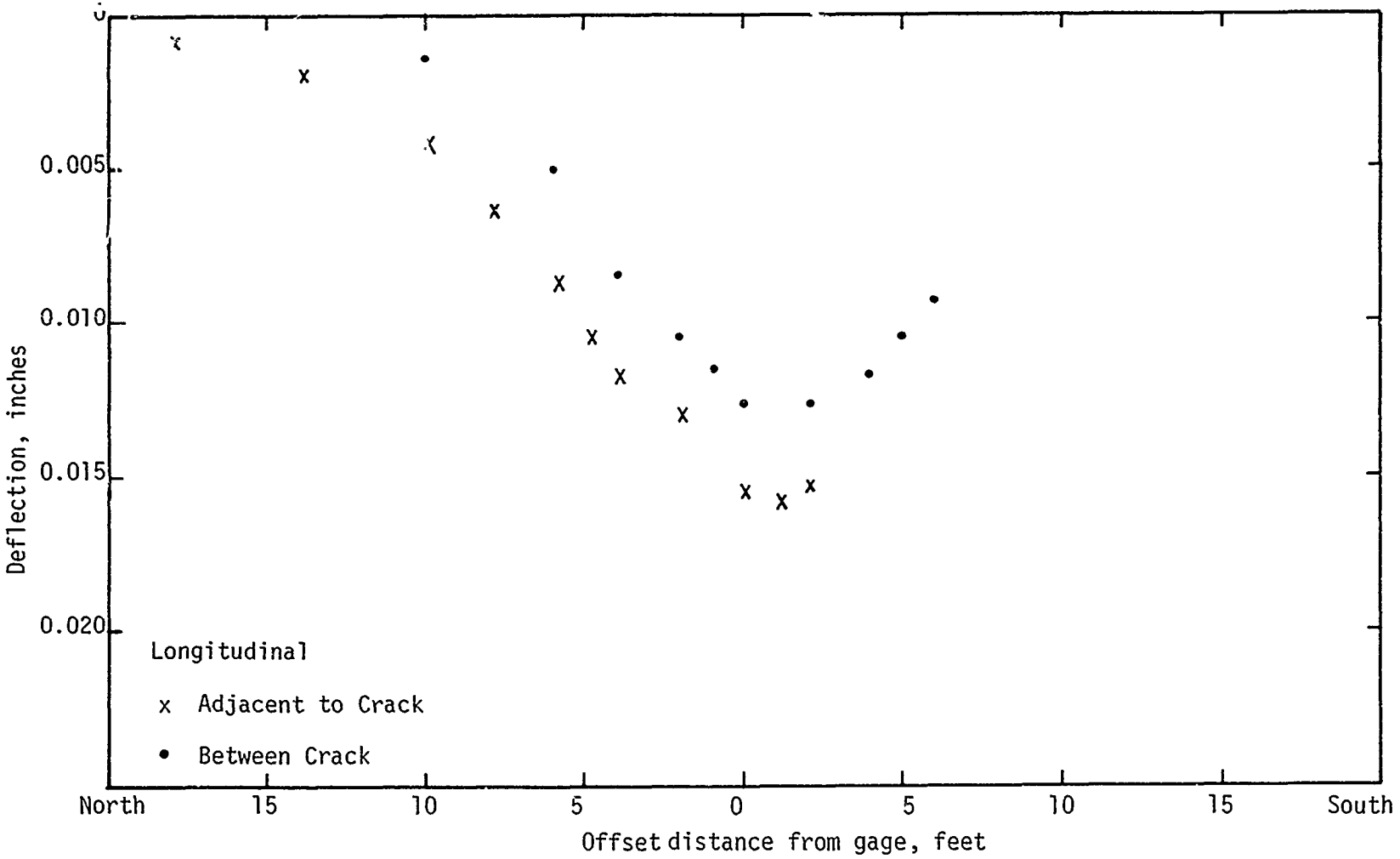

Figure 18. Boeing 727 aircraft load deflection data for Site 4 (sta 305 + 77) on Runway 4R-22L.

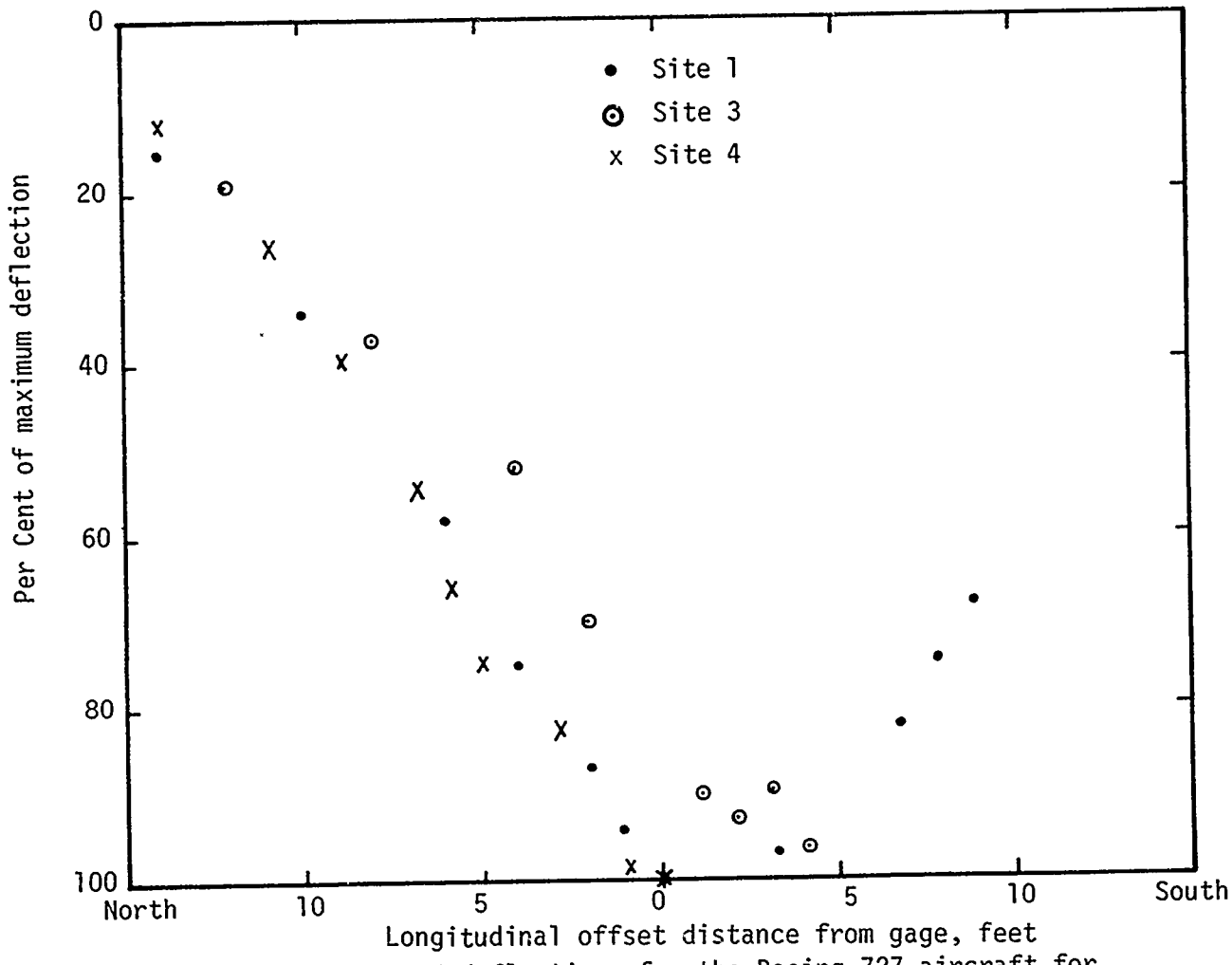

Figure 19. Normalized deflections for the Boeing 727 aircraft for adjacent to crack measurements.

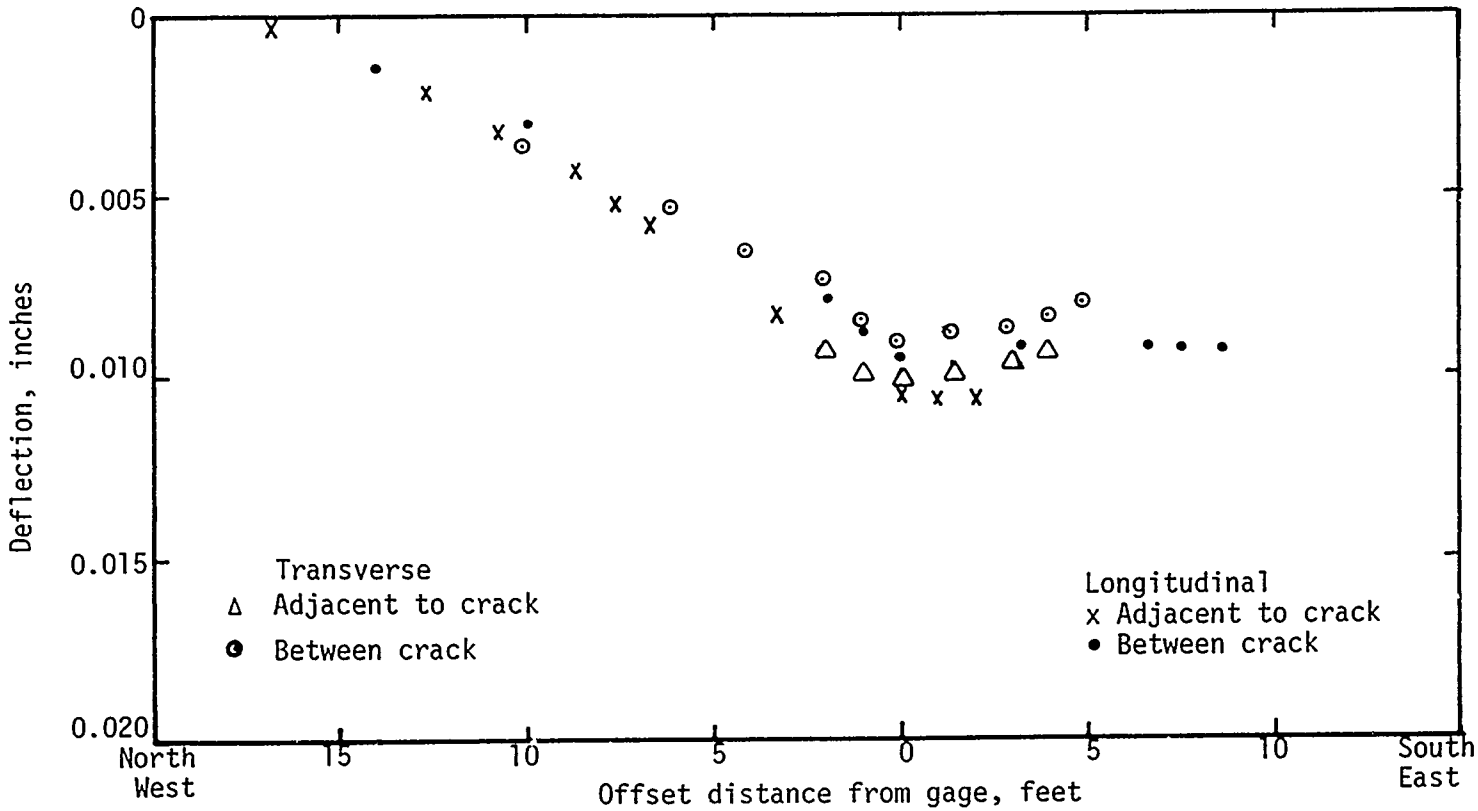

Figure 20. Aircraft tug (B747) load deflection data for Site 1 (sta 329 + 48) on Runway 4R-22L.

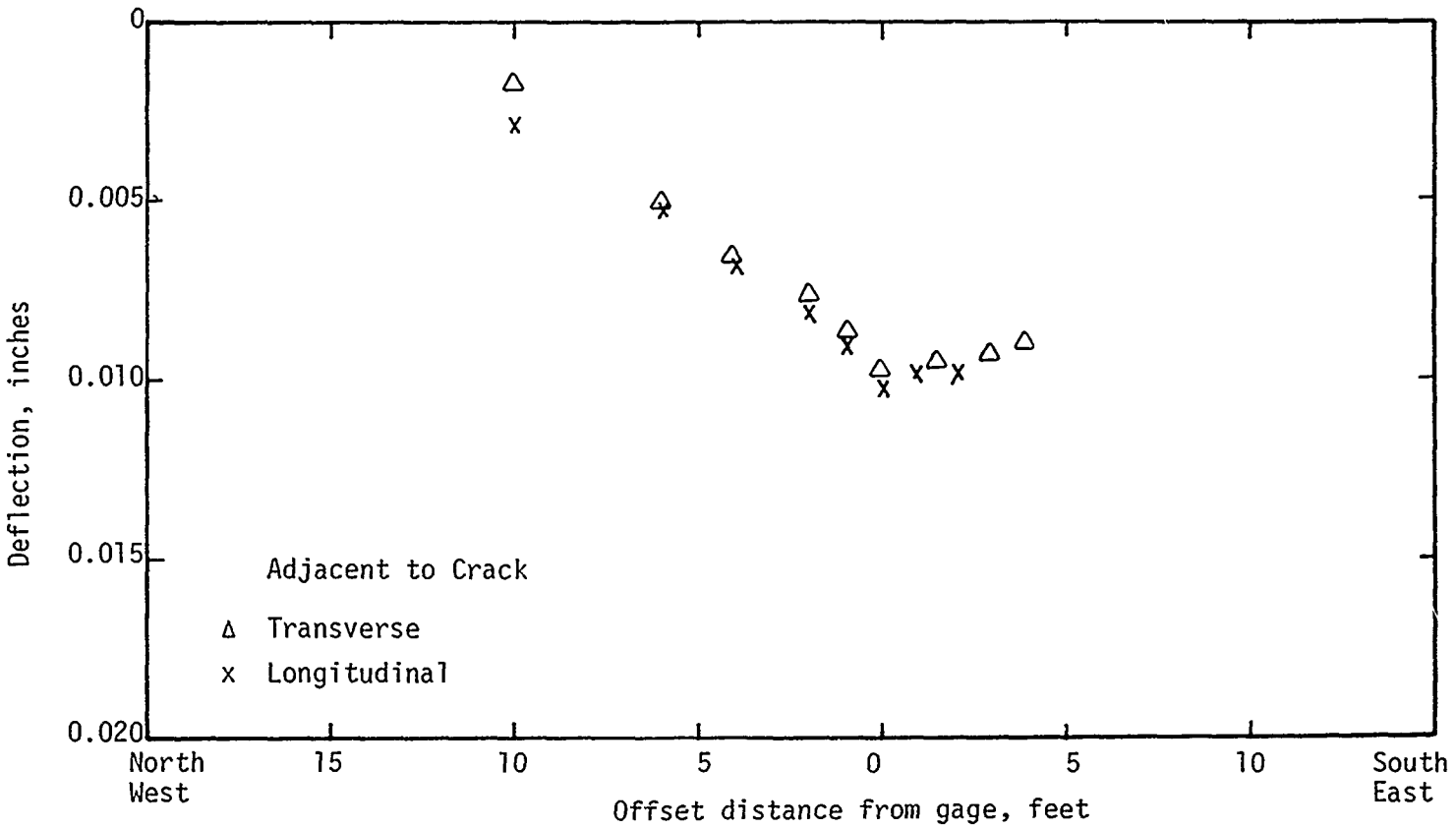

Figure 21. Aircraft tug (B747) load deflection data for Site 3 on Runway 4R-22L.

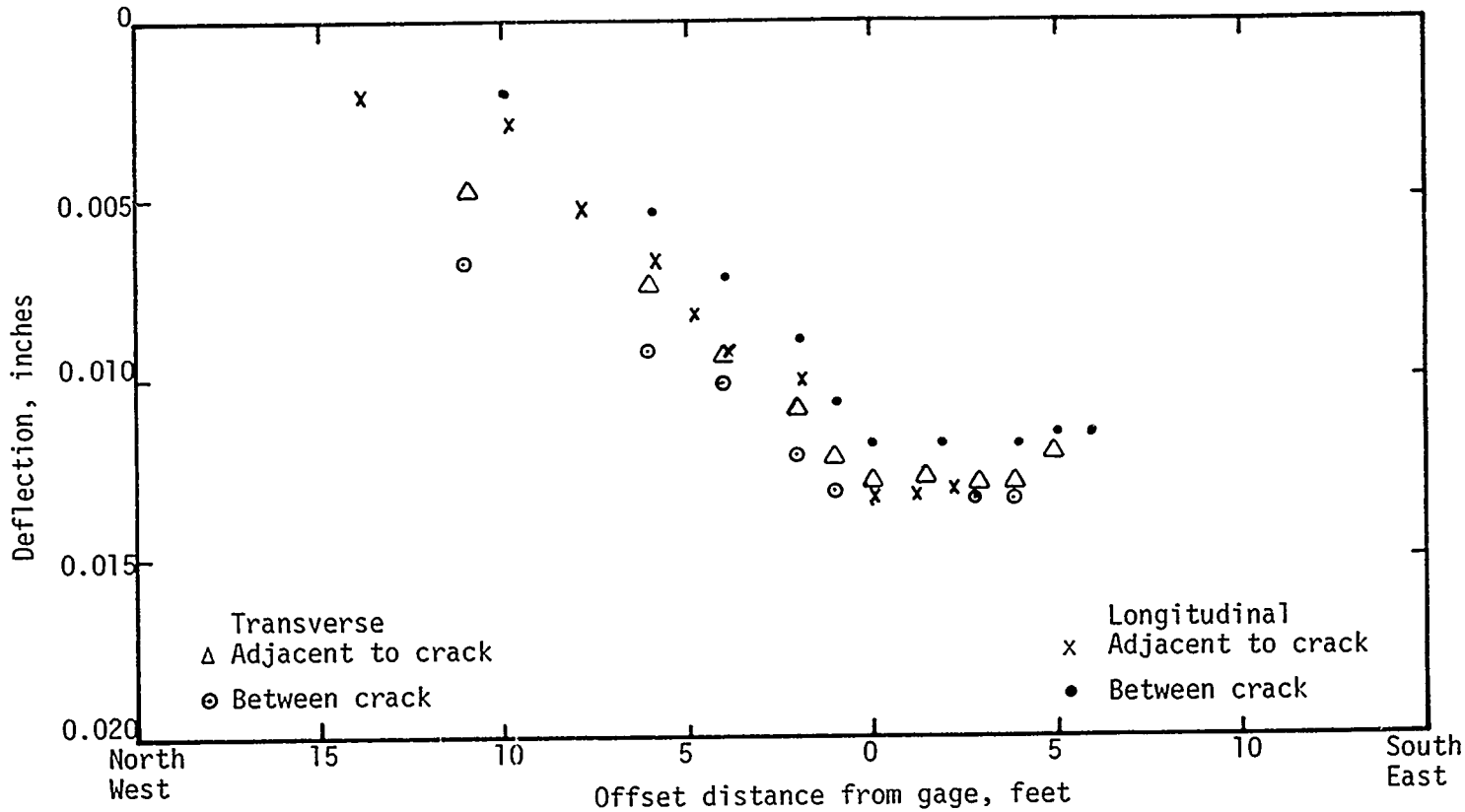

Figure 22. Aircraft tug (B747) load deflection data for Site 4 (sta 305 + 77) on Runway 4R-22L.

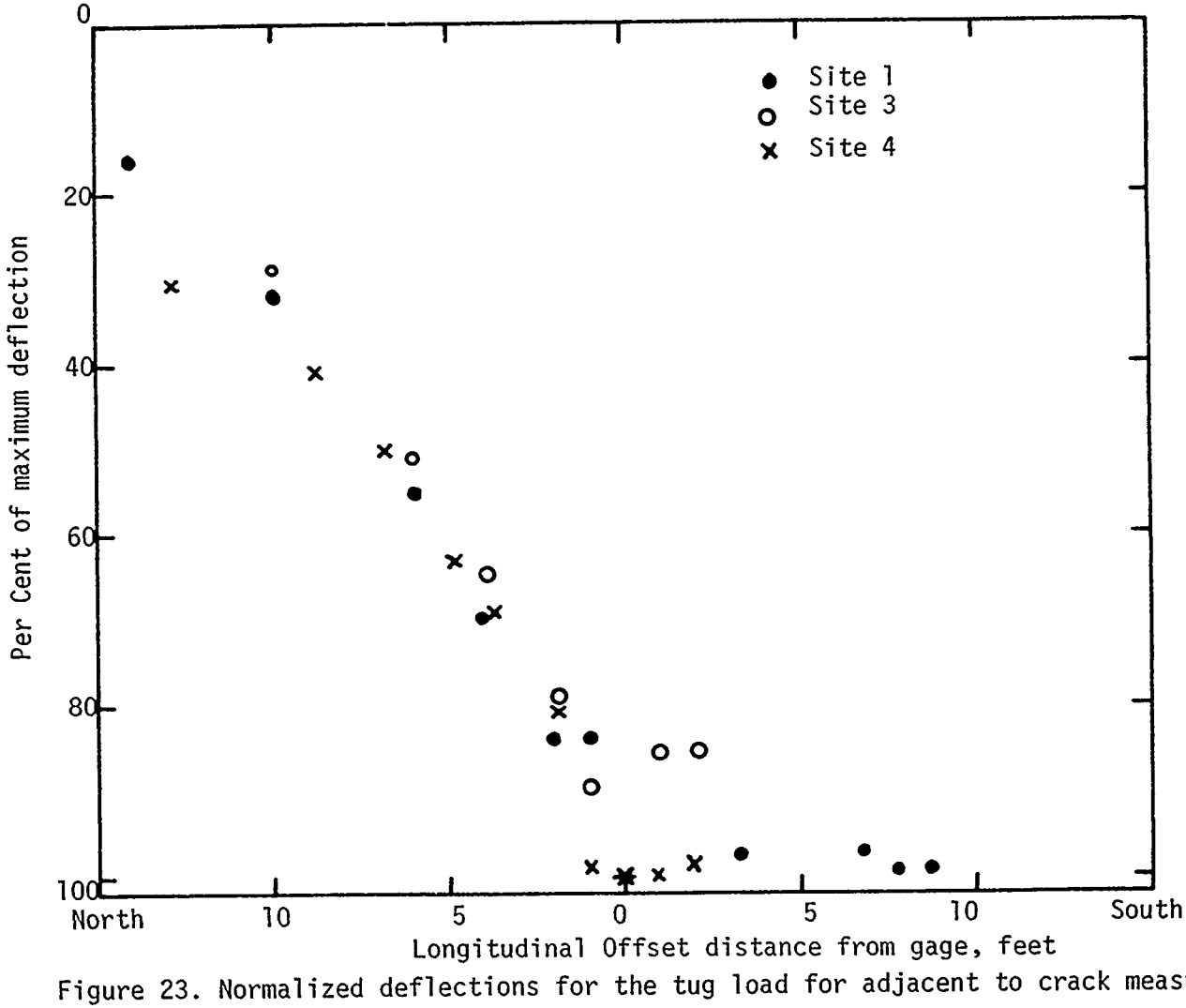

Figure 23. Normalized deflections for the tug load for adjacent to crack measurements.

At Sites 1 and 3, all loads produced similar basin shapes. At sites 4, the Boeing 727 and tug (B747) loads produced similar basin shapes, but the plate load produced a larger deflection basin.

17. The deflections are increasing at a small rate with time as seen from the Dynaflect and WES Vibrator data. Therefore when using the design procedure to characterize the pavement for each test load, the 1975 WES Vibrator deflections should be sufficient for the plate, B727 and tug (B747) loads.

Strain Measurements

18. Measurements of strain in the portland cement concrete slab and the cement aggregate mixture (CAM) were attempted using the in-place Bison Gauges installed in the pavement structure in 1973. However no meaningful results could be obtained. Therefore no data were obtained in 1973 or 1975.

Pavement Condition Observations

19. The condition survey included crack patterns of the entire runway, a few crack width measurements, and a record of any distress (longitudinal cracking, spalling, concrete surface popouts, etc.) that has occurred. The only distress observed over the entire runway was surface popouts (Figure 24 and 25.) There was a very small amount of longitudinal cracking but it was practically invisible to the casual observer. No problems were observed on any longitudinal construction joints.

Crack Spacing

20. Crack spacing data were collected after construction in September 1971 and May 1975. Data for both periods were measured to the nearest foot. Runway 4R-22L was constructed in 1970 and 1971. Station 254-294 was constructed in the spring of 1971, the average crack spacing was found to be 5.7 feet (Ref 9) in 1971 and 3.3 in 1975. Station 294-332 was constructed in the fall of 1970, its average crack spacing was found to be 6.1 feet (Ref 9) in 1971 and 5.8 in 1975. The average crack spacing of each section in Figure 1 for 1971 and 1975 is tabulated in Table 4. In general a spacing of 3 to 10 feet will produce acceptably

Figure 24. General view of transverse cracking and aggregate popout along Runway 4R-22L.

Figure 25. Close-up of an aggregate popout with some distress developing around popout.

Table 4

Average Crack Spacing for Each Section Along Runway 4R-22L

Section Number	Location Along Runway, Station	Average Crack Spacing (ft) 1971 (Ref 9)	1975
A	258-263	5.8	2.9
B	268-273	7.3	3.3
C	278-283	5.1	3.4
D	286-291	6.1	4.2
E	303-308	6.0	4.9
F	319-324	6.2	6.4
Entire Runway		5.9	4.2

small crack widths (Ref 26). Cracking, resulting from shrinkage and temperature change, starts within a few days after construction and almost all will occur within a few years after construction (Ref 26, 27). The change in crack spacing distribution with time is shown in Figures B1-B6 Appendix B in the form of cumulative frequency diagrams of crack spacing. The average crack spacing has reduced with time for every section with the exception of Section F, which is in the touchdown area, and due to the accumulation of rubber from aircraft tires, some cracks were probably not counted in 1975 because they were covered with rubber.

21. No severe closely spaced cracking has occurred in any of the sections which is documented by the shape of the cumulative frequency diagram for both time periods. Thus, it may be hypothesized that most of the cracks are developing because of temperature stresses, rather than excessive load stresses.

22. Application of the Kolomogorov-Smirnov Test (Ref 25) checked if the distribution of crack spacing, for each section, had changed with time. The test is based on a maximum absolute difference between two observed cumulative distributions. Based on the Kolmogorov-Smirnov Test, only section F has the same distribution for the two time periods, 1971 and 1975 while Sections A-D do not have the same distribution. The 1975 distributions for sections A-D are all the same, i.e. not different from each other. This supports the hypothesis that the larger crack spacing in 1971 have reduced due to a balancing of temperature and shrinkage stresses and the tensile strength of the concrete. The crack patterns obtained from the field survey, for each section of the 1975 data, are shown in Figures B7-B12 Appendix B.

Crack Width

23. Crack width data, listed in Appendix C, was collected in 1972, 1973, and 1975. The September 1972 and May 1975 data were collected using a microscope with a graduated eye piece. The 1973 data was collected with Whitmore strain gage. This data represents movement of the crack and not crack width. Measurements were made at three different seasons in 1973, May 16, August 3, and Nov. 14. No temperature changes were recorded,

therefore it can not be determined how the slab length changes with a change in temperature. Movement between the plugs is also a function of crack spacing which is illustrated in Figures 26-28. An equation can be written for 2 of the 3 sections investigated, which is listed in the figure of the corresponding location. It can also be observed that the greatest slope occurs on the edge lane which supports the supposition that cracks may be wider at the outside edge than in the interior (Ref 26). It may also be observed from Figures 26-28 that temperature and shrinkage affect movement of the cracks because the line does not go through the origin. Therefore, movement of the CRC pavement is a function of change in temperature, shrinkage and average crack spacing, assuming that other properties of the concrete and reinforcing steel remain constant.

Material Properties

24. In order to analyze the pavements structural behavior under various loads and environmental conditions, it was necessary to determine the physical properties of the individual layers. These properties include the modulus of elasticity, thickness, and Poisson's ratio. For this field study portland cement concrete and cement aggregate mixture (CAM) cores were taken at each site. Disturbed samples of the granular subbase were obtained and undisturbed samples of the subgrade were taken at several depths.

Concrete

25. The modulus of elasticity of the portland cement concrete shown in Table 5 was determined during two previous studies (Ref 5,9). Although additional concrete cores were taken in 1975, these cores were not tested for strength because of the existing data. The modulus of elasticity used in this analysis was determined by averaging all data. A modulus of 3,000,000 psi, overall average, was used at each site in the analysis. A high coefficient of variation exists for the modulus for samples obtained throughout the runway length and concrete thickness (Table 5).

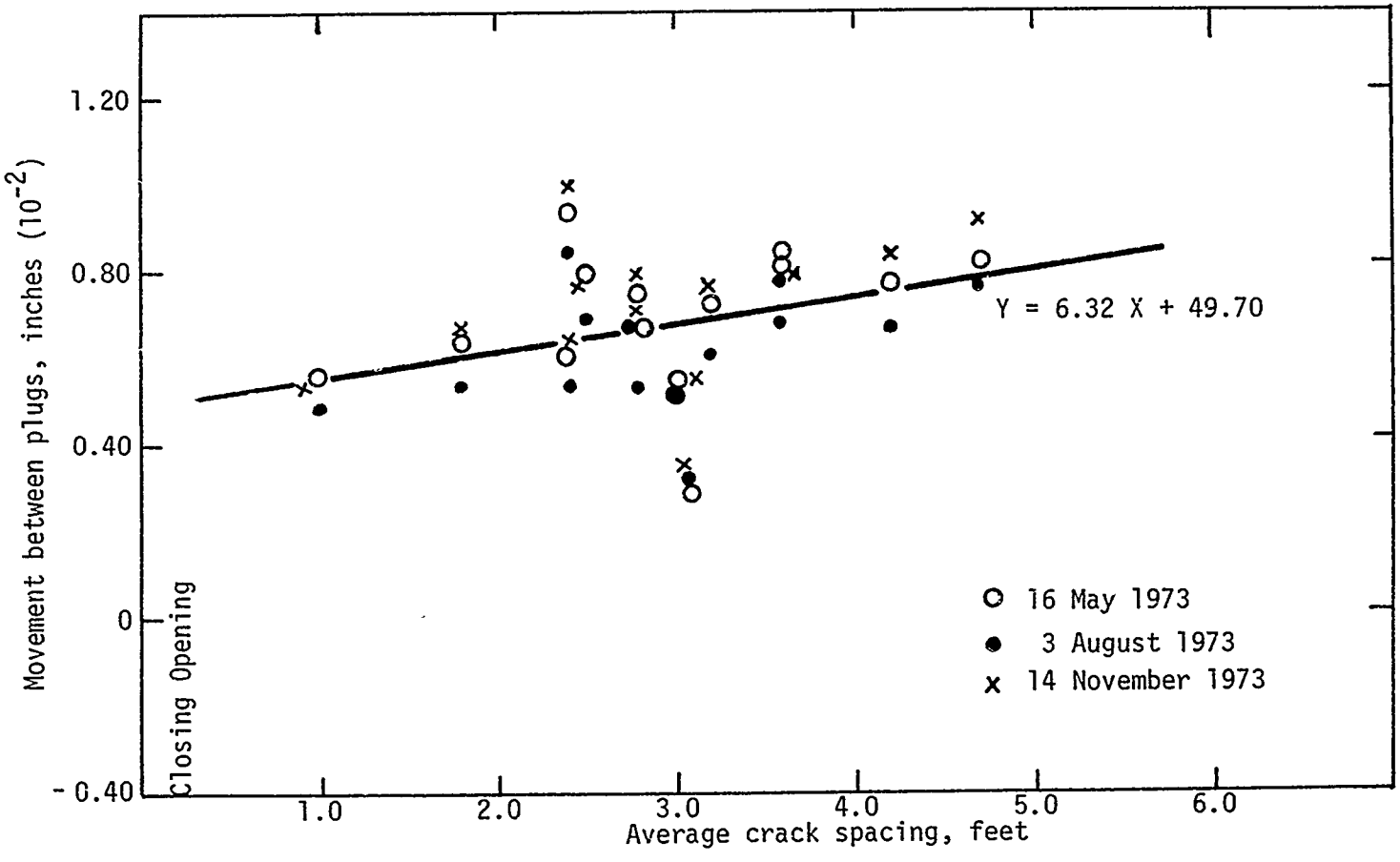

Figure 26. Crack width measurements taken with the Whitmore Strain gage at Station 306 + 50 (Interior lane) expressed as a function of crack spacing.

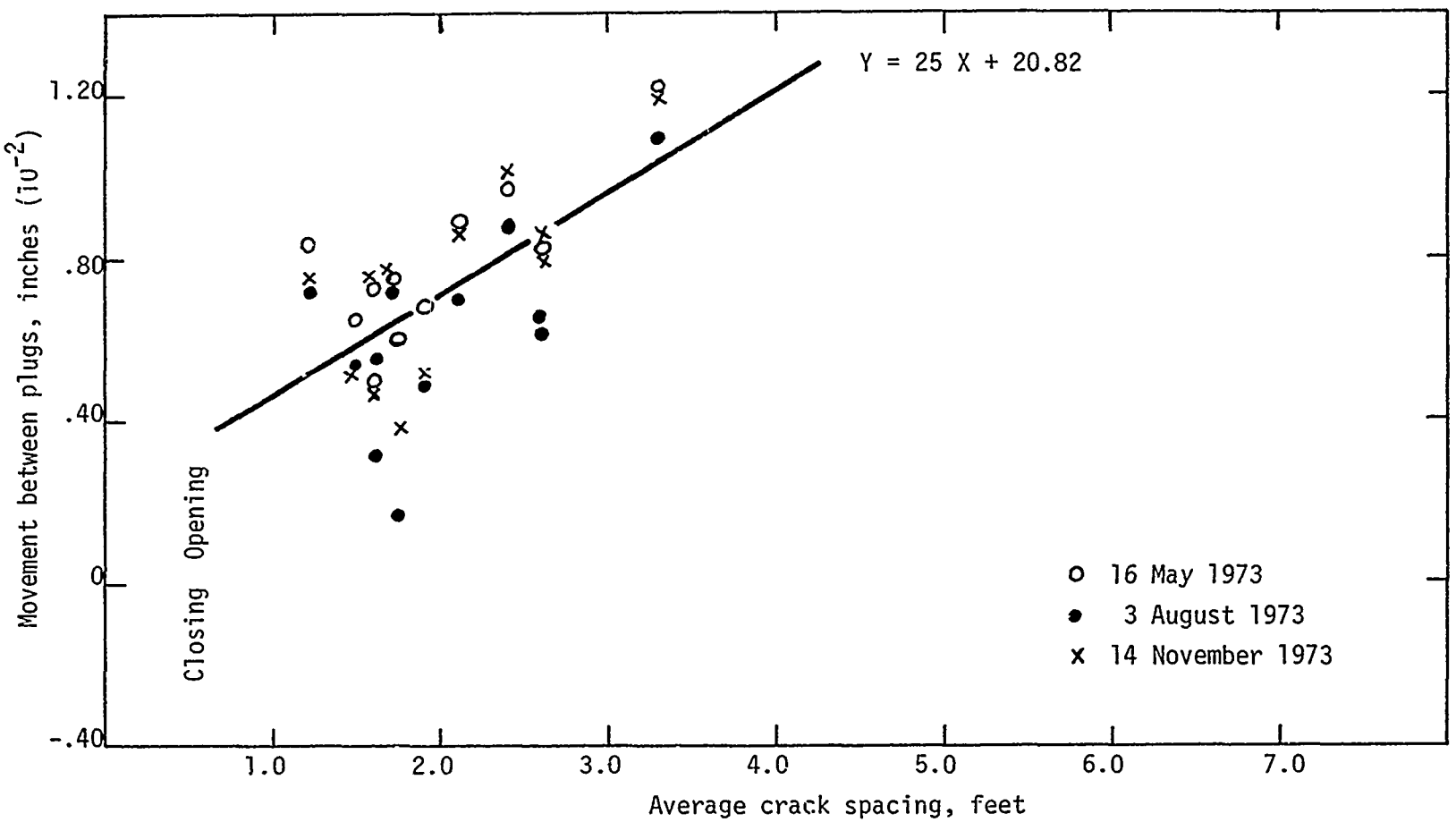

Figure 27. Crack width measurements taken with the Whitmore Strain gage at Station 305 + 50 (outer lane) expressed as a function of crack spacing.

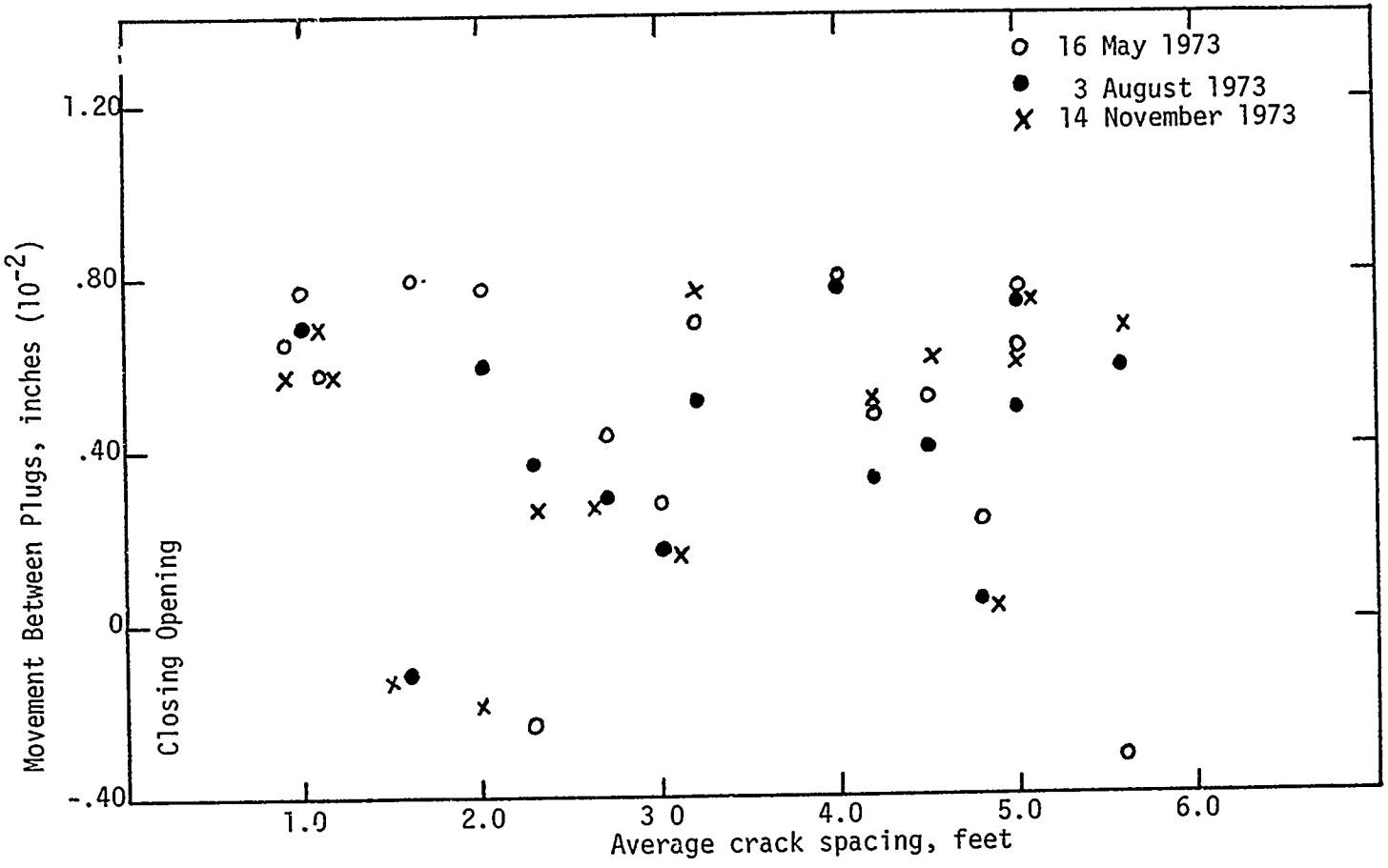

Figure 28. Crack width measurements taken with the Whitmore Strain gage at Station 304 + 60 (outer lane) expressed as a function of crack spacing.

Table 5

Summary of Portland Cement Concrete Test Data
Available For Runway 4R-22L (Ref 5,9)

Location Station-Station		Slab Thickness (inches)		Modulus of Elasticity (psi x 10^3)		Tensile Strength (psi)		Unit Weight (pcf)	
Oct 71	Nov. 72	Oct. 71		Oct. 71	Nov. 72	Oct. 71	Nov. 72	Oct. 71	Nov. 72
319-324	322	14.50	*T	2125	2830	614	656	146.6	146.0
				4159	3919	589	946	142.2	150.2
				1918	3155	547	906	142.7	150.2
			*B	1300	2848	859	640	152.0	145.6
303-308	304	14.00	T	1430	1418	573	621	147.1	145.6
				6747	1835	817	707	146.9	141.5
			B	4848	2141	785	570	150.2	137.6
286-291	288	14.25			2247	774	605	146.9	147.6
			T	2923	2676	737	610	145.9	143.9
				3625	2939	734	573	149.2	146.8
				2262	3424	707	733	149.2	146.2
			B	4269	3098	914	843	151.4	146.4
278-283	282	14.75	T	9117	2456	790	543	160.0	145.9
				1200	2685	461	753	142.7	143.4
				2700	2532	697	479	143.9	145.2
			B	3437	3308	725	707	146.2	146.5
268-273	270	15.25	T	2024	5148	487	912	147.5	152.2
				2089	3174	545	403	147.8	151.2
				3088	2827	772	736	146.7	148.0
			B	2666	3398	695	653	147.5	150.1
258-263		14.00	T	2319		716		147.8	
				3309		685		148.0	
				1342		605		144.6	
			B	4699		768		147.0	
Mean				3200	2900	690	680	147.5	146.5
Coefficient of Variation				58.4	27.1	16.8	21.1	2.5	2.3

*T - Core section from top of pavement

*B - Core section from bottom of pavement

The concrete thickness was determined from cores taken in 1975 near each test site. The thicknesses used in the analysis are given below.

Site 1 (sta 329)	13.5 inches
Site 3 (sta 306)	14.5 inches
Site 4 (sta 306)	14.8 inches

Other thickness values, obtained in 1971 (Ref 9) are given in Table 5. Poisson's Ratio for the concrete, was not determined by test, but was assumed to be 0.20 in the analysis (Ref 18).

Cement Aggregate Mixture

26. The cement aggregate mixture (CAM) was cored in 1972 (Ref 9) and in 1975. The 1972 cores were tested for strength and modulus of elasticity (Table 6). The cores taken in 1975 were not tested because sufficient data existed. The modulus of the CAM layer was chosen to be 1,410,000 psi, since this value represents an average modulus of all the data. The subbase stiffness had a high coefficient of variation with runway length and thickness as shown in Table 6. It was observed, from the cores obtained at each site, that the bottom of the cores contained loose material and voids. This could be the result of a variation in cement content and/or compactive effort which would cause the large variation in stiffness and strength (Ref 14, 28). The thicknesses of the CAM layer at each site as determined from the 1975 cores are as follows:

Site 1 (sta 329)	8 inches
Site 3 (sta 306)	8 inches

Table 6

Summary of Cement Aggregate Mixture (CAM) Test Data (Ref. 9)

Location	Thickness (in)	Modulus of Elasticity (psi) ($x10^3$)	Tensile Strength (psi)	Unit Weight (pcf)
255-T*	8.00	1138	171	127.6
B*		475	124	122.1
260-T*	8.00	1512	287	137.1
B		962	209	130.5
265-T	8.00	2122	432	143.0
-B		2898	345	138.3
270-T	10.00	919	276	144.0
B		1908	329	139.1
275-T	10.75	678	110	144.7
-B		1034	201	132.8
280-T	9.75	2562	296	140.5
-B		759	204	132.7
285-T	9.00	2396	392	146.9
-B		1226	158	126.0
290-T	8.00	1605	307	142.6
-B		1646	356	138.4
288-T	-	616	224	141.3
-B		973	273	142.2
Mean		1410	260	137.2
Coefficient of variation,%		50.8	35.1	5.1

*T - Core section from top of layer
*B - Core section from bottom of layer

Site 4 (sta 306)	8.5 inches	

Other thickness values obtained are given in Table 6 (Ref 9). Poisson's ratio for the CAM layer was not determined by test but was assumed to be 0.3 for the analysis.

Subbase

27. Granular subbase material was obtained in 1971 and 1975. The material sampled in 1971 (Ref 10) was compacted and tested triaxially with a repeated vertical load at moisture contents of 4.3 and 7.0 percent. At 4.3% moisture the material was found to have a resilient modulus (M_R) value of 44,000 psi. The M_R value at 7.0% moisture was very small. The material taken in 1975 was compacted into two samples for laboratory testing. Sample #1 and #2 were compacted to a dry density of 147.1 pcf and 146.9 pcf (Figure 29) with a moisture content of 4.1 and 4.3% respectively. These two samples were also tested triaxially with a repeated vertical load. Sample #1 was tested at a confining pressure of 0 and 3 psi. A zero confining pressure was used to represent the most critical condition to occur, and 3 psi was to represent the estimated overburden pressure. As observed from Figure 29, based on averages, the material had a greater modulus at a confining pressure of 3 psi. Figure 29 shows a large variation in the resilient modulus and that the M_R is independent of deviator stress level. This is usually not the case, since untreated gravel or crushed stone is normally considered stress sensitive relative to the confining pressure. This large variation of modulus and independence of stress level could have resulted from the sampling technique, augering loose material, which affected the material gradation.

Subgrade

28. The undisturbed subgrade samples collected were tested triaxially with a repeated vertical load at different confining pressures depending on the depth of the sample. For performing the test, the confining pressure was determined by calculating the expected overburden pressure and estimating the lateral stress produced by the applied load. The

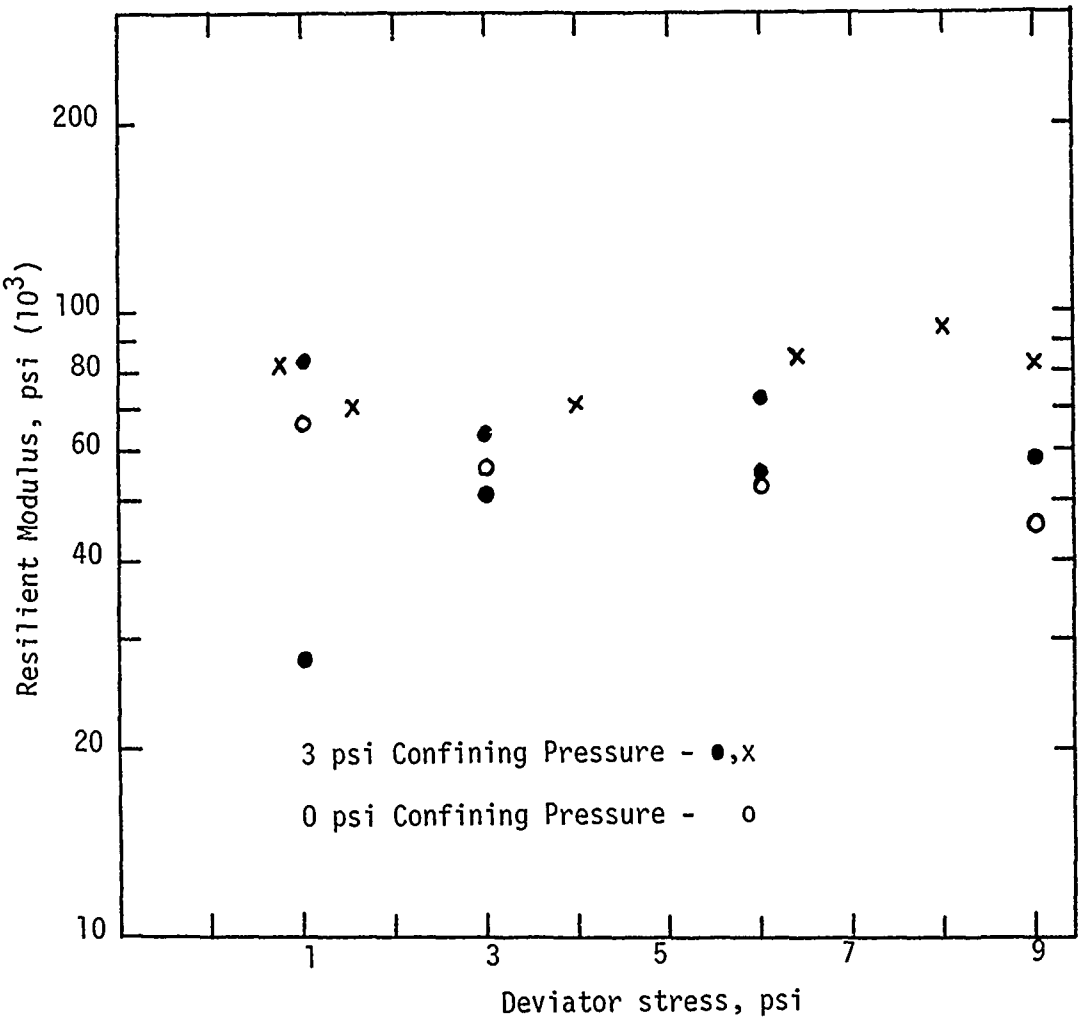

Subbase Sample No.	1	2
Symbol	●, o	x
Moisture Content, %	4.1	4.3
Dry Density, pcf	141.4	140.8
Curing Time, days	11	0

Figure 29. Laboratory test data for the granular subbase material sampled in May 1975.

confining pressures used to simulate the conditions at each depth sampled, are listed below.

Depth (feet)	Confining Pressure (psi)
3.5 - 6	5
6 - 8	7
8 - 11	9

Each sample was tested over a range in deviator stresses, since the subgrade is stress sensitive, as shown in Figures 30-32. The resilient modulus was determined for each deviator stress after 1200 cycles of load applications were applied. The slopes of the lines in Figures 30-32 are very similar indicating the same response to load. Poisson's Ratio was not determined in the laboratory, but was assumed to be 0.450.

29. The subsurface conditions are tabulated in Table 7 for three different time periods. Figure 33 shows the moisture content has generally increased with time in the bandwidth shown on the graph. The data shown indicates that the moisture content is stabilizing with time which is important in stress prediction. Figure 34 illustrates that the dry density has also decreased with time although no explanation can be deducted for this observation. A review of the soil profile along the runway centerline developed by the City of Chicago's Department of Public Works revealed the following conditions:

Site 1 - 5 ft of compacted fill material; 5½ ft of topsoil and original clay fill, 1½ ft of silt and clay; and a very tough and hard clay.

Site 3 - 0.5 ft compacted fill material; 6 ft topsoil and original silty, clay fill; and a very tough and hard silty clay.

Since transverse soil profile data were not available, Site 4 was assumed to have the same conditions as Site 3. The data presented

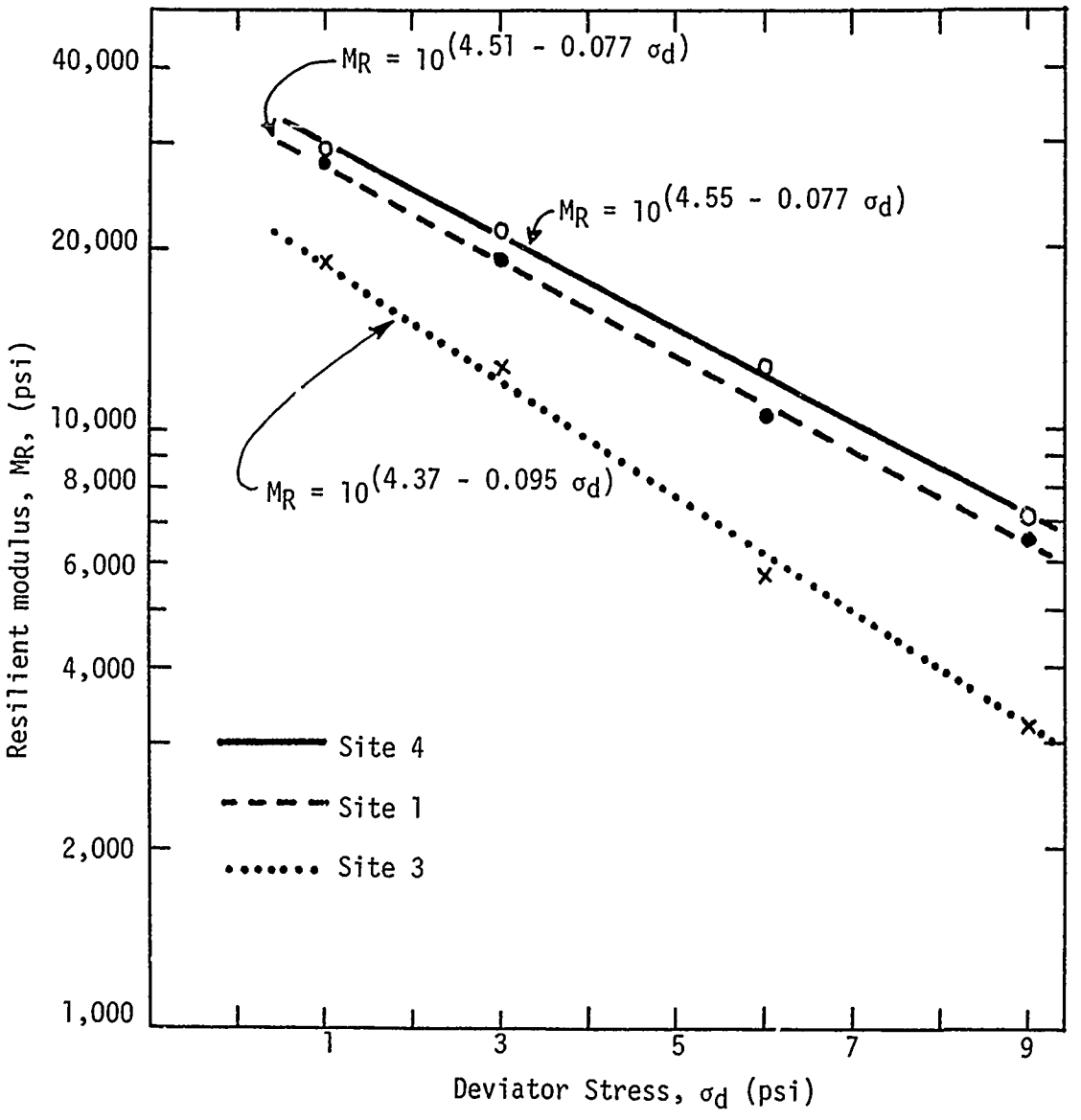

Figure 30. Laboratory test results of the subgrade material at a depth of 3.5 - 6 feet below the surface. (Confining pressure = 5 psi)

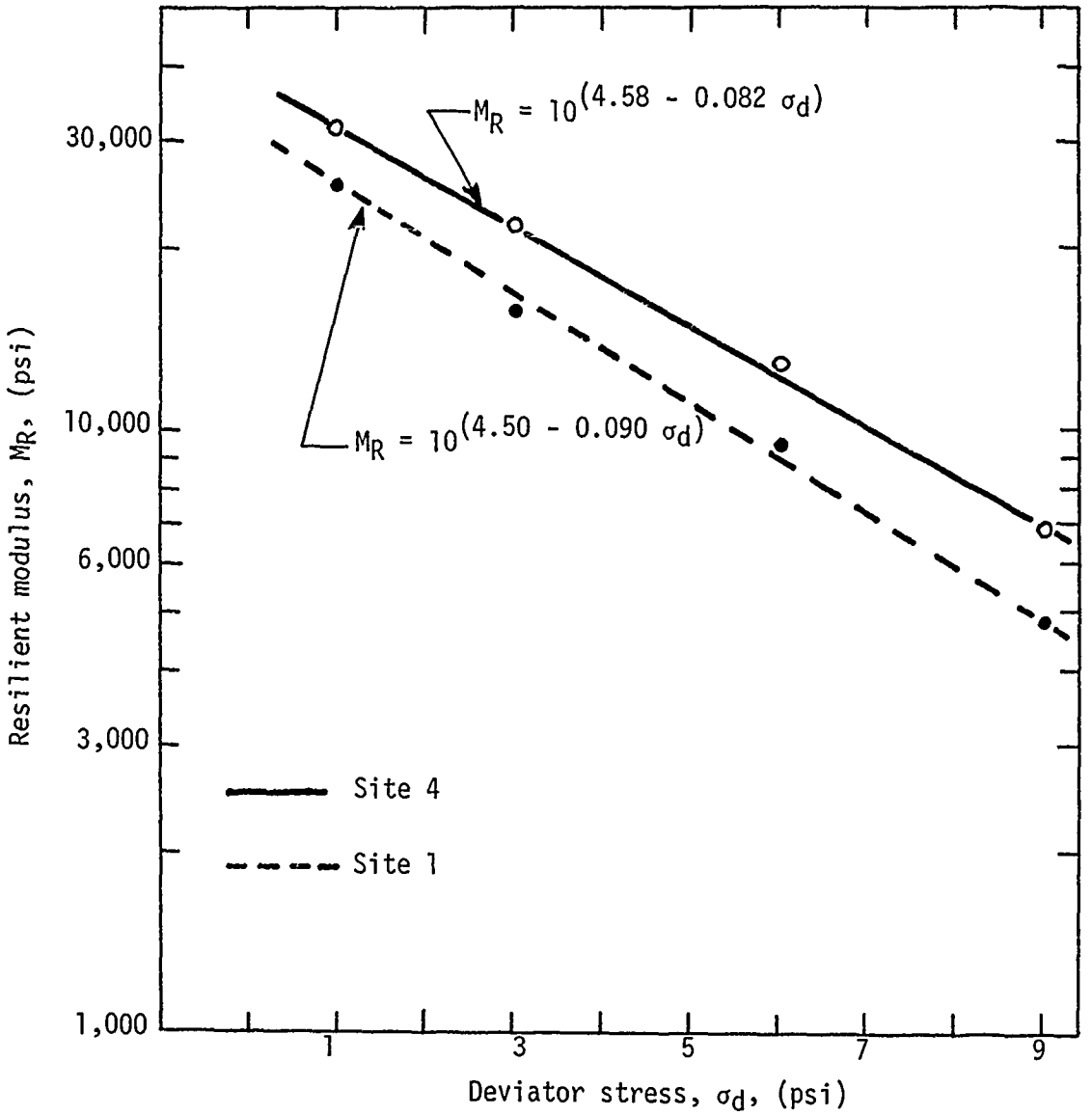

Figure 31. Laboratory test results of the subgrade material at a depth of 8-11 feet below the surface. (Confining pressure = 9 psi)

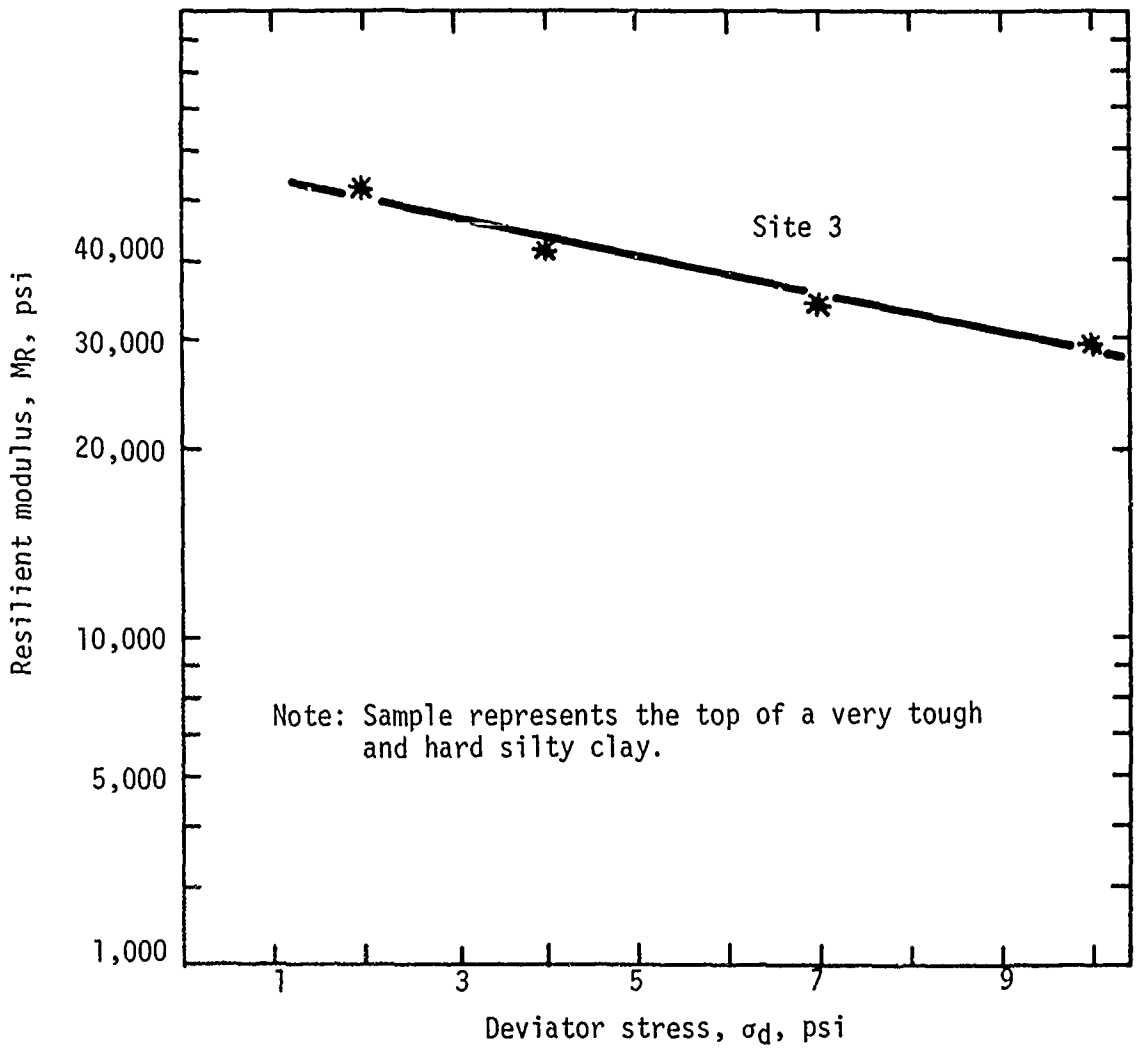

Figure 32. Laboratory test results of the subgrade material at a depth of 6-8 feet below the surface (confining pressure = 7 psi).

Table 7

Subsurface Soil Condition Beneath

Centerline of Runway 4R-22L

Date	Location	Moisture Content (%)	Dry Density (pcf)	Depth (ft)
Nov. 1971	260	14.2	122.0	3.5-6.5
(Ref.9)	270	15.1	113.2	"
	280	15.3	114.0	"
	288*	11.7	124.7	"
	300	16.2	111.7	"
	320	14.1	117.8	"
Oct. 1972	270	16.1	119.1	"
(Ref. 5)	288	17.6	110.2	"
	304	14.6	117.8	"
	322	18.0	115.7	"
June 1975	330 + 60***	18.2	107.2	4-6½
		17.1	112.6	9-11½
	305 + 99	19.1	109.6	3½-6
		18.1	113.1	6-7½
	306**	17.3	108.8	3½-6
		16.0	116.4	8½-11

* Substituted for zero recovery at sta 290,sample taken in edge lane.
** Sample taken near edge of runway (Lane 1).
*** Wet layer found to exist at a depth of about 7.0 ft.

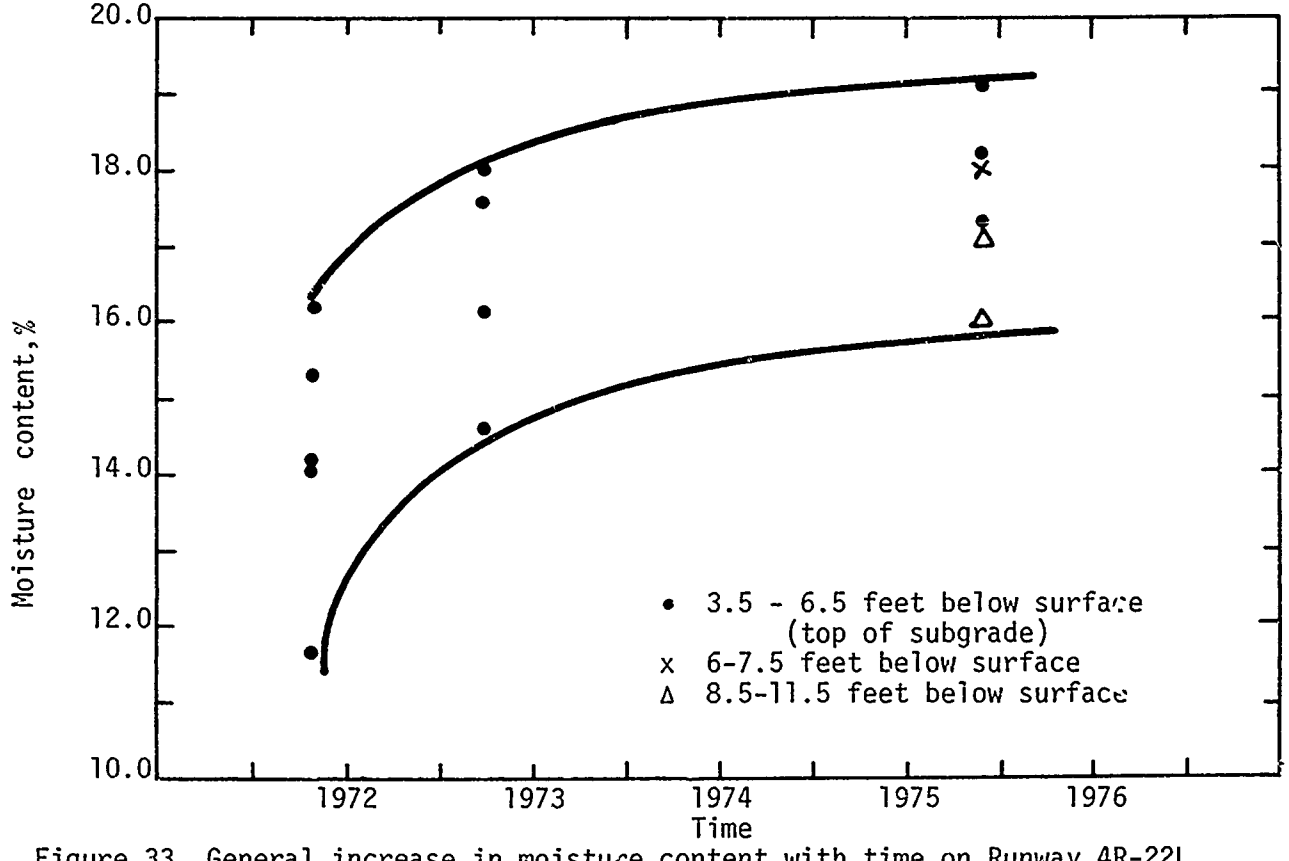

Figure 33. General increase in moisture content with time on Runway 4R-22L.

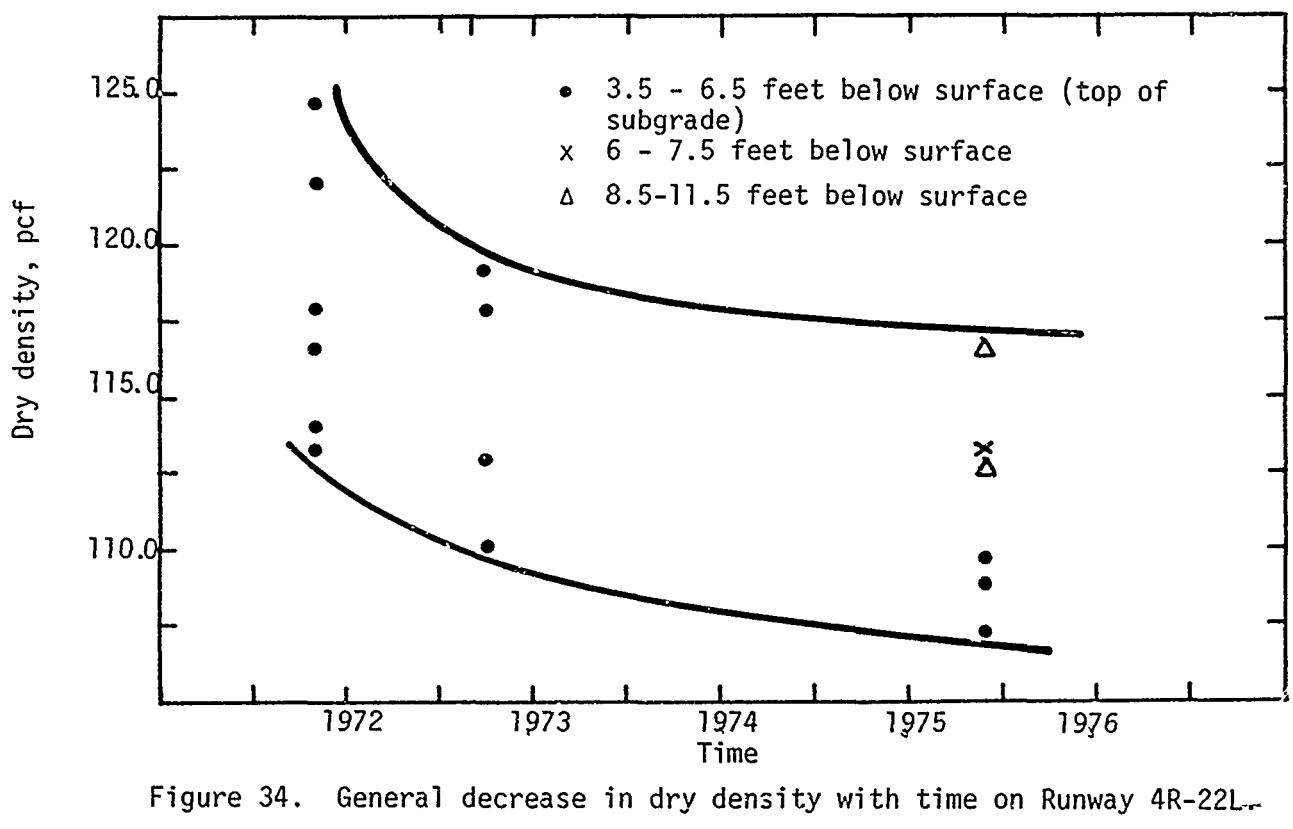

Figure 34. General decrease in dry density with time on Runway 4R-22L.

in Figures 33 and 34 show some interesting observations, but probably do not constitute a large enough sample on which to base any definite conclusions other than what the data infer.

Environmental Data

30. Temperature and rainfall data were collected from the U.S. Department of Commerce, National Climatic Center in Asheville, North Carolina. At O'Hare International Airport temperatures are relatively warm in the summer and relatively cold in the winter. Figure 35 gives the average monthly high and low temperatures for the period from 1972-1975. Figure 36 gives the snow and ice in equivalent inches of water, and Figure 37 illustrates the rainfall throughout the year. Summer thundershowers are frequently heavy and variable (Ref 19). Normally, a more continuous rainfall is common in the spring and autumn. The snowfall from year to year varies over a wide range.

36. Since the temperature of the slab varies with depth, thermistors were placed in Runway 4R-22L to observe the temperature difference with depth. The differences in temperature between the top and bottom of the slab is important, because deflection is a function of the temperature differential. As the top of the slab becomes warmer than the bottom, the deflection decreases, and when the top of the slab becomes cooler than the bottom, the deflection increases (Ref 16). Temperature readings were taken with the thermistors on 21 May 1975 (Figure 38). The temperature near the top of the slab changes directly with a change in air temperature, but the bottom of the CRC does not seem to be affected by any sudden change in temperature at the surface.

Traffic Survey

32. A traffic survey was taken on the 22nd of May 1975 to determine the distribution of aircraft for the entire airport. The survey was conducted over three different time periods during the day, 8:30 - 10:30 a.m., 12:30 - 3:00 p.m., and 5:30 -7:30 p.m. Figure 39 gives a distribution of arrivals and departures during the day of the 22nd. There were more departures than arrivals in the morning

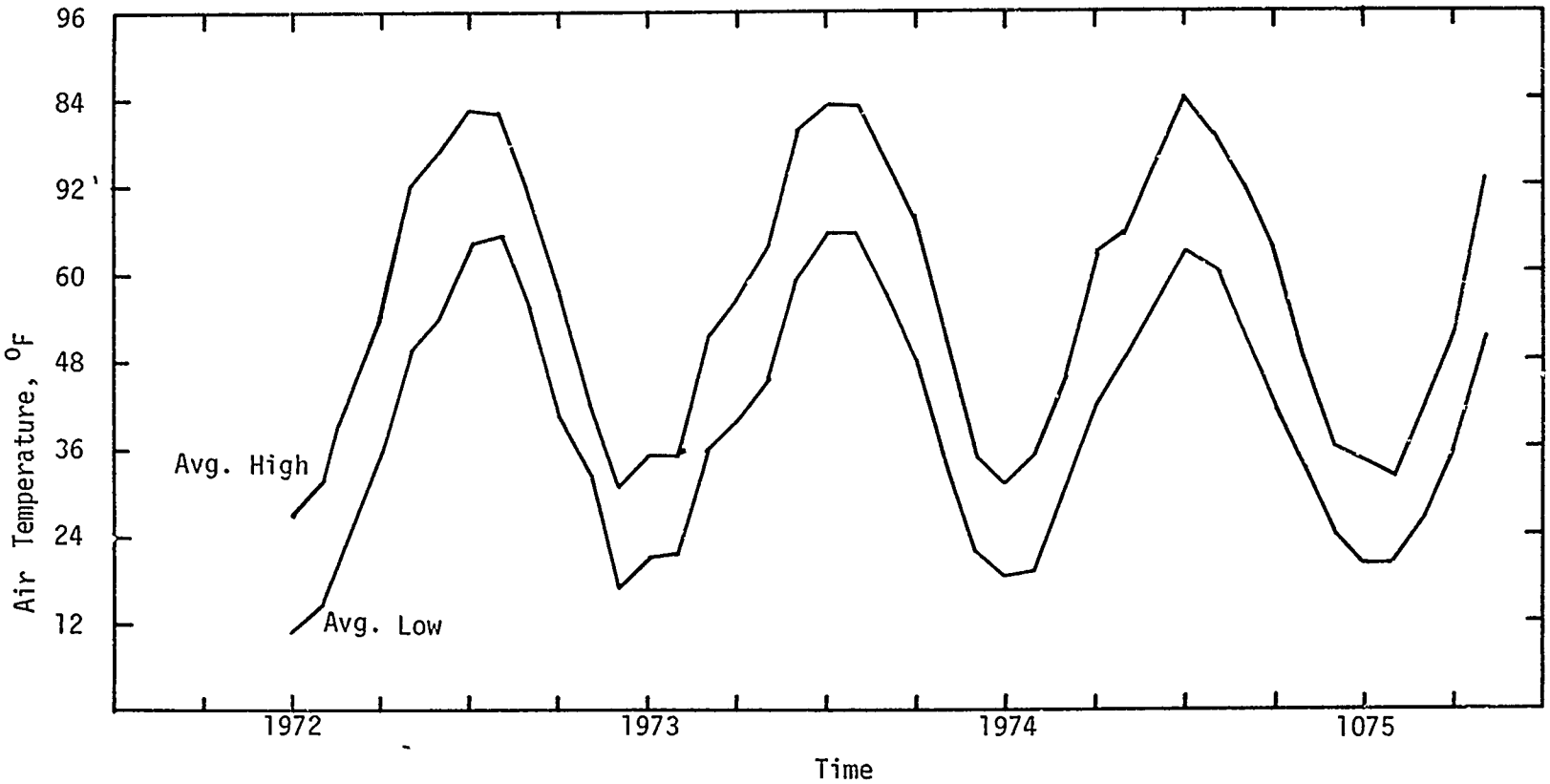

Figure 35. Average monthly high and low air temperatures, for the O'Hare International Airport.

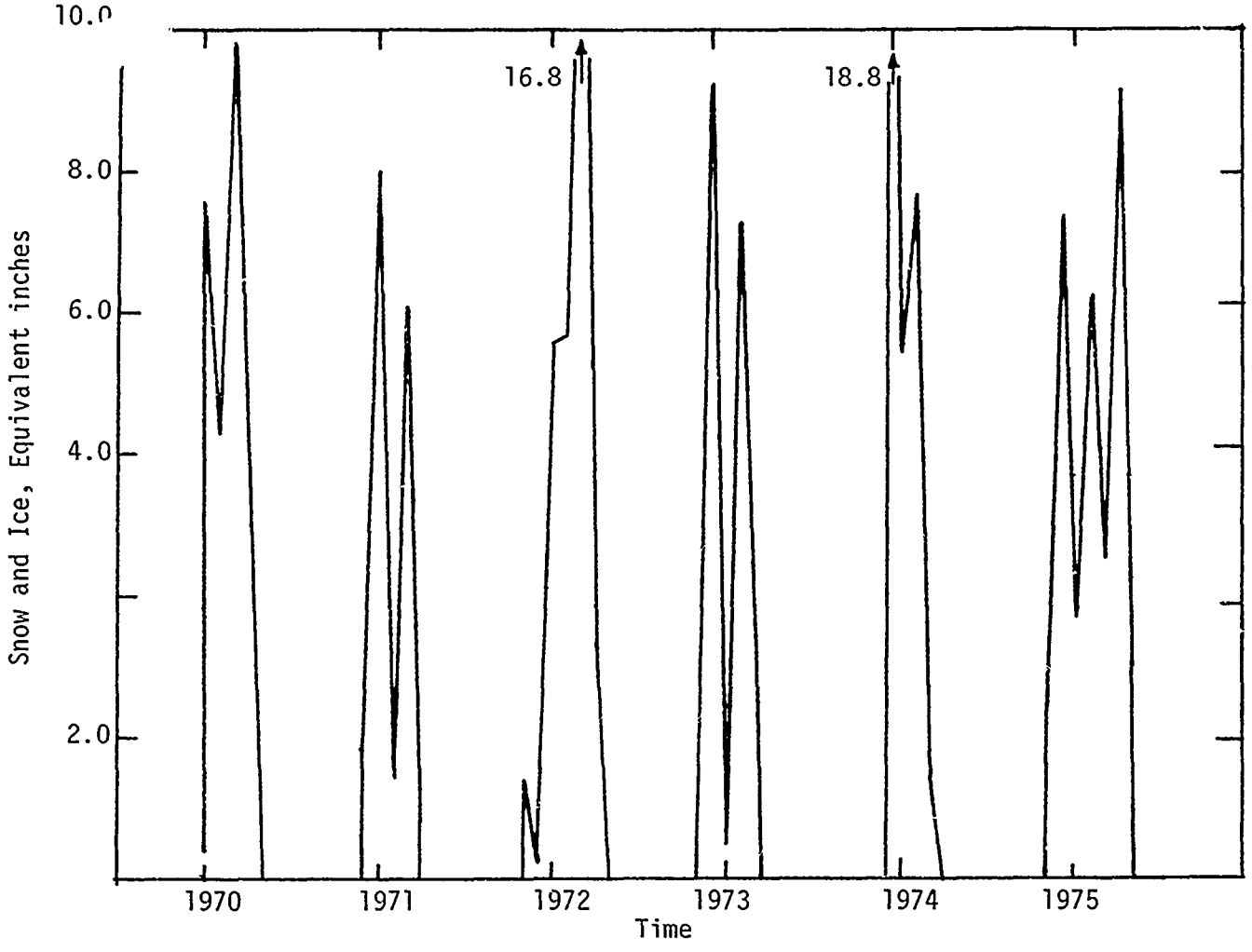

Figure 36. Yearly snow and ice precipitation of O'Hare International Airport.

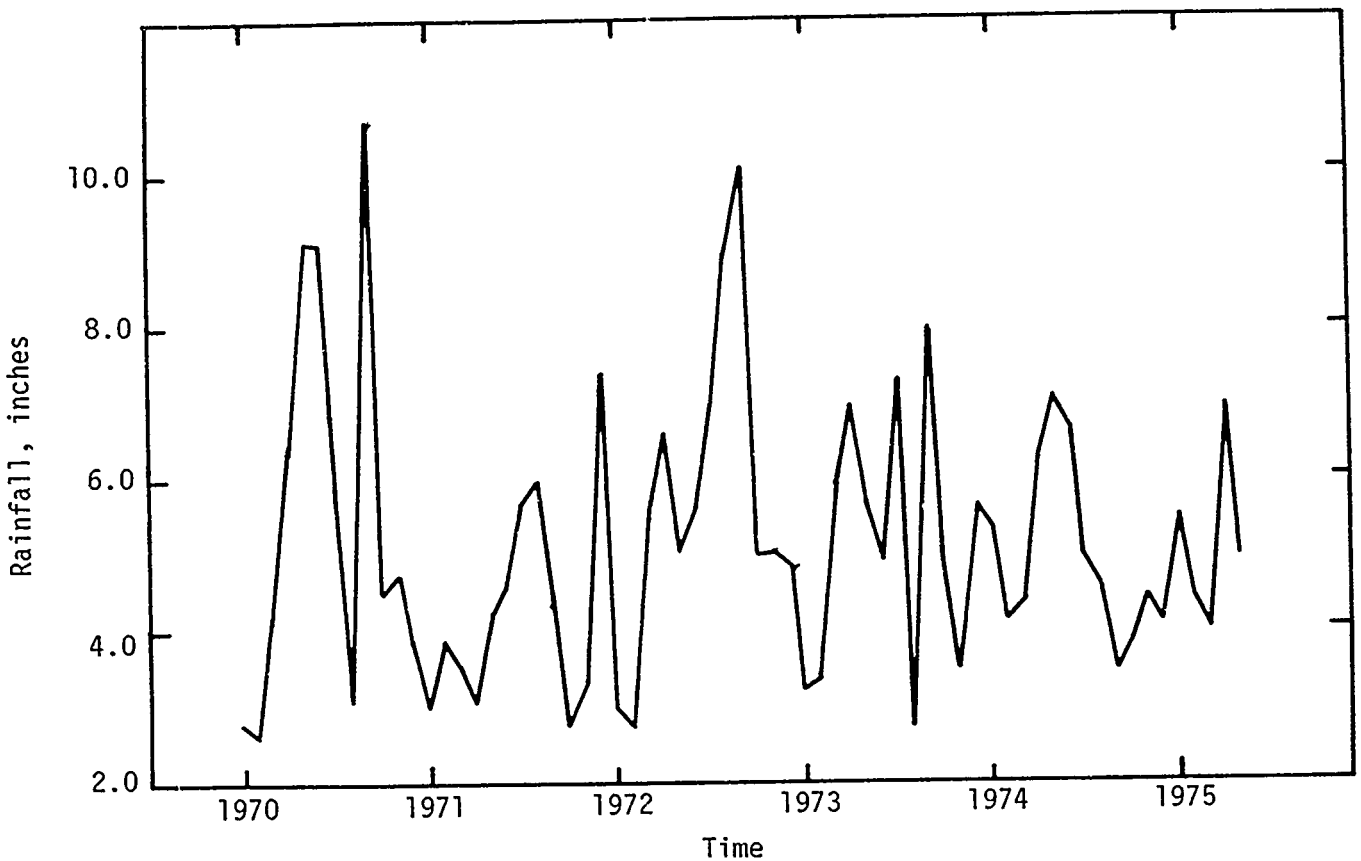

Figure 37. Monthly rainfall for O'Hare International Airport.

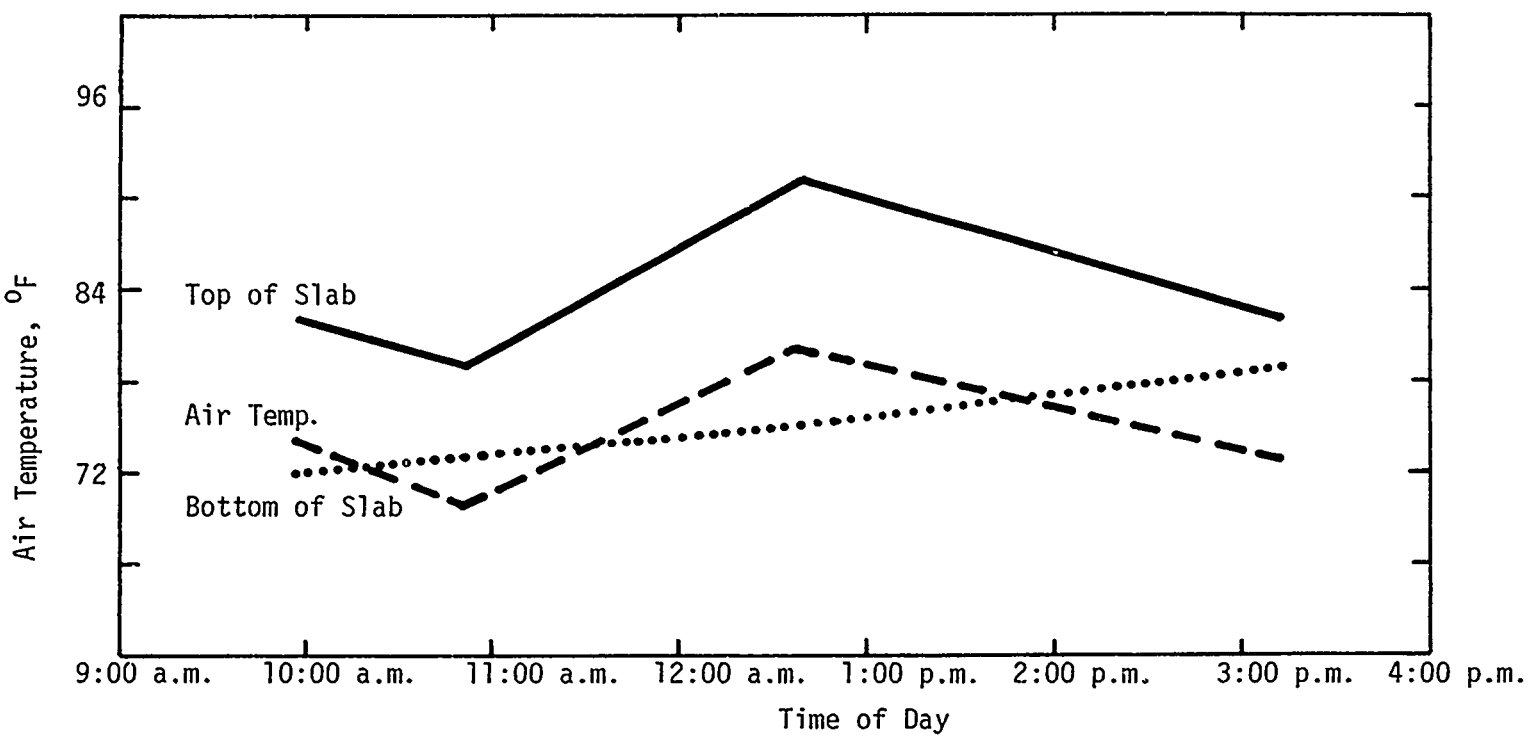

Figure 38. Temperature variation with depth of CRCP, taken with thermistors located at Site 4 on 21 May 1975.

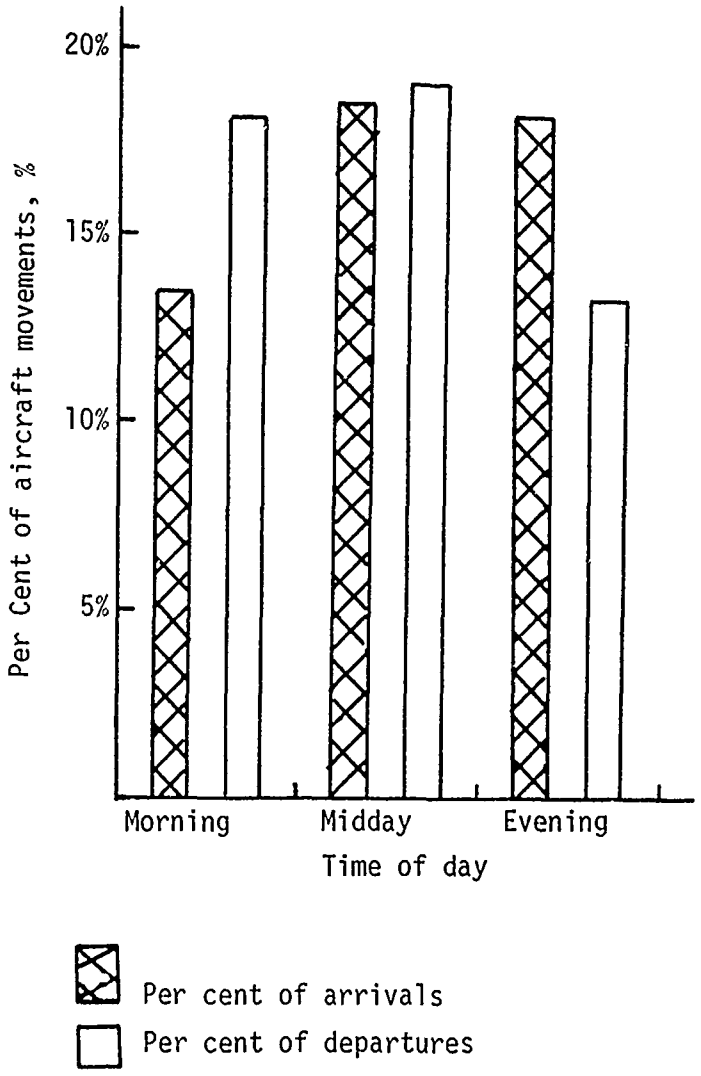

Figure 39. Distribution of arrivals and departures of the traffic survey on 22 May 1975 for O'Hare International Airport.

hours, but more arrivals than departures during the early evening hours. By using the distribution of aircraft (Table 8) and the number of movements the actual traffic distribution can be determined. The movements are normally obtained from runway utilization logs which are monthly recordings of all departures and arrivals for each runway at O'Hare International Airport. These runway utilization logs were not available therefore the actual traffic distribution can not be determined, for any given runway. Table 8 gives the distribution of aircraft for different time periods.

Table 8

Traffic Survey Comparisons for O'Hare International Airport, Chicago, Illinois

Percent of Total Operations On:

Type of Aircraft	All Runways 1975	Runways* 1973 (Ref 5)	Runway 9R-27L 1975	Runway 9R-27L 1971 (Ref 9)	Runway 9R-27L 1970 (Ref 9)
B747	1.9	2.5	1.7	-	-
B727/200	17.2	12.5	24.7	17	13
B727	17.0	19.4	15.5	22	28
B720	3.7	0.2	3.4	15	2
B737	5.4	4.8	6.0	5	7
B707	3.7	9.0	3.3	15	13
DC10	7.5	2.8	2.2	-	-
DC9	14.8	22.4	18.7	21	19
DC8	4.8	3.5	3.8	-	-
DC-8-50	-	-	-	3	4
DC-8-61	-	-	-	1	2
DC-8 Super	3.1	2.9	1.6	-	-
L1011	1.6	0.6	1.1	-	-
Convair 340/440/580	5.4	10.5	2.7	-	-
Convair 880	-	2.7	-	3	5
Small Jets	1.1	-	1.1	-	-
Fairchild	2.2	6.2	3.8	-	-
Small Props	9.5	-	10.4	-	-
Air Force Planes	1.1	-	-	-	-

* Includes only Runways 4R-22L, 9R-27L, and 14R-32L.

PART III PAVEMENT CHARACTERIZATION AND ANALYSIS

33. In characterizing the pavement structure, all material properties are based on mean test values with the exception of the subgrade layer which is stress sensitive. In order to simulate the pavement's behavior two analytical models are available. 1) elastic layer theory (Ref 13) and 2) the discrete element method, slab theory (Ref 11, 12).

Elastic Layer Theory

34. When the pavement response is predicted analytically by the use of elastic layer theory, the material properties of each layer must be determined. The laboratory test data presented in the previous chapter were used as input data to analyze the deflections which were measured with the WES Vibrator for each site. The subgrade modulus of elasticity was computed with consideration of the type load since it is stress sensitive. The characterization of the pavement was based on laboratory determined properties for all layers except the subgrade. The subgrade was characterized using a combination of the deflection measurements, laboratory soil tests and layered analyses of the pavement structure.

Subgrade Modulus Determination

35. The selection of the design subgrade modulus of elasticity for each load was accomplished using the laboratory resilient modulus data along with the subgrade modulus estimated from deflection measurements on the existing runway (Ref 6,7). The laboratory evaluation of materials produced curves as exhibited in Figures 30-32, where the resilient modulus decreased as the deviator stress increased. Elastic layer theory was used to calculate deflections and deviator stresses (top of subgrade) produced by the nondestructive test (NDT) equipment, i.e. WES Vibrator and Dynaflect. The relations shown in Figures 40-42 were determined for Sites 1, 3, and 4, respectively, for a range of subgrade moduli. In addition to these, the relation of subgrade

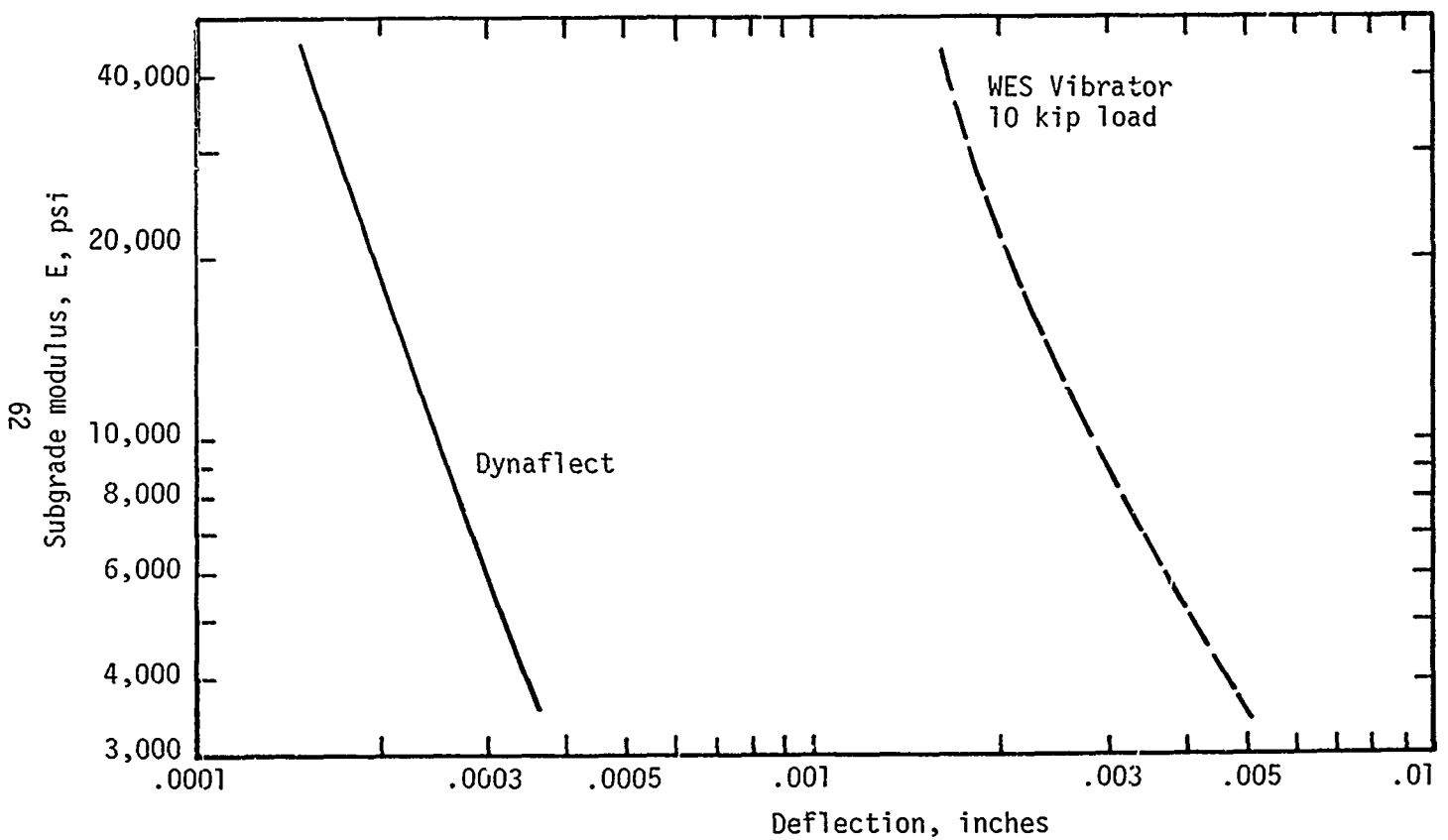

Figure 40. Theoretical deflection versus subgrade modulus for dynamic load conditions at Site 1.

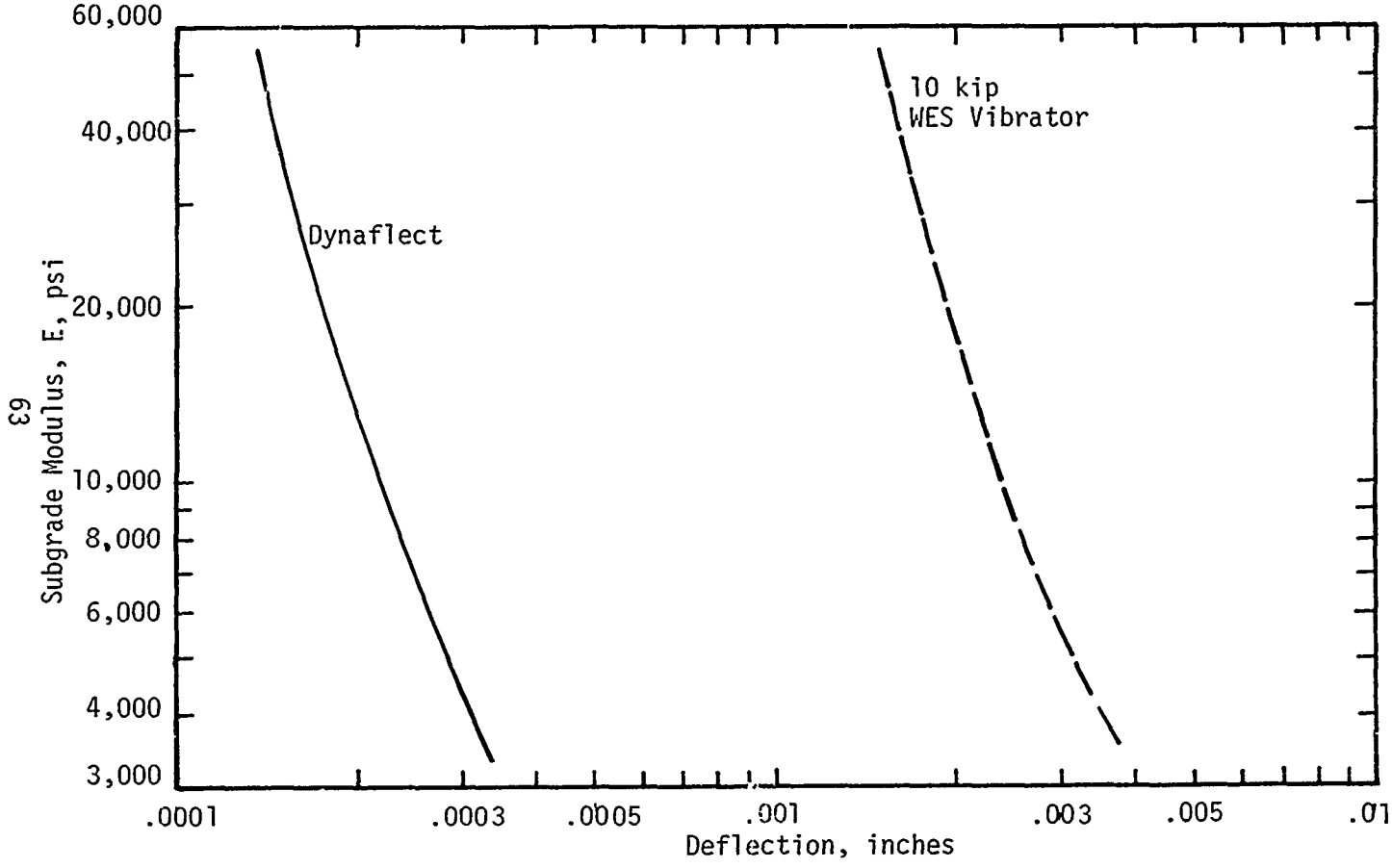

Figure 41. Theoretical deflection versus subgrade modulus for dynamic load conditions at Site 3.

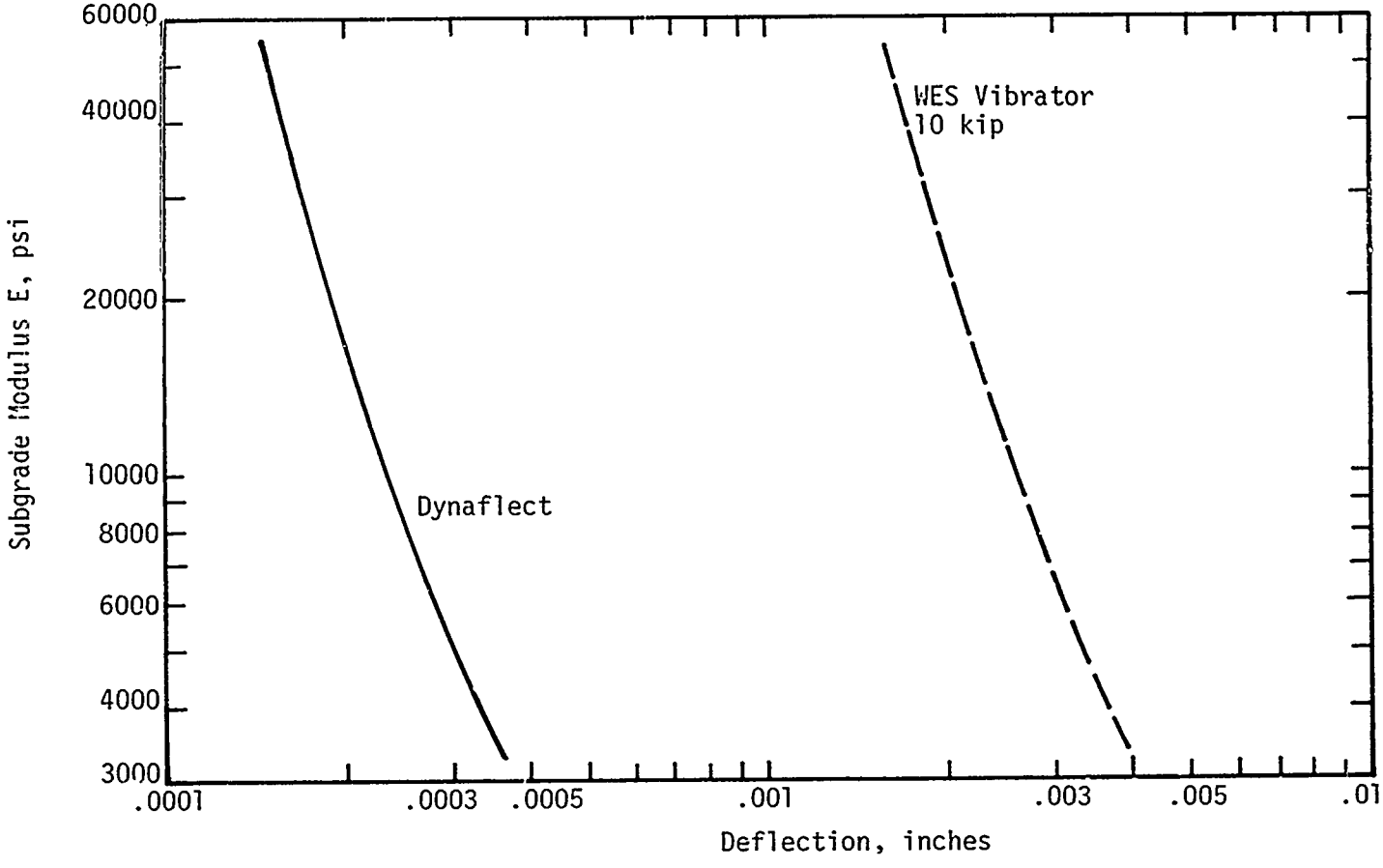

Figure 42. Theoretical deflection versus subgrade modulus for dynamic load conditions at Site 4.

modulus and deviator stress were developed for each of the NDT loads and the heavy experimental test loads. Figures 43-45 show these relations for Sites 1, 3, and 4 respectively.

36. The subgrade modulus values for the NDT loads and also the large test loads (aircraft/tug) were determined using the following stepwise procedure:

a. The subgrade modulus for the NDT loads was determined by using the mean measured deflection for each site (Table 9) and entering it in Figures 40-42 to determine the subgrade modulus representative of the NDT load.

b. The subgrade modulus values representative of the NDT load from Step 1 were entered in Figures 43-45, respectively, to obtain the deviator stress at the top of the subgrade for each site. The values of modulus were entered on the vertical scale and projected horizontally to the curve labeled WES Vibrator and projected vertically downward to determine the value of deviator stress.

c. In Figures 43-45 a line was drawn through the coordinate determined for each site in the two foregoing steps. For Figure 43, this line was parallel to the laboratory line developed for Site 1 (Figure 30), likewise in Figures 44 and 45 for sites 3 and 4.

d. The subgrade modulus for each large test load as obtained by simply projecting horizontally fromthe intersections of the analysis curve and curves for each test load curve (tug, B727, Plate)

The results of this procedure yielded the subgrade moduli for all the loads considered in the study. These values of subgrade moduli are summarized in Table 10.

37. The data in Table 10 are the subgrade modulus values used in the computations to predict deflections for comparisons with those measured under the B727 aircraft, the B727 aircraft tug and the

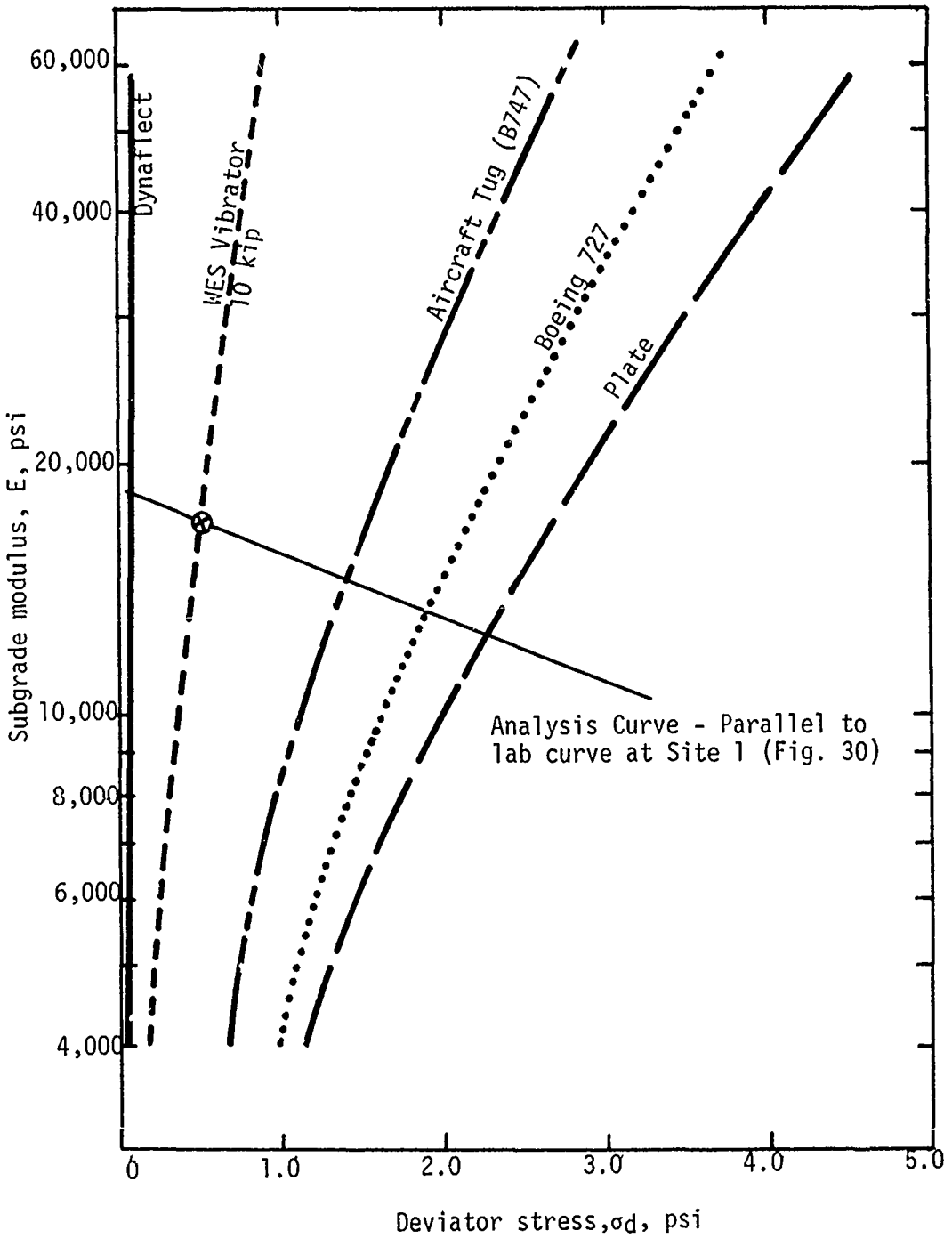

Figure 43. Theoretical deviator stress (top of subgrade) versus subgrade modulus for dynamic and static load conditions at Site 1.

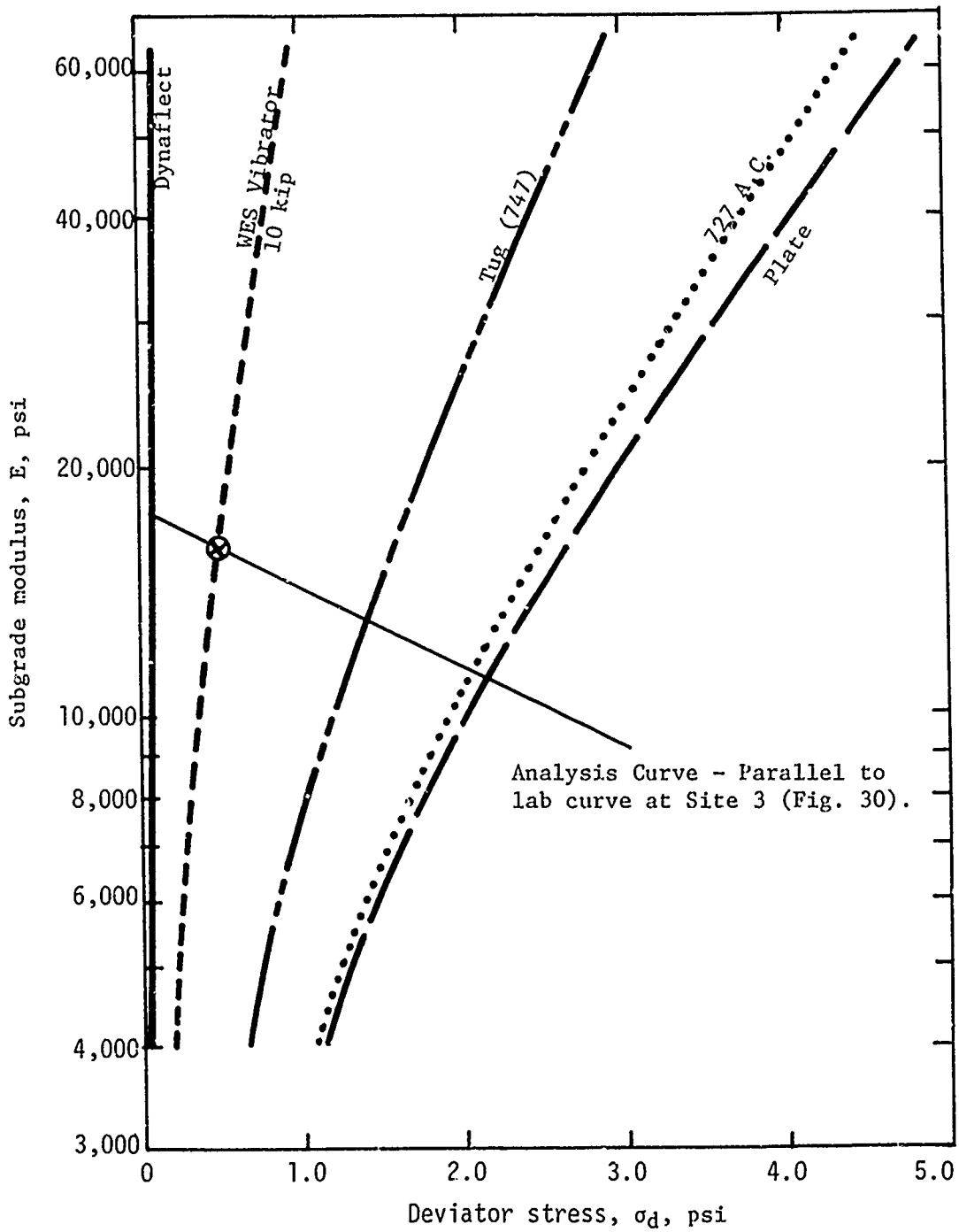

Figure 44. Theoretical deviator stress (top of subgrade) versus subgrade modulus for dynamic and static load conditions at Site 3.

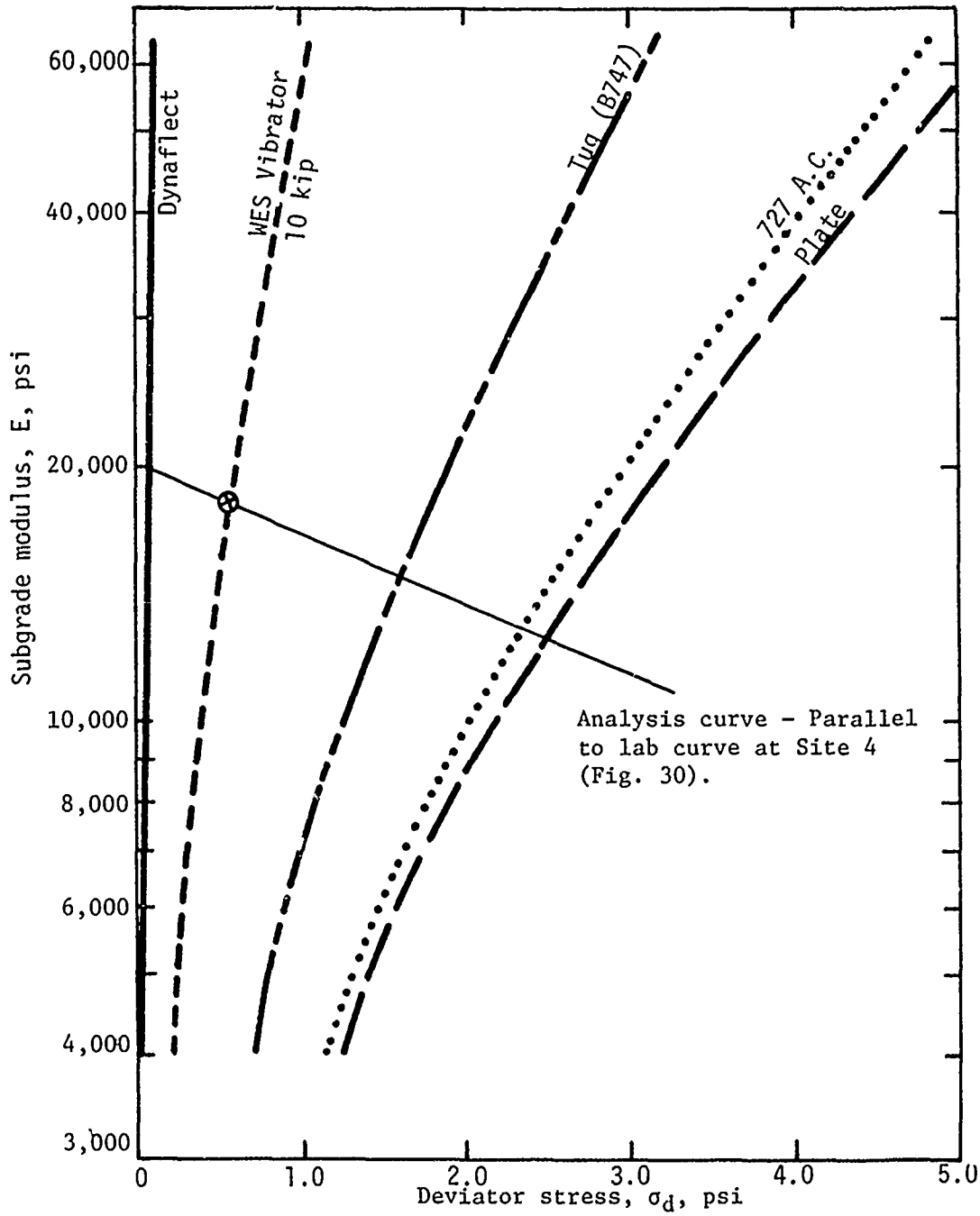

Figure 45. Theoretical deviator stress (top of subgrade) versus subgrade modulus for dynamic and static load conditions at Site 4.

Table 9

Deflection Values Used to Characterize Each Site

Site	Deflection, inches (10^{-3}) WES Vibrator (1975)	Dynaflect (1972)
1	2.25*	.199
3	2.02**	.224
4	2.10**	.192***

* Measurement represents the average deflection within 500 ft. of site since deflection at site 1 was believed to be in error (Table 2).

** Measurements represent average deflection within 500 ft. of site.

*** Measurement taken in 1971 since no data in lane 1 exists for 1972.

Table 10

Subgrade Resilient Modulus Based On
the Dynaflect and WES Vibrator Loads
Considering Concept of Stress Sensitivity

Test Site	Type of Load	WES Vibrator (1975) Deviator Modulus psi	WES Vibrator (1975) Subgrade Modulus psi	Dynaflect (1972) Deviator Stress psi	Dynaflect (1972) Subgrade Modulus psi
1		0.08	18,500	0.08	18,500
3	Dynaflect	0.07	17,500	0.07	13,000
4		0.08	20,000	0.08	19,000
1		0.50	17,000	0.50	17,000
3	Wes Vibrator	0.48	16,000	0.40	12,200
4		0.57	18,000	0.55	17,500
1		2.27	12,500	2.27	12,500
3	Plate	2.14	11,000	1.88	8,900
4		2.49	12,500	2.41	12,000
1		1.90	13,000	1.90	13,000
3	727 A.C.	2.06	11,500	1.80	9,000
4		2.35	13,000	2.30	12,500
1		1.40	14,500	1.40	14,500
3	Tug (747)	1.40	13,200	1.20	10,200
4		1.60	15,000	1.58	14,500

plate load simulation of the B727. The modulus of elasticity values determined for the subgrade material for the various loads (Table 10) indicates that the material is load sensitive as was first determined in the laboratory.

38. An important factor in characterizing the existing inplace pavement was the consideration of the depth of the subgrade. Soil surveys by the City of Chicago (Ref 9) were used to approximate the depth of the subgrade layer immediately beneath the pavement. These depths were 10, 7, and 7 feet respectively for sites 1, 3, and 4. The material beneath this layer was defined as a very tough clay and was assigned a modulus of 150,000 psi. This procedure is an attempt to simulate the stiff material response at very low stress levels. This procedure has been used with success previously in design studies (Ref 20, 21).

39. Another important factor is the consideration of the variability in stiffness of the CAM layer. As was noted in Chapter II, the CAM cores contained loose material near the bottom, therefore it was decided to reduce the CAM modulus by 1½ standard deviations (230,000 psi). This is the value that was used in the final analysis. In the first analysis an infinite subgrade depth was used with a mean value of modulus of the CAM layer, but there was difficulty in predicting basin shape as will be noted in Chapter IV. Therefore, after close evaluation of the existing layers a reduced CAM modulus and rigid layer were used to predict deflection magnitude and basin shape.

Prediction of Deflection for Test Loads

40. Using the pavement component properties defined previously, Sites 1, 3, and 4 were analyzed for loadings with a B727 aircraft, B747 aircraft tug, and a plate load simulation of a B727 aircraft. The deflection on the pavement surface was predicted for distances from the load similar to the offsets considered in the field. The stresses in the pavement werw also noted for each of the test loads. The predicted deflections

for each of the test loads on each of the three sites are shown in Figures 46-54. The comparisons are actually a comparison of a predicted deflection basin and a measured influence line. The data shown are for movement of the test load in a line parallel to the centerline of the runway. Also shown on the graphs in Figures 46-54 are the data taken with the test load as they were moved transversely to the runway centerline at each site.

Slab Theory

41. The second theoretical methodology used for analysing the pavement is slab theory (Ref 11, 12). Considerations with slab theory are offered as an addition to the elastic layer analyses. Extensive destructive testing is required for evaluation with slab theory, therefore its application here is only as extensive as the nondestructive testing allows really applicable. No testing of inplace k-values was performed in the field. Also the nature of the pavement structure is such that a k-value of the built-up layers (subbase & subgrade) maybe somewhat misleading.

Composite k-value determination

42. In an earlier study (Ref 9), deflection tests were made on the pavement of Runway 4R-22L using the Benkelman Beam. These data were used together with slab theory to evaluate a composite k-value of the subgrade, subbase and base layers. The k-value on top of the CAM layer from this study was 420 psi/in. Similarly, in this research, the deflection measurements from the WES Vibrator were used together with slab theory and a current composite k-value was determined. This was accomplished by developing a theoretical relation shown in Figure 55 for the WES Vibrator load on the pavement under study and entering it with the measured deflection (Figure 55 is based on computations using discrete-element slab code). The theoretical k-value for the composite of the layers in the pavement foundation was 470 psi/in.

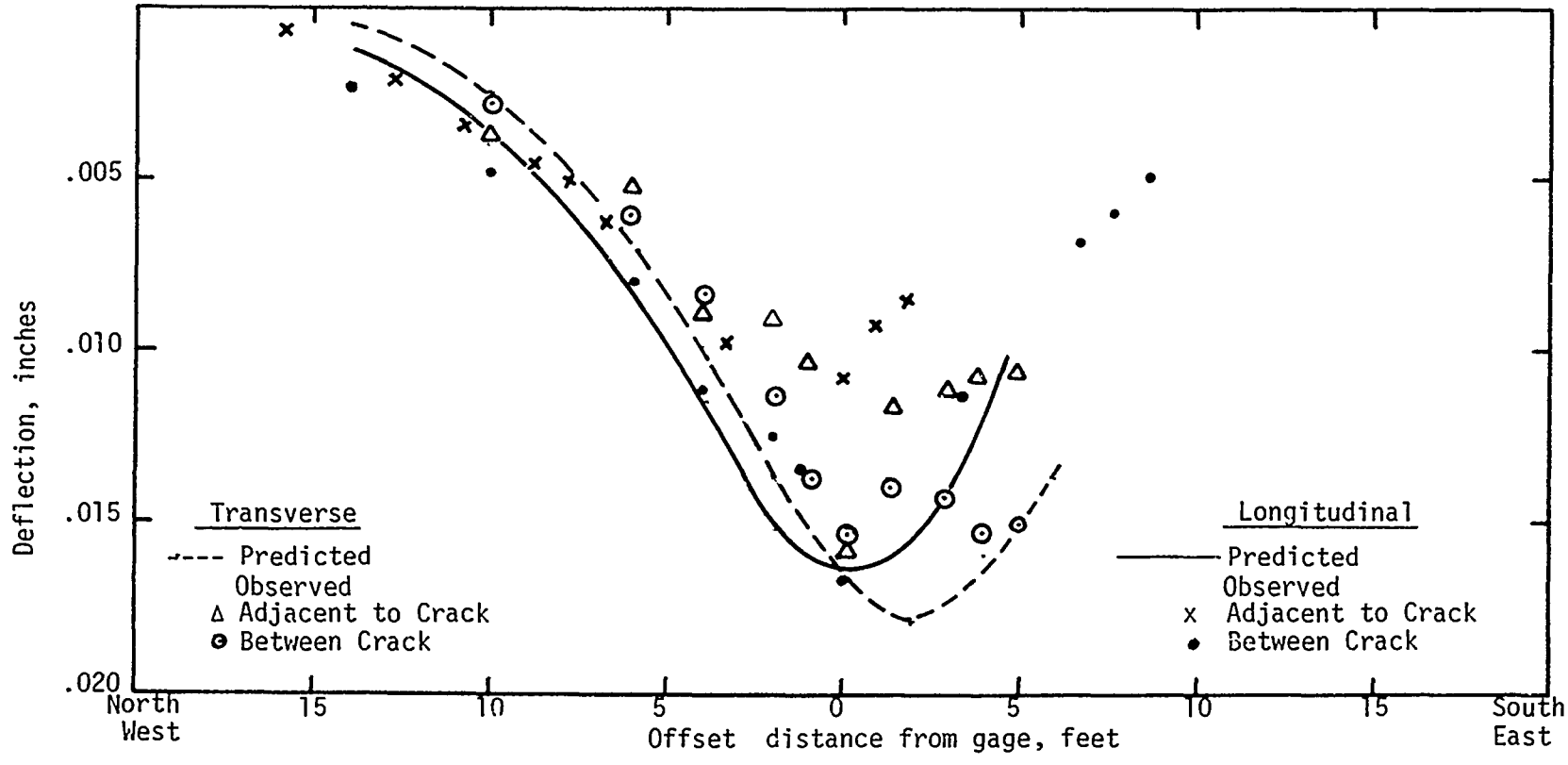

Figure 46. Comparison of predicted and observed deflections for the plate load at Site 1.

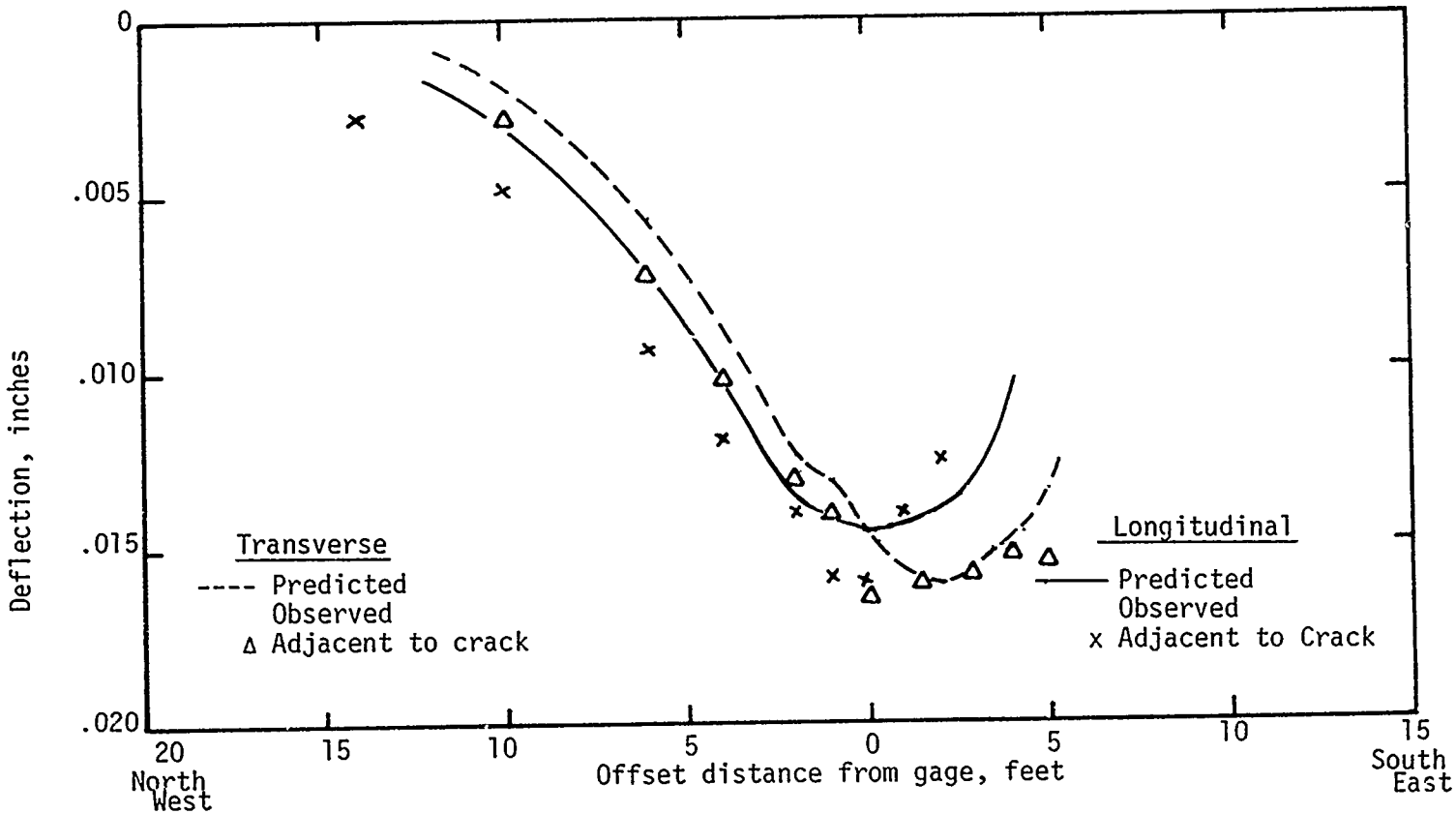

Figure 47. Comparison of predicted and observed deflections for the plate load at Site 3.

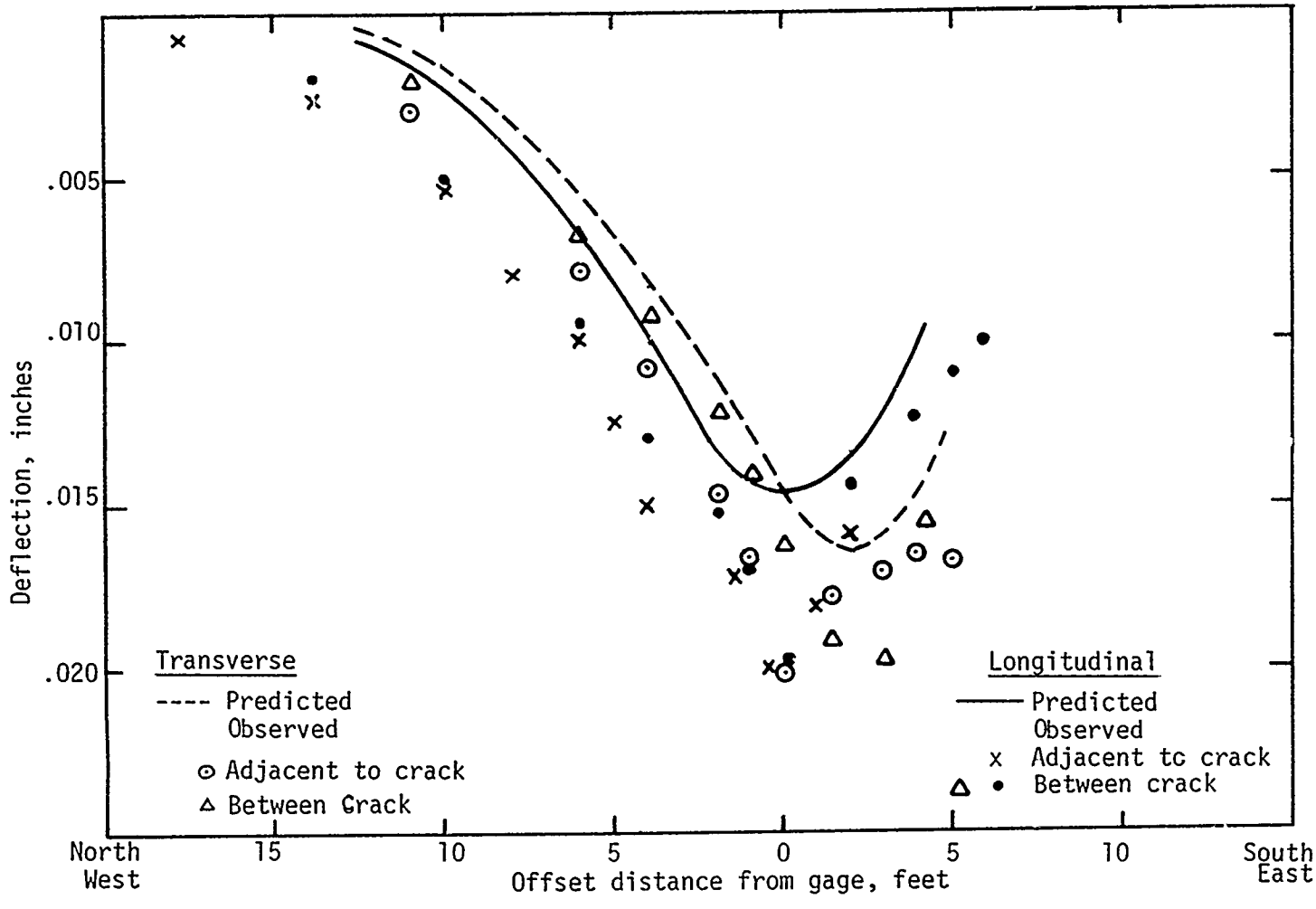

Figure 48. Comparison of predicted and observed deflections for the plate load at Site 4.

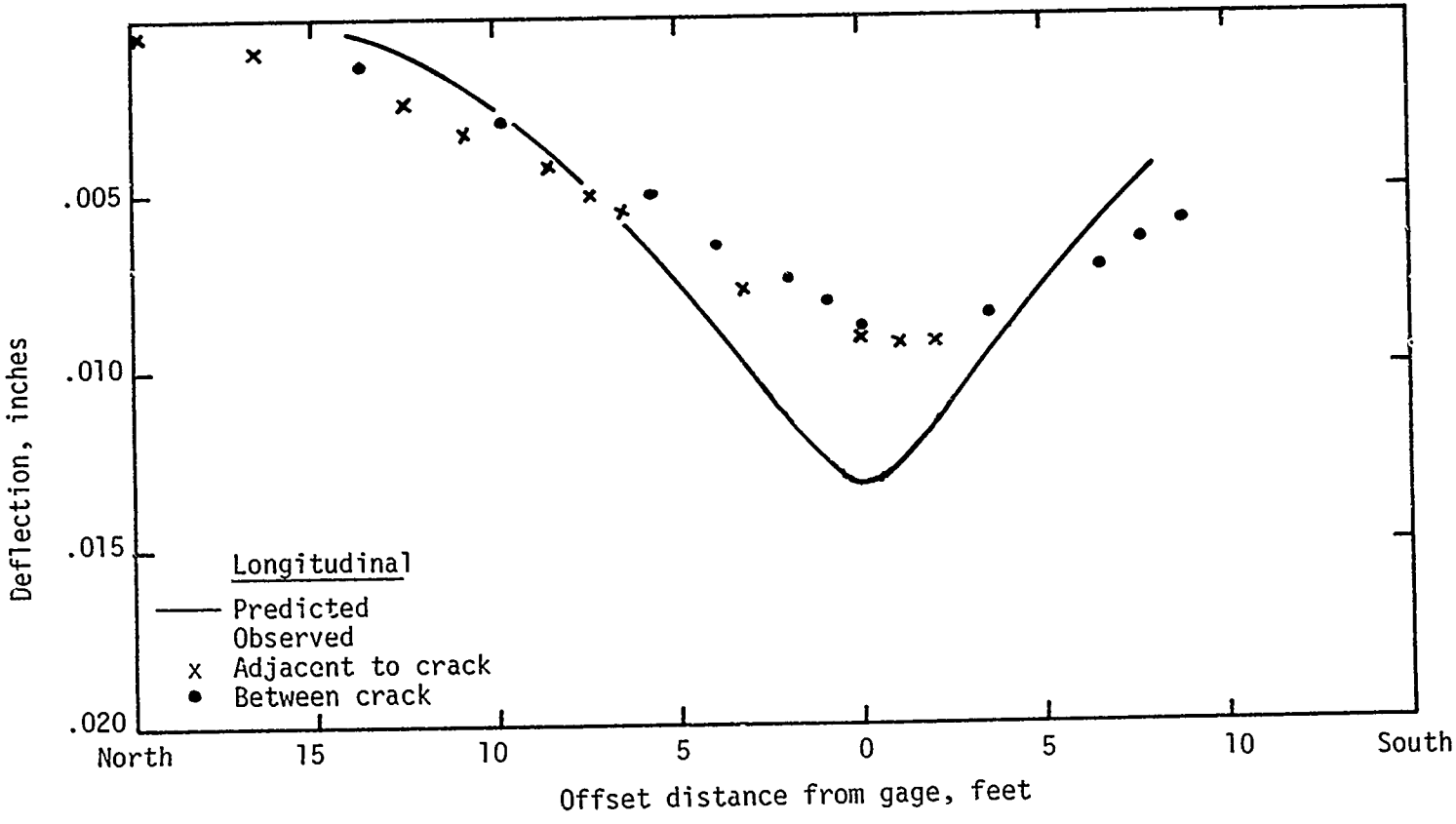

Figure 49. Comparison of predicted and observed deflections for the B727 load at Site 1.

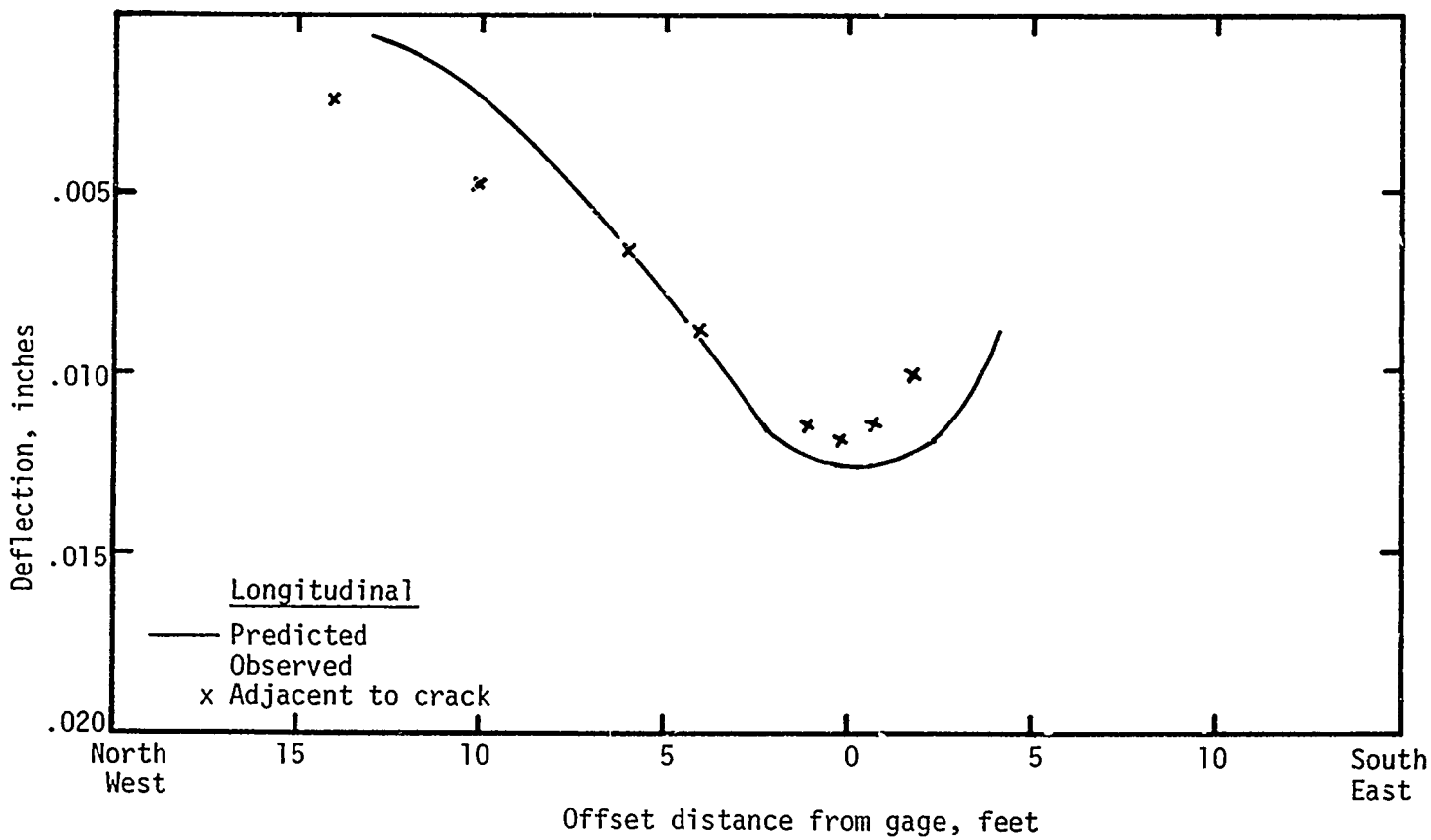

Figure 50. Comparison of predicted and observed deflections for B727 load at Site 3.

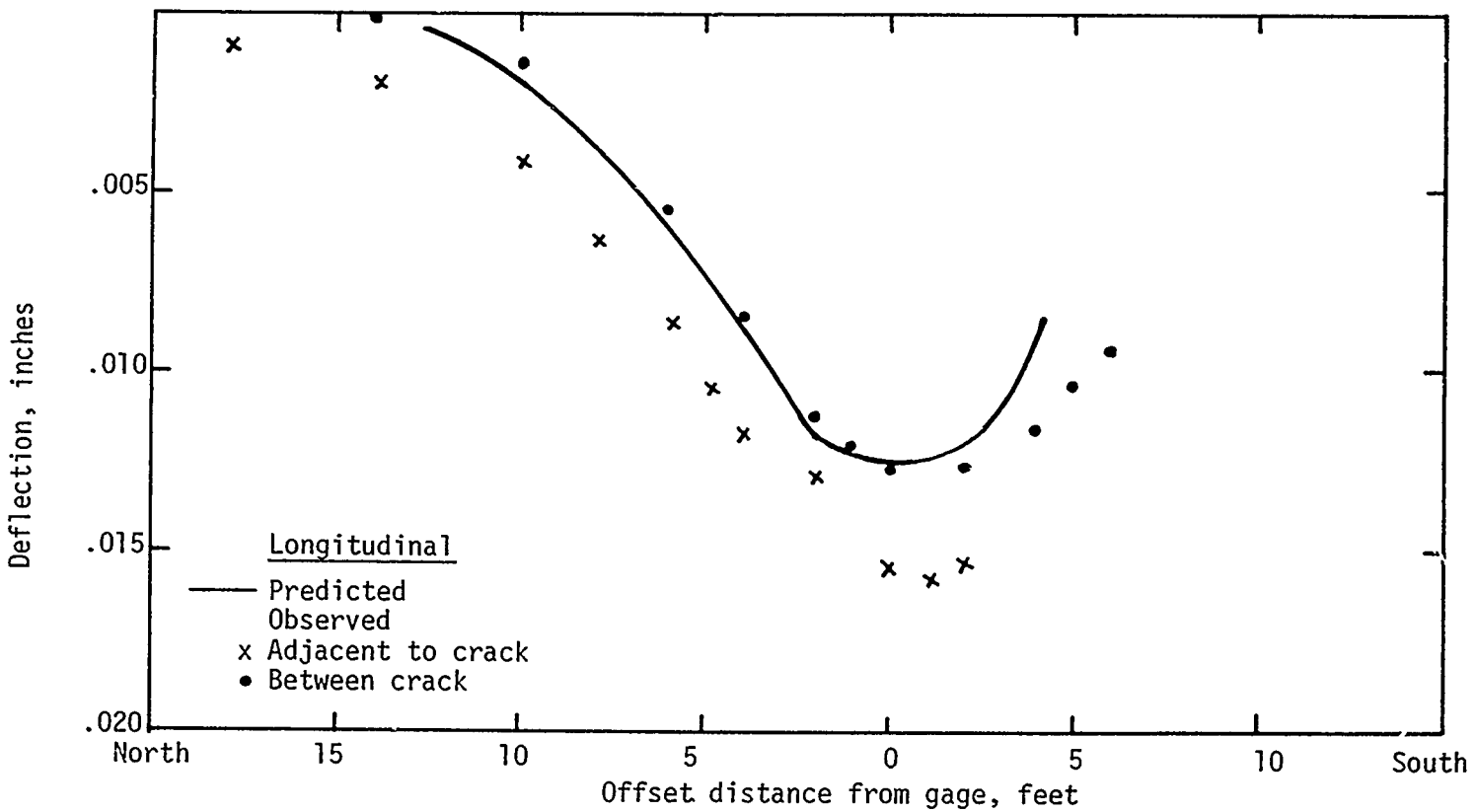

Figure 51. Comparison of predicted and observed deflections for B727 the load at Site 4.

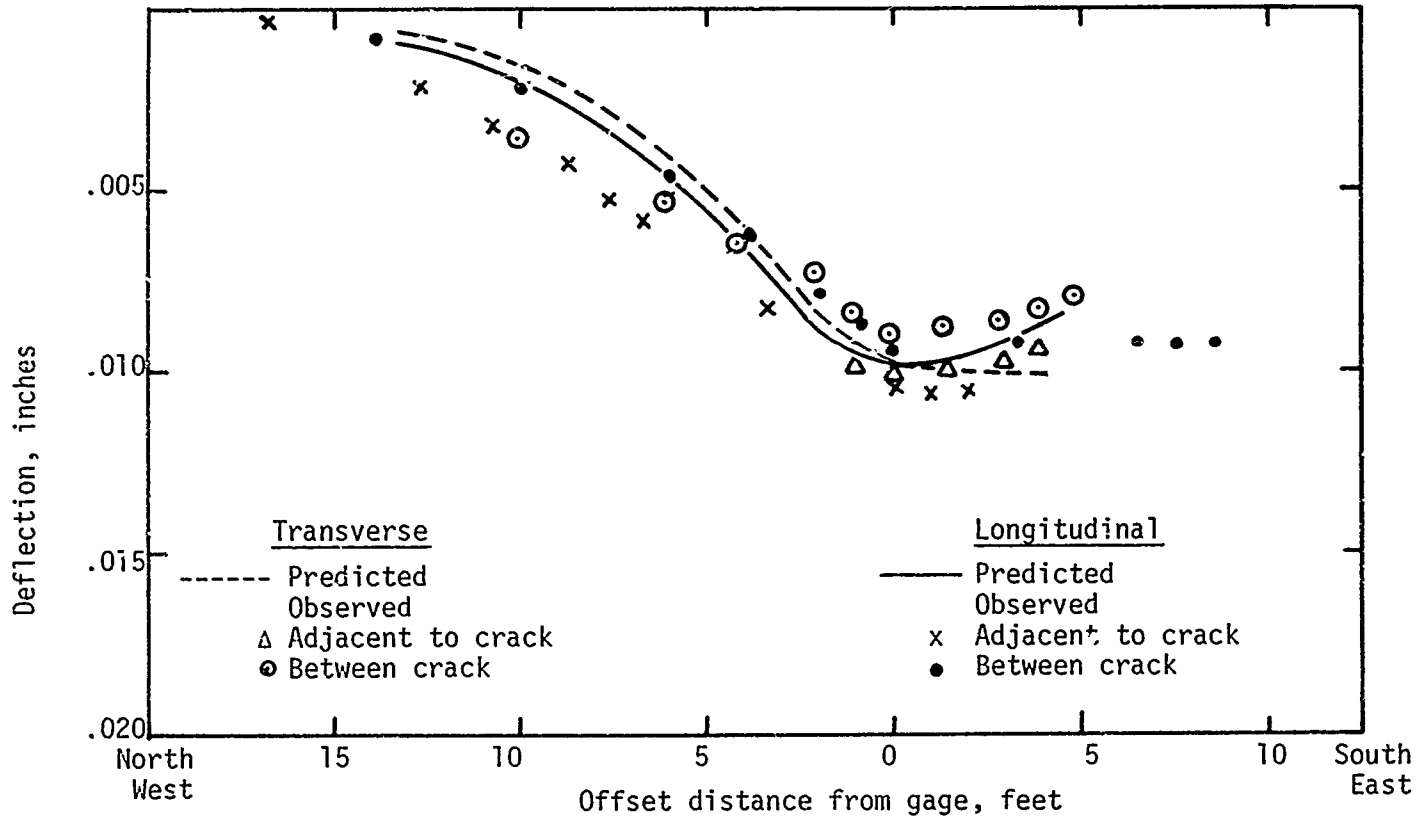

Figure 52. Comparison of predicted and observed deflections for the tug (B747) load at Site 1.

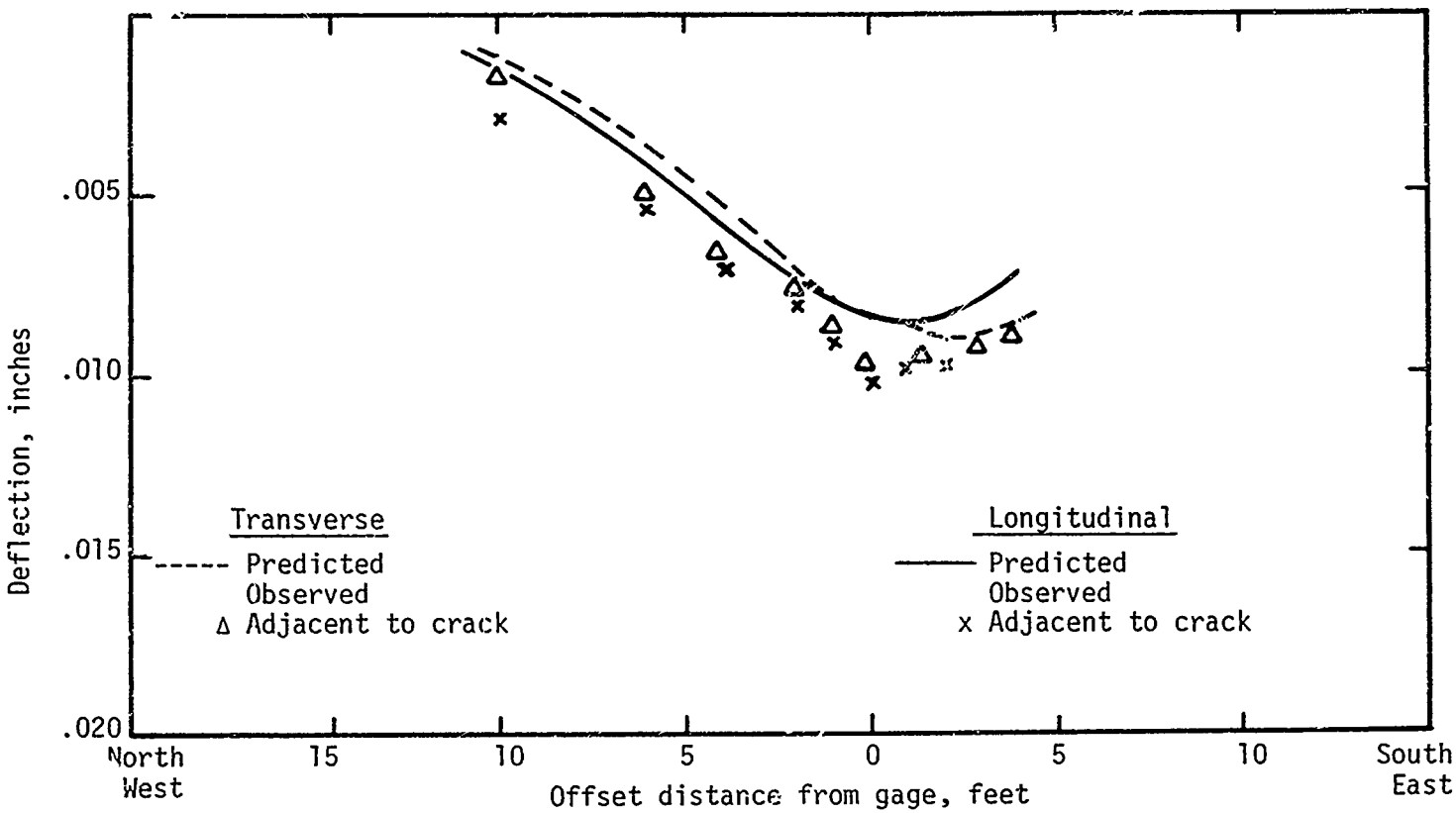

Figure 53. Comparison of predicted and observed deflections for Tug (B747) load at Site 3.

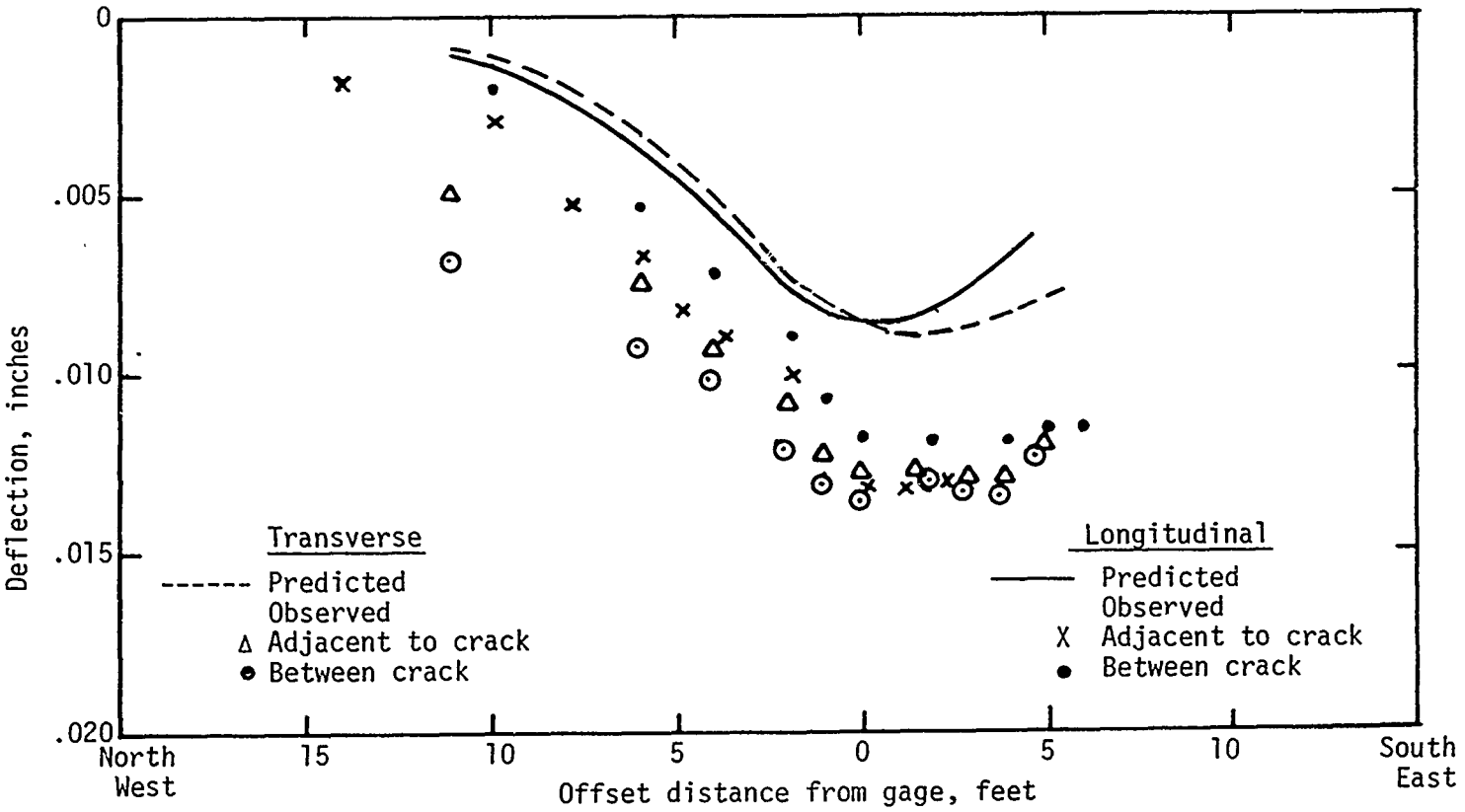

Figure 54. Comparison of predicted and observed deflections for the tug (B747) load at Site 4.

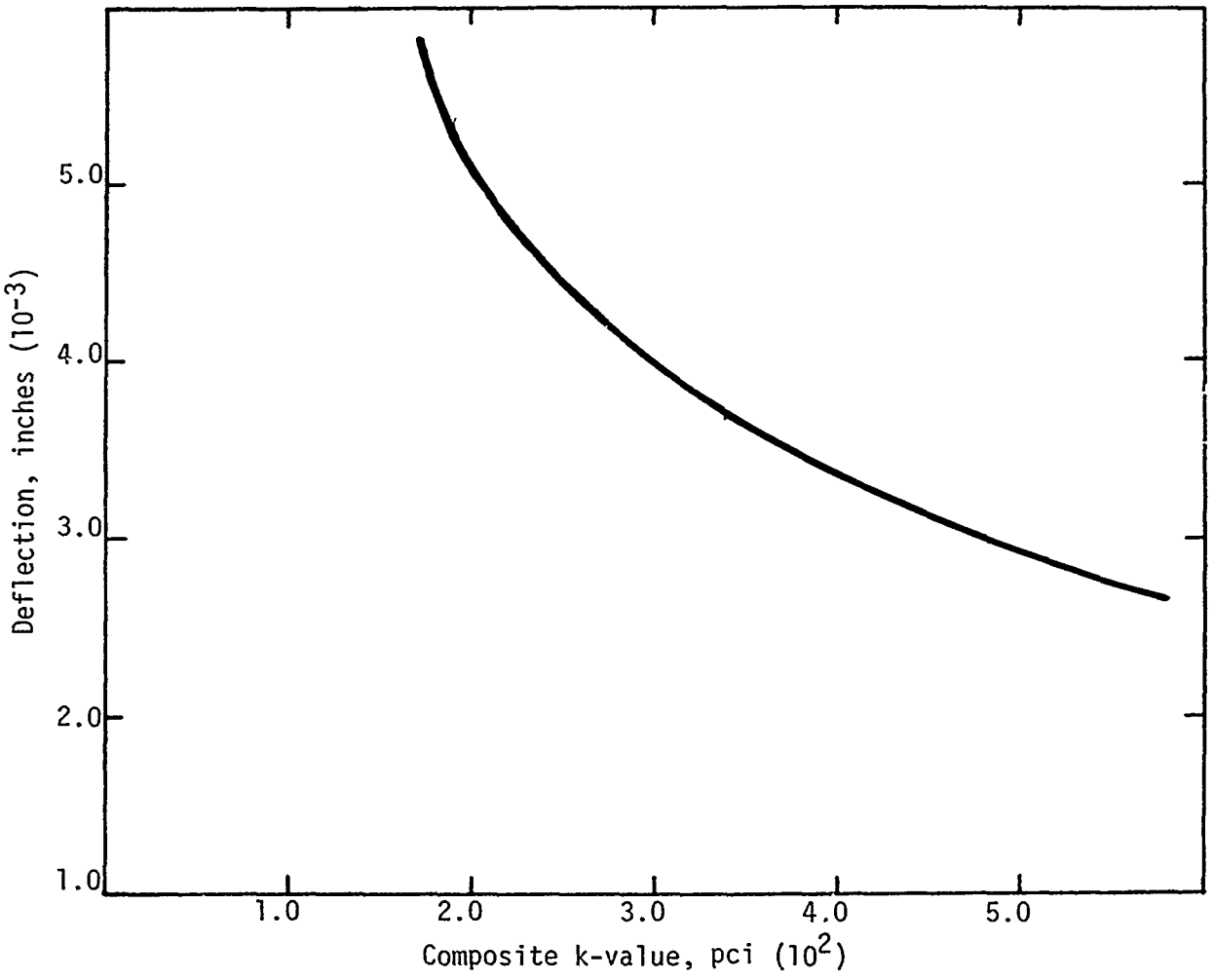

Figure 55. Determination of the composite k-value from deflection using the WES Vibrator.

43. It is believed that the k-value is stress sensitive as is the resilient modulus of the clay subgrade. Thus, the resilient modulus for the subgrade for each of the test loads (Table 10) was used together with the subbase design chart from the CRCP design manual (Ref 7) to develop composite k-values. In this analysis, the granular layer was treated as subgrade as the technique used can handle only one subbase layer and in this case the CAM was considered. This was accomplished by converting resilient modulus values to k-values (natural subgrade only). For Site 3 the composite k-values were as follows:

WES Vibrator Plate Simulation of B727	470 psi/in 420
B727	437
Tug (B747)	448

Because of the very close results of k-value from the various analyses a single value was selected at 420 psi/in as was determined in previous investigation using NDT and similar analysis techniques.

Deflection Prediction for Test Loads

44. Using slab theory (Ref 11, 12) along with the portland cement concrete thickness and modulus of elasticity, the deflections were predicted for each of the test loads for the respective sites. Figures 56-64 show the comparison of the predicted deflections with the observed data for each test load for each site. The comparisons of the observed and computed deflections in Figures 56-64 are discussed and interpreted in the next chapter.

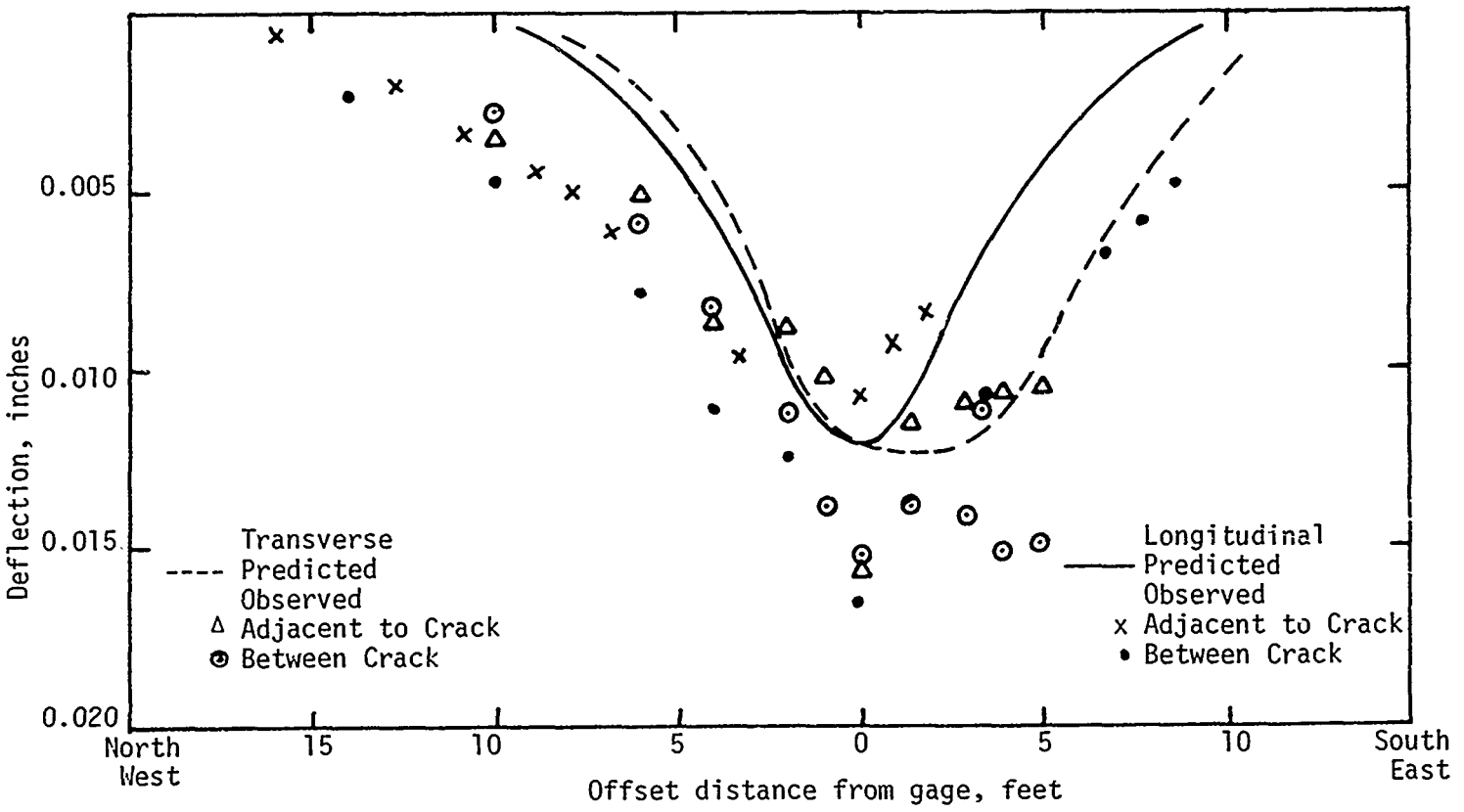

Figure 56. Comparison of predicted deflections, using plate theory, and observed deflections for the plate load at Site 1.

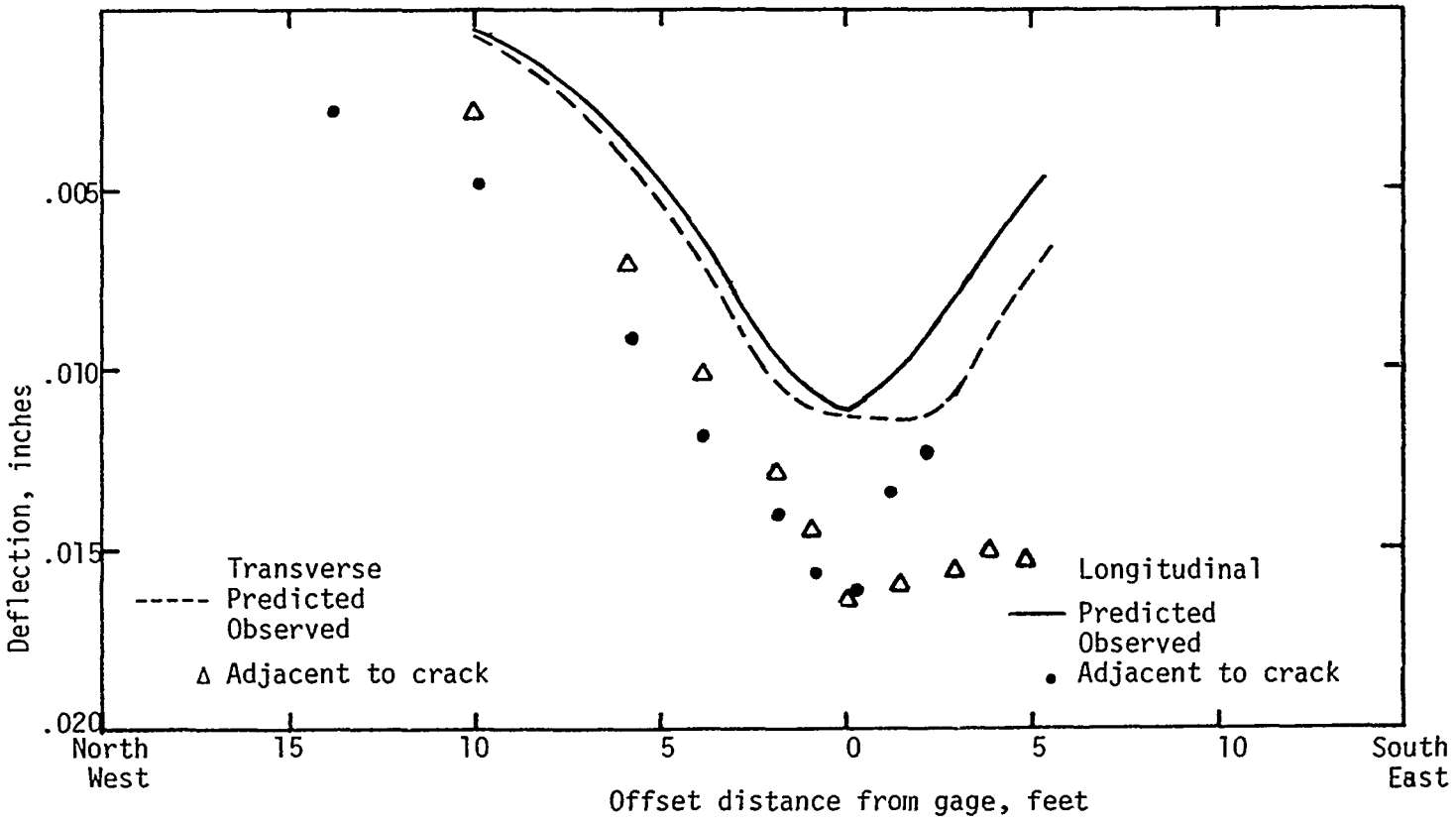

Figure 57. Comparison of predicted deflections, using plate theory, and observed deflections for the plate load at Site 3.

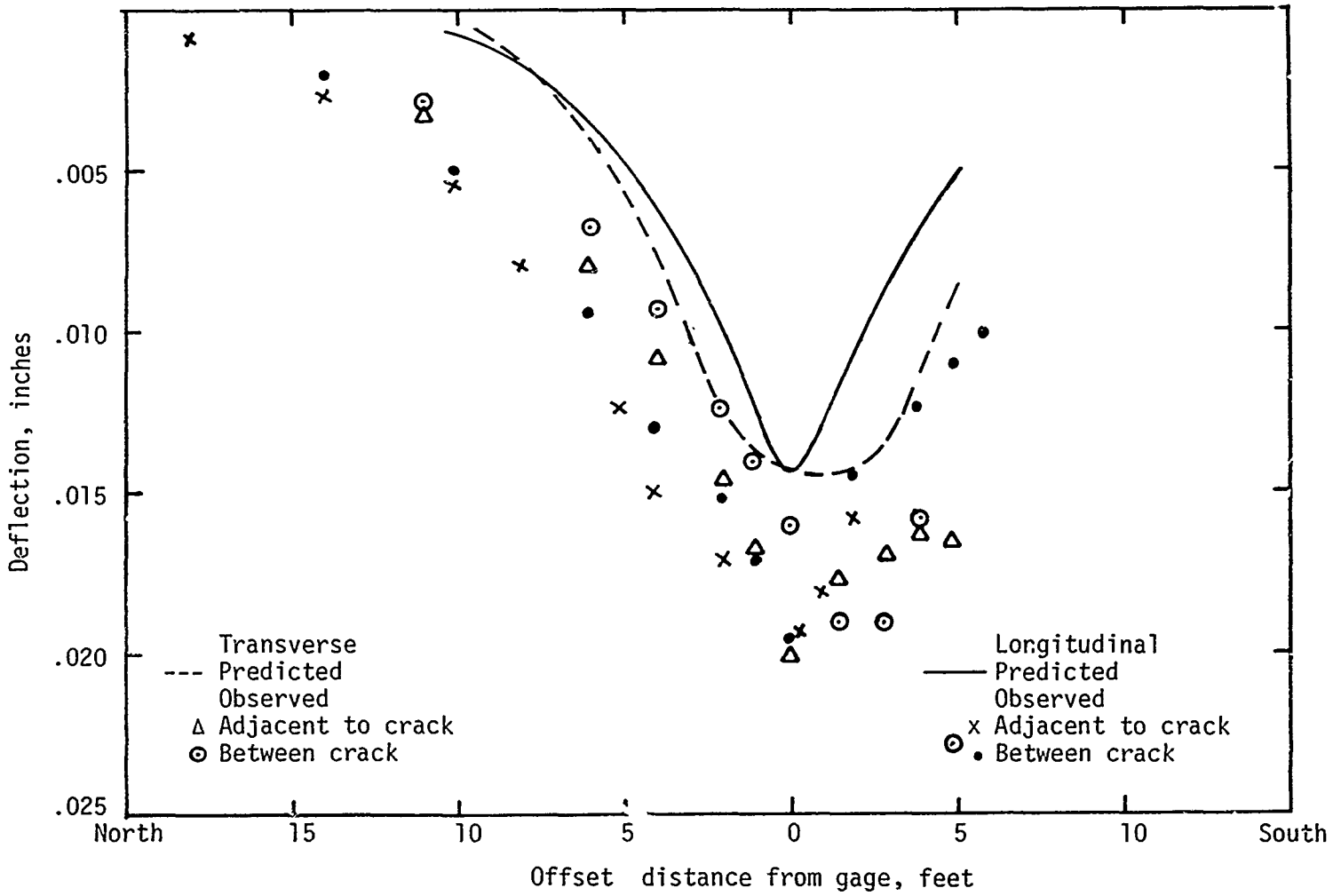

Figure 58. Comparison of predicted deflections, using plate theory, and observed deflections for the plate load at Site 4.

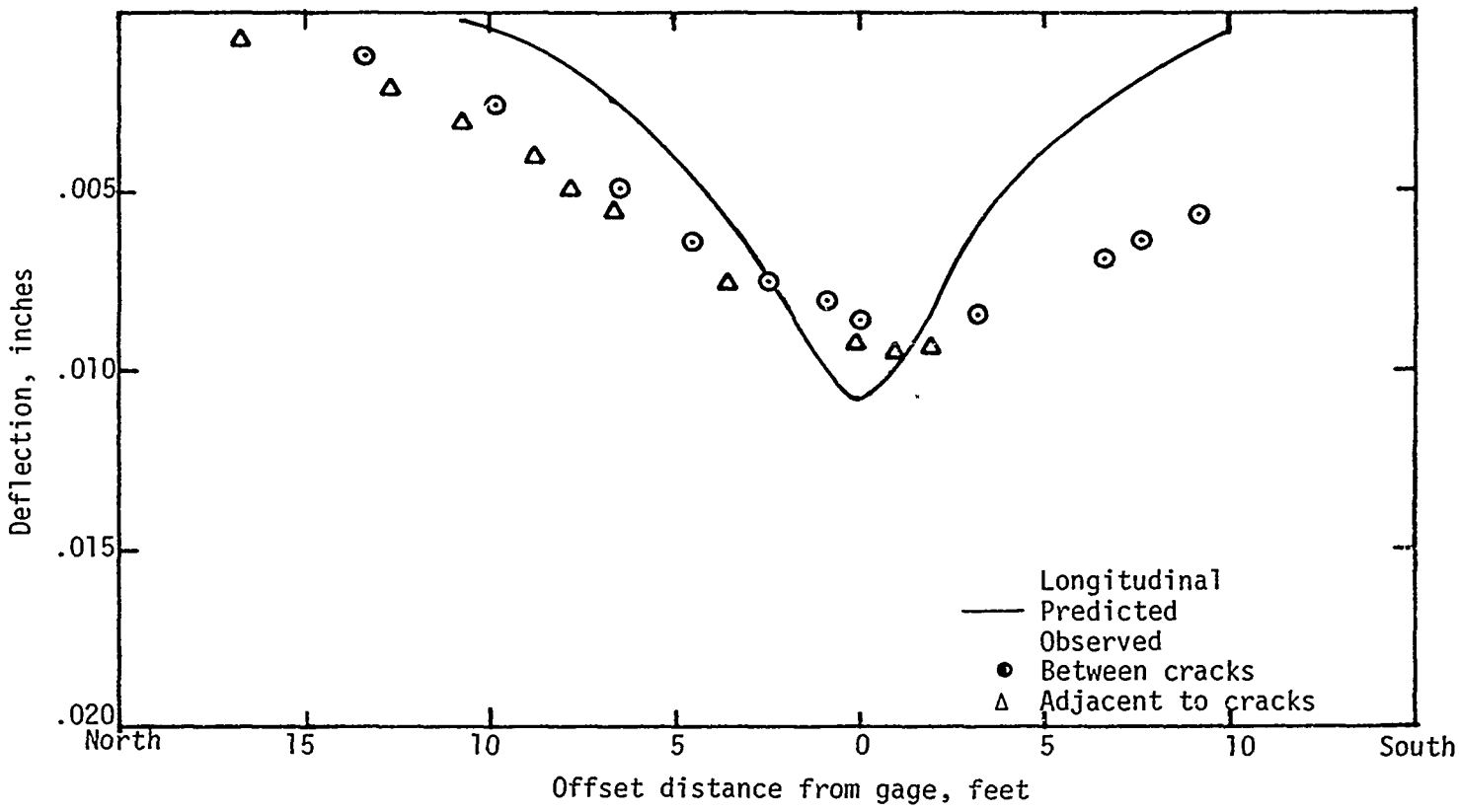

Figure 59. Comparison of predicted deflections, using plate theory, and observed deflections for the B727 load at Site 1.

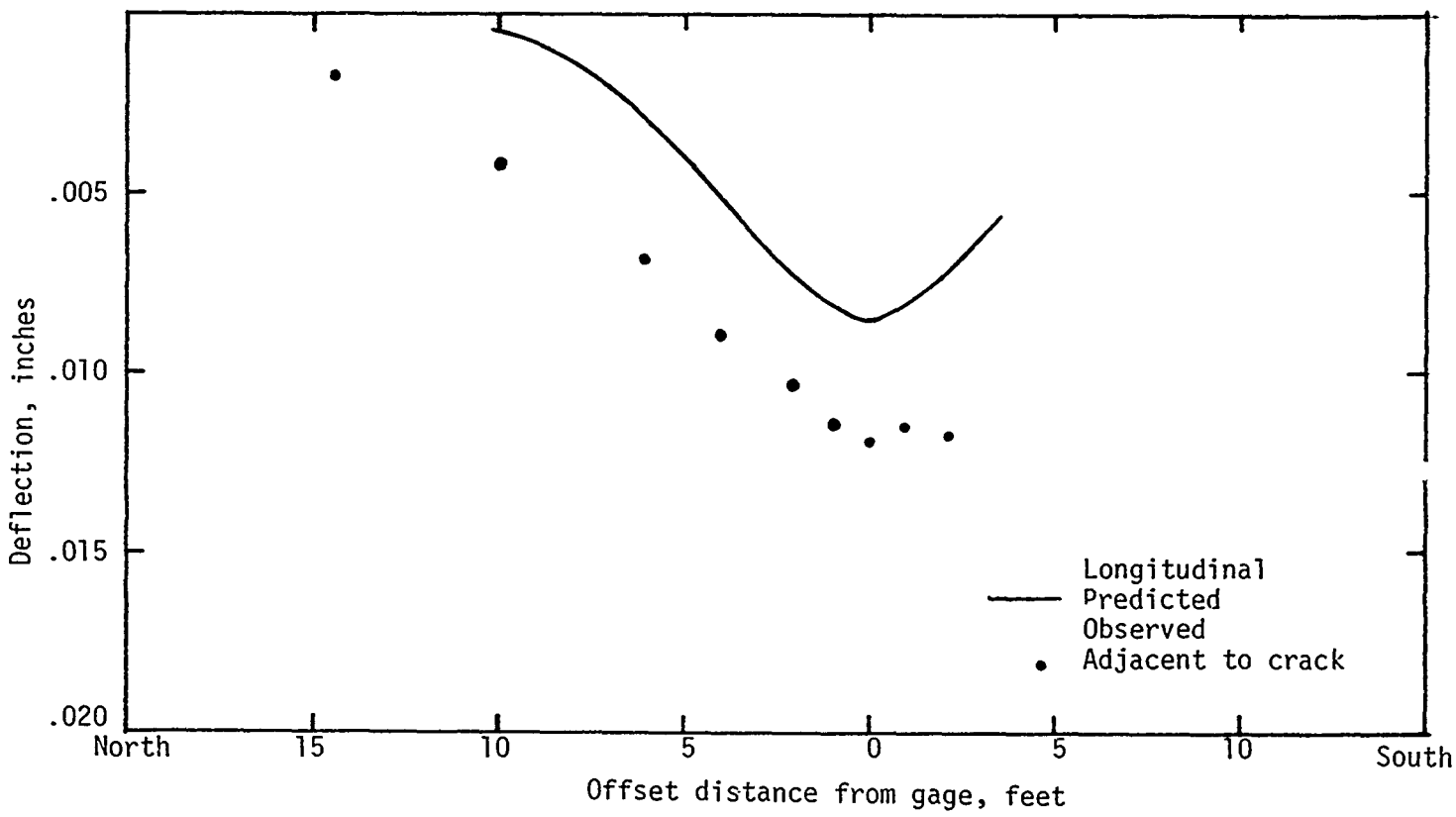

Figure 60. Comparison of predicted deflections, using plate theory, and observed deflections for the B727 load at Site 3.

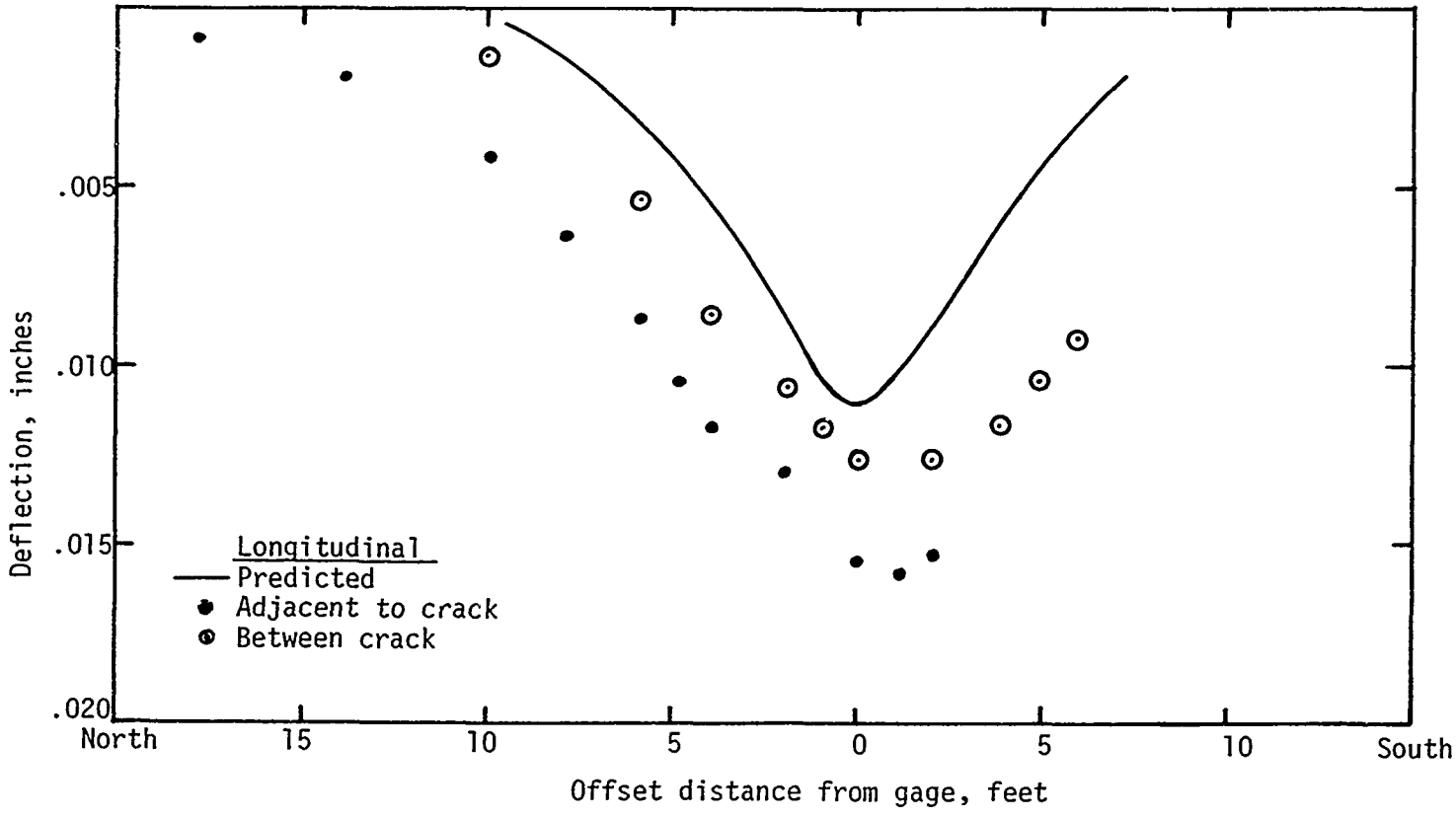

Figure 61. Comparison of predicted deflections, using plate theory, and observed deflections for the B727 load at Site 4.

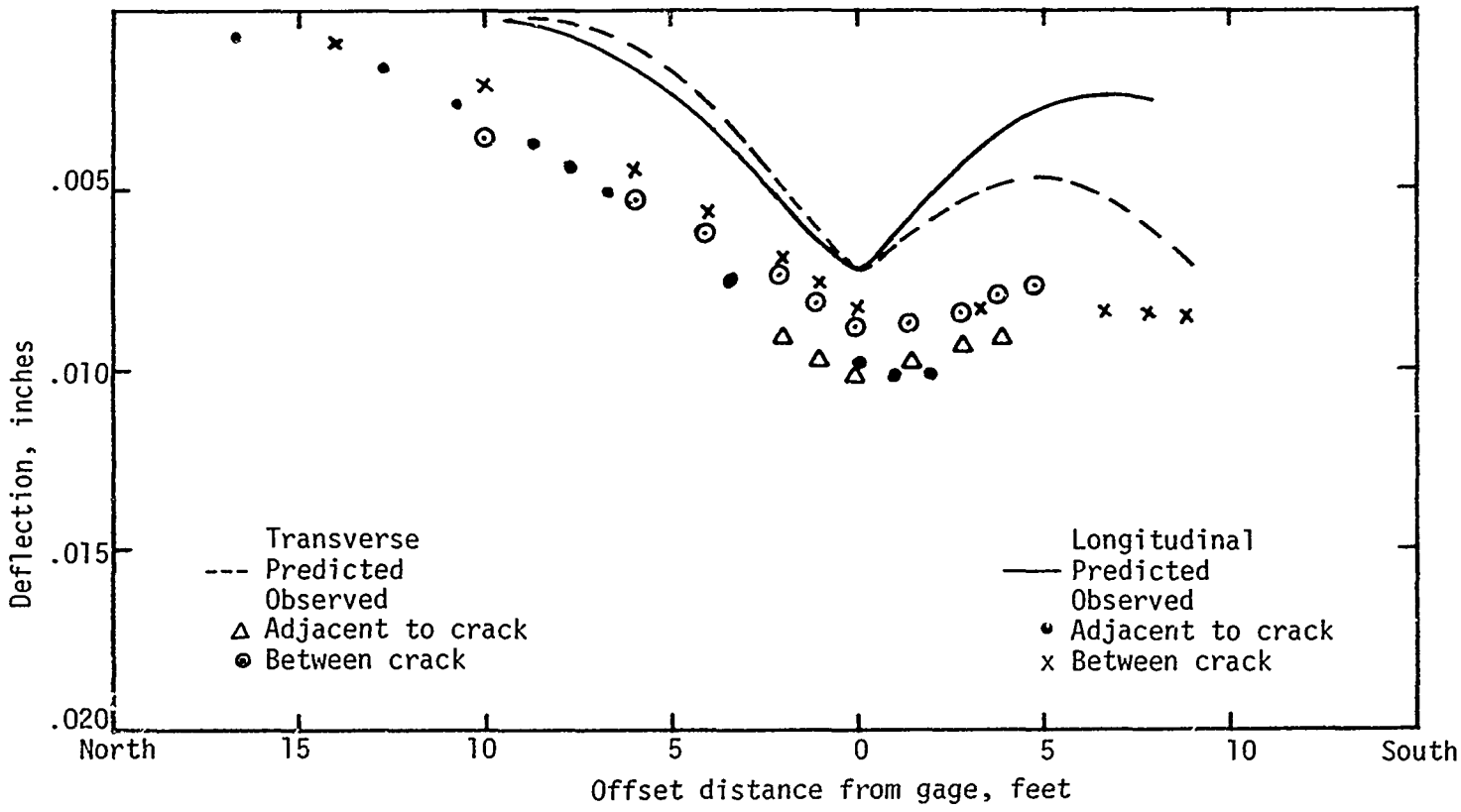

Figure 62. Comparison of predicted deflections, using plate theory, and observed deflections for the tug (B747) load at Site 1.

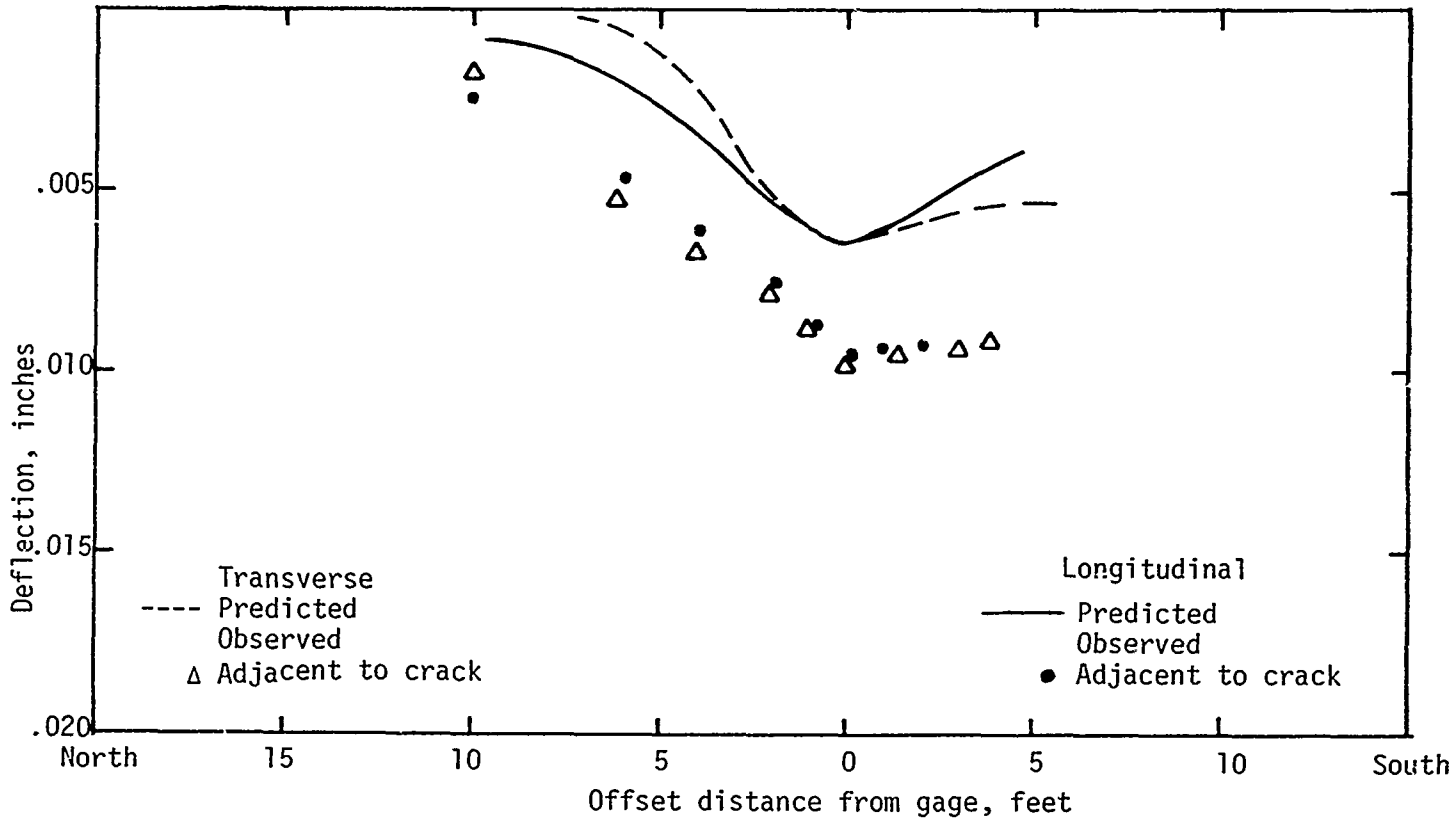

Figure 63. Comparison of predicted deflections, using plate theory, and observed deflections for the tug (B747) load at Site 3

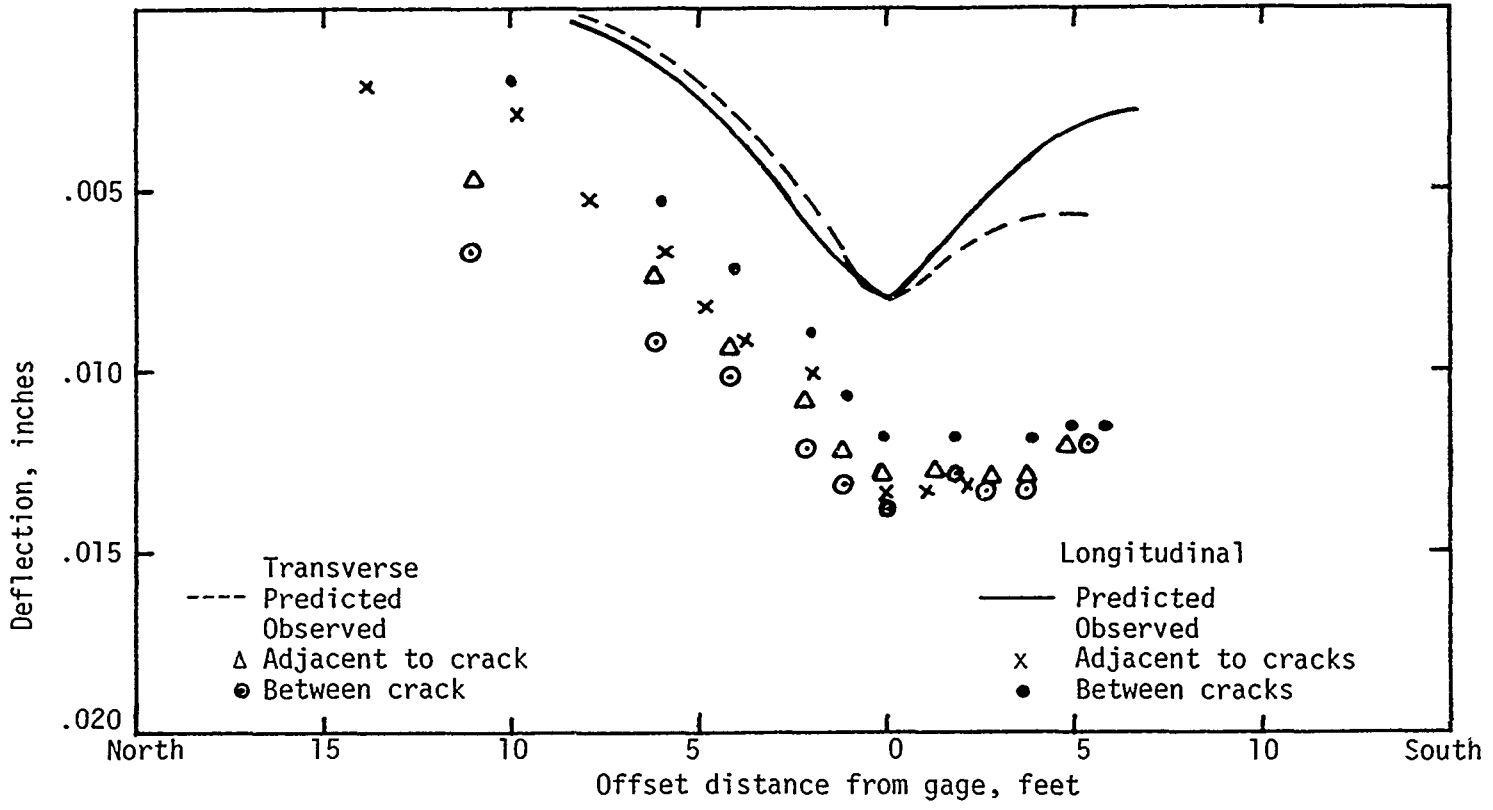

Figure 64. Comparison of predicted deflections, using plate theory, and observed deflections for the tug (B747) load at Site 4.

PART IV DISCUSSION AND INTERPRETATION OF RESULTS

45. As discussed in Part I, one objective of this effort is to establish creditibility for the proposed CRCP design procedures (Ref 6, 7). The following paragraphs describe, for the two analytical models presented in the procedure, their ability to predict the behavior of the pavement based on the resilient modulus modification. The differences in observations and predictions are discussed for each theory. The data are also interpreted relative to the design procedures.

Comparison of Observed and Predicted Deflections

46. The following paragraphs present the comparisons of the observed and predicted deflections. The differences relative to each are discussed.

Elastic Layer Theory

47. In the application of elastic layered theory, several principles offered in the CRCP design manuals (Ref 6, 7) were applied. These being the consideration of stress sensitivity in the subgrade and also the depth of subgrade. By applying both these principles, it was possible to both predict the deflections as well as the shape of the deflection basin. In this analysis, all the deflections were predicted within one standard deviation of the measured WES Vibrator measurements. Furthermore, the predicted deflections were greater than the measured deflections in some cases and less than the measured values in other cases. The actual comparison of the observations and predictions are made in Figures 46-54, where the data are plotted together with the predicted basin.

48. When the concept of subgrade depth was not applied, the deflection predictions under the load were similar to the measured deflections except that the predictions in this case were consistently less than the measured values. This difference was initially rationalized on the basis that elastic layer theory does not consider stiffness loss due

to cracks in a pavement structure. The theory does not consider material variability with depth as exists in the field (Part II). The observed deflections at the cracks were slightly greater than those between the cracks. The most important reason for applying the subgrade depth principle was that without it, the shape of the predicted deflection basin gave a poor comparison to the measured influence line. An example of the poor comparison of deflection basin measurements and predictions is shown in Figure 65. This is considered significant because the shape of the deflection basin is indicative of the state of stress in the pavement. The model could be predicting the deflection under the load accurately but still be a poor stress prediction model. This problem is alleviated by considering the depth of subgrade as a design parameter, which is a conservative approach.

49. The consideration of the concept of subgrade stress sensitivity is important as evidenced by the range in subgrade modulus values determined for the wide range of loadings (Table 10). A direct comparison of the important of stress sensitivity is made in Table 11 where the measured deflection is compared with the deflection predicted with and without consideration of stress sensitivity. The comparison of measured and predicted deflections in Table 11 shows that consideration of stress sensitivity was not important in all cases, however it was significant in six of the nine comparisons, thus is believed to be a valid technique.

Slab Theory

50. In the application of slab theory, it is impossible to give consideration to the components of the slab supporting medium other than the k-value. The k-value of the composite support for runway 4R-22L was estimated by several means. All three of these techniques yielded about the same k-value (420-470 psi/in). These comparisons extend credibility to the methods of estimating k-value, but do not explain the poor comparison of observed deflection and measured deflection (Figures 56-64). There may be several reasons for the poor comparisons,

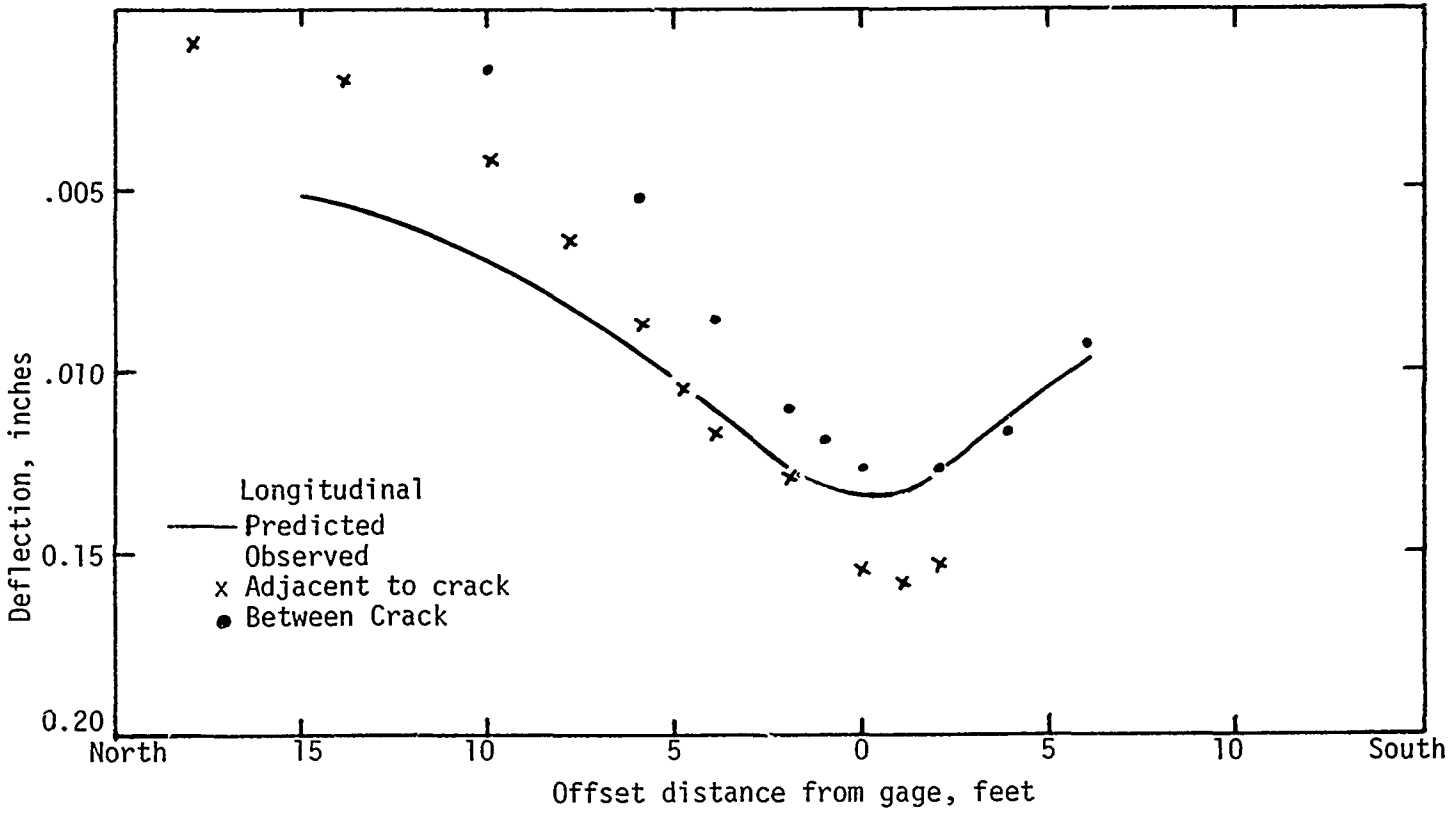

Figure 65. Typical comparison of predicted and observed deflections (B727 load at Site 3) that occurred in the first analysis(with reduced CAM modulus and w/o rigid layer).

Table 11
Comparison of Deflection Measurements and Predictions
With and Without Stress Sensitivity Considerations

Site	Load		Average Measured Deflection (inches)	Predicted Deflections, (inches) With Stress Sensitivity	Predicted Deflections, (inches) Without Stress Sensitivity
	Plate	A*	.01548	.01612	.01390
		B**	.01600		
1	B727	A	.00942	.01400	.01230
		B	.00875		
	Tug (B747)	A	.01002	.00983	.00900
		B	.00868		
	Plate	A	.01639	.01457	.01270
		B	-		
3	B727	A	.01191	.01352	.01220
		B	-		
	Tug (B747)	A	.00968	.00848	.00850
		B			
	Plate	A	.01984	.01462	.01280
		B	.01783		
4	B727	A	.01557	.01349	.01220
		B	.01287		
		A	.01297	.00847	.00840
		B	.01203		

*A - Adjacent ot Crack Measurements
**B - Between Crack Measurements

these being:

a. K-value is based on a uniform, homogeneous, semi-infinite media.

b. The response of a system of layers beneath a slab to load may or may not be the same as the assumption in No. 1 above, and,

c. Excessively large k-values may be misleading because the stress sensitivity properties of k-value are not well established (data presented was on the basis of elastic moduli considerations).

51. It has been shown in previous parameter studies that bending moments or stresses are not very sensitive to k-values greater than 250 or 300 psi/in (Ref 22). Deflection is, however, significantly influenced by the k-value as illustrated in Figure 55. The observed deflections and predicted deflections noted in Figures 56-64 for the three sites reflect significant differences in deflection magnitude, but excellent comparisons of basin shapes. In a previous analysis of highway pavements, it was also found that in most cases, the measured deflection was larger than that computed using slab theory (Ref 23). This indicates for high values of composite k-value that the stresses (bending) would be reasonably accurate, even though the magnitude of deflection predicted was low.

Design Implications of Data

52. The following paragraphs relate to the various elements of the design procedure which are reinforced or substantiated by the data and analyses developed in this research.

Subbase Design

53. The subbase design chart developed previously (Ref 5,7) was checked in the analysis of the pavement using slab theory. The composite k-value from the chart (Figure 11, Ref 7) and the k-value determined from the deflection testing and analysis compared well. This not only establishes confidence in the subbase design procedure, but also indicates the resilient modulus correlation with k-value

are reasonable for use with the subbase chart. This is a technique that may be used in subbase design.

Crack Pattern

54. The transverse crack pattern has changed between 1971 and 1975, the two time periods for which data are available. The mean spacing is decreasing as evidenced by the data summarized in Table 4. The crack patterns may continur to change slightly with time as has been observed on CRC highway pavements (Ref 24). The changes which have taken place are obviously related to a continued balancing of temperature stress, shrinkage stress and concrete tensile strength as the changes are distributed throughout the entire runway length. The crack pattern as observed is quite typical of CRC pavement in general. The results of the statistical test (Part II) indicate the distribution of the crack spacings is changing. Since the cracking has occurred uniformly along the runway length, it is reasonable to assume that cracking attributed to load stresses is very minimal. This is also substantiated by the very small stresses predicted for the large test loads (Table 12).

55. In the survey, a few longitudinal cracks were noted. This is not surprising because it was also found that in some of the borings that the CRC slab and the CAM subbase were bonded very securely. This is a significant factor in explaining longitudinal cracking as well as the increased number of transverse cracks. The longitudinal cracks noted were about the same width at the surface as the transverse cracks. This implies that the transverse reinforcement is needed and that it is at least adequate. There was no structural damage observed on the runway nor was there any predicted for the stress levels in the pavement.

Table 12

Maximum Tensile Stress That Occurs
At The Bottom Of The CRC Layer

Site	Type of Load	Maximum Tensile Stress (psi)
	Plate	189
1	727 AC	156
	Tug (747)	123
	Plate	194
3	727 AC	180
	Tug (747)	127
	Plate	205
4	727 AC	192
	Tug (747)	138

PART V SUMMARY

56. The general objective of this report was to check the reliability and/or recommend any changes in the concepts and techniques used in the development of the proposed design procedures for CRC pavements and overlays. The data collected from runway 4R-22L, O'Hare International Airport and the analyses of these data form the basis for the following conclusions and recommendations.

Conclusions

57. Based on the analyses of the data (observations versus predictions) the design method, in general, is reliable. The following conclusions are offered pertaining to the components of the design method (pavement evaluation, materials characterization, load analysis models, and reinforcement).

Pavement Evaluation

58. The following conclusions are offered relative to pavement evaluation.

a. The methodology for pavement evaluation and design as configured with nondestructive testing is both sound and workable as evidenced by the comparison of observations and analyses.

b. Nondestructive testing used with the method may be of a wide variety, e.g. the loads may range from 1,000 lb (Dynaflect) to 10,000 lb or greater (WES Vibrator).

c. As observed from the analysis moisture stabilizes with time. Thus, characterization on an existing pavement for an overlay design is a sound principle since it presents field conditions. In contrast, the pavement design does not recognize this change in moisture content with time. By obtaining additional data in the future, the method could be easily changed to account for this moisture stabilization.

Materials Characterization

54. The following conclusions are offered relative to materials characterization.

a. The development of modulus or subgrade reaction values from nondestructive tests and slab theory analyses compare very well with

k-values determined from the subbase design chart in the design manuals, thus establishing confidence in the subbase design.

b. It is believed that the stress sensitivity characteristics of subgrades should be accounted for in design analyses, otherwise, the stress predictions and damage predictions may be erroneous.

c. The depth of subgrade layers when less than ten feet should be considered in design to properly model the real pavement with layer theory.

Analytical Models

60. The following conclusions are offered relative to the analytical models.

a. The analytical response models used in the proposed design procedures (Refs 11, 12, 13) i.e. elastic layer theory and slab theory, are applicable for continuously reinforced concrete pavements,

b. The performance model used in the design methods cannot be checked by an evaluation of a new pavement. Validation is not offered other than that the analysis method used to develop the model is rational and applicable, thus, the model must be used on the merits of its data base.

c. The theoretical development of composite k-values for layered base/subbase/subgrades are valid but when used in conventional slab theory predicted deflections and observed deflections do not match. K-values of composite layers are not in harmony with the assumptions associated with k-value, furthermore, k has little meaning when evaluated experimentally, particularly on layered systems.

d. The elastic models are applicable when good load transfer is achieved as was apparent in this case, since the deflection adjacent to the cracks was approximately equal to the deflection between cracks.

e. The absence of small crack spacings indicates that the slabs are not overstressed as would be expected for a runway with few load applications.

Reinforcement Design

61. The following conclusions are offered relative to reinforcement design.

a. The narrow crack width measured shows adequate longitudinal steel. Also, the deflections, between and adjacent to cracks which are approximately equal, show good load transfer. Therefore, the longitudinal reinforcement on this project is adequate.

b. Although crack spacing is critical in CRCP, the present design method does not predict mean crack spacing or change in crack spacing with time. From further evaluation and measurements of runway 4R-22L, it would be possible to incorporate, in the design method, the crack spacing due to internal (shrinkage and thermal effects) and external (wheel loads) loading conditions.

c. The longitudinal cracking which was very small on runway 4R-22L, should be checked in future years to indicate if there is a need for transverse steel.

Reliability of Analytical Models

62. The design procedures for CRC airfield pavement make use of the two basic theories, elastic layer and slab theory (Ref 11, 12, 13). These analytical models have been used to evaluate the CRC pavement on runway 4R-22L at O'Hare and the results of the predictions and observations are believed to be acceptable. The magnitude of deflection is satisfactorily predicted by elastic layer theory and the shape of the deflection basin is accurately predicted by both layer and slab theory. The checks performed indicate the reliability to be good for both models. Elastic layer theory is utilized for both deflection and stress analysis (Ref 6) while slab theory is used only for stress analysis (Ref 7). Each model was found reliable for its application in the design procedures.

Reliability of NDT

63. The feasibility of using nondestructive testing (NDT) for characterization of existing pavement structures is demonstrated by

thegood comparisons between observed and predicted deflection. This is true for both the heavy load, WES Vibrator, and the lighter test load, Dynaflect, as evidenced by the very nearly identical subgrade properties determined from deflection measurements (Table 10). The application of NDT is validated by the results presented and adds significant creditibility to both the CRC pavement design procedures as well as the analytical models used in them.

Recommendations

64. The following recommendations are offered which relate to various items which would further enhance the CRC airfield pavement design procedures.

a. Observations of performance must continue on CRC airfield pavement to verify or form the basis for changing the performance model used in the design procedures.

b. Runway 4R-22L should continue to be monitored for deflections (NDT), damage, and crack spacings at the ages of 5, 8, and 12 years. Deflections measurements with the simulated 727 (plate) should be repeated also.

c. Although not a part of the scope of this research, the reinforcement design procedure should be revised to reflect the effects of crack spacing and the crack width as recent technological developments will now permit (Ref 26, 29).

d. Design procedure should be changed to reflect the effects of seasonal variations on properties of materials.

e. Methods or techniques are noted for considering the effect of variations in materials properties on design values as well as the effective elastic properties of cracked layers of cemented paving materials.

f. The design procedures are of necessity very complex and as a result should be completely automated or at least developed into a series of programs for the engineer to interact with, and

g. At the earliest opportunity, the procedures should be applied in real design problems on air carrier airports.

REFERENCES

1. "Continuously Reinforced Pavement News," Continuously Reinforced Pavement Group, Chicago, Winter, 1970.

2. Treybig, Harvey J., "Performance of Continuously Reinforced Concrete Pavement in Texas," Highway Research Board Record 291, pp 32-47, 1969.

3. McCullough, B. F., W. R. Hudson, and Harvey J. Treybig, "Evaluation of Distress on Runway 9R-27L, O'Hare Field, Chicago," A Report submitted to the Committee of Concrete Reinforcing Bar Producer, American Iron and Steel Institute, December 1970.

4. McCullough, B. F., and John H. Frederick, Jr., "Pavement Evaluation Study Runway 7-25, USAF Plant 42, Palmdale, California" for Materials Research and Development, Inc., May 1968.

5. Treybig, Harvey J., B. Frank McCullough and W. Ronald Hudson, "Continuously Reinforced Concrete Airfield Pavement - Volume I, Tests on Existing Pavement and Synthesis of Design Methods", Report No. FAA-RD-73-33-1, Prepared for Air Force Weapons Laboratory, U.S. Army Engineer Waterways Experiment Station and Federal Aviation Administration, May 1974.

6. Treybig, Harvey J., B. Frank McCullough and W. Ronald Hudson, "Continuously Reinforced Concrete Airfield Pavement - Volume II, Design Manual for Continuously Reinforced Concrete Overlay Pavements," Report No. FAA-RD-73-33-2, Prepared for Air Force Weapons Laboratory, U.S. Army Engineer Waterways Experiment Station and Federal Aviation Administration, May 1974.

7. Treybig, Harvey J., B. Frank McCullough and W. Ronald Hudson, "Continuously Reinforced Concrete Airfield Pavement - Volume III, Design Manual for Continuously Reinforced Concrete Pavements," Report No. FAA-RD-73-33-3, Prepared for Air Force Weapons Labora tory, U.S. Army Engineer Waterways Experiment Station and Federal Aviation Administration, May 1974.

8. Treybig, Harvey J., B. Frank McCullough and W. Ronald Hudson "Continuously Reinforced Concrete Airfield Pavement - Volume IV, Guide Specifications," Report No. FAA-RD-73-33-4, Prepared for Air Force Weapons Laboratory, U.S. Army Engineer Waterways Experiment Station and Federal Aviation Administration May 1974.

9. Treybig, Harvey J., W. R. Hudson and B. F. McCullough, "First Phase Pavement Evaluation -- Runway 4R-22L, O'Hare International Airport," A Report for the Continuously Reinforced Pavement Group, Chicago, Illinois, June 1972.

10. McCullough, B.F., W. Ronald Hudson, and Harvey J. Treybig, "Evaluation of Distress on Runway 9R-27L O'Hare International Airport, Chicago, a report for the Committee of Concrete Reinforcing Bar Producers, American Iron and Steel Institute, April 1971.

11. Panak, John J. and Hudson Matlock, "A Discrete-Element Method of Analysis for Orthogonal Slab and Grid Bridge Floor Systems, Preliminary Research Report 56-25, Center for Highway Research University of Texas at Austin, August 1971.

12. Hudson, W. R., and Hudson Matlock, "Discontinuous Orthotropic Plates and Pavement Slabs," Research Report 56-6, Center for Highway Research The University of Texas, Austin, May 1966.

13. Warren H., and W. L. Eieckmann, "Numerical Computations of Stresses and Strains in a Multiple-Layer Asphalt Pavement System" Internal Report, Unpublished, Chevron Research Corporation,September 1963.

14. Anagnos, James N., Thomas W. Kennedy, and W. Ronald Hudson, "Evaluation and Prediction of Tensile Properties of Cement-Treated Materials," Research Report 98-8, Center for Highway Research, University of Texas at Austin, October 1970.

15. McCullough, B.F., "A Pavement Overlay Design System Considering Wheel Loads, Temperature Changes, and Performance," The Institute of Transportation and Traffic Engineering, University of California, Berkeley, 1969.

16. McCullough, B.F., and Harvey J. Treybig, "Determining the Relationships of Variables in Deflection of Continuously Reinforced Concrete Pavement," Highway Research Board 131, Highway Research Board, 1966.

17. Abou-Ayyash, Adnan and W. Ronald Hudson, "Analysis of Bending Stiffness Variation at Cracks in Continuous Pavements," Research Report 56-22, Center for Highway Research University of Texas at Austin, April 1972.

18. Richards, Cedric W., Engineering Materials Science, Brooks/Cole Publishing Co., Belmont Cal., Sept 1968.

19. Local Climatological Data, Annual Summary with Comparative Data, O'Hare International Airport, Chicago, Illinois, National Climatic Center, Asheville, North Carolina, 1972-1975.

20. Hudson, W. R., B. F. McCullough, H. J. Treybig, "Subbase Recommendations for Dallas-Fort Worth Regional Airport," Report FC-1/3 Submitted to Forrest and Cotton--Carter and Burgess, Austin Research Engineers, Inc., September 1971.

21. Hudson, W. R., B. F. McCullough, and H. J. Treybig, "Pavement Recommendations for the Dallas-Forth Worth Regional Airport," Report FC-1/4 Submitted to Forrest and Cotton--Carter and Burgess, Austin Research Engineers Inc, September 1971.

22. Rauhut, J. Brent and B. Frank McCullough, "Performance Study of Large Area Slabs on Grade" Report No. WR-3, Submitted to Wire Reinforcement Institute by ARE Inc, July 1974.

23. Treybig, Harvey J., "Observation and Analyses of Continuously Reinforced Concrete Pavement." Research Report No. 46-7, Texas Highway Department, April 1968.

24. Shelby, M.D. and B. F. McCullough, "Determining and Evaluating the Stresses in an In-Service Continuously Reinforced Concrete Pavement" Highway Research Record No. 5. Washington, D.C., National Academy of Sciences, January 1963.

25. Miller, Irwin, and John E. Freund, Probability and Statistics for Engineers, Prentice-Hall Inc., Englewood Cliffs, New Jersey, 1965.

26. McCullough, B. Frank, Adnan Abou-Ayyash, W. Ronald Hudson, and Jack P. Randall, "Design of Continuously Reinforced Concrete Pavements for Highways," NCHRP 1-15 Parts 1 and 2, August 1974.

27. "Continuously Reinforced Concrete Pavements", National Cooperative Highway Research Program Synthesis 16, Highway Research Board, 1973.

28. Pendola, Humberto J., Thomas W. Kennedy, and W. Ronald Hudson, "Evaluation of Factors Affecting the Tensile Properties of Cement-Treated Materials," Research Project 98-3, Center for Highway Research, University of Texas at Austin, September 1969.

29. Vallejo, Felipe Rivero and B. Frank McCullough, "Drying Shrinkage and Temperature Drop Stresses in Jointed Reinforced Concrete Pavement." Research Report 177-1, Center for Highway Research, University of Texas at Austin, August 1975.

APPENDIX A: DEFLECTION MEASUREMENTS ON RUNWAY 4R-22L

1. This appendix contains deflection data and figures that illustrate the locations where the measurements were made. Figures A1-A4 show the general layout of each test site, including crack location with respect to LVDT's and Bison gages. Deflection measurements, for each test load (plate, B727, tug) were taken at specified transverse and longitudinal offsets. These transverse and longitudinal offsets are shown in Figure A5 and A6. The loading devices were moved longitudinally and transversely so that deflection influence lines could be observed. Figure A5 and A6 illustrate the positioning of each test load at the various sites.

2. Tables A1-A6 give the deflection profile measurements for the Dynaflect and WES Vibrator along Runway 4R-22L. Table A7 gives WES Vibrator deflection values at each test site. Tables A8-A16 show the deflection measured at each test site for the three test loads (plate, B727, tug).

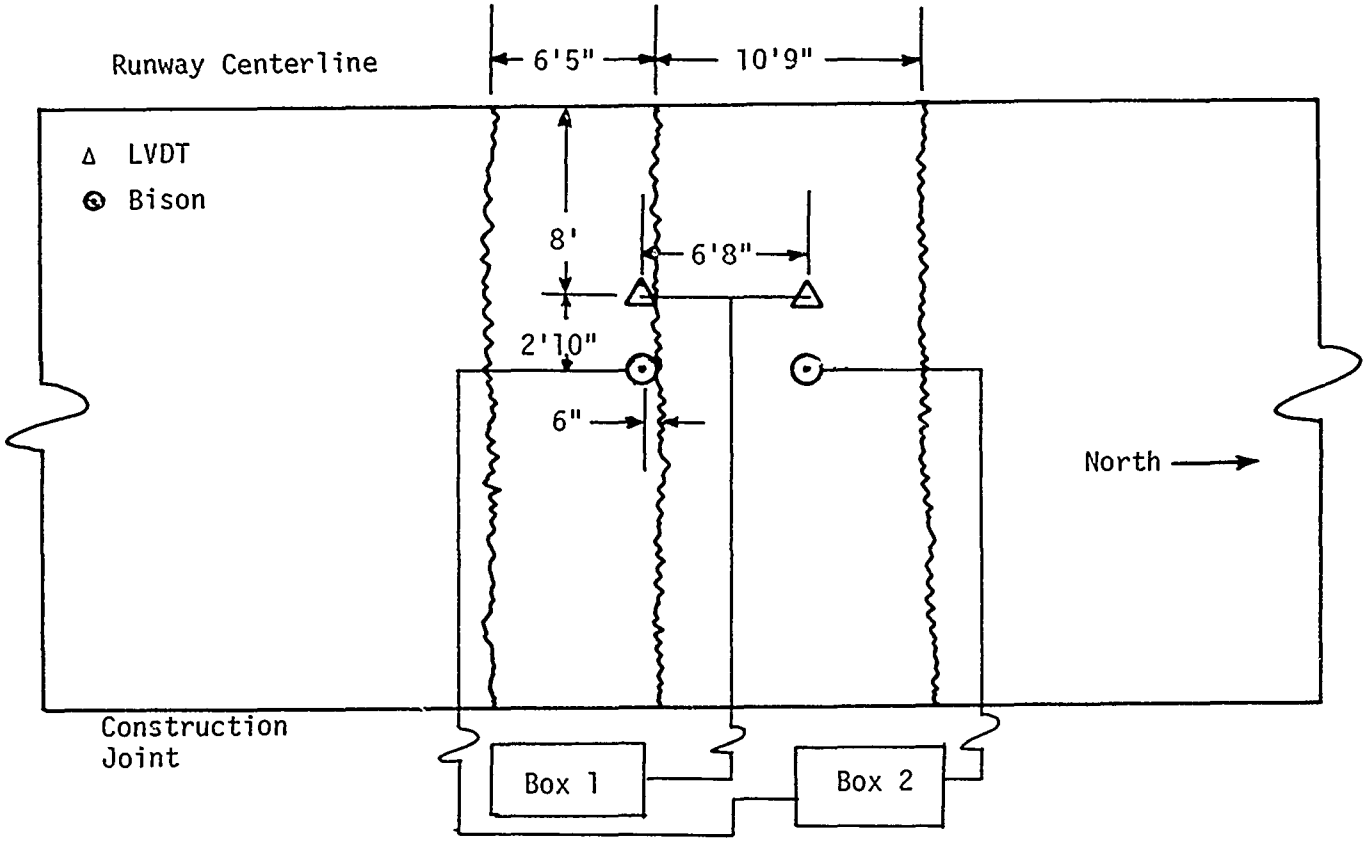

Figure A1. Site 1 Station 328 + 48, End of runway in wheel path of B727, either interior paving lane.

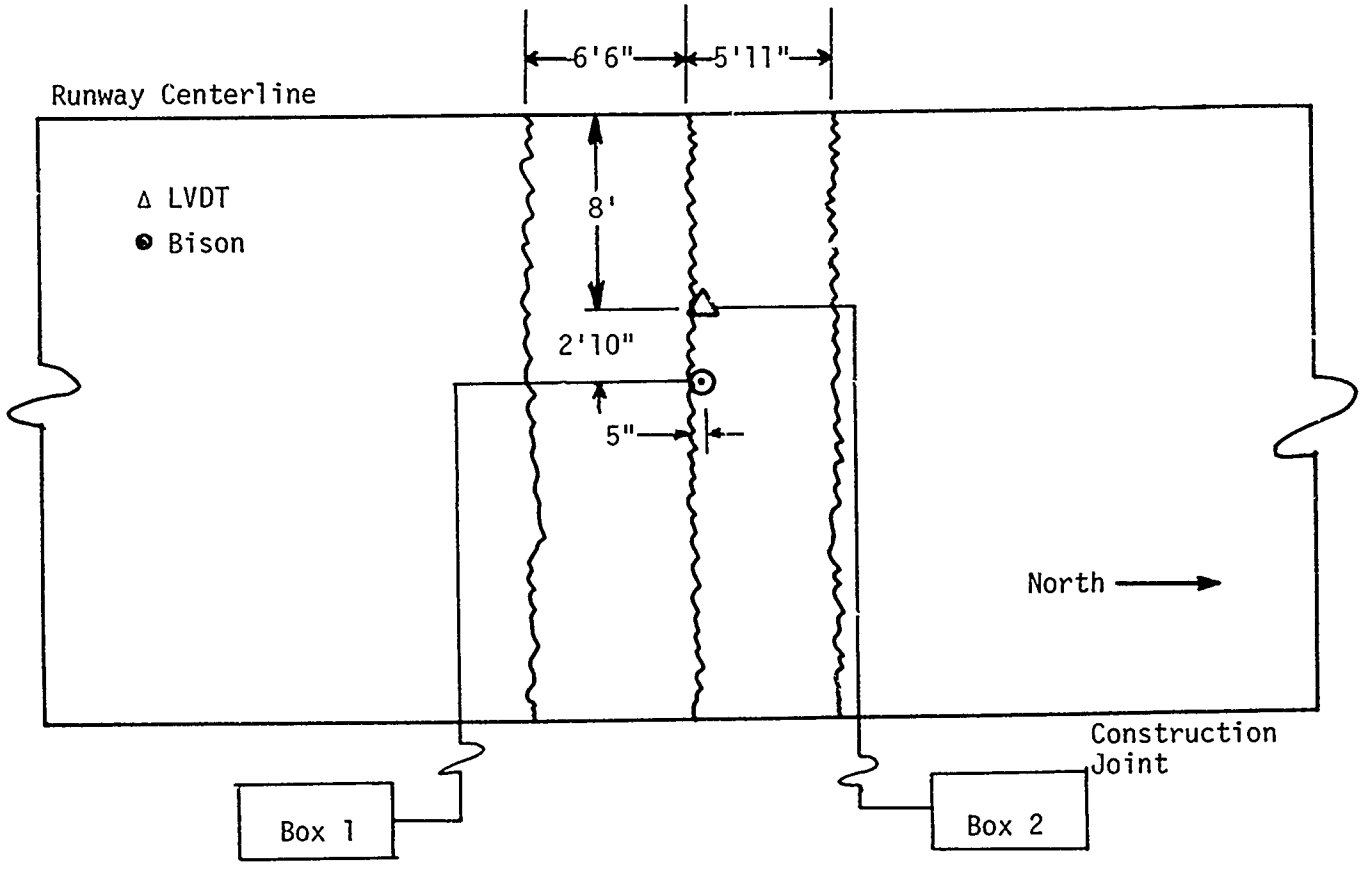

Figure A2. Site 2 Station 320 + 88, Touchdown area, in wheel path of B727, either interior paving lane.

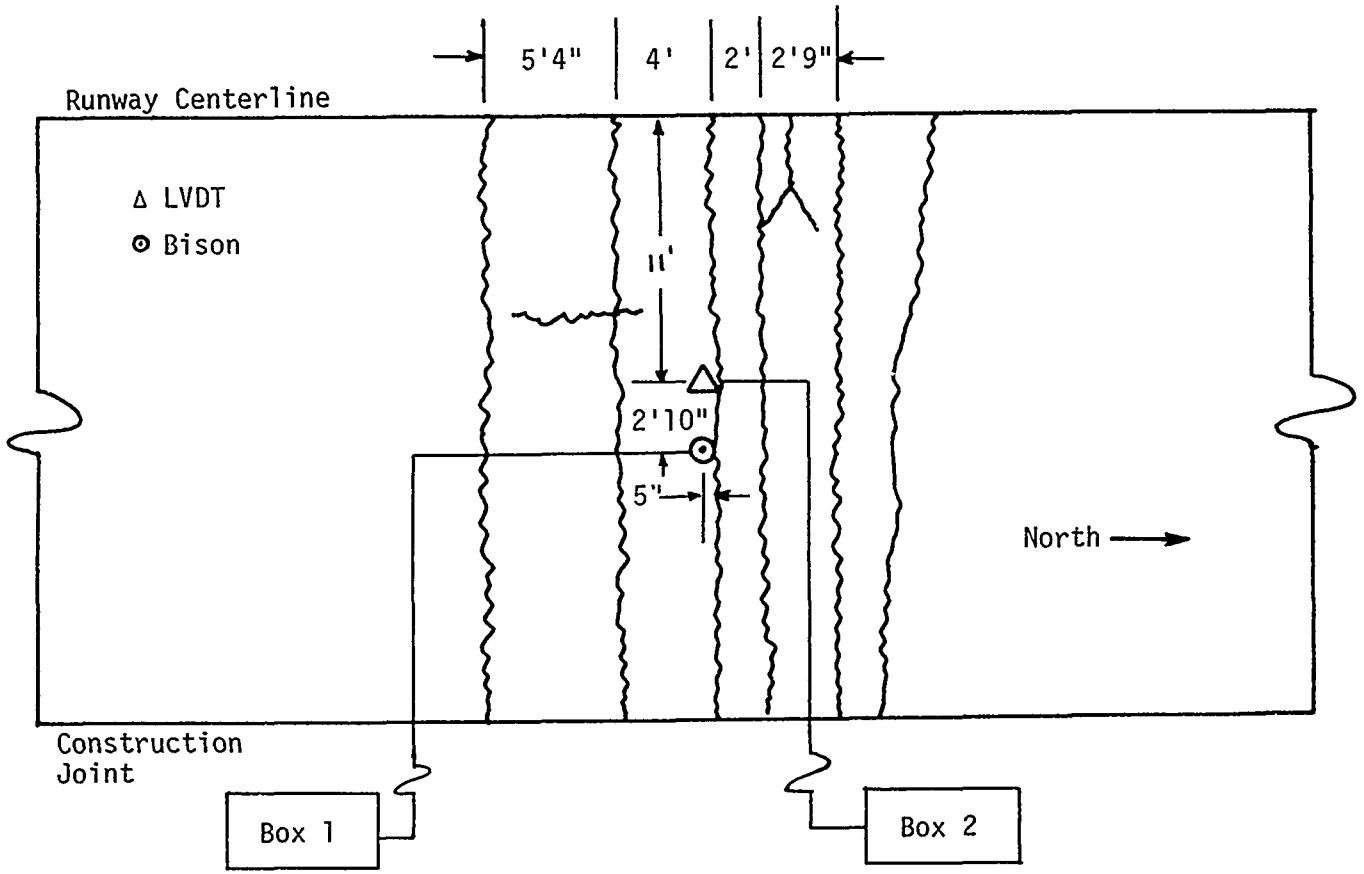

Figure A3. Site 3 Station 305 + 66, Rotation area in wheel path of B727, either interior paving lane.

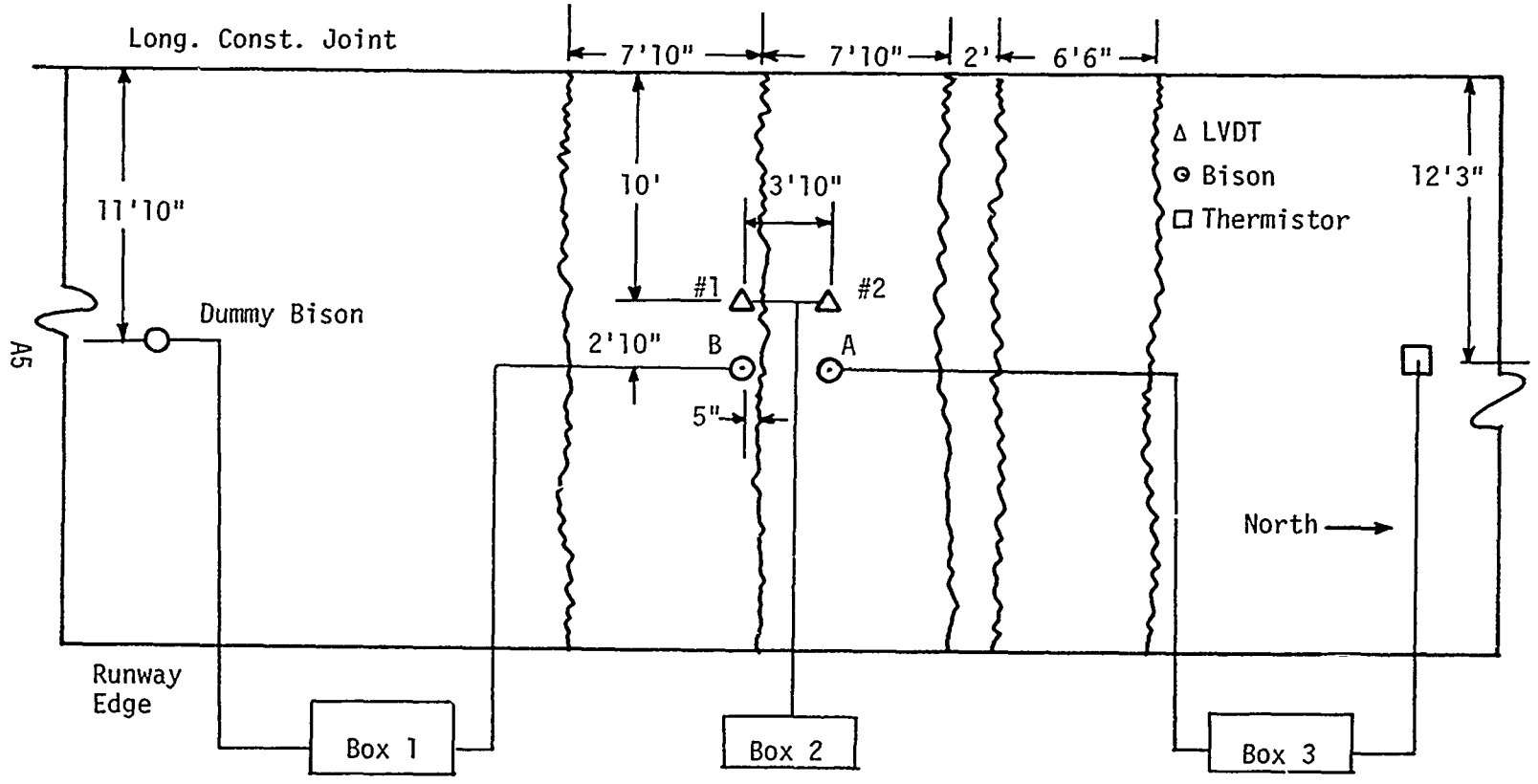

Figure A4. Site 4 - Station 305 + 77, No traffic, outer paving lane, (adjacent to site 3).

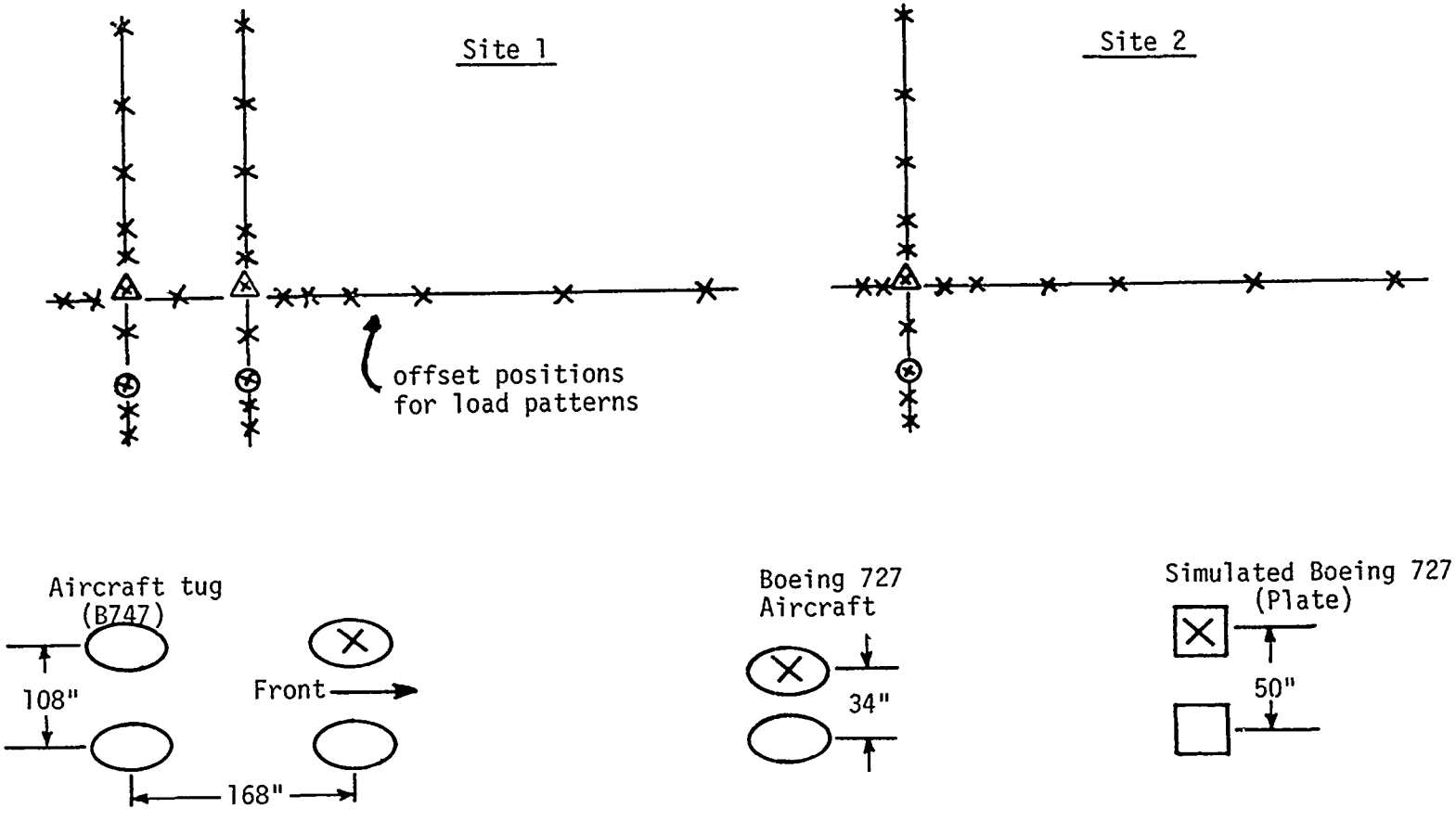

Figure A5. General layout for longitudinal and transverse offsets at Sites 1 and 2 for the three test loads (not to scale).

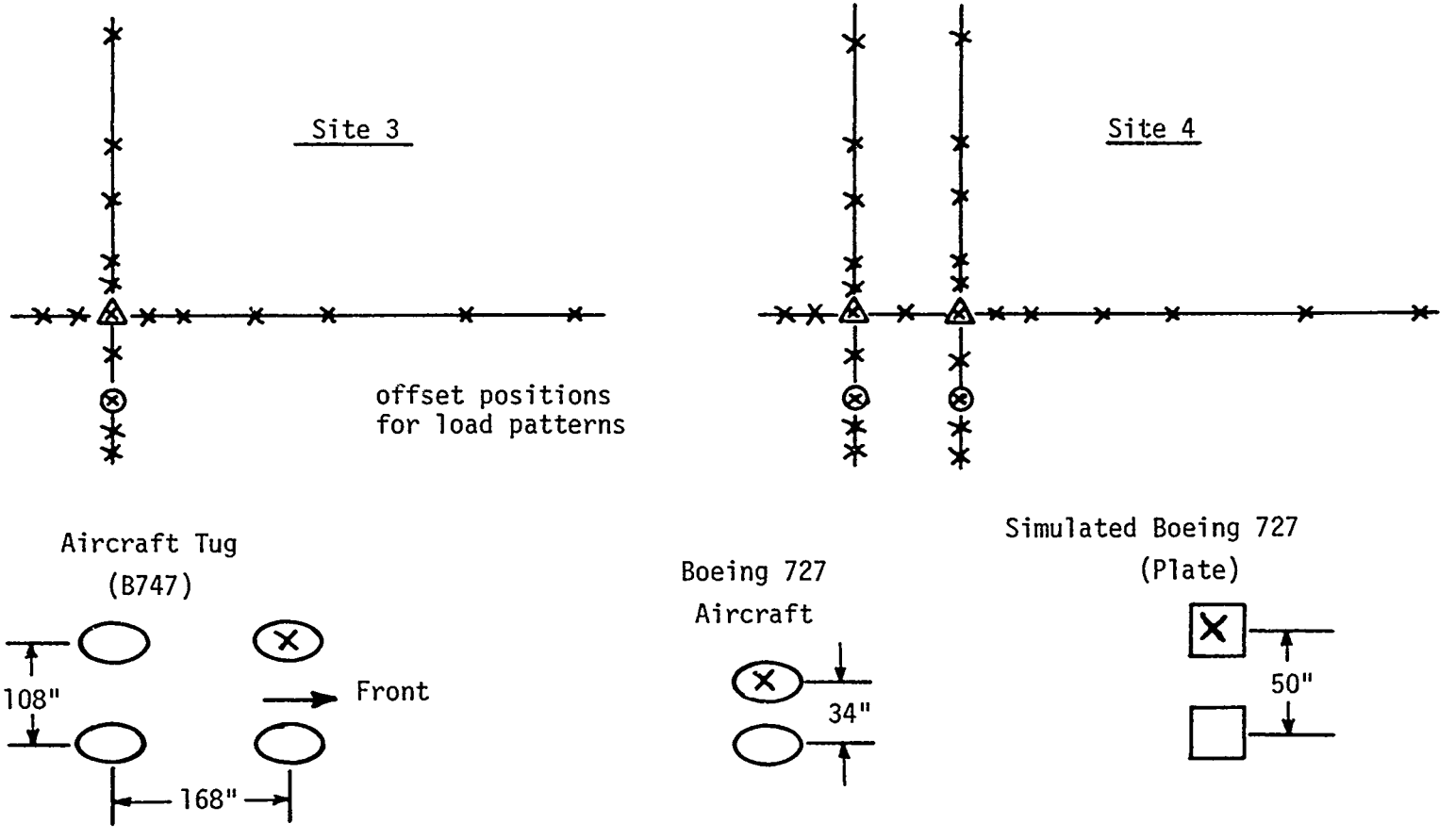

Figure A6. General layout for longitudinal and transverse offsets at sites 3 and 4 for the three test loads (not to scale).

Table A1

Dynaflect Deflection Collected on Runway 4R-22L, O'Hare International Airport

October 1971

Centerline Profile

Location of Measurement	Deflection, inches (10^{-3})				
	Sensor 1	Sensor 2	Sensor 3	Sensor 4	Sensor 5
254 + 00	.177	.174	.159	.159	.138
254 + 50	.180	.174	.165	.156	.144
255 + 00	.210	.200	.177	.168	.150
255 + 50	.220	.210	.186	.174	.156
256 + 00	.230	.220	.200	.180	.162
256 + 50	.240	.220	.200	.186	.174
257 + 00	.240	.220	.200	.192	.174
257 + 50	.220	.210	.200	.180	.162
258 + 00	.210	.200	.174	.168	.153
258 + 50	.200	.180	.162	.153	.138
259 + 00	.200	.186	.171	.165	.150
259 + 50	.200	.189	.174	.162	.144
260 + 00	.145	.192	.177	.168	.153
260 + 50	.240	.220	.200	.171	.156
261 + 00	.220	.210	.200	.174	.162
261 + 50	.200	.189	.168	.159	.144
262 + 00	.162	.159	.153	.144	.132
262 + 50	.162	.159	.150	.141	.129
263 + 00	.186	.183	.174	.162	.147
263 + 50	.198	.192	.180	.171	.153
264 + 00	.240	.220	.200	.183	.171
264 + 50	.210	.200	.180	.171	.156
265 + 00	.220	.210	.200	.180	.162
265 + 50	.220	.220	.210	.183	.165
266 + 00	.260	.250	.220	.210	.174
266 + 50					

Table A1 continued
Dynaflect Deflection Collected on Runway
4R-22L, O'Hare International Airport

October 1971

Centerline Profile

Location of measurement	Deflection, inches (10^{-3})				
	Sensor 1	Sensor 2	Sensor 3	Sensor 4	Sensor 5
266 + 50	.200	.200	.171	.162	.147
267 + 00	.230	.220	.210	.200	.162
267 + 50	.250	.240	.220	.210	.177
268 + 00	.180	.180	.165	.159	.144
268 + 50	.210	.210	.180	.168	.150
269 + 00	.159	.156	.144	.138	.129
269 + 50	.171	.171	.162	.150	.141
270 + 00	.220	.210	.200	.174	.159
270 + 50	.192	.195	.183	.171	.159
271 + 00	.210	.200	.180	.171	.156
271 + 50	.192	.186	.177	.162	.147
272 + 00	.183	.183	.168	.159	.144
272 + 50	.192	.192	.180	.168	.156
273 + 00	.230	.220	.200	.180	.162
273 + 50	.180	.177	.165	.159	.144
274 + 00	.189	.183	.168	.162	.147
274 + 50	.174	.171	.162	.156	.144
275 + 00	.192	.189	.183	.174	.162
275 + 50	.177	.174	.168	.159	.150
276 + 00	.171	.171	.156	.147	.132
276 + 50	.189	.189	.183	.174	.165
277 + 00	.195	.192	.180	.174	.156
277 + 50	.180	.174	.165	.159	.150
278 + 00	.195	.192	.180	.174	.171
278 + 50	.230	.220	.210	.200	.171
279 + 00	.220	.210	.200	.180	.174

Table A1 continued

Dynaflect Deflection Collected on Runway
4R-22L, O'Hare International Airport

October 1971

Centerline Profile

Location of measurement	Deflection, inches (10^{-3})				
	Sensor 1	Sensor 2	Sensor 3	Sensor 4	Sensor 5
279 + 50	.220	.220	.210	.200	.174
280 + 00	.230	.230	.220	.210	.200
280 + 50	.240	.240	.230	.220	.200
281 + 00	.210	.200	.180	.171	.156
281 + 50	.220	.200	.200	.165	.150
282 + 00	.200	.186	.174	.165	.150
282 + 50	.174	.174	.162	.156	.144
283 + 00	.240	.230	.210	.200	.168
283 + 50	.180	.174	.165	.156	.147
284 + 00	.171	.171	.162	.150	.141
284 + 50	.177	.171	.159	.153	.138
285 + 00	.159	.156	.150	.141	.129
285 + 50	.156	.153	.144	.138	.126
286 + 00	.168	.162	.150	.144	.132
286 + 50	.165	.159	.150	.141	.132
286 + 00	.168	.162	.150	.144	.132
286 + 50	.165	.159	.150	.141	.132
287 + 00	.168	.165	.153	.147	.135
287 + 50	.168	.168	.156	.147	.132
288 + 00	.168	.165	.156	.150	.138
288 + 50	.159	.156	.144	.138	.129
289 + 00	.150	.147	.138	.132	.123
289 + 50	.156	.150	.144	.138	.129
290 + 00	.153	.150	.126	.135	.126
290 + 50	.168	.162	.156	.150	.138
291 + 00	.174	.171	.165	.156	.144

Table A1 continued
Dynaflect Deflection Collected on Runway
4R-22L, O'Hare International Airport

October 1971
Centerline Profile

Location of Measurement	Deflection, inches (10^{-3}) Sensor 1	Sensor 2	Sensor 3	Sensor 4	Sensor 5
291 + 50	.162	.162	.147	.144	.132
292 + 00	.174	.165	.156	.150	.141
292 + 50	.204	.189	.174	.168	.156
293 + 00	.300	.280	.250	.240	.200
293 + 50	.210	.200	.171	.165	.150
294 + 00	.220	.210	.180	.174	.156
294 + 50	.230	.220	.200	.174	.159
295 + 00	.192	.180	.168	.159	.144
295 + 50	.198	.180	.168	.156	.141
296 + 00	.195	.171	.159	.150	.135
296 + 50	.189	.171	.159	.147	.132
297 + 00	.174	.165	.153	.141	.129
297 + 50	.186	.165	.150	.141	.129
298 + 00	.168	.156	.144	.132	.114
298 + 50	.165	.156	.144	.135	.123
299 + 00	.180	.165	.153	.144	.132
299 + 50	.180	.168	.153	.141	.126
300 + 00	.192	.180	.161	.150	.135
300 + 50	.220	.200	.162	.150	.132
301 + 00	.220	.210	.200	.171	.156
301 + 50	.204	.186	.168	.159	.144
302 + 00	.195	.183	.171	.162	.147
302 + 50	.240	.230	.210	.200	.168
303 + 00	.240	.230	.210	.200	.165
303 + 50	.220	.200	.180	.174	.162
304 + 00	.250	.210	.180	.174	.159
304 + 50	.195	.180	.168	.162	.150

Table A1 (continued)

Dynaflect Deflection Collected on Runway 4R-22L, O'Hare International Airport

October 1971

Centerline Profile

Location of Measurement	Deflection, inches (10^{-3}) Sensor 1	Sensor 2	Sensor 3	Sensor 4	Sensor 5
305 + 00	.230	.220	.200	.180	.162
305 + 50	.230	.210	.200	.168	.150
306 + 00	.201	.189	.180	.168	.150
306 + 50	.171	.159	.144	.138	.123
307 + 00	.240	.210	.180	.165	.150
307 + 50	.204	.186	.171	.162	.147
308 + 00	.198	.192	.180	.168	.159
308 + 50	.192	.177	.162	.150	.138
309 + 00	.186	.171	.153	.141	.126
309 + 50	.183	.171	.159	.144	.132
310 + 00	.168	.162	.150	.138	.126
310 + 50	.192	.174	.162	.150	.135
311 + 00	.174	.168	.156	.150	.132
311 + 50	.192	.177	.159	.147	.132
312 + 00	.177	.168	.153	.144	.132
312 + 50	.168	.162	.150	.138	.120
313 + 00	.180	.168	.150	.135	.120
313 + 50	.168	.156	.144	.135	.123
314 + 00	.204	.186	.168	.156	.141
314 + 50	.192	.180	.165	.156	.144
315 + 00	.240	.210	.174	.162	.147
315 + 50	.201	.192	.174	.168	.153
316 + 00	.168	.156	.150	.141	.126
316 + 50	.174	.162	.153	.141	.126
317 + 00	.171	.159	.150	.138	.126
317 + 50	.183	.174	.162	.150	.138

Table A1 (continued)

Dynaflect Deflection Collected on Runway
4R-22L, O'Hare International Airport

October 1971
Centerline Profile

Location of measurement	Deflection, inches (10^{-3})				
	Sensor 1	Sensor 2	Sensor 3	Sensor 4	Sensor 5
318 + 00	.201	.186	.165	.150	.135
318 + 50	.198	.186	.168	.156	.141
319 + 00	.198	.186	.168	.162	.147
319 + 50	.204	.198	.183	.171	.156
320 + 00	.186	.174	.162	.153	.138
320 + 50	.180	.168	.156	.150	.138
321 + 00	.180	.174	.168	.156	.138
321 + 50	.207	.195	.177	.165	.150
322 + 00	.186	.177	.165	.156	.144
322 + 50	.183	.177	.168	.162	.147
323 + 00	.204	.195	.180	.171	.159
323 + 50	.192	.180	.168	.156	.144
324 + 00	.189	.177	.162	.156	.144
324 + 50	.198	.189	.174	.165	.150
325 + 00	.250	.240	.220	.200	.174
325 + 50	.207	.195	.180	.171	.159
326 + 00	.198	.186	.174	.165	.153
326 + 50	.240	.220	.200	.174	.165
327 + 00	.207	.195	.180	.174	.159
327 + 50	.189	.177	.165	.156	.141
328 + 00	.250	.230	.200	.171	.156
328 + 50	.198	.186	.168	.159	.144
329 + 00	.207	.189	.174	.165	.150
329 + 50	.183	.174	.162	.153	.141
330 + 00	.171	.156	.144	.135	.126
330 + 50	.168	.156	.144	.132	.126

Table A1 continued

Dynaflect Deflection Collected on Runway
4R-22L, O'Hare International Airport

October 1971
Centerline Profile

Location of Measurement	Deflection, inches (10^{-3}) Sensor 1	Sensor 2	Sensor 3	Sensor 4	Sensor 5
331 + 00	.165	.153	.144	.138	.126
331 + 50	.162	.150	.138	.129	.117
332 + 00	.150	.138	.129	.123	.114
332 + 50	.144	.132	.120	.114	.105
333 + 00	.159	.144	.126	.120	.108
333 + 50	.135	.126	.114	.108	.099
Mean	.196				
Coefficient of Variation	13.9%				

Table A2

Dynaflect Deflection Collected on Runway 4R-22L, O'Hare International Airport

October 1971

Edge Profile (Lane 1)

Location of Measurement	Deflection, inches (10^{-3})				
	Sensor 1	Sensor 2	Sensor 3	Sensor 4	Sensor 5
Sta 254	.162	.153	.150	.147	.138
Sta 255	.168	.165	.159	.153	.141
Sta 256	.180	.168	.162	.153	.187
Sta 257	.219	.210	.201	.186	.179
Sta 258	.240	.220	.210	.200	.192
Sta 259	.220	.210	.200	.198	.192
Sta 260	.219	.201	.195	.186	.177
Sta 261	.250	.240	.240	.230	.210
Sta 262	.240	.230	.220	.200	.186
Sta 263	.230	.210	.200	.195	.186
Sta 264	.280	.270	.270	.266	.250
Sta 265	.240	.230	.220	.210	.200
Sta 266	.250	.240	.230	.220	.200
Sta 267	.240	.230	.220	.210	200
Sta 268	.260	.240	.240	.230	.220
Sta 269	.210	.200	.186	.174	.162
Sta 270	.240	.220	.210	.200	.177
Sta 271	.220	.200	.192	.186	.174
Sta 272	.230	.220	.200	.186	.171
Sta 273	.200	.186	.183	.177	.168
Sta 274	.183	.177	.168	.165	.156
Sta 275	.171	.162	.159	.156	.153
Sta 276	.195	.180	.177	.174	.162
Sta 277	.174	.165	.156	.150	.147
Sta 278	.250	.230	.220	.210	.200
Sta 279	.220	.200	.198	.195	.192

Table A2 (continued)

Dynaflect Deflection Collected on Runway
4R-22L, O'Hare International Airport

October 1971
Edge Profile (Lane 1)

Location of Measurement	Deflection, inches (10^{-3})				
	Sensor 1	Sensor 2	Sensor 3	Sensor 4	Sensor 5
Sta 280	.189	.171	.168	.162	.156
Sta 281	.192	.183	.174	.162	.153
Sta 282	.192	.177	.171	.162	.150
Sta 283	.270	.240	.230	.210	.186
Sta 284	.165	.162	.159	.150	.147
Sta 285	.168	.16	.156	.153	.144
Sta 286	.177	.162	.159	.153	.144
Sta 287	.189	.180	.174	.171	.165
Sta 288	.165	.156	.150	.144	.138
Sta 289	.171	.159	.156	.150	.144
Sta 290	.165	.159	.147	.144	.138
Sta 291	.165	.162	.159	.147	.138
Sta 292	.168	.159	.153	.150	.141
Sta 293	.240	.220	.200	.180	.168
Sta 294	.250	.240	.230	.220	.230
Sta 295	.171	.165	.159	.159	.156
Sta 296	.192	.183	.18	.179	.174
Sta 297	.165	.162	.156	.156	.150
Sta 298	.204	.195	.186	.177	.174
Sta 299	.168	.165	.165	.165	.165
Sta 300	.204	.180	.171	.165	.156
Sta 301	.171	.165	.159	.156	.156
Sta 302	.171	.165	.162	.159	.156
Sta 303	.165	.153	.150	.150	.144
Sta 304	.204	.198	.198	.192	.186

Table A2(continued)

Dynaflect Deflection Collected on Runway
4R-22L, O'Hare International Airport

October 1971
Edge Profile (Lane 1)

Location of Measurement	Deflection, inches (10^{-3})				
	Sensor 1	Sensor 2	Sensor 3	Sensor 4	Sensor 5
Sta 305	.210	.204	.204	.201	.195
Sta 306	.177	.162	.162	.159	.150
Sta 307	.180	.165	.156	.150	.144
Sta 308	.213	.204	.198	.198	.189
Sta 309	.180	.174	.174	.165	.159
Sta 310	.219	.198	.186	.168	.156
Sta 311	.168	.168	.159	.147	.138
Sta 312	.153	.144	.144	.141	.141
Sta 313	.153	.144	.141	.138	.138
Sta 314	.213	.198	.177	.159	.144
Sta 315	.240	.220	.210	.200	.192
Sta 316	.174	.174	.171	.168	.156
Sta 317	.156	.147	.147	.144	.144
Sta 318	.162	.156	.147	.141	.141
Sta 319	.186	.174	.171	.171	.162
Sta 320	.204	.186	.174	.162	.156
Sta 321	.195	.186	.177	.168	.165
Sta 322	.250	.210	.200	.171	.165
Sta 323	.210	.192	.192	.186	.174
Sta 324	.219	.198	.192	.186	.180
Sta 325	.204	.198	.192	.186	.180
Sta 326	.186	.180	.177	.174	.171
Sta 327	.250	.230	.220	.220	.220
Sta 328	.220	.200	.180	.174	.174
Sta 329	.180	.174	.165	.156	.153

Table A2 (continued)

Dynaflect Deflection Collected on Runway
4R-22L, O'Hare International Airport

October 1971
Edge Profile (Lane 1)

Location of Measurement	Deflection, inches (10^{-3}) Sensor 1	Sensor 2	Sensor 3	Sensor 4	Sensor 5
Sta 330	.159	.150	.144	.141	.138
Sta 331	.165	.162	.156	.153	.153
Sta 332	.147	.135	.135	.132	.132
Sta 333	.132	.129	.123	.123	.120
Sta 334	.114	.111	.108	.102	.102
Mean	0.198				
Coefficient of Variation	17.4%				

Table A3

Dynaflect Deflection Collected on Runway

4R-22L, O'Hare International Airport

September 1972

Centerline Profile

Station		Deflection, inches (10^{-4}) Sensor 1	Sensor 2	Sensor 3	Sensor 4	Sensor 5
25400	1*	4.000	3.400	3.200	2.800	2.600
25400	2**	2.040	1.980	1.860	1.740	1.650
25500	2	2.160	2.010	1.950	1.770	1.680
25500	1	2.370	2.220	2.130	1.920	1.800
25600	2	2.340	2.310	2.250	2.040	1.950
25600	1	2.800	2.700	2.600	2.130	2.010
25700	2	2.370	2.250	2.220	2.010	1.920
25700	1	2.800	2.600	2.600	2.040	1.950
25800	2	2.070	1.920	1.830	1.680	1.590
25800	1	2.280	2.100	1.980	1.770	1.650
25900	2	2.100	2.010	2.010	1.800	1.740
25900	1	2.130	2.040	1.980	1.800	1.710
26000	2	2.280	2.130	2.040	1.830	1.710
26000	1	2.340	2.220	2.100	1.890	1.770
26100	2	2.400	2.280	2.220	2.040	1.950
26100	1	2.800	2.600	2.600	2.070	1.950
26200	2	2.040	1.980	1.920	1.740	1.650
26200	1	2.130	1.980	1.920	1.740	1.650
26300	2	2.430	2.280	2.220	1.980	1.890
26300	1	2.430	2.310	2.220	1.980	1.890
26400	2	2.370	2.280	2.250	2.070	1.980
26400	1	2.900	2.700	2.600	2.400	2.040
26500	2	2.900	2.700	2.600	2.100	1.980
26500	1	2.600	2.600	2.400	1.980	1.890
26600	2	3.000	3.000	3.000	2.700	2.500
26600	1	3.200	3.000	2.900	2.600	2.500
26700	2	2.900	2.800	2.800	2.600	2.500
26700	1	3.000	2.800	2.800	2.500	2.400
26800	2	2.160	2.070	2.070	1.920	1.830
26800	1	2.100	2.010	1.980	1.830	1.770
26900	2	1.950	1.920	1.920	1.710	1.620

*1 Adjacent to crack
**2 Between crack

Table A3

Dynaflect Deflection Collected on Runway

4R-22, O'Hare International Airport

September 1972

Centerline Profile

Station		Deflection, inches (10^{-4}) Sensor 1	Sensor 2	Sensor 3	Sensor 4	Sensor 5
26900	1	2.130	1.980	1.920	1.680	1.620
27000	2	2.070	1.950	1.950	1.860	1.800
27000	1	2.160	2.070	2.010	1.830	1.770
27100	2	2.280	2.250	2.160	1.920	1.770
27100	1	2.370	2.160	2.040	1.830	1.680
27200	2	1.950	1.890	1.890	1.740	1.710
27200	1	2.100	2.100	2.070	1.830	1.740
27300	2	2.070	2.010	2.010	1.920	1.860
27300	1	2.130	2.010	2.010	1.830	1.800
27400	2	1.980	1.920	1.950	1.830	1.770
27400	1	1.950	1.860	1.920	1.740	1.710
27500	2	2.220	2.160	2.160	2.070	2.040
27500	1	2.190	2.130	2.130	1.800	1.920
27600	2	1.770	1.740	1.740	1.650	1.590
27600	1	1.800	1.740	1.680	1.590	1.500
27700	2	2.040	1.980	1.980	1.800	1.740
27700	1	2.190	2.040	2.040	1.800	1.740
27800	2	2.400	2.340	2.340	2.190	2.190
27800	1	2.700	2.600	2.600	2.400	2.160
27900	2	2.100	2.040	2.040	1.980	1.890
27900	1	2.340	2.220	2.160	1.950	1.860
28000	2	2.190	2.100	2.100	1.920	1.860
28000	1	2.250	2.130	2.130	1.920	1.860
28100	2	2.340	2.190	2.130	1.920	1.830
28100	1	2.430	2.220	2.220	1.920	1.860
28200	2	2.460	2.220	2.160	1.920	1.830
28200	1	2.220	2.100	2.100	1.860	1.800
28300	2	2.340	2.220	2.220	1.980	1.830
28300	1	2.800	2.600	2.500	2.040	1.920
28400	2	1.920	1.860	1.830	1.710	1.620
28400	1	1.950	1.860	1.830	1.680	1.620
28500	2	1.620	1.530	1.530	1.440	1.380
28500	1	1.680	1.560	1.560	1.500	1.380
28600	2	2.010	1.920	1.860	1.680	1.620
28600	1	2.220	2.040	2.010	1.770	1.650
28700	2	2.010	1.920	1.920	1.830	1.800
28700	1	2.040	1.980	1.920	1.800	1.770

Table A3 (continued)

Dynaflect Deflection Collected on Runway 4R-22L, O'Hare International Airport

September 1972

Centerline Profile

Station		Deflection, inches (10^{-4}) Sensor 1	Sensor 2	Sensor 3	Sensor 4	Sensor 5
28800	2	1.740	1.710	1.680	1.620	1.560
28800	1	1.800	1.740	1.740	1.590	1.530
28900	2	1.620	1.530	1.530	1.440	1.380
28900	1	1.680	1.590	1.590	1.440	1.380
29000	2	1.680	1.620	1.620	1.470	1.410
29000	1	1.740	1.590	1.590	1.500	1.470
29100	2	1.860	1.800	1.800	1.650	1.590
29100	1	1.950	1.800	1.800	1.620	1.590
29200	2	1.710	1.620	1.620	1.500	1.470
29200	1	1.770	1.680	1.650	1.530	1.440
29300	2	3.200	3.000	2.900	2.600	2.400
29300	1	3.200	3.000	2.900	2.600	2.400
29400	2	2.340	2.220	2.220	1.980	1.890
29400	1	2.310	2.160	2.130	1.950	1.860
29500	2	2.040	1.950	1.950	1.740	1.680
29500	1	1.980	1.890	1.890	1.680	1.650
29600	2	2.160	2.100	2.100	1.830	1.770
29600	1	2.100	1.980	1.980	1.800	1.710
29700	2	2.040	1.920	1.920	1.710	1.620
29700	1	2.040	1.920	1.860	1.740	1.620
29800	2	1.830	1.740	1.740	1.560	1.500
29800	1	2.070	1.860	1.740	1.590	1.500
29900	2	1.980	1.890	1.860	1.680	1.620
29900	1	2.010	1.890	1.890	1.680	1.620
30000	2	2.130	1.980	1.950	1.740	1.650
30000	1	2.100	1.920	1.920	1.800	1.650
30100	2	2.250	2.220	2.160	2.010	1.920
30100	1	2.220	2.100	2.040	1.860	1.770
30200	2	2.190	2.100	2.100	1.920	1.860
30200	1	2.430	2.250	2.220	1.980	1.920
30300	2	2.460	2.370	2.370	2.160	2.130
30300	1	2.460	2.340	2.340	2.160	2.070

Table A3 (continued)

Dynaflect Deflection Collected on Runway

4R-22L, O'Hare International Airport

September 1972

Centerline Profile

Station		Deflection, inches (10^{-4}) Sensor 1	Sensor 2	Sensor 3	Sensor 4	Sensor 5
30425	2	2.190	2.130	2.130	1.950	1.920
30425	1	2.250	2.160	2.130	1.980	1.920
30500	2	2.250	2.160	2.160	1.980	1.920
30500	1	2.340	2.220	2.220	2.010	1.950
30600	2	2.250	2.100	2.100	1.860	1.740
30600	1	2.040	1.980	1.980	1.800	1.680
30700	2	2.160	2.040	2.040	1.800	1.710
30700	1	1.980	1.920	1.920	1.740	1.680
30800	2	2.160	2.100	2.100	1.920	1.830
30800	1	2.370	2.250	2.160	1.920	1.800
30900	2	2.040	1.980	1.920	1.740	1.650
30900	1	2.070	1.920	1.920	1.710	1.650
31000	2	1.740	1.710	1.710	1.560	1.500
31000	1	1.920	1.800	1.740	1.590	1.500
31100	2	1.950	1.860	1.860	1.680	1.620
31100	1	1.950	1.830	1.830	1.650	1.590
31200	2	1.920	1.830	1.770	1.620	1.560
31200	1	1.920	1.830	1.830	1.620	1.530
31300	2	1.770	1.680	1.680	1.530	1.470
31300	1	1.770	1.710	1.680	1.500	1.470
31400	2	1.860	1.770	1.740	1.620	1.560
31400	1	2.070	1.920	1.830	1.680	1.620
31500	2	2.010	1.950	1.950	1.770	1.710
31500	1	2.100	1.980	1.980	1.800	1.770
31600	2	1.740	1.680	1.680	1.560	1.500
31600	1	1.890	1.800	1.770	1.590	1.530
31700	2	1.770	1.680	1.680	1.560	1.500
31700	1	1.860	1.740	1.680	1.560	1.500
31800	2	1.800	1.680	1.680	1.530	1.500
31800	1	1.830	1.830	1.740	1.710	1.500
31900	2	2.100	2.040	2.040	1.800	1.710
31900	1	2.040	1.980	1.980	1.770	1.680
32000	2	1.830	1.740	1.740	1.620	1.590
32000	1	1.860	1.770	1.830	1.620	1.560
32100	2	1.800	1.710	1.710	1.560	1.530
32100	1	1.680	1.680	1.680	1.590	1.560

Table A3 (continued)

Dynaflect Deflection Collected on Runway
4R-22L, O'Hare International Airport

September 1972
Centerline Profile

Station		Deflection, inches (10^{-4}) Sensor 1	Sensor 2	Sensor 3	Sensor 4	Sensor 5
32200	2	1.860	1.830	1.830	1.710	1.650
32200	1	1.890	1.830	1.830	1.680	1.650
32300	2	2.040	1.920	1.920	1.740	1.680
32300	1	2.010	1.920	1.890	1.740	1.740
32400	2	1.830	1.740	1.740	1.620	1.560
32500	2	2.160	2.070	2.130	1.920	1.860
32500	1	2.130	2.070	2.040	1.920	1.830
32600	2	2.250	2.160	2.100	1.920	1.860
32600	1	2.400	2.280	2.250	1.980	1.920
32700	2	2.070	2.040	2.040	1.920	1.860
32700	1	2.100	2.040	2.040	1.860	1.800
32800	2	2.160	2.130	2.040	1.920	1.860
32800	1	2.160	2.130	2.100	1.920	1.830
32900	2	2.250	2.100	2.040	1.920	1.860
32900	1	2.100	1.980	2.040	1.830	1.800
33000	2	1.800	1.650	1.650	1.680	1.470
33000	1	1.830	1.710	1.710	1.590	1.500
33100	2	1.740	1.680	1.680	1.530	1.500
33100	1	1.740	1.680	1.680	1.560	1.500
33200	2	1.560	1.530	1.530	1.470	1.440
33200	1	1.740	1.560	1.560	1.410	1.380
33300	2	1.740	1.620	1.620	1.440	1.410
33400	2	1.410	1.290	1.290	1.170	1.140
33420	1	6.900	5.800	5.200	4.100	3.400

Location of Sensor 1	Mean Deflection inches (10^{-4})	Coefficient of Variation of
1) Adjacent to crack	2.17	15.9
2) Between crack	2.08	15.1
Combined 1 & 2	2.13	15.6

Table A4

WES Vibrator Deflection Data for Runway 4R-22L, O'Hare International Airport

September 1972
Centerline Profile (Lane 3)

Location of measurement	Deflection* inches (10^{-3})	Location to** Crack
334 + 00	1.24	
332 + 00	1.61	1
331 + 88	1.11	2
330 + 00	2.08	1
329 + 99	1.46	2
328 + 00	2.00	1
327 + 98	1.65	2
326 + 00	1.75	1
325 + 99	1.72	2
324 + 03	2.12	1
324 + 00	1.75	2
322 + 00	1.65	1
321 + 94	1.55	2
318 + 00	1.87	1
317 + 97	1.65	2
314 + 00	1.85	1
313 + 98	2.25	2
310 + 00	2.25	1
309 + 98	1.80	2
306 + 00	2.25	1
305 + 99	1.98	2

* Deflection values for a load of 10 kips and a frequency of 15 cps taken 12.5 ft. East of runway centerline.

** 1 - Adjacent to a crack
2 - Between cracks

Table A4 (continued)

WES, Vibrator Deflection Data for Runway 4R-22L, O'Hare International Airport

September 1972

Centerline Profile (Lane 3)

Location of measurement	Deflection* inches (10^{-3})	Location to** Crack
304 + 25	1.50	1
304 + 23	1.60	2
302 + 00	2.00	1
301 + 98	2.10	2
298 + 00	2.20	1
297 + 97	1.70	2
294 + 00	2.20	1
293 + 98	1.91	2
290 + 00	1.30	1
289 + 99	1.58	2
286 + 00	1.63	1
278 + 00	2.62	1
270 + 00	1.90	1

	Overall	Between cracks	Adjacent to crack
Mean	1.82	1.72	1.93
Coefficient of variation	18.0%	15.9%	16.8%

* Deflection values for a load of 10 kips and a frequency of 15 cps taken 12.5 ft. East of runway centerline.

** 1 - Adjacent to a crack
2 - Between cracks

Table A5

WES Vibrator Deflection Data for
Runway 4R-22L, O'Hare International Airport

May 1975

19 ft. East of Centerline (Lane 3)

Location of measurement	Deflection**, inches (10^{-3}) 10,000 lb load	15,000 lb. load	Location of measurement	Deflection**, inches (10^{-3}) 10,000 lb load	15,000 lb load
254 + 60	1.20	2.30	301 + 98*	2.50	3.30
256 + 50	1.70	2.60	302 + 00*	2.15	3.25
258 + 50	1.75	2.80	304 + 00	1.75	2.65
260 + 50	2.10	3.25	304 + 23*	1.85	2.75
262 + 50	1.55	2.40	304 + 25*	2.00	3.00
264 + 50	2.30	3.50	305 + 99*	2.75	4.25
266 + 50	2.20	3.25	306 + 00*	2.15	3.30
268 + 50	3.20	4.90	308 + 00	2.15	3.25
270 + 00*	2.15	3.25	309 + 98*	1.85	2.75
272 + 50	1.70	2.60	310 + 00*	2.20	3.25
274 + 50	2.15	3.20	311 + 00	2.90	3.55
276 + 50	1.70	2.70	313 + 00	1.80	2.75
278 + 00*	1.75	2.65	313 + 98*	2.70	3.95
281 + 00	2.00	3.05	314 + 00	2.45	3.65
283 + 00	1.85	2.90	316 + 00	3.70	5.57
285 + 00	2.90	4.50	317 + 97*	1.85	2.75
286 + 00*	1.45	2.30	318 + 00	1.70	2.70
289 + 00	1.90	2.90	321 + 00	1.30	2.00
290 + 00	1.40	2.10	321 + 94*	1.50	2.25
292 + 00	2.10	3.30	322 + 00*	1.60	2.40
293 + 98*	2.25	3.50	323 + 00	2.00	3.00
294 + 00	2.90	2.70	324 + 00	1.65	2.50
296 + 00	1.75	2.70	324 + 03*	2.20	3.25
297 + 97*	1.75	2.70	325 + 99*	1.90	3.00
298 + 00	1.80	2.85	326 + 00*	1.75	2.70
300 + 00	1.55	2.35	327 + 98*	2.05	3.20

Table A5 (cont.)

WES Vibrator Deflection Data for
Runway 4R-22L, O'Hare International Airport

May 1975

19 ft. East of Centerline (Lane 3)

Location of measurement	Deflection**, inches (10^{-3}) 10,000 lb. load	15,000 lb. load
328 + 00*	1.75	2.50
329 + 99*	1.70	2.50
330 + 00*	1.75	2.80
331 + 88*	1.25	1.85
332 + 00*	1.40	2.25
334 + 00*	1.30	2.00
Mean	1.97	
Coefficient of Variation	25.2%	

* These measurements were 12.5 feet east of centerline rather than the 19 feet.

** Measurements taken at a frequency of 15 cps.

Table A6

WES Vibrator Deflection Data for

Runway 4R-22L, O'Hare International Airport

May 1975

19 ft. West of Centerline (Lane 4)

Location of measurement	Deflection**, inches (10^{-3}) 10,000 lb. load	15,000 lb. load	Location of measurement	Deflection**, inches (10^{-3}) 10,000 lb load	15,000 lb load
255 + 50	2.10	3.20	307 + 00	2.25	3.55
257 + 50	2.75	4.20	309 + 00	2.05	3.20
259 + 50	3.20	4.90	312 + 00	2.10	3.25
261 + 50	2.00	3.25	315 + 00	1.75	2.75
253 + 50	2.60	4.15	317 + 00	2.30	3.50
265 + 50	2.25	3.70	319 + 00	2.00	3.00
267 + 50	2.25	4.10	325 + 00	1.85	2.85
271 + 50	2.25	3.20	329 + 00	2.25	3.55
273 + 50	1.95	3.10	333 + 00	1.75	2.75
277 + 50	2.00	3.20			
280 + 00	2.10	3.30	Mean	2.24	
282 + 00	2.40	3.00	Coefficient of Variation	13.4%	
284 + 00	2.25	3.50			
287 + 00	2.25	3.25			
291 + 00	2.10	3.25			
293 + 00	2.50	4.00			
295 + 00	2.25	3.50			
297 + 00	2.35	3.60			
299 + 00	2.55	3.95			
301 + 00	2.35	3.75			
303 + 00	2.50	3.85			

* Measurements taken at a frequency of 15 cps.

Table A7

WES Vibrator Deflection Data for
Runway 4R-22L, O'Hare International Airport

May 1975

SITE 1

Location of measurement	Deflection*, inches (10^{-3}) 10,000 lb. load	15,000 lb. load
329 + 28	2.50	3.80
329 + 38	3.00	4.50
329 + 43	2.85	4.40
329 + 48**	3.20	4.70
329 + 53	2.80	4.25
329 + 58	3.55	5.50
329 + 68	2.35	3.60

SITE 2

Location of measurement	Deflection*, inches (10^{-3}) 10,000 lb. load	15,000 lb. load
320 + 28	1.75	2.60
320 + 38	2.15	3.40
320 + 43	2.80	4.35
320 + 48**	2.00	3.40
320 + 53	1.50	2.25
320 + 58	1.95	2.95
320 + 63	2.15	3.25

* Measurements taken at a frequency of 15 cps.

** Approximate location of LVDT's

Table A7 (continued)

WES Vibrator Deflection Data for

Runway 4R-22L, O'Hare International Airport

May 1975

SITE 3

Location of measurement	Deflection*, inches (10^{-3}) 10,000 lb. load	15,000 lb. load
305 + 46	2.00	3.00
305 + 56	1.85	2.75
305 + 61	2.00	2.95
305 + 66**	1.90	2.75
305 + 71	2.00	2.90
305 + 76	1.85	2.75
305 + 86	2.20	3.40

SITE 4

Location of measurement	Deflection*, inches (10^{-3}) 10,000 lb. load	15,000 lb. load
305 + 57	1.90	3.00
305 + 67	2.00	3.00
305 + 72	2.70	4.15
305 + 77**	2.35	3.70
305 + 82	1.95	2.90
305 + 87	1.75	2.65
305 + 97	2.05	3.15

*Measurements taken at a frequency of 15 cps.

**Approximate location of LVDT's

Table A8

Plate Load Deflection Data
for Site 1 on Runway 4R-22L

May 21, 1973

LVDT Adjacent to Cracks		LVDT Between Cracks	
Location of offset from LVDT	Deflection, inches	Location or offset from LVDT	Deflection, inches
0	.01548	0	.01534
1W	.01037	1W	.01378
2W	.00895	2W	.01122
4W	.00852	4W	.00838
6W	.00511	6W	.00597
10W	.00369	10W	.00269
1'5"E	.01165	1'5"E	.01392
2'10"E	.01108	2'10"E	.01420
3'10"E	.01079	3'10"E	.01520
4'10"E	.01065	4'10"E	.01506
6'8"N	.00625	0*	.01661
7'8"N	.00511	1N	.01364
8'8"N	.00454	2N	.01250
10'8"N	.00341	4N	.01108
12'8"N	.00199	6N**	.00796
16'8"N	.00071	10N	.00469
20'8"N	-0-	14N***	.00227
3'4"N	.00966	3'4"S	.01134
0	.01093	6'8"S	.00696
1S	.00923	7'8"S	.00597
2S	.00866	8'8"S	.00497

Temperature Beginning of Test = 80°F
*Temperature at 2:15 = 74°F
Contact Pressure = 148 psi

**Temperature at 2:40 = 70°F
***Temperature at 2:45 = 68°F(Hard Rain)
Gross Weight = 76,000 lbs

Table A9

Plate Load Deflection Data for

Site 3 on Runway 4R-22L

May 20, 1975

LVDT Adjacent to Crack

Location or offset from LVDT	Deflection, inches
0	.01630
1S	.01350
2S	.01250
1N	.01580
2N	.01480
4N	.01250
6N	.00910
10N	.00480
14N	.00270
0	.01647
1'5"E	.01619
2'10"E	.01577
3'10"E	.01520
4'10"E	.01548
1W	.01406
2W	.01307
4W	.01023
6W	.00724
10W	.00298

Temperature Range: 85-90^{o}F
Gross Weight = 76,000 lbs.
Contact Pressure = 148 psi

Table A10

Plate Load Deflection Data for

Site 4 on Runway 4R-22L

May 20, 1975

LVDT Adjacent to crack		LVDT Between Crack	
Location or Offset from LVDT	Deflection inches	Location or Offset from LVDT	Deflection inches
3'10"N	.0151	0	.01960
4'10"N	.0125	1N	.01690
5'10"N	.0099	2N	.01530
7'10"N	.0081	4N	.01310
9'10"N	.0055	6N	.00950
13'10"N	.0026	10N	.00510
17'10"N	.0011	14N	.00210
1'11"N	.0172	1'11"S	.01490
0	.0195	3'10"S	.01250
1S	.0182	4'10"S	.01110
2S	.0158	5'10"S	.01010

Temperature Range: 76°F

May 21, 1975

0	.02017	0	.01605
1W	.01676	1W	.01406
2W	.01463	2W	.01236
4W	.01093	4W	.00937
6W	.00795	6W	.00682
1W	.00312	11W	.00227
1'5"E	.01776	1'5"E	.01903
2'10"E	.01704	2'10"E	.01974
3'10"E	.01648	3'10"E	.01577
4'10"E	.01662	4'10"E	.02372

Temperature Range: 76°F Gross Weight = 76,000 lb. Contact Press.=148 psi

Table A11

727 Aircraft Load Deflection Data
for Site 1 on Runway 4R-22L

June 14, 1973

LVDT Adjacent to Cracks

Location of offset from LVDT	Deflection, inches Run 1	Run 2	Location of offset from LVDT	Deflection, inches Run 1	Run 2
20'8"N	.00047	.00042	14N	.00129	.00129
16'8"N	.00099	.00085	10N	.00294	.00269
12'8"N	.00235	.00212	6N	.00509	.00504
10'8"N	.00319	.00300	4N	.00652	.00637
8'8"N	.00418	.00414	2N	.00754	.00759
7'8"N	.00493	.00479	1N	.00818	.00813
6'8"N	.00559	.00541	0	.00867	.00882
3'4"N	.00780	.00771	3'4"S	.00842	.00862
0	.00916	.00968	6'8"S	.00715	.00666
1S	.00925	.00982	7'8"S	.00647	.00612
2S	.00925	.00964	8'8"S	.00593	.00549

Gross Weight = 120,400 lbs.

Tire Pressure = 175 psi

Table A12

727 Aircraft Load Deflection Data

for Site 3 on Runway 4R-22L

June 12, 1973

LVDT Adjacent to Crack

Location or Offset from LVDT	Deflection, inches Run 1	Run 2
14N	.00250	.00188
10N	.00480	.00418
6N	.00668	.00710
4N	.00898	.00877
2N	.01265	.01024
1N	.01149	.01149
0	.01191	.01191
1S	.01149	.01128
2S	.01107	.01107

Gross Weight = 138,000 lbs.
Tire Pressure = 175 psi

Table A13

727 Aircraft Load Deflection Data

for Site 4 on Runway 4R-22L

June 12, 1973

LVDT Adjacent to Cracks			LVDT Between Cracks		
Location of offset from LVDT	Deflection, inches Run 1	Run 2	Location of offset from LVDT	Deflection, inches Run 1	Run 2
17'10"N	.00104	.00062	14N	-0-	-0-
13'10"N	.00188	.00188	10N	.00154	.00132
9'10"N	.00418	.00438	6N	.00506	.00594
7'10"N	.00627	.00647	4N	.00836	.00902
5'10"N	.00856	.00877	2N	.01056	.01100
4'10"N	.01040	.00982	1N	.01144	.01232
3'10"N	.01170	.01170	0	.01276	.01298
1'11"N	.01295	.01337	1'11"S	.01276	.01276
0	.01546	.01567	3'10"S	.01166	.01100
1S	.01567	.01525	4'10"S	.01056	.00814
2S	.01525	-	5'10"S	.00946	-

Gross Weight = 138,000 lbs.

Tire Pressure = 175 psi

Table A14

Tug (747) Load Deflection Data
for Site 1 on Runway 4R-22L

June 14, 1973

LVDT Adjacent to Cracks			LVDT Between Cracks		
Location or offset from LVDT	Deflection, inches Run 1	Run 2	Location of offset from LVDT	Deflection, inches Run 1	Run 2
20'8"N	.000379	-0-	14N	.001383	.000148
16'8"N	.001137	-0-	10N	.002964	.001383
12'8"N	.002180	.000954	6N	.005119	.003902
10'8"N	.003318	.002038	4N	.006471	.005236
8'8"N	.004313	.003128	2N	.007805	.006619
7'8"N	.005166	.003555	1N	.008645	.007113
6'8"N	.005830	.004455	0	.009336	.007904
3'4"N	.008389	.006636	3'4"S	.009188	.007805
0	.010490	.009290	6'8"S	.009188	.007755
1S	.011044	.009432	7'8"S	.009287	.007805
2S	.011091	.009385	8'8"S	.009287	.007755
4'10"E	.00456*		4'10"E	.00788	.00852
3'10"E	.00498*	.00930	3'10"E	.00823	.00852
2'10"E	.00507*	.00958	2'10"E	.00857	.00887
1'5"E	.00521*	.00987	1'5"E	.00877	.00867
0	.00507*	.01029	0	.00891	.00857
1W	.00488*	.00987	1W	.00833	.00823
2W	.00398*		2W	.00735	.00769
4W	.00398*		4W	.00642	
6W	.00352*		6W	.00529	
10W	.00244*		10W	.00367	

* Readings appear to be low by a factor of 2
Gross weight = 125,000 Tire Pressure = 115 psi

Table A15

Tug (747) Load Deflection Data

for Site 3 on Runway 4R-22L

June 12, 1973

LVDT Adjacent to Crack

Location or Offset from LVDT	Deflection, inches Run 1	Run 2
10N	.00292	.00209
6N	.00522	.00438
4N	.00668	.00564
2N	.00815	.00710
1N	.00919	.00815
0	.01024	.00898
1S	.01024	.00898
2S	.00982	.00898
3'10"E	.00919	
2'10"E	.00940	
1'5"E	.00961	
0	.00982	
1W	.00877	
2W	.00773	
4W	.00668	
6W	.00522	
10W	.00188	

Gross Weight = 125,000 lbs.
Tire Pressure = 115 psi

Table A16

Tug (747) Load Deflection Data

for Site 4 on Runway 4R-22L

June 11, 1973

LVDT Adjacent to crack			LVDT Between Crack		
Location or Offset from LVDT	Deflection inches Run 1	Run 2	Location or Offset from LVDT	Deflection, inches Run 1	Run 2
13'10"N	.00215	.00193	10N	.00204	.00204
9'10"N	.00408	.00365	6N	.00544	.00476
7'10"N	.00537	.00494	4N	.00726	.00681
5'10"N	.00666	.00623	2N	.00908	.00839
4'10"N	.00838	.00731	1N	.01067	.00976
3'10"N	.00924	.00827	0	.01180	.01089
1'11"N	.01075	.01053	1'11"S	.01180	.01089
0	.01333	.01268	3'10"S	.01180	.01066
1S	.01333	.01247	4'10"S	.01157	.01066
2S	.01311	.01225	5'10"S	.01157	.01044
4'10"E	.01204		4'10"E	.01203	
3'10"E	.01290		3'10"E	.01339	
2'10"E	.01290		2'10"E	.01339	
1'5"E	.01268		1'5"E	.01294	
0	.01290		0	.01339	
1W	.01225		1W	.01316	
2W	.01096		2W	.01203	
4W	.00946		4W	.01066	
6W	.00752		6W	.00931	
10W	.00494		10W	.00681	

Gross Weight = 125,000 lbs.

Tire Pressure = 115 psi

APPENDIX B: CRACK SPACING

1. Crack spacing is an important aspect in the design of CRCP, therefore this appendix contains figures which illustrate the distribution of cracking and give the actual crack spacings for different pavement sections. Figures B1- B6 are cumulative frequency diagrams of the crack spacing for various test sections along Runway 4R-22L for different time periods. Figures B7 - B12 show the actual crack spacing in May 1975 for the same test sections as in Figures B1 - B6.

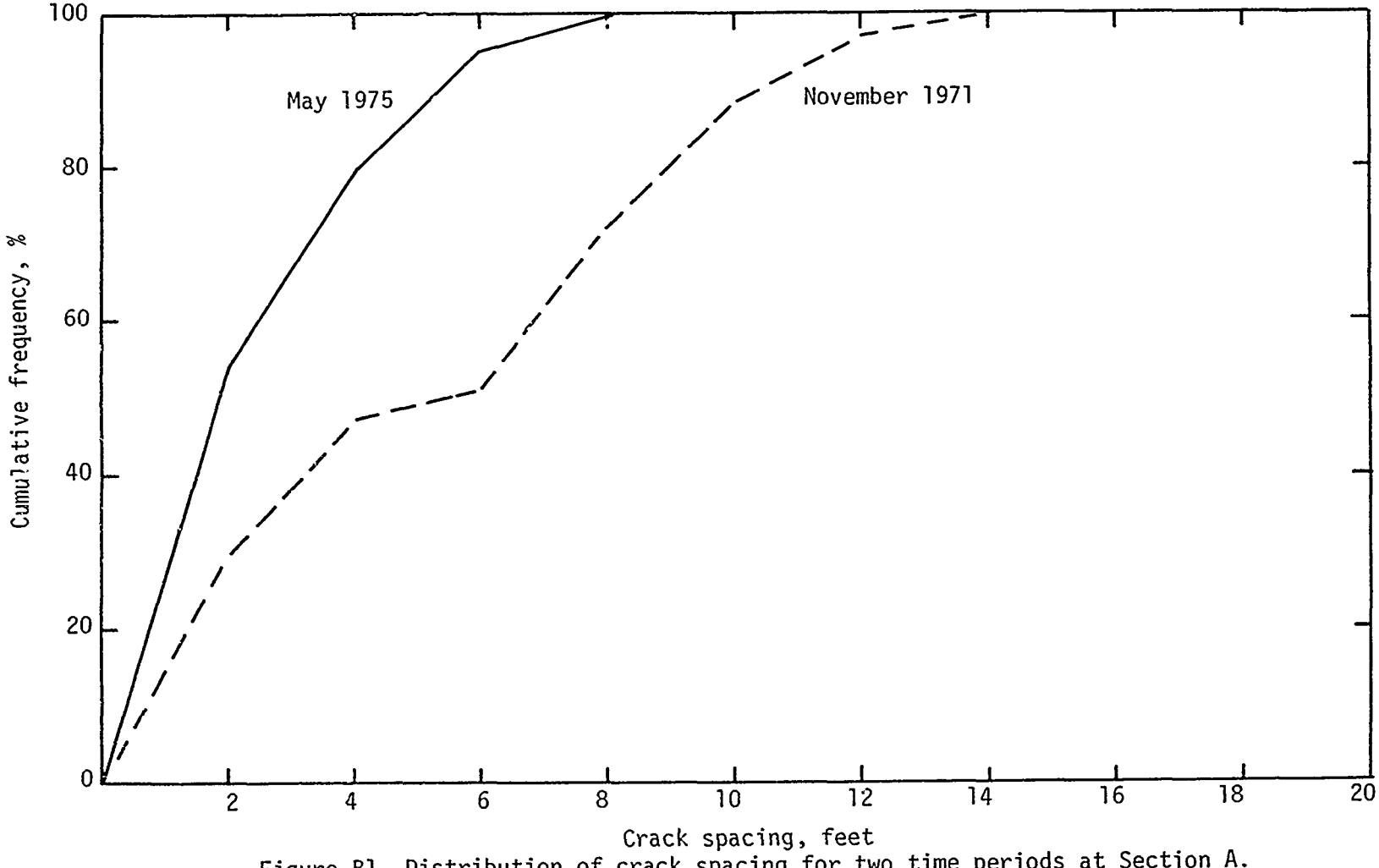

Figure B1. Distribution of crack spacing for two time periods at Section A.

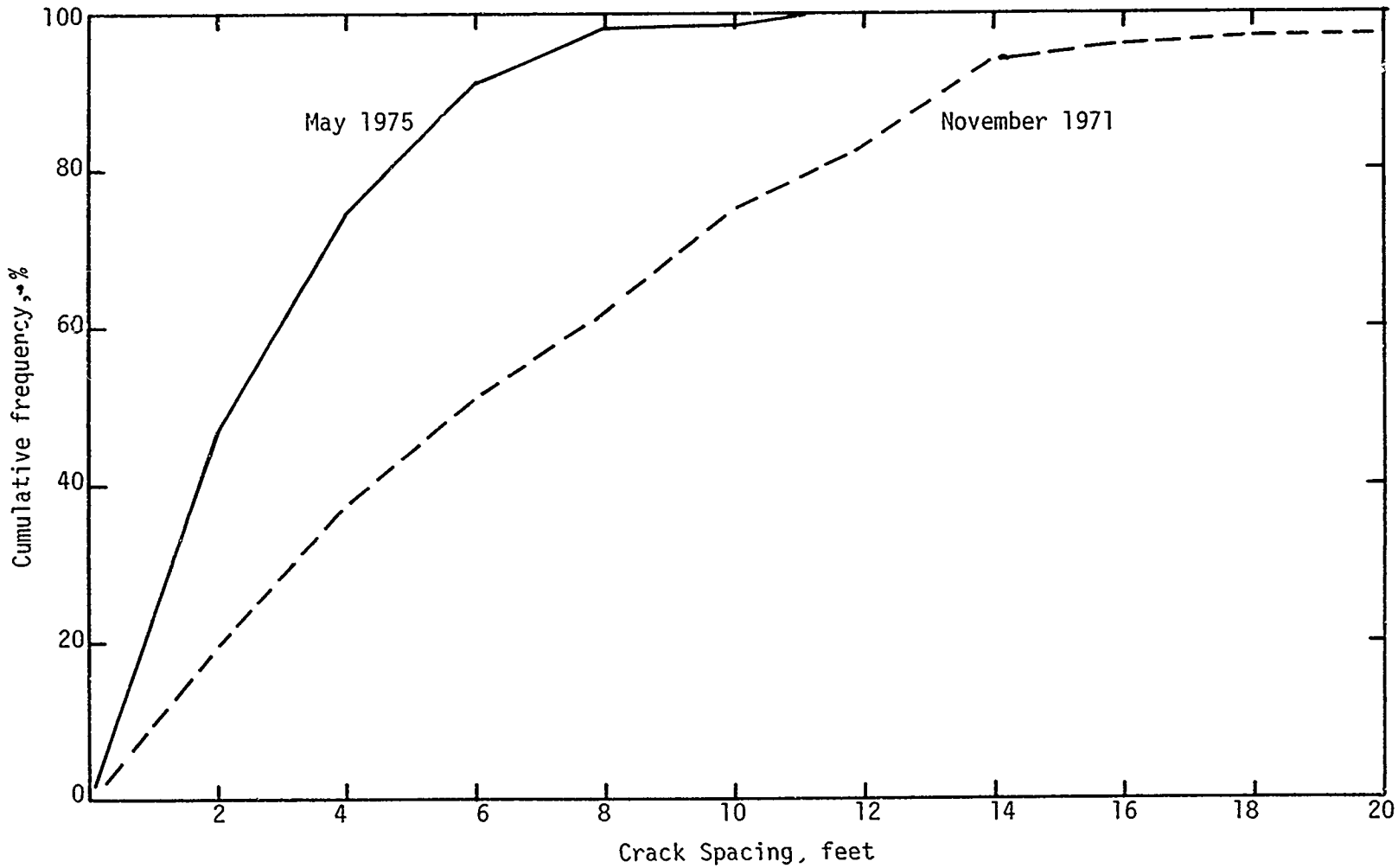

Figure B2. Distribution of crack spacing for two time periods at Section B.

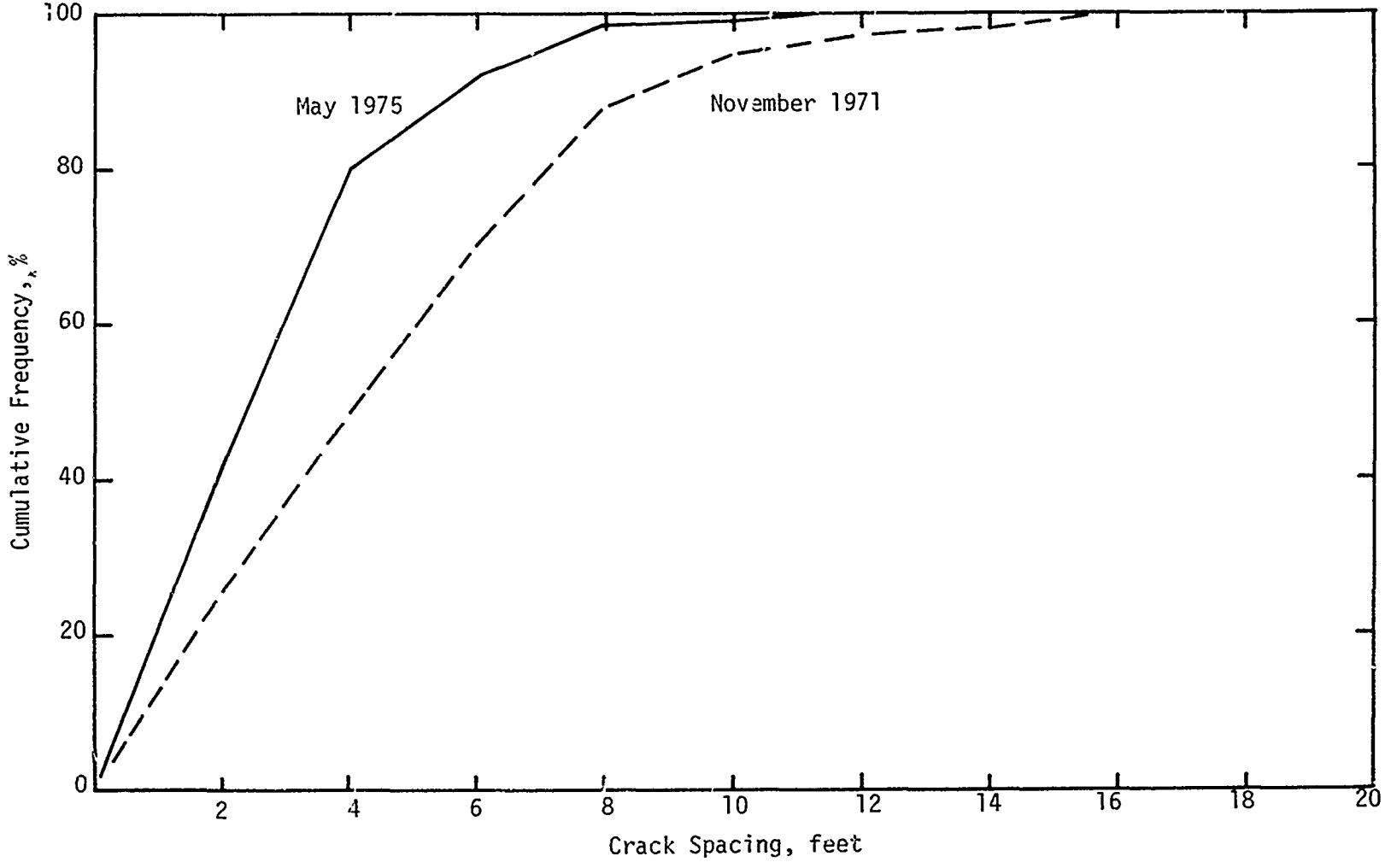

Figure B3. Distribution of crack spacing for two time periods at Section C.

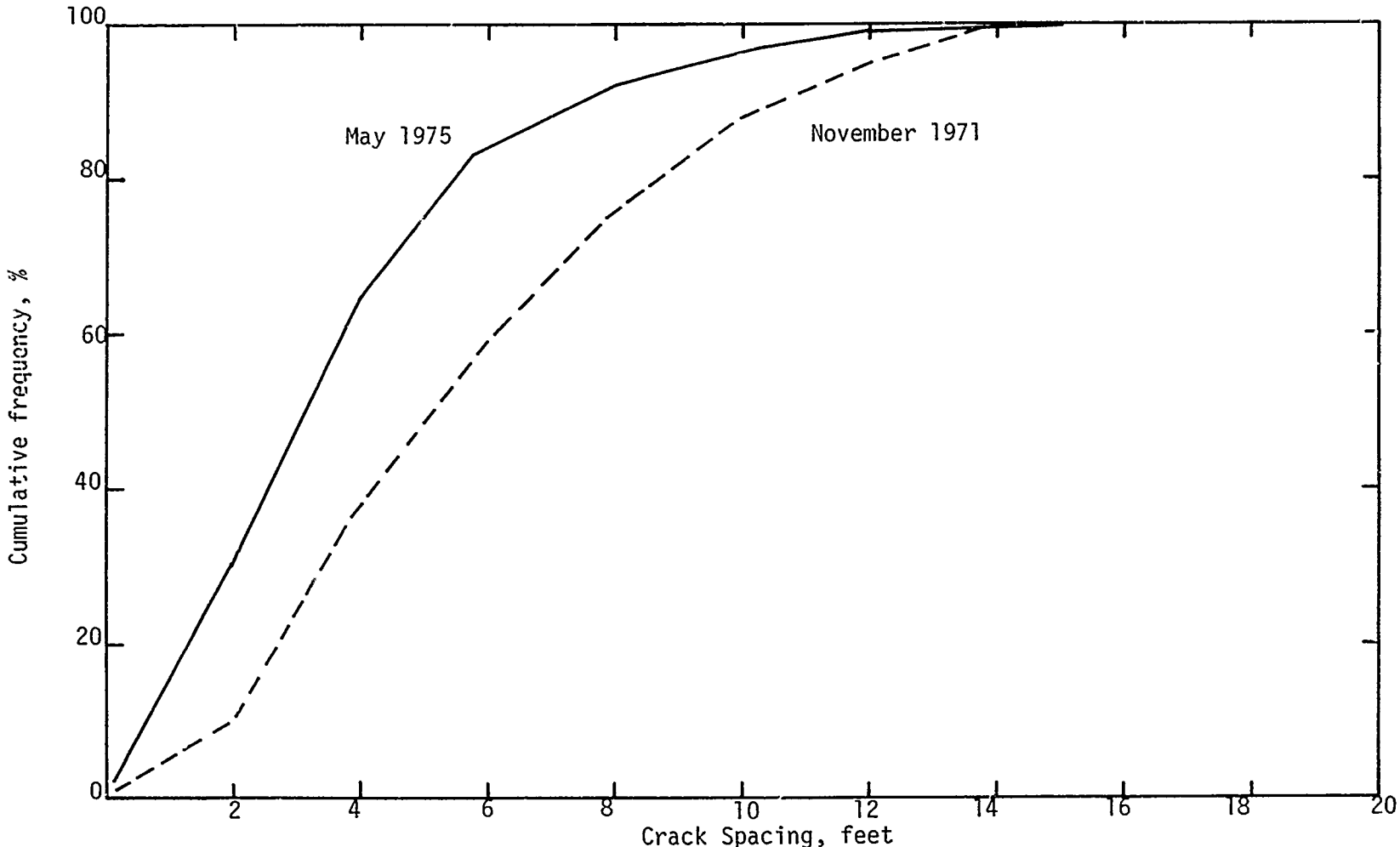

Figure B4. Distribution of crack spacing for two time periods at Section D.

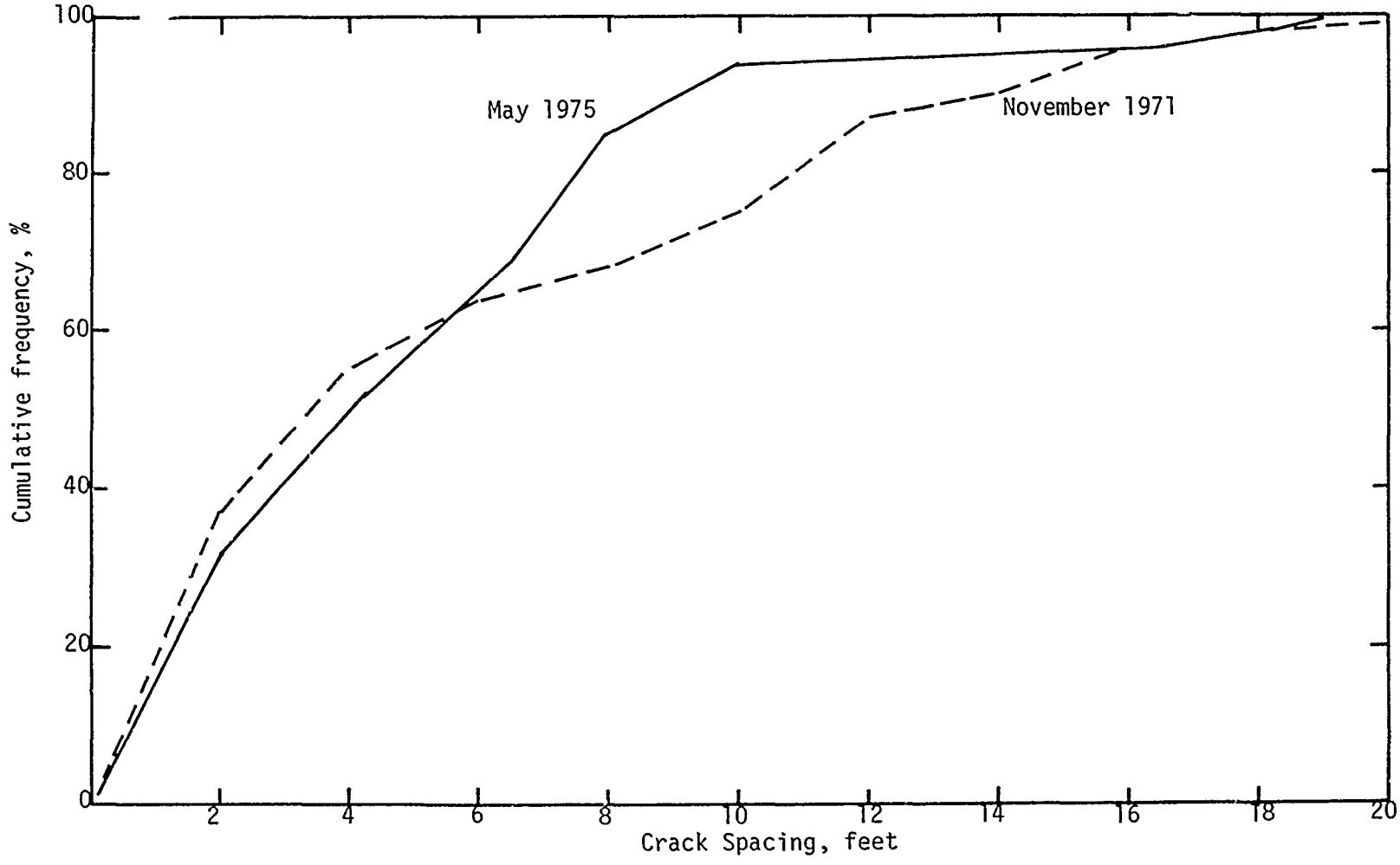

Figure B5. Distribution of crack spacing for two time periods at Section E.

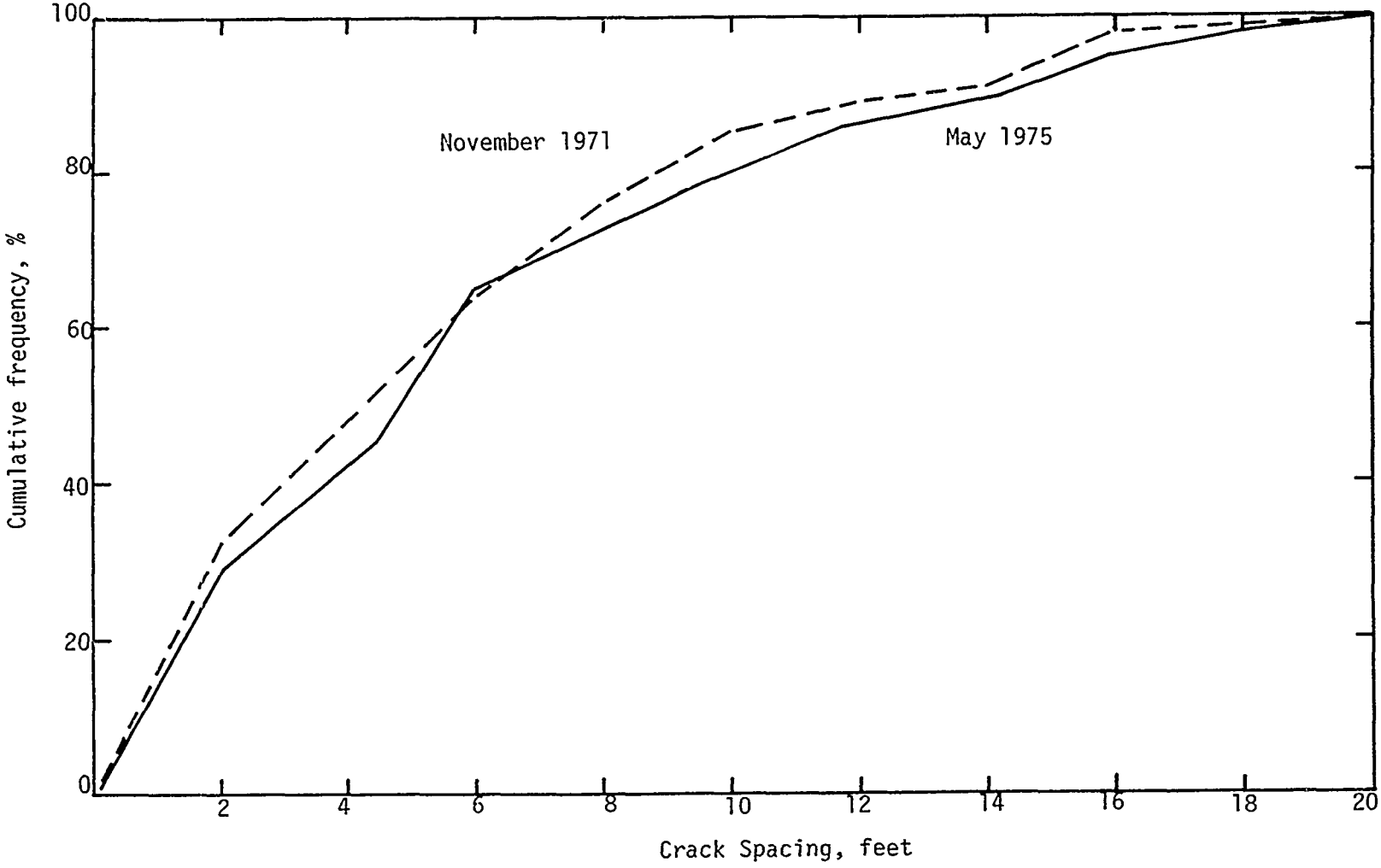

Figure B6. Distribution of crack spacing for two time periods at Section F.

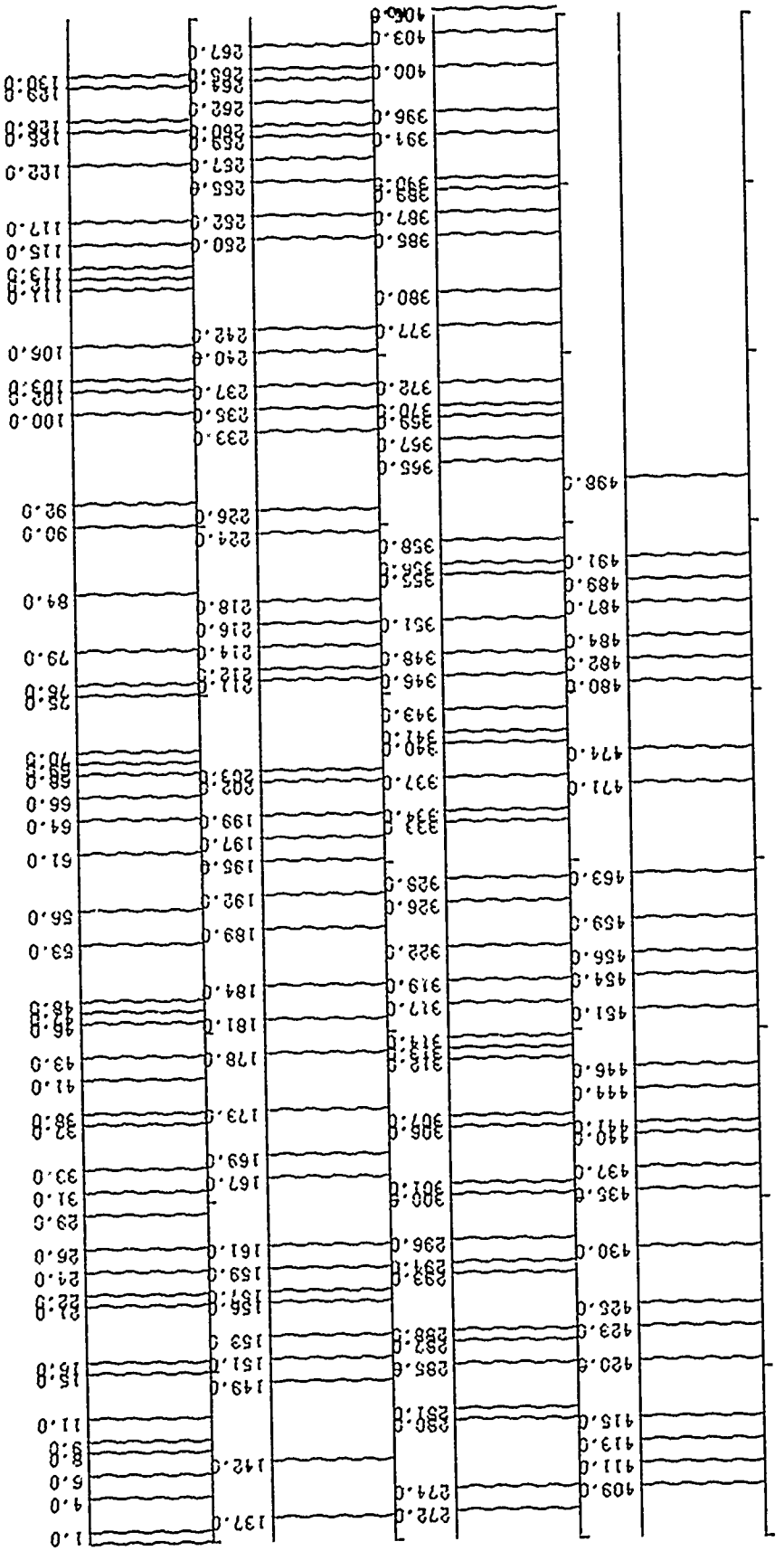

Figure B7. Crack pattern, in feet, for Section A from the May 1975 condition survey.

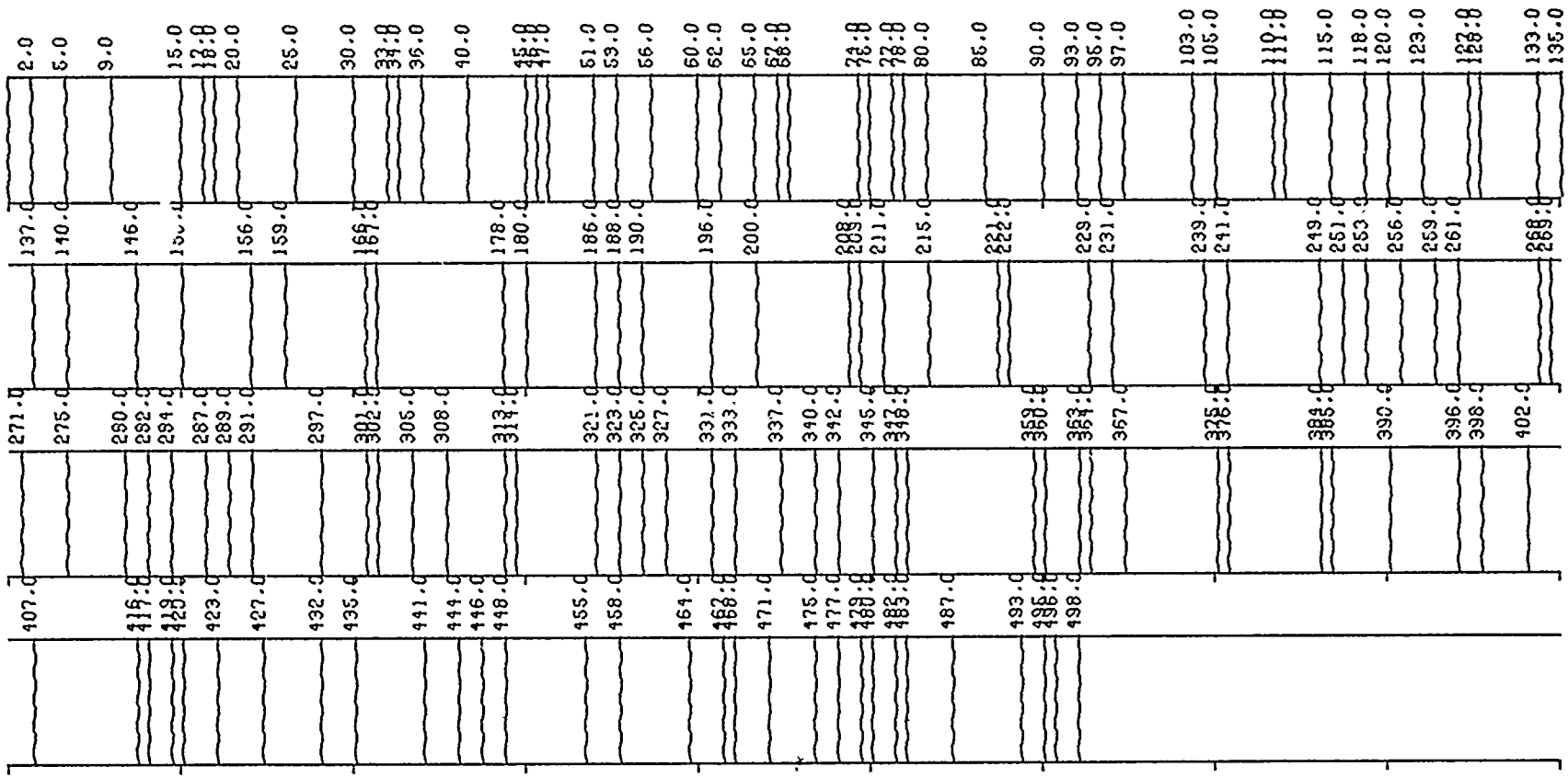

Figure B8. Crack pattern, in feet, for Section B from the May 1975 condition survey.

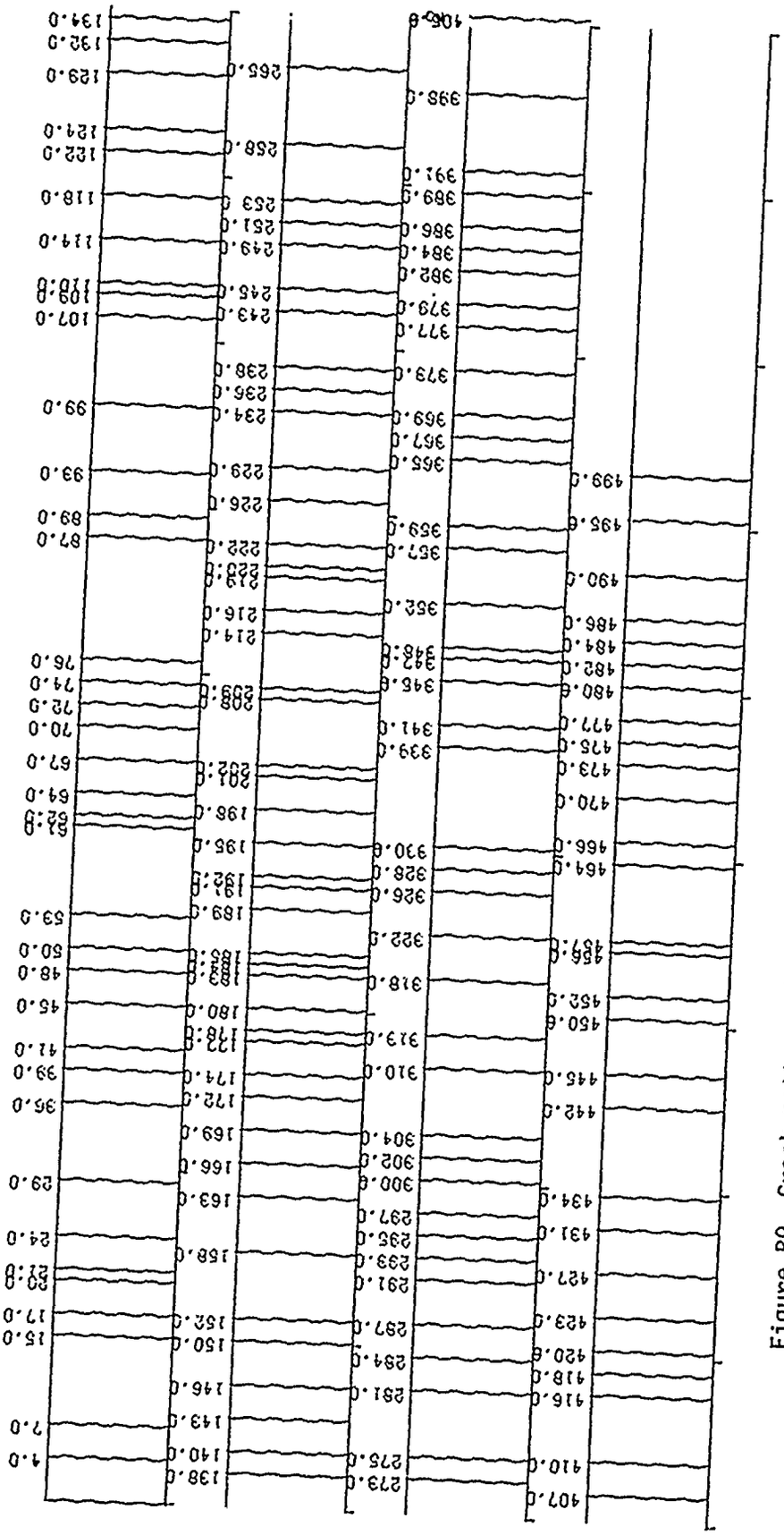

Figure B9. Crack pattern, in feet, for Section C from the May 1975 condition survey.

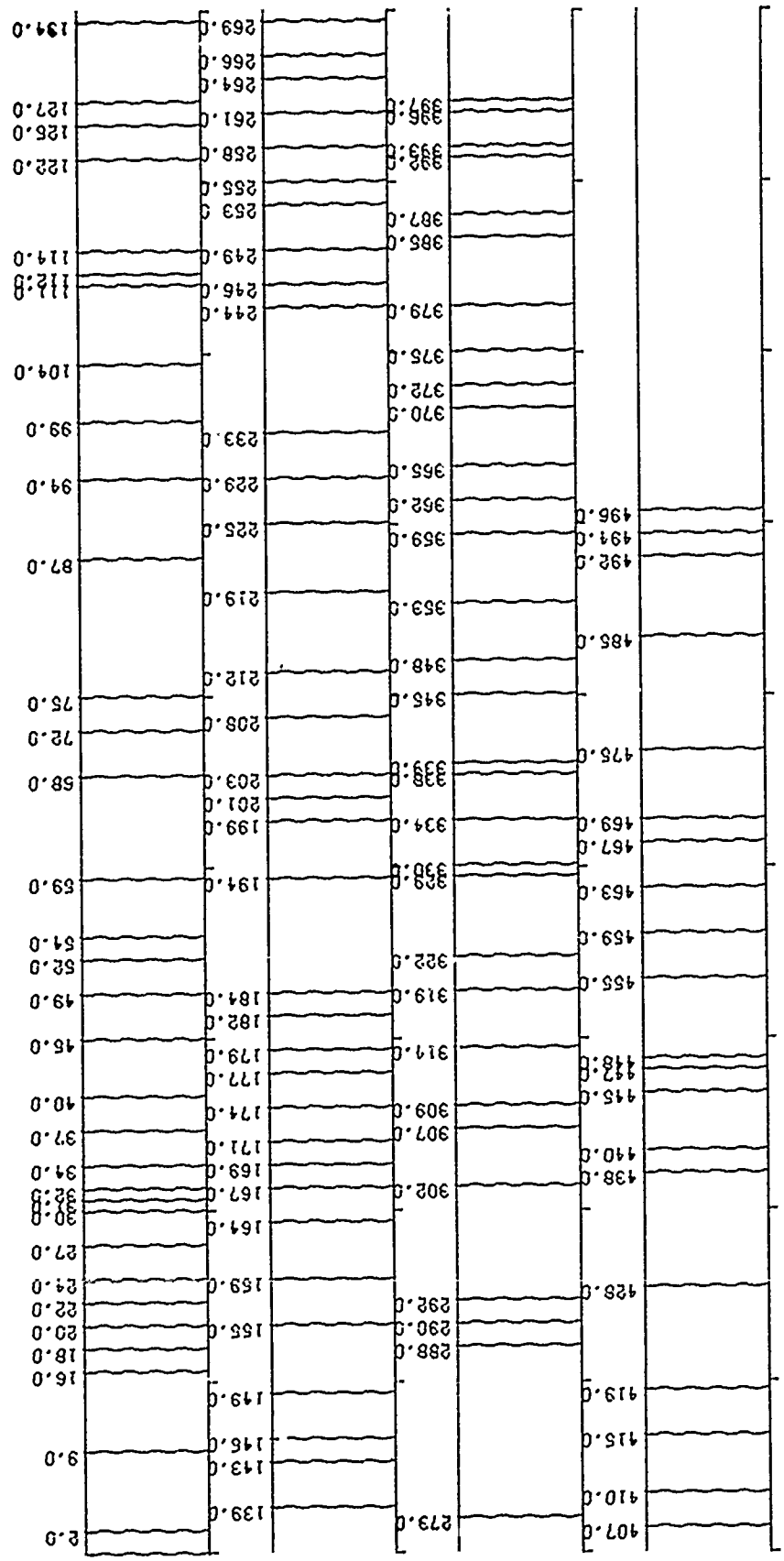

Figure B10. Crack pattern, in feet, for Section D from the May 1975 condition survey.

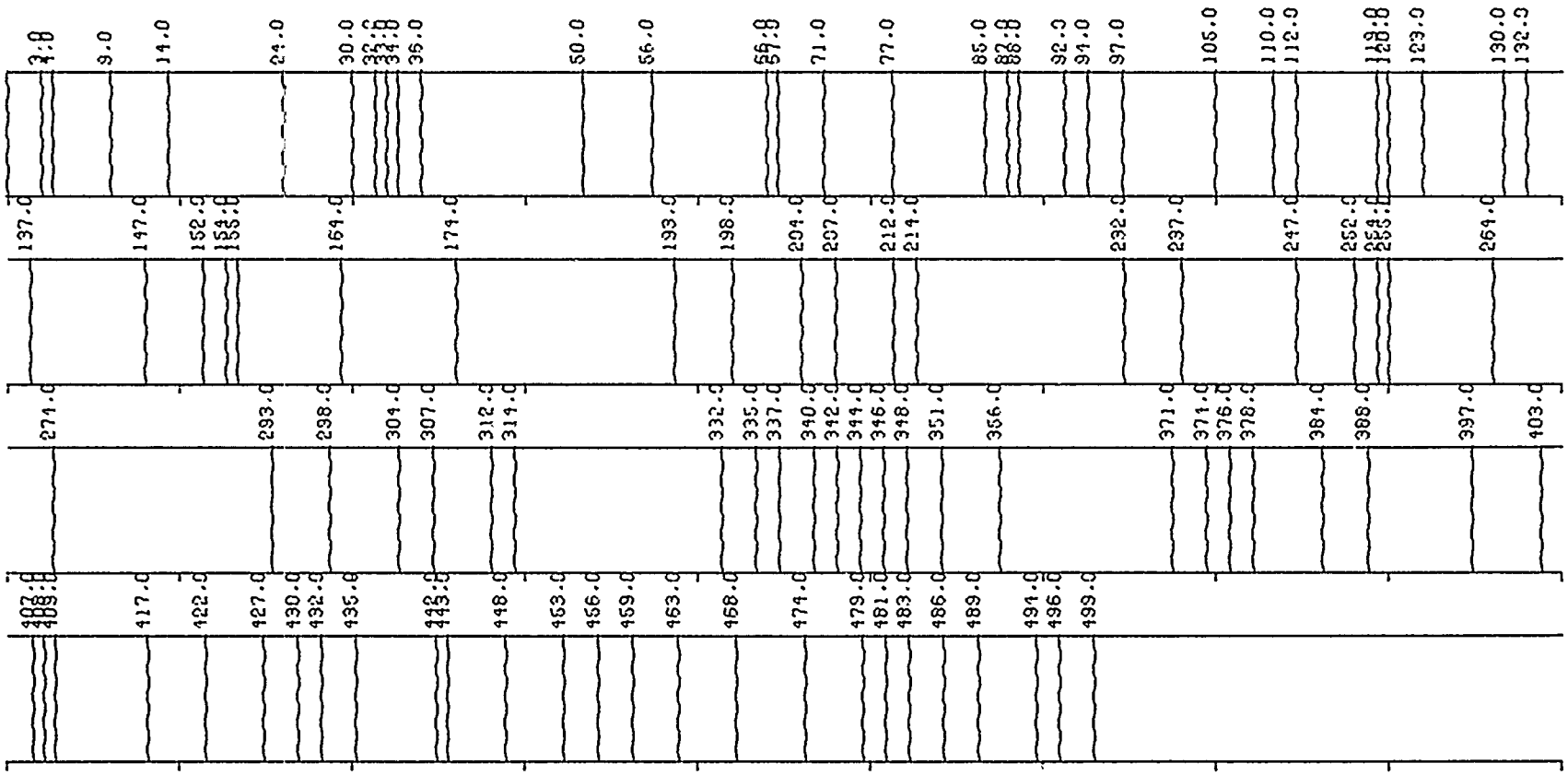

Figure B11. Crack pattern, in feet, for Section E from the May 1975 condition survey.

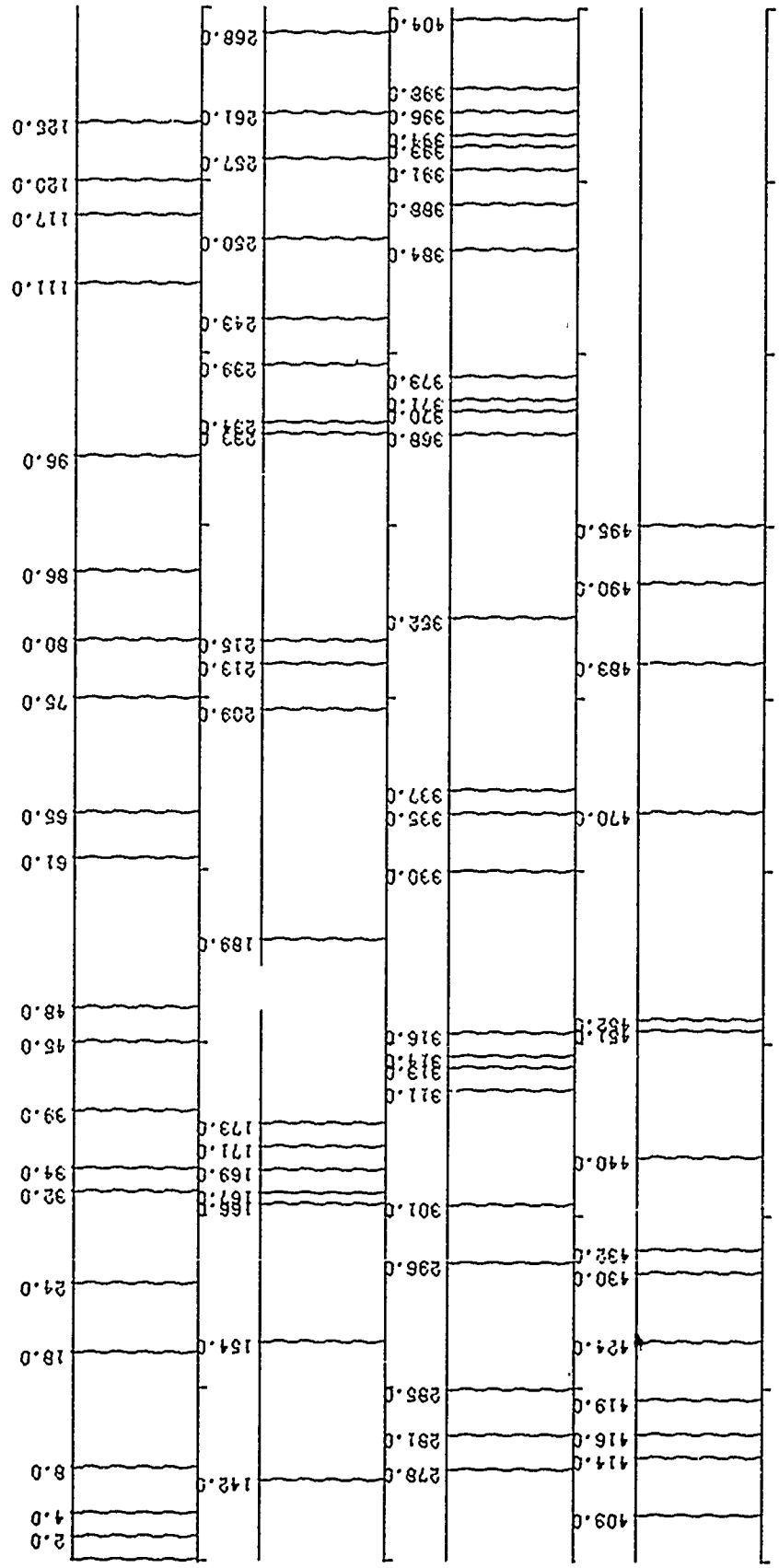

Figure B12. Crack pattern, in fact, for Section F from the May 1975 condition survey.

APPENDIX C: CRACK WIDTH AND CONCRETE MOVEMENT

1. This appendix contains crack width data (Table C1) and concrete movement (Table C2). Movement of the concrete was taken with a Whitmore Strain Gage for three different seasons, spring, summer, and fall. Measurements were made at three locations on Runway 4R-22L, which are illustrated in Figures C1-C3. The data collected is given in Table C2.

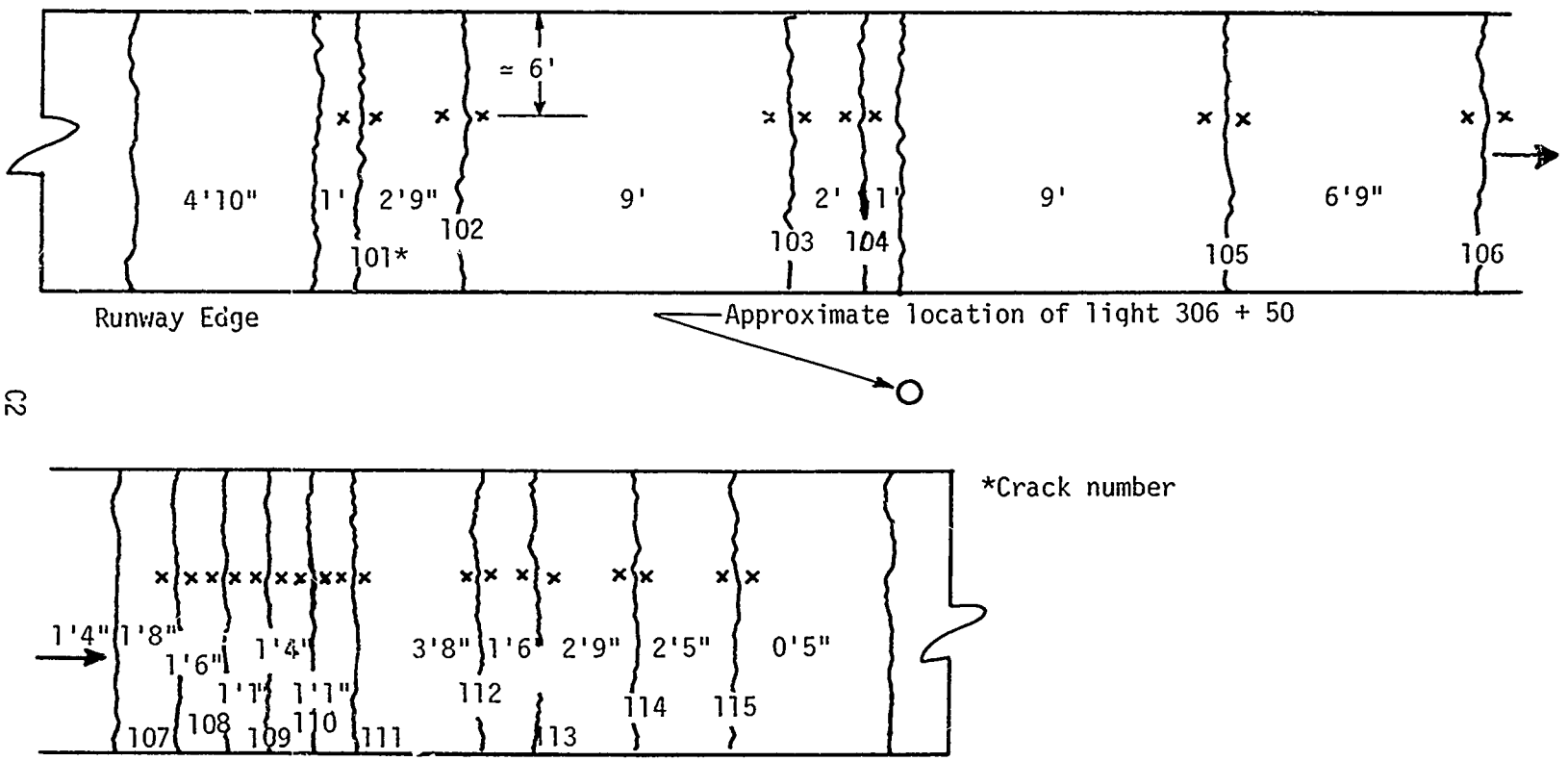

Figure C1. General layout for Whitmore Gage measurements at about station 306 + 50 (outer lane)

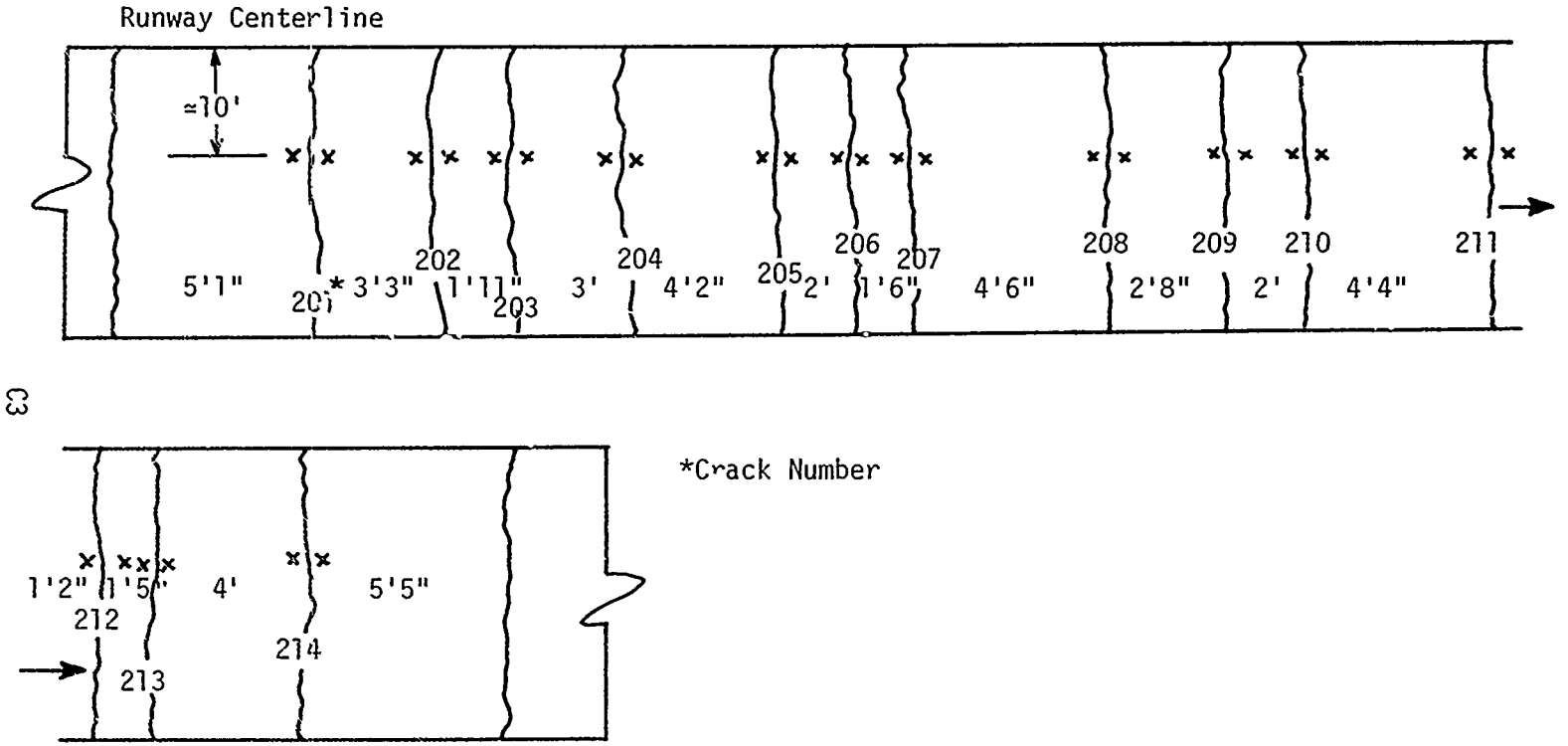

Figure C2. General layout for Whitmore Gage measurements at about station 306 + 50 (interior lane)

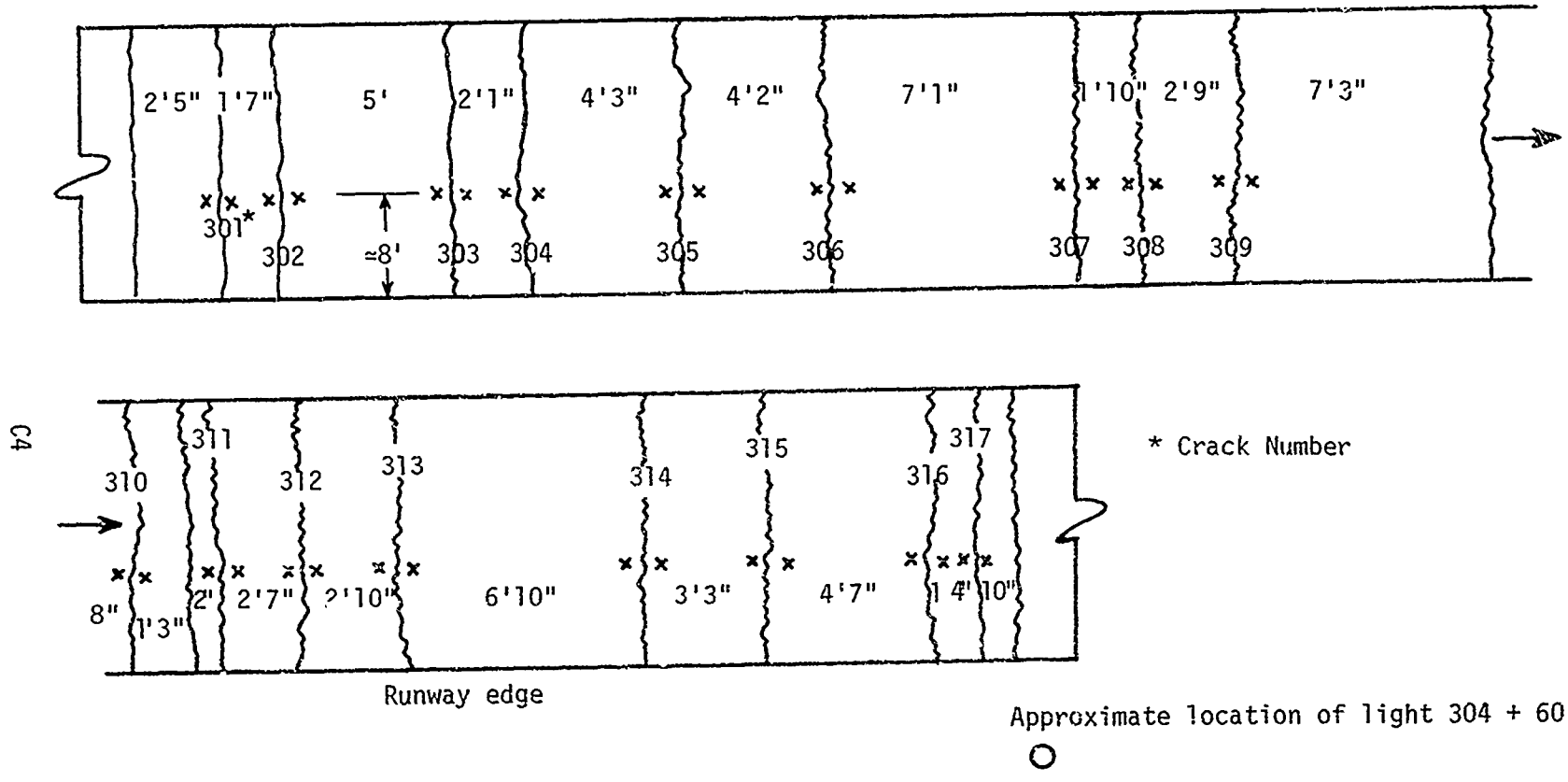

Figure C3. General layout for Whitmore Gage measurements at about station 304 + 60 (outer lane).

Table C1

Crack Width Measurements Taken With A Microscope on Runway 4R-22L

Date	Location	Number of Measurements	Mean Crack Spacing (feet)	Mean Crack Width (inches)	Approximate Air Temp (^{o}F)
9/22/72	sta 272	-	2.5	.010	69
	sta 273	-	2.5	.007	71
	sta 288	-	3.0	.018	71
	sta 290	-	2.0	.012	71
	sta 292	-	3.5	.009	71
5/19/75	site 4 Lane 1	12	-	.014	96
	site 2 Lane 3	3	-	.007	96
5/21/75	site 1 Lane 3	11	-	.011	75
	sta 328 Lane 3	4	-	.035	80
	sta 324 Lane 3	2	-	.016	80
	sta 324 Lane 2	7	-	.012	80
	sta 324 Lane 1	10	-	.010	80

Table C2

Crack Width Data Taken with the Whitmore Strain Gage on Runway 4R-22L

Crack Number	Average Crack Spacing (feet)	Whitmore Gage Readings 5-16-73	8-3-73	11-4-73
Initial Standard		465	462	464
101	1.9	397	409	413
102	1.8	425	423	445
103	5.5	394	390	414
104	1.5	400	409	408
105	3.8	461	459	469
106	4.0	456	458	478
107	1.6	415	413	431
108	1.7	390	386	390
109	1.6	392	386	407
110	1.2	381	377	390
111	2.4	368	377	390
112	2.6	383	380	396
113	2.1	376	374	392
114	2.6	381	377	401
115	3.3	343	341	352
Final Standard		465		
Initial Standard		461		
201	4.2	384	377	395
202	2.6	368	362	377
203	2.5	383	383	393
204	3.6	381	377	393
205	3.1	434	428	432
206	1.8	398	395	408

Table C2 (continued)

Crack Width Data Taken with the Whitmore Strain Gage on Runway 4R-22L

Crack Number	Average Crack Spacing (feet)	Whitmore Gage Readings 5-16-73	8-3-73	11-4-73
Initial Standard				
207	3.0	407	406	410
208	3.6	380	382	385
209	2.3	401	396	408
210	3.2	390	385	401
211	2.8	386	382	394
212	1.0	406	406	413
213	2.8	394	390	408
214	4.7	479	369	386
Final Standard		463		
Initial Standard		460		
301	2.0	483	478	403
302	3.2	491	385	412
303	4.2	413	411	429
304	5.6	491	393	403
305	4.5	409	402	422
306	2.3	484	411	436
307	5.0	383	373	389
308	4.0	381	375	384
309	1.0	383	367	394
310	0.9	395	393	405
311	1.6	381	374	374
312	2.7	417	412	433
313	4.8	437	430	457
314	5.0	397	393	413

Table C2 (continued)

Crack Width Data Taken with the

Whitmore Strain Gage on Runway 4R-22L

Crack Number	Average Crack Spacing (feet)	Whitmore Gage Readings 5-16-73	8-3-73	11-4-73
Initial Standard				
315	7.8	414	409	426
316	3.0	433	430	446
317	1.1	403	395	405
Final Standard		460	460	460

In accordance with ER 70-2-3, paragraph 6c(1)(b), dated 15 February 1973, a facsimile catalog card in Library of Congress format is reproduced below.

Treybig, Harvey J
Data collection and analysis, Runway 4R-22L, O'Hare International Airport, by Harvey J. Treybig, Harold L. Von Quintus, [and] B. Frank McCullough, Austin Research Engineers, Inc., Engineering Consultants, Austin, Texas. Vicksburg, U. S. Army Engineer Waterways Experiment Station, 1976.
1 v. (various pagings) illus. 27 cm. (U. S. Waterways Experiment Station. Contract report S-76-11)
Prepared for Federal Aviation Administration, Systems Research and Development Service, Washington, D. C., under Contract DACW39-75-C-0090.
Includes bibliography.
1. Continuously reinforced concrete. 2. Data collection. 3. Data processing. 4. O'Hare International Airport. 5. Overlays (Pavements). 6. Reinforced concrete. 7. Rigid pavements. 8. Runways. I. McCullough, B. Frank, joint author. II. Von Quintus, Harold L., joint author. III. Austin Research Engineers, Inc. IV. U. S. Federal Aviation Administration. (Series: U. S. Waterways Experiment Station. Contract report S-76-11)
TA7.W34c no.S-76-11